



Technische Universität München

Lehrstuhl für Analytische Lebensmittelchemie

Development and application of two-dimensional separation
systems coupled to mass spectrometry incorporating
capillary electrophoresis

Kevin Jooß

Vollständiger Ausdruck der von der Fakultät Wissenschaftszentrum Weihenstephan für Ernährung, Landnutzung und Umwelt der Technischen Universität München zur Erlangung des akademischen Grades eines

Doktors der Naturwissenschaften

genehmigten Dissertation.

Vorsitzender: Prof. Dr. rer. nat. Erwin Grill

Prüfer der Dissertation: 1. apl. Prof. Dr. agr. Philippe Schmitt-Kopplin
2. Prof. Dr. Bernhard Küster
3. Prof. Dr. rer. nat. Gerhard Scriba

Die Dissertation wurde am 15.01.2019 bei der Technischen Universität eingereicht und durch die Fakultät Wissenschaftszentrum Weihenstephan für Ernährung, Landnutzung und Umwelt am 02.06.2019 angenommen.

Man merkt nie, was schon getan wurde, man sieht immer nur, was noch zu tun bleibt.

- Marie Curie -

Acknowledgements

I want to thank all the people who supported me during the ups and especially the downs of my doctorate. They are an indispensable and cherished part of my life. Without them, I am sure I would not be the same person. Special thanks goes to the following people:

Prof. Dr. Christian Neusüß for providing me the opportunity to do my doctorate in his laboratory undertaking this challenging and exciting project. He supported me substantially during my entire doctorate with great guidance and supervision. He has shown great patience when needed and I especially appreciate his kind nature.

Prof. Dr. Philippe Schmitt-Kopplin, who enabled my doctorate with his external supervision. I particularly appreciate the scientific discussions we had at the Helmholtz Zentrum München.

Prof. Dr. Dirk Flottmann, who always had a sympathetic ear. He had a major influence on my interest in chemometrics. It was a pleasure to develop the related lecture in the master curriculum.

Oliver Höcker, who was of great help during my entire doctorate not only professionally but also personally. He turned out to be one of my closest friends.

Dr. Jens Meixner, who worked with me on several projects. He taught me how efficient and organized a person can be. In this way, he inspired me to improve myself constantly.

Dr. Cristina Montealegre, Dr. Sabine Neuberger, Johannes Schlecht, Jennifer Römer, Alex Stolz, Lukas Naumann and Dr. Nora Tromsdorf who were valuable colleagues over the past years. It was a pleasure to work in such a comfortable environment.

All short-term members of the working group including bachelor and master students who contributed to our work and the friendly atmosphere in the lab.

I also would like to thank the rest of the faculty members, especially Peter Pfundstein and Andreas Haible for their technical and administrative support.

My parents, to who I owe my greatest gratitude. They always supported me in every decision I made no matter what. They are an important supporting pillar in my life and I deeply love and respect them.

My grandfather, who sadly passed away a few years ago. He had a huge influence in evoking my passion for science and always believed that I will succeed in following my dreams.

My grandmother, for her constant support and encouragement during my entire doctorate. Her meals are just delicious.

My brother, who was a great motivation and inspiration for me to follow the path of an analytical scientist.

Summary

Demands imposed on analytical techniques are constantly increasing, especially for the analysis of complex samples. In this regard, capillary electrophoresis (CE) coupled to mass spectrometry (MS) is becoming more and more important in the academic field as well as in the pharmaceutical industry. This is mainly due to the separation mechanism of CE based on the electrophoretic mobility of ions in liquid phase, which is for instance well-suited for the separation of intact proteins with only small structural differences. However, certain restrictions still remain impeding the broader application of CE-MS: (i) considerable interference with electrospray ionization (ESI) of many commonly applied electrolytes, (ii) low concentration sensitivity due to minor injection volumes (typically few nL), and (iii) deficient resolution and separation in particular cases. Multidimensional separation methods coupled to MS, including capillary zone electrophoresis (CZE) as one separation dimension, represent an auspicious approach to overcome these challenges and their development and application were the core objective of the presented thesis.

The first part of this thesis was dedicated to the development of CZE-CZE-MS methods. In the 1st dimension, ESI-interfering CZE methods were applied. Analytes of interest were transferred to the 2nd dimension using a mechanical 4-port valve as CE-CE interface. There, co-transferred ESI-interfering electrolyte compounds were separated from the analyte prior to MS detection. Reliable and precise sample transfer from the 1st to the 2nd separation dimension represents the crucial part of this CE-CE-MS system, which was realized by implementing a hydrodynamic heart-cut sample transfer strategy. In this way, interference-free mass spectra could be obtained despite the utilized ESI-interfering electrolytes. The first application involved the identification of previously unknown degradation products resulting from the combination of acetylsalicylic acid and ascorbic acid in effervescent tablets. Subsequently, a CZE-CZE-MS method was developed for monoclonal antibody (mAb) charge variant characterization utilizing an exceedingly efficient, but ESI-interfering electrolyte as 1st dimension. In this way, separation and mass spectrometric differentiation between main and deamidated forms of a model mAb ($\Delta m = 1$ Da) on intact protein level was achieved for the first time. The CE-CE-MS system is expected

to be applicable to any kind of CE method as 1st dimension, making online MS detection accessible for a wide range of ESI-interfering CE electrolytes.

The second part of the thesis involved the development of a heart-cut nano liquid chromatography (nanoLC)-CZE-MS method, utilizing the aforementioned 4-port valve interface, to improve sensitivity and separation performance in regards to intact (glyco)protein analysis compared to direct CZE-MS. The hyphenation of nanoscale reversed phase liquid chromatography (nanoRPLC) and CZE is of major interest in the scientific/industrial community due to their nearly orthogonal separation mechanism as well as their matching geometries and dimensions. In a proof-of-concept study, a model protein mix was first separated by nanoLC followed by efficient sample transfer of individual protein species and subsequent separation and characterization of their proteoforms, e.g. from ribonuclease B, by CZE-MS. Besides utilizing the higher loading capacity of the nanoLC system, improved separation efficiency for intact proteins was achieved compared to the individual separation dimensions.

In addition, the combination of CZE and drift-tube ion mobility mass spectrometry (DTIM-MS) technology was investigated as an interesting and auspicious alternative to traditional 2D liquid based separation. Prior to this work, the hyphenation of CZE and DTIM-MS has not been investigated in detail. A CZE-DTIM-MS method was developed for the characterization of native and labeled *N*-glycans exhibiting superior separation performance compared to the 1D methods. Each individual glycan signal separated in CZE resolved in an unexpectedly high number of peaks in the arrival time distribution of the DTIM-MS. Furthermore, without initial separation by CZE, the complexity of certain *N*-glycans could not be resolved by DTIM-MS alone.

Summarized, the different 2D methods developed during this thesis embody compelling analytical tools to strongly improve the power and possibilities of CZE-MS.

Zusammenfassung

Die Anforderungen an analytische Techniken nehmen stetig zu, insbesondere hinsichtlich der Analytik von komplexen Proben. Kapillarelektrophorese (CE) gekoppelt mit Massenspektrometrie (MS) gewinnt dabei zunehmend an Bedeutung, sowohl im akademischen als auch pharmazeutisch industriellen Umfeld. Der Trennmechanismus von CE, der auf der unterschiedlichen elektrophoretischen Mobilität von Ionen in der flüssigen Phase basiert, spielt dabei eine wichtige Rolle. CE ist beispielsweise für die Trennung von intakten Proteinen mit nur geringen strukturellen Unterschieden gut geeignet. Es gibt jedoch gewisse Limitierungen, die die breitere Anwendung von CE-MS erschweren: (i) Störung der Elektrospray Ionisierung (ESI) einer Vielzahl der häufig verwendeten Elektrolyte, (ii) niedrige Konzentrationsempfindlichkeit aufgrund der geringen Injektionsvolumina (üblicherweise wenige nL), und (iii) in bestimmten Fällen unzureichende Auflösung und Trenneffizienz. Zweidimensionale Trennmethode, unter Verwendung von Kapillarzonenelektrophorese (CZE) als eine der Trenndimensionen, stellen einen vielversprechenden Ansatz dar, um diese Herausforderungen zu bewältigen. Die Entwicklung und Anwendung solcher Methoden bilden den Kern dieser Arbeit.

Während des ersten Teils dieses Projekts stand die Entwicklung und Anwendung von CZE-CZE-MS Methoden im Vordergrund. In der 1. Dimension wurden CZE Methoden verwendet, die auf ESI-störenden Elektrolyten basieren. Analyte wurden mit einem mechanischen 4-Wege Ventil in die 2. Dimension übergeben. Dort wurden die kotransferierten ESI-störenden Elektrolytbestandteile der 1. Dimension vor der MS Detektion vom Analyten abgetrennt. Ein wichtiger Aspekt des CE-CE-MS Systems ist die zuverlässige und präzise Probenübergabe von der 1. in die 2. Trenndimension. Dies wurde durch die Implementierung einer hydrodynamisch basierten „heart-cut“ Probenübergabe realisiert. Trotz der Verwendung von ESI-störenden Elektrolyten konnten störungsfreie MS-Spektren generiert werden. In der ersten Anwendung konnten zuvor unbekannte Abbauprodukte von Acetylsalicylsäure und Ascorbinsäure in Brausetabletten identifiziert werden. Anschließend wurde eine CZE-CZE-MS Methode für die Charakterisierung von Ladungsvarianten monoklonalen Antikörper entwickelt. In der 1. Trenndimension wurde hier ein sehr effizienter, aber ESI-störender Elektrolyt verwendet. Die Trennung und massenspektrometrischer

Differenzierung von Hauptform und deamidierten Varianten eines Modellantikörpers ($\Delta m = 1 \text{ Da}$) war auf diese Weise möglich. Dies konnte erstmals auf intakter Proteinebene erreicht werden. Das CE-CE-MS System ist grundsätzlich für jede beliebige CE Methode in der 1. Dimension zugänglich, um damit online MS Detektion für eine große Bandbreite an ESI-störenden CE Elektrolyten zugänglich zu machen.

Im zweiten Teil dieser Thesis wurde eine „heart-cut“ nano-Flüssigkeitschromatographie (nanoLC)-CZE-MS Methode entwickelt. Hier wurde ebenfalls das 4-Wege Ventil als Interface verwendet. Ziel war es die Sensitivität und Trennleistung für die Analyse von intakten (Glyko-)Proteinen im Vergleich zur direkten CZE-MS zu verbessern. Aufgrund der nahezu orthogonalen Trennmechanismen als auch den zueinander passenden Geometrien ist die Kopplung von nano-Umkehrphasenchromatographie (nanoRPLC) und CZE sowohl im wissenschaftlichen als auch industriellen Umfeld von besonderem Interesse. In einer „Proof-of-Concept“ Studie wurde ein Modellproteinmix zunächst mittels nanoLC getrennt und einzelne Proteinspezies (z.B. RNase B) in die 2. Dimension übergeben. Anschließend wurden Proteoformen mittels CZE-MS getrennt und charakterisiert. Neben der höheren Beladbarkeit des nanoLC Systems wurde eine höhere Trenneffizienz für intakte Proteine im Vergleich zu den individuellen Trenndimensionen erreicht.

Als vielversprechende Alternative zur klassischen zweidimensionalen Trennung in flüssiger Phase wurde die Kombination von CZE und Driftrohr-Ionenmobilitäts-Massenspektrometrie (DTIM-MS) getestet. Die Kopplung dieser beiden Trenntechniken wurde bisher noch nicht im Detail untersucht. In der hier vorgestellten Arbeit wurde eine CZE-DTIM-MS Methode zur Charakterisierung von nativen und derivatisierten *N*-Glykanen entwickelt. Die CZE-DTIM-MS Methode wies ebenso eine verbesserte Trennleistung im Vergleich zu den jeweiligen 1D Methoden auf. Für jedes in der CZE detektierte Glykansignal wurde eine unerwartet hohe Anzahl an Peaks in der „Arrival Time Distribution“ des DTIM-MS beobachtet. Ohne die vorrangegangene Trennung in der CZE überlagern bestimmte Signale im DTIM-MS und könnten somit nicht aufgelöst werden.

Zusammengefasst konnten während dieser Thesis neuartige und effiziente 2D Methoden entwickelt werden um die Leistung und Möglichkeiten von CZE-MS erheblich zu verbessern.

Contents

List of abbreviations	xii
Introduction & methods	1
1 Protein structure and synthesis.....	1
1.1 Glycosylation of proteins	3
1.2 Glycoproteins of the immune system: antibodies.....	5
1.3 Monoclonal antibodies as biotherapeutics	6
2. Electrophoretic based separation systems	9
2.1 Capillary zone electrophoresis.....	9
3. Chromatographic based separation systems	13
3.1 Reversed-phase liquid chromatography.....	15
4. Mass spectrometry.....	15
4.1 Electrospray ionization	16
4.2 ESI-interfering CE electrolytes	18
4.3 Time-of-flight mass analyzer	19
4.4 Quadrupole mass analyzer	20
4.5 Quadrupole time-of-flight mass spectrometer	21
5 Ion mobility spectrometry based separation	23
5.1 Drift-tube ion mobility mass spectrometry.....	24
6 Two-dimensional separation systems	26
6.1 CE-CE-MS	28
6.2 LC-CE-MS.....	32
6.3 CE-IM-MS.....	33
Objectives	35
List of manuscripts	37
I. Setup of CZE-CZE-MS system and first application to small pharmaceuticals..	39

II: Extension of CZE-CZE-MS applications towards intact protein analysis.....	53
III: Overview of CE-CE-MS applications developed for ESI-interfering electrolytes	65
IV: Setup of LC-CE-MS system and first application to intact glycoprotein analysis	73
V: Development of a CZE-DTIM-MS method for the analysis of protein glycosylation	85
Discussion	97
7. Setup of CZE-CZE-MS system and first application to small pharmaceuticals .	97
7.1 CZE-CZE-MS of small pharmaceuticals	97
7.2 CE-CE-MS utilizing a 4-port valve interface.....	98
7.3 Development of heart-cut strategy	100
7.4 Identification of ASA/ASC degradation products	103
8. Extension of CZE-CZE-MS applications towards intact protein analysis.....	104
8.1 CZE-CZE-MS of mAb charge variants	104
8.2 CZE-CZE-MS method development.....	105
8.3 Mass accuracy of intact mAbs	106
8.4 Deamidated charge variants of Trastuzumab	109
9. Overview of CE-CE-MS applications developed for ESI interfering electrolytes	110
9.1 Application of different CE modes as 1 st dimension	110
10. Setup of LC-CE-MS system and first application to intact glycoprotein analysis	111
10.1 NanoLC-CZE-MS of glycoproteins.....	111
10.2 Development of nanoLC-CZE-MS method	112
10.3 Heart-cut of RNase B from protein mix.....	113
11. Development of a CZE-DTIM-MS method for the analysis of protein glycosylation	115

11.1 CZE-IM-MS of <i>N</i> -glycans	115
11.2 Analysis of APTS-labeled mAb <i>N</i> -glycans	116
11.3 Analysis of native <i>N</i> -glycans	118
Conclusion.....	121
References	125
Appendix.....	141
List of Figures	141
Supplementary Information Manuscript II.....	143
Supplementary Information Manuscript IV	144
Supplementary Information Manuscript V	147
Scientific contributions	151
Eidesstattliche Erklärung	155
Short Curriculum Vitae – Kevin Jooß	157

List of abbreviations

1D	-	one-dimensional
2D	-	two-dimensional
AA	-	amino acid
ASC	-	ascorbic acid
AC	-	alternating current
AGP	-	α -1-acid glycoprotein
APTS	-	8-aminopyrene-1,3,6-trisulfonic acid
ASA	-	acetylsalicylic acid
Asn	-	asparagine
ATD	-	arrival time distribution
BGE	-	background electrolyte
CE	-	capillary electrophoresis
CEM	-	charge ejection model
CGE	-	capillary gel electrophoresis
CIEF	-	capillary isoelectric focusing
CRM	-	charge residue model
CZE	-	capillary zone electrophoresis
DC	-	direct current
diAc-ASC	-	diacetylated ascorbic acid
DNA	-	deoxyribonucleic acid
DTIM-MS	-	drift tube ion mobility mass spectrometry
EACA	-	ϵ -aminocaproic acid

EOF	-	electroosmotic flow
ESI	-	electrospray ionization
EV	-	external vial
FAc	-	formic acid
FAIMS-MS	-	field asymmetric mobility spectrometry mass spectrometry
Fuc	-	fucose
FS	-	fused-silica
Gal	-	galactose
GlcNAc	-	N-acetylglucoseamine
Gln	-	glutamine
HAc	-	acetic acid
HETP	-	height equivalent to theoretical plate
HPLC	-	high-performance liquid chromatography
HV	-	high voltage
IEM	-	ion evaporation model
IEX	-	ion exchange chromatography
Ig	-	immunoglobulin
IgG	-	immunoglobulin G
IMS	-	ion mobility spectrometry
IM-MS	-	ion mobility mass spectrometry
ITP	-	isotachopheresis
LC	-	liquid chromatography
LIF	-	laser-induced fluorescence
Man	-	mannose

mAb	-	monoclonal antibody
mAc-ASC	-	monoacetylated ascorbic acid
mRNA	-	messenger ribonucleic acid
<i>m/z</i>	-	mass-to-charge ratio
MS	-	mass spectrometry
NSA	-	2-naphthalenesulfonic acid
NeuNAc	-	<i>N</i> -acetylneuraminic acid
UHPLC	-	ultra-high-performance liquid chromatography
PTM	-	post-translational modification
PVA	-	poly(vinyl alcohol)
Q	-	quadrupole
RF	-	radio frequency
RNase	-	ribonuclease
RPLC	-	reversed-phase liquid chromatography
SDS	-	sodium dodecyl sulfate
Ser	-	serine
SIM	-	selected ion monitoring
SL	-	sheath liquid
Thr	-	threonine
TOF	-	time-of-flight
tRNA	-	transfer ribonucleic acid
TIMS-MS	-	trapped ion mobility spectrometry mass spectrometry
TWIM-MS	-	travelling wave ion mobility mass spectrometry

Introduction & methods

The presented thesis can be divided into 5 major parts: (i) an introduction to proteins and related post-translational modifications such as glycosylation followed by the separation, hyphenation and detection techniques applied in this work including an overview of state-of-the-art technology; (ii) the core objectives of this work; (iii) relevant publications accompanied by a brief summary and candidate's contributions; (iv) a discussion section focusing on accomplishments in the overall context of the project; (v) a conclusion and future perspectives following this project.

1 Protein structure and synthesis

Peptides and proteins are polymers of amino acids (AAs) which are chained together covalently via amidation called "peptide bond" as depicted in Figure 1. These chains are composed of up to 20 different types of standard (proteinogenic) AAs which possess characteristic side chains [1] (pp. 108-112). In addition, the non-standard AAs L-selenocysteine and L-pyrrolysine can be incorporated by particular translation mechanisms [2]. Peptides consist of at least 2 AAs (dipeptide) up to several thousands. The transition between peptide and protein is fluent and thus not exactly defined. Still, if the mass of the AA sequence exceeds 10,000 Da and tertiary or quaternary structures are formed, these macromolecules are typically referred to as proteins [1] (pp. 108-112). Proteins are involved in a majority of biological functions including (i) biochemical reactions, (ii) transport/storage of small ions and molecules, (iii) immune response, (iv) transition of signals to coordinate biological processes, and (v) structure and support of cells [1] (pp. 201-303). It is highly remarkable that the combination of 20 (or 22) different AAs results in such a variety of structures and characteristics. The biosynthesis of proteins in eukaryotes is considered one of the most complex biological processes. Nevertheless, it can be simplified and divided into three major steps as illustrated in Figure 2: (1) transcription, (2) translation, and (3) post-translational modification [1] (pp. 1409-1467). The transcription takes place in the nucleus where the double-stranded deoxyribonucleic acid (DNA) is untangled and transcribed into single-stranded messenger ribonucleic acid (mRNA) by the enzyme RNA polymerase.

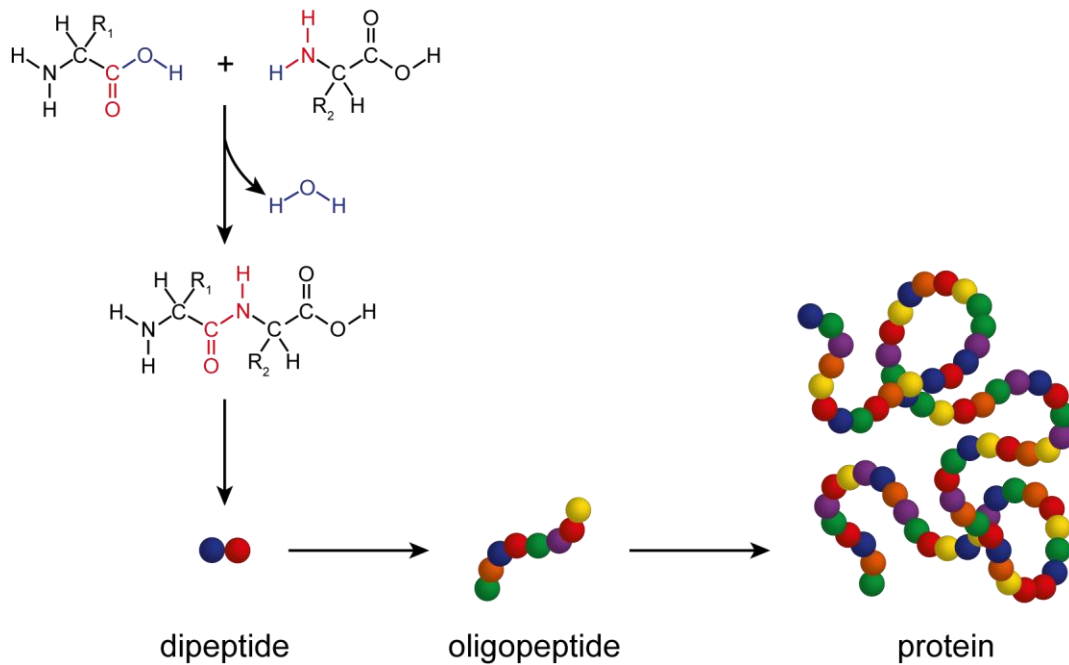


Figure 1: Basic structural composition of peptides and proteins. Peptides (< 100 AAs) and proteins (> 100 AAs) are composed of amino acids which are linked covalently via peptide bonds involving elimination of water.

In fact, the mRNA is complementary to the original single-stranded transcribed DNA and able to leave the nucleus to migrate towards the ribosomes located at the rough endoplasmic reticulum in the cytosol. It is translated by the ribosome to a protein sequence with the help of transfer-RNA (tRNA). Three bases of the mRNA represent one codon for the recognition of a tRNA which transports a specific AA. This AA is transferred to the next tRNA, the AA chain is prolonged and the protein is released after the stop codon is reached. The protein gets folded either during or after the primary peptide chain is synthesized. Subsequently, additional post-translational modifications (PTMs) occur. PTMs are covalent and generally enzymatic modification of proteins usually taking place after the translation and help to regulate localization, activity, and interactions with other cellular molecules [3]. They can occur at any time at the life cycle of a protein. Many proteins are modified after the translation process is completed to mediate correct folding, increase stability or help to localize the protein to a distinct cellular compartment. Other PTMs can occur after the folding process is completed. These PTMs serve to alter the biological activity of the protein, e.g. activation or deactivation of catalytic activity. Thus, PTMs represent a common

mechanism to regulate the overall cellular activity. PTMs include e.g. methylation [4], acetylation [5], phosphorylation [6], lipidation [7] and glycosylation [8].

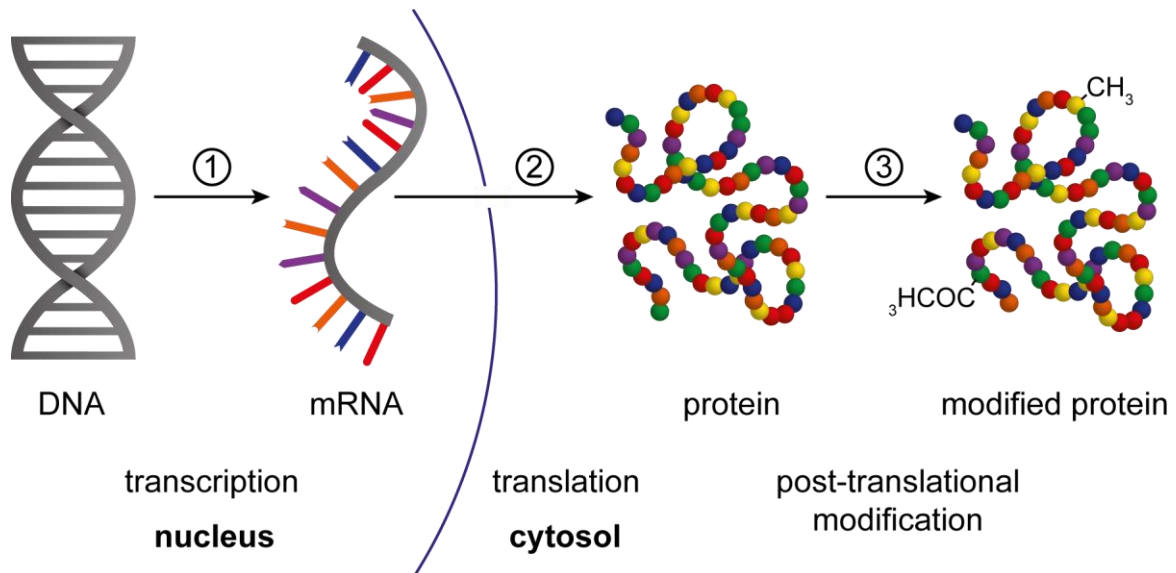


Figure 2: Simplified concept of protein synthesis divided into three major steps: (1) transcription, (2) translation, and (3) posttranslational modification.

1.1 Glycosylation of proteins

Glycosylation is one of the most common PTMs, usually taking place in the endoplasmatic reticulum and the Golgi apparatus [9]. Approximately 50% of all proteins are glycosylated in eukaryotic organisms [10]. Glycoproteins exhibit at least one potential glycosylation site with a covalently attached glycan. Generally speaking, glycans are “oligosaccharide trees” comprised of different monosaccharides linked together via α - and β -glycosidic bonds [11, 12]. The most common monosaccharides are *N*-acetylglucosamine (GlcNAc), mannose (Man), galactose (Gal), fucose (Fuc) and *N*-acetylneuraminic acid (NeuNAc). Glycans are attached either on asparagine (*N*-glycans) or on serine/threonine (*O*-glycans) residues [13]. Each *N*-glycan is derived from the same core structure of $\text{Man}\alpha 1-6(\text{Man}\alpha 1-3)\text{Man}\beta 1-4\text{GlcNAc}\beta 1-4\text{GlcNAc}\beta 1-\text{Asn}$ as shown in Figure 3. *N*-glycosylation represents a sequence-specific modification and can only be found at asparagine (Asn) residues followed by any amino acid (except for proline) and serine or threonine (Asn-X-Ser/Thr) [14]. *N*-glycans are divided in three basic structure classes: (i) high-mannose type, containing further mannose units extending the branches, (ii) complex type, in which

“antennae” instigated by *N*-acetylglucosaminyl-transferases are attached to the core and (iii) hybrid type, a combination of the two previous ones. In general, a distinction is made between macro- and micro-heterogeneity of glycosylation [15]. Macro-heterogeneity describes which potential glycosylation sites are occupied. On the other hand, micro-heterogeneity is related to the variety of *N*-glycan structures themselves. In addition, even glycans with the same elemental composition can exhibit highly complex micro-heterogeneity due to stereoisomers of monomer units, several potential linkage sites, anomeric configurations of glycosidic bonds, and the presence of multiple branching patterns [16]. Thus, the analysis of glycosylation still remains a challenging task usually requiring several orthogonal analytical methods.

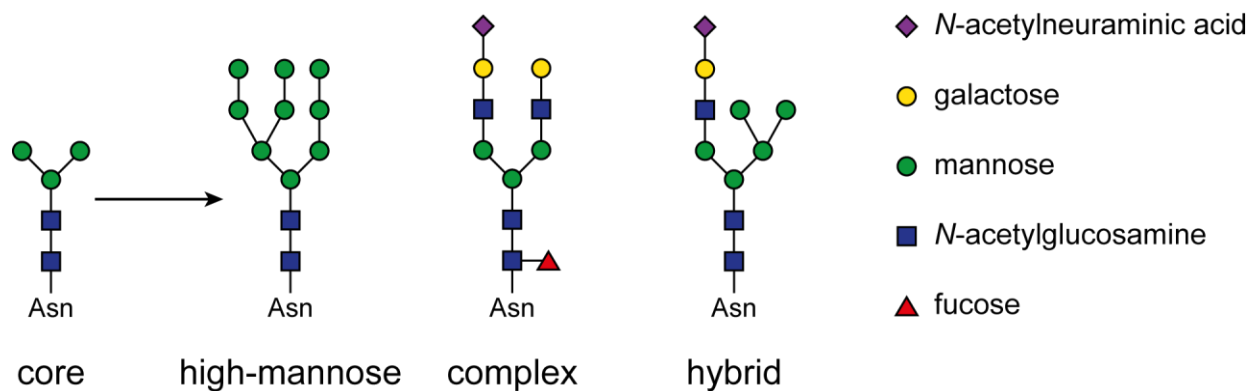


Figure 3: Three general types of *N*-glycans: high-mannose, complex and hybrid type. All *N*-glycans are derived from the same core structure (left side). Each type of *N*-glycan can be potentially fucosylated.

Several biological functions are associated with protein glycosylation including immune response, protein regulation and interactions, apoptosis and recognition of signals on the cell surface [17]. In addition, glycosylation is known to be involved in the development and progression of human diseases especially cancer, inflammatory diseases, rheumatoid arthritis, and Alzheimer’s disease [18]. Increased insight in the molecular and structural characteristics of glycans in biological processes led to the development of biotherapeutics, e.g. monoclonal antibodies (mAbs) with well-defined glycoforms [19]. For the above-mentioned reasons, the analysis of glycosylation represents one of the most important endeavors of glycoprotein characterization with plenty of scope for methodological and technical improvements.

1.2 Glycoproteins of the immune system: antibodies

Antibodies, also known as immunoglobulins (Igs), are glycoproteins that are an essential part of our body's immune system against pathogens and cancer cells [20] (pp. 225-241). They are produced and secreted by plasma cells (B-cells) and are based on a small number of building blocks that are exposed to somatic recombination and hypermutation during cell maturation. Though very similar in structure, these processes enable an extreme variability of antibodies with only a limited number of antibody coding genes in the progenitor B-cell. In this context, B-cells producing high affinity antibodies proliferate more frequently by antigen stimulation, referred to as affinity maturation. This results in the selection of antibodies with increasing affinities. The process to develop specific antibodies in our body usually takes around two weeks and the memory (dendritic) cells will remember the pathogenic antigen for the rest of the host's life.

The most common and archetypical Ig in mammals is the immunoglobulin G (IgG) illustrated in Figure 4. IgGs exhibit a molecular weight of approximately 150 kDa based on four polypeptide chains: two light chains (2x 25 kDa) and two heavy chains (2x 50 kDa) leading to its typical "Y" shape [21]. Both, light and heavy chains contain a variable and a constant region. Light chains comprise one variable domain (V_L) and one constant domain (C_L), whereas heavy chains contain one variable (V_H) and three constant (C_{H1-3}) domains. The variable regions of the IgG contain the antigen-binding site, referred to as paratope. In general, antigens ("antibody generating") are defined as any pathogenic molecule stimulating antibody production by the immune system. In some cases antigens are part of the host itself, e.g. considering autoimmune diseases or cancer cells. The shape of a paratope is specific to only one site of an antigen, called epitope, enabling these two structures to bind together precisely. In this way, an antibody can mark an infected cell or a microbe for attacks by other parts of the immune system, such as macrophages. Alternatively, it can neutralize a pathogen directly, such as affecting the target's metabolism.

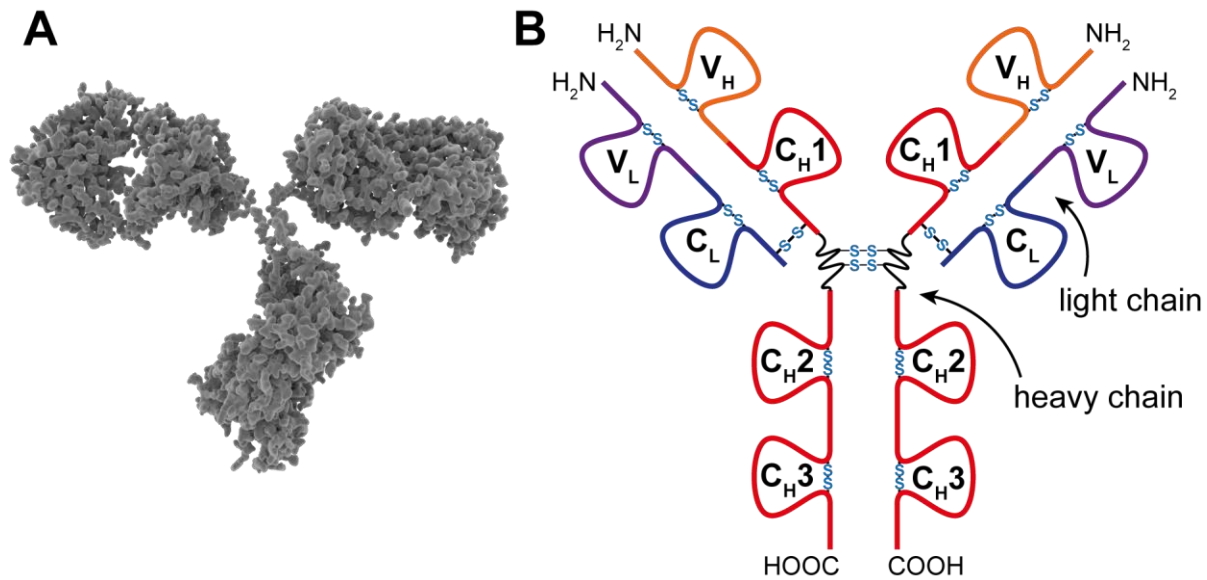


Figure 4: (A) Three-dimensional depiction of IgG class. (B) Scheme of general structure of IgG: Two heavy and two light chains connected via disulfide bonds resulting in a characteristic "Y" shape. Both, heavy and light chains possess a constant (C_H1-3 and C_L) and a variable region (V_H and V_L).

Many antigens exhibit multiple epitopes. As a consequence, different B-cells produce antibodies that bind to different epitopes of the same antigen to create a more effective immune response, known as polyclonal antibodies. Contrary, monoclonal antibodies (mAbs) are formed from one type of B-cell and always bind to a single epitope.

1.3 Monoclonal antibodies as biotherapeutics

Antibodies, including mAbs, are highly effective for treating a variety of different diseases, due to their important immunologic characteristics. In fact, biotherapeutics based on mAbs represent the fastest growing group of pharmaceuticals already achieving sales of almost \$75 billion in 2013 [22] and are expected to reach nearly \$125 billion in 2020 [23]. Starting with the first therapeutic mAb in 1986, 76 mAbs are currently available on the market and approved by the US Food and Drug Administration and the European Medicine Agency in 2017 [24]. The fields of application of mAbs encompass, among other things, the treatment of cancer, transplantations and cardiovascular, infectious or chronic inflammatory diseases [25].

Polyclonal antibodies are rather simple to produce by injection of an antigen into a living organism, drawing blood after few weeks followed by subsequent purification.

This process gets extensively more complex concerning mAbs. It is desired to target specific antibodies arising from a single type of B-cell, however, their isolation from an organism quickly leads to cell death [26]. To overcome this issue, immortal plasma cells are used derived from a type of cancer cell called multiple myeloma, which can proliferate indefinitely outside a living organism. This approach, referred to as hybridoma technology, is considered a major revolution in the entire pharmaceutical field and can be divided into four major steps [27]: (i) injection of a target antigen into an animal and incubation followed by (ii) extraction of spleen cells containing high concentrations of B-cells. (iii) Myeloma cells are mixed with the extracted spleen cells. The resulting hybrid cells incorporate features of both originator cells, including immortality and immunologic activity. (iv) These cells are screened with various assays to determine and isolate the antibody of interest. However, animal derived mAbs produced in this way (e.g. murine mAbs) exhibited severe side effects that could not be neglected, including allergic reactions, immune response against the applied mAb and decreased therapeutic efficacy [28]. Over the years, the development of mAbs based on genetic engineering was improved leading to chimeric, humanized, and finally to full-human mAbs which are illustrated in Figure 5. [29]. Most therapeutic mAbs on the market are humanized and produced in genetically modified Chinese Hamster Ovary cells [30]. In this way, the therapeutic efficacy and safety can be increased minimizing the aforementioned side effects [31].

Besides the selection of a desired cell line, the development of the large-scale production (upstream) and purification methods (downstream) is an essential part for the manufacturing of therapeutic mAbs [32]. After initial filtration, the downstream process typically contains three chromatographic purification steps: (i) protein A affinity, (ii) cation exchange, and (iii) anion exchange chromatography [33]. Protein A chromatography is applied to capture the mAb, whereas the subsequent ion exchange columns are additional clean-up steps to remove impurities, including host cell proteins, aggregates, endotoxins, DNA, and viruses [34].

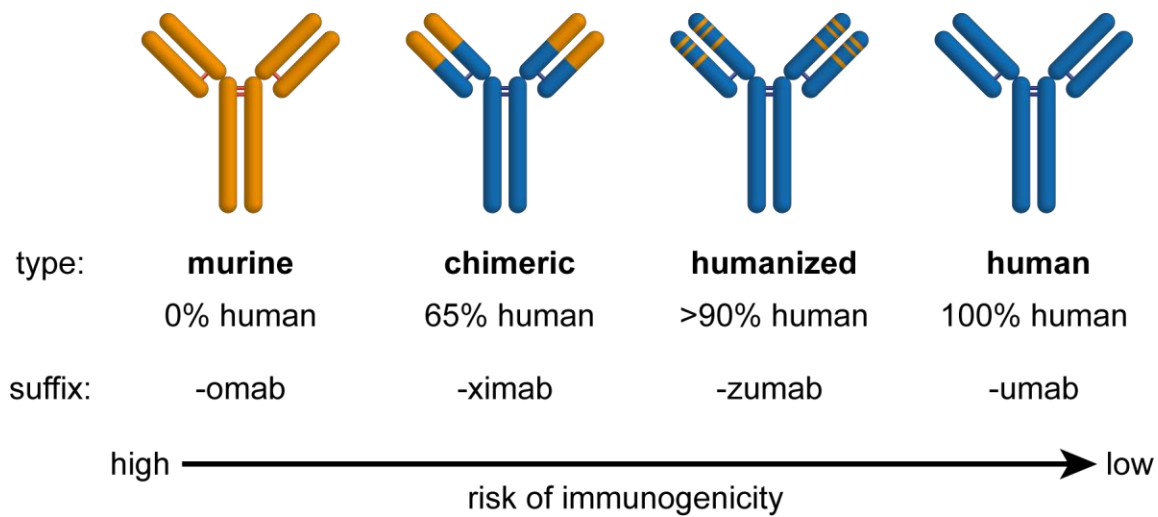


Figure 5: Graphical representation of four general types of biotherapeutic mAbs, including the ratio of human protein sequence and the corresponding suffix. The risk of immunogenicity is decreased ranging from murine to full-human mAbs.

Despite all these efforts, product- and degradation-related impurities of mAbs represent a common issue during synthesis, purification and storage of these complex glycoproteins. Impurities include, among others, aggregation, denaturation, fragmentation. In addition, unintended chemical modifications comprise e.g. disulfide bond scrambling, change in glycosylation pattern, deamidation, pyroglutamate formation, loss of C-terminal lysine, oxidation and amino acid substitution [35]. The characterization of such variants is crucial regarding product quality including technical development, release testing, control of manufacturing processes and safety of the drug [36]. In this context, deamidation represents the most common chemical degradation pathway of therapeutic mAbs originating from the hydrolysis of the amide side-chains of glutamine (Gln) and/or Asn [37]. Deamidation of therapeutic mAbs is well characterized on peptide and fragment level and it has been demonstrated to decrease potency, activity and stability of mAbs [38]. Yet, the characterization of intact mAb charge variants, especially deamidated forms, is highly desired due to the risk of artificially induced modifications caused by sample preparation such as digestion procedures. One promising and already applied technique to not only achieve an effective separation of intact mAb charge variants, but also in regards to glycosylation analysis, represents capillary electrophoresis which is described in the following chapter.

2. Electrophoretic based separation systems

The general concept of electrophoresis describes the differential movement of charged molecules by attraction and repulsion in a medium applying an electric field [39] and was already introduced by Tiselius in 1937 earning him the Nobel Prize [40]. Nevertheless, separation efficiency in free solution was limited by convection and diffusion caused by Joule heating (heat generated by electric current flowing through a conductive medium) [41]. Therefore, traditional electrophoresis is performed in slab gels based on polyacrylamide or agarose. Though being considered one of the most widely applied techniques for protein separation up to date, these methods are time-consuming, labor-intensive, suffer from low efficiencies, and are difficult to be automated. Open tubular capillaries with small inner capillary diameters ($\leq 150 \mu\text{m}$) generate only minor portions of heat and thus can be considered anti-convective. This approach was first described by Hjerten *et al.* in 1967 [42] and later improved by Jorgenson *et al.* in the early 1980s [43]. Techniques that emerged from these early works are generally referred to as capillary electrophoresis (CE).

2.1 Capillary zone electrophoresis

Capillary zone electrophoresis (CZE) is the simplest but also the most versatile form of CE. The generic instrumental setup is based on a narrow-bore, fused-silica (FS) capillary filled with a conductive liquid, the background electrolyte (BGE), as illustrated in Figure 6 [39]. Both ends of the capillary are dipped into different BGE reservoirs, respectively. Electrodes are placed in the BGE reservoirs closing an electrical circuit comprised of the capillary, the reservoirs and a high voltage (HV) source. Injection is performed by either applying small pressure (hydrodynamic) or HV (electrokinetic) for a short time resulting in injection volumes in the low to mid nL-range [44]. Typical separation voltages are in the range of -30 to +30 kV, resulting in relatively low currents in the low to mid μA -range. Even today, optical detection (e.g. UV-Vis) is mostly performed.

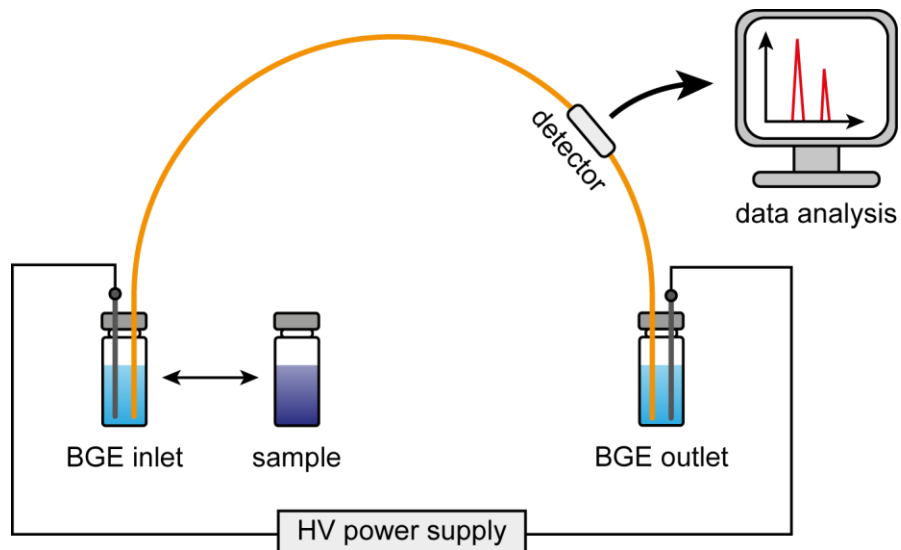


Figure 6: Scheme of general CZE setup: Fused-silica capillary is dipped into different BGE reservoirs (inlet and outlet) including electrodes connected to an HV power supply. For hydrodynamic/electrokinetic injection, the BGE inlet is replaced by a sample vial. Afterwards, a voltage up to ± 30 kV is applied for separation. (Optical) detection is performed near the outlet of the separation capillary.

These detectors are placed in proximity to the capillary outlet to maximize the effective separation length. The velocity (v) of ions in an electric field can be described mathematically as shown in equation 2.1 [39]:

$$v = \mu_e \cdot E \quad (2.1)$$

v	:	ion velocity
μ_e	:	electrophoretic mobility
E	:	electric field strength

The electric field strength (E) is the quotient of applied voltage and capillary length (V/cm). The electrophoretic mobility (μ_e) is constant for the same type of ions in a defined conductive medium. This constant can be derived from balancing the electric force an ion is exposed by the frictional force it experiences while traversing the given medium. This mathematical relationship can be substituted and solved for the electrophoretic mobility resulting in equation 2.2:

$$\mu_e = \frac{q}{6 \cdot \pi \cdot \eta \cdot r} \quad (2.2)$$

- q : ion charge
 η : viscosity of medium
 r : hydrodynamic radius of ion

Consequently smaller, highly charged ions exhibit a higher electrophoretic mobility than larger, minor charged ions. An important factor that needs to be addressed is that this equation strictly applies to fully dissociated molecules. Thus, the dissociation rate (α_i) in a given medium needs to be considered resulting in the so called effective electrophoretic mobility (μ_{eff}) described in equation 2.3:

$$\mu_{eff} = \alpha_i \cdot \mu_e \quad (2.3)$$

- μ_{eff} : effective electrophoretic mobility
 α_i : degree of dissociation of molecule

A major factor in CZE represents the electroosmotic flow (EOF), which is a concomitant of CE in general as shown in Figure 7. The surface of the inner wall of FS capillaries is comprised of silanol groups. At weak acidic to basic pH the silanol groups are partly to entirely deprotonated, carrying a negative charge. Consequently, cations of the electrolyte are attracted by the deprotonated silanol groups forming a fixed layer, referred to as "Stern layer". Additional cations are attracted creating a second, diffuse mobile layer containing an excess of cations. If HV is applied, the positively charged diffuse layer creates a bulk flow towards the cathode end of the capillary, called EOF. It is evident that the pH of the electrolyte plays a crucial role considering the strength of the EOF.

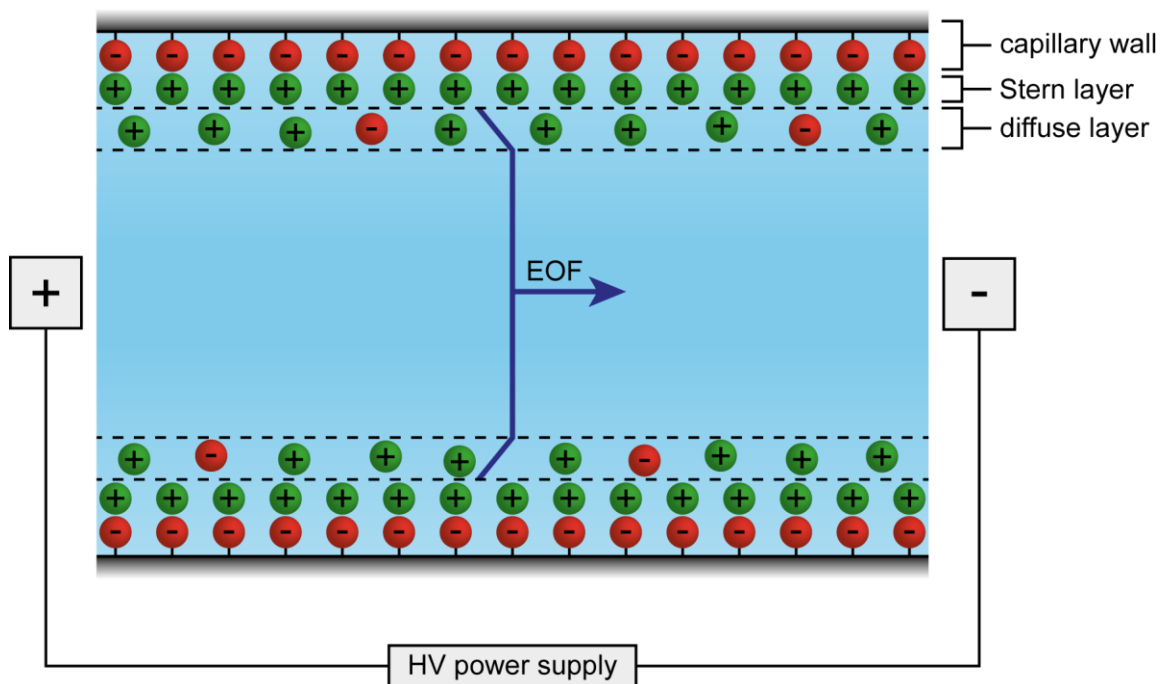


Figure 7: Formation of EOF in FS capillaries: Cations accumulate at the deprotonated silanol groups of the capillary wall building an immobile layer, the "Stern layer". In proximity a diffuse layer is formed containing an excess of cations. If HV is applied, the diffuse layer moves towards the cathode resulting in the EOF.

A unique characteristic of EOF is the formed flat "stamp-like" flow profile, which is beneficial in comparison to the laminar flow profiles obtained by applying pressure e.g. utilized in chromatographic based approaches. As a consequence, the EOF does not contribute to the dispersion of the sample zone leading to comparable narrow signals. In addition, eddy diffusion and mass transfer phenomena as described for liquid chromatography (see chapter 3) are not affecting peak widths in CE. However, a major limitation of CZE is its sensitivity, which can be primarily attributed to the small injection volumes (low to mid nL range). Nevertheless, there has been major progress regarding improvement of sensitivity, especially considering the hyphenation with MS instrumentation [45]. Due to the above-mentioned characteristics of CZE and recent technical developments, CZE gained more importance lately as an alternative separation technique to the well-established liquid chromatography systems. This is particularly true for the characterization of proteins. Minor differences in the protein structure, e.g. deamidation, result in considerable changes in electrophoretic mobilities. Thus, CZE based methods exhibit high separation performance for charge variants of intact proteins often superior to

chromatographic based methods [46]. An additional example represents the analysis of glycan profiles which is routinely performed using CZE coupled to laser-induced fluorescence (LIF) detection [47].

3. Chromatographic based separation systems

Over the last decades liquid chromatography (LC) has been the method of choice for the separation of compounds in non-volatile samples. The instrumental setup of a basic LC system comprises the following components: pumps, degasser, sampling unit, column (and LC oven) and detection unit. The pumps usually deliver a constant flow of a defined mobile phase composition through the LC system. The sampling unit is used to inject a specified volume of sample into the mobile phase flow which carries it into the column. The detector generates a signal proportional to the amount of sample compound eluted from the column. The separation mechanism of LC is based on the partition of analyte molecules between a mobile and a stationary phase. The longer a molecule resides in the stationary phase the longer it takes to reach the detector. This phenomenon is described by the retention factor (k) and can be expressed by the following equation:

$$k = \frac{t_R - t_0}{t_0} = \frac{t'_R}{t_0} \quad (3.1)$$

k	:	retention factor
t_R	:	retention time
t_0	:	void time
t'_R	:	adjusted retention time

Presuming there is no interaction with the stationary phase, the time it takes for a molecule to reach the detector is defined as void time (t_0). The retention factor is the quotient between adjusted retention time (t'_R) and void time and represents an independent parameter to describe the elution of compounds. The selectivity (α) is used to determine the elution relationship between two different compounds as shown in equation 3.2:

$$\alpha = \frac{k_2}{k_1} \quad (3.2)$$

α : selectivity

However, the selectivity does not take the respective peak widths into consideration. Therefore, the resolution (R) has been established to describe the quality of separation (see equation 1.5).

$$R = \frac{t_{R2} - t_{R1}}{\frac{1}{2}(w_1 + w_2)} = 1.18 \cdot \left(\frac{t_{R2} - t_{R1}}{w_{0.5h,1} + w_{0.5h,2}} \right) \quad (3.3)$$

R : chromatographic resolution

w_i : peak width at baseline of compound i

$w_{0.5h,i}$: full width at half maximum of compound i

The resolution can be calculated either based on the peak width at baseline or the full width at half maximum (FWHM). For poorly resolved peaks ($R \leq 1.5$), it is oftentimes easier to determine the FWHM. The peak width is dependent on three major phenomena which are described by the Van-Deemter equation devised in 1956 [48]:

$$HETP = A + \frac{B}{u} + C \cdot u \quad (3.4)$$

$HETP$: height equivalent to a theoretical plate

A : Eddy diffusion parameter

B : longitudinal diffusion coefficient

C : mass transfer coefficient

u : linear flow rate

The Eddy diffusion (A) describes the peak broadening occurring due to the multiple potential flow paths through a column packed with particles. Longitudinal diffusion

(*B*) refers to diffusion of individual analyte molecules in the mobile phase along the longitudinal direction and is inversely proportional to the linear flow rate (*u*). Contrary, the mass transfer term (*C*) describes molecule interchange from the mobile to the stationary phase and *vice versa*. Thus, the faster the flow rate the larger the peak broadening attributed to mass transfer. It is aspired to minimize the HETP in order to improve the separation performance, which can be achieved e.g. by decreasing the particle diameter. This is associated with a significant increase in backpressure and led to the development of high-performance liquid chromatography (HPLC) and finally ultra-high-performance liquid chromatography (UHPLC) systems exhibiting improved peak capacities [49]. The latter ones are capable to handle pressures exceeding 1000 bar.

3.1 Reversed-phase liquid chromatography

Reversed-phase liquid chromatography (RPLC) still represents the most commonly applied mode of LC. In RPLC, the stationary phase is typically based on silica gel which is functionalized with C₄, C₈ or C₁₈ chains to generate a hydrophobic particle surface [50]. Consequently, hydrophobic molecules are stronger retained than hydrophilic compounds. Samples are injected at aqueous conditions and the hydrophobicity of the mobile phase is increased over time to elute compounds from the stationary phase. The exact separation mechanism is still under discussion but it is assumed that both partitioning and adsorption play a critical role [51]. RPLC is one of the standard separation techniques for the characterization of proteins and peptides [52]. Still, the field of proteomics is constantly improving due to the increasing demand for better analytical performance including e.g. nanoRPLC or multidimensional concepts, which is one of the objectives of the here presented work [53].

4. Mass spectrometry

Nowadays, mass spectrometry (MS) represents one of the most important analytical techniques not only in proteomics but in the entire field of separation science [54]. The type of ionization and mass spectrometers that were used during this project are described in the following.

4.1 Electrospray ionization

Electrospray ionization (ESI) is used to generate and transfer ions from liquid phase to the gas phase at atmospheric pressure and was introduced by Yamashita and Fenn in 1984 [55]. ESI is a “soft” ionization technique and is considered the gold standard for hyphenation of liquid separation techniques with MS, such as LC or CE. The general concept of ESI in positive ion mode in combination with preceding CE separation as applied in this thesis is depicted in Figure 8.

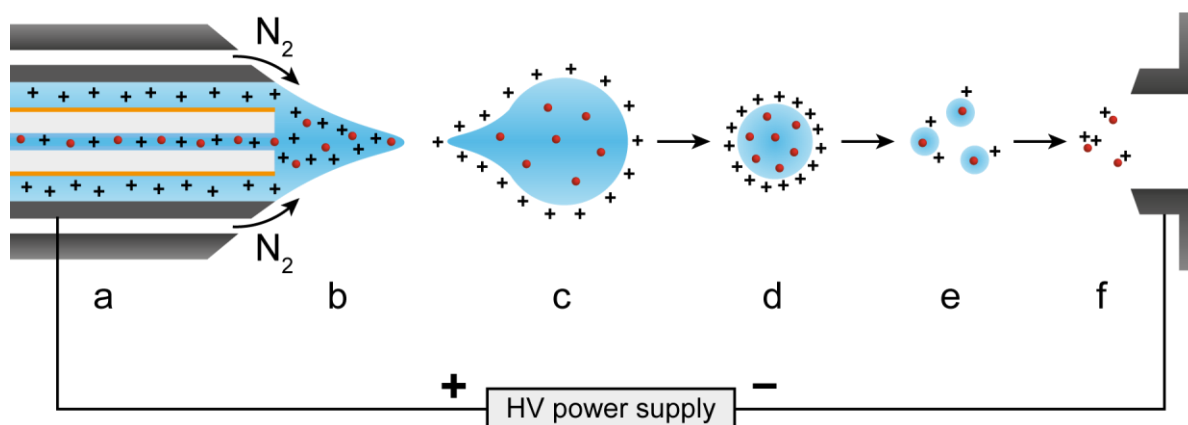


Figure 8: ESI process in positive ion mode applying CE-MS: (a) tip of coaxial sheath liquid interface, (b) Taylor cone, (c) nebulization resulting in multiple charged droplets, (d) desolvation until Rayleigh limit is reached, (e) smaller multiple charged droplets formed after coulomb explosion, and (f) transition of ions to gas-phase before entering the orifice to the MS instrument.

ESI is produced by applying an electric field (typically 3-6 kV) between a metal needle filled with liquid and the inlet of an MS instrument. Typical flow rates of LC are in the range of 1-1000 $\mu\text{L}/\text{min}$ which is sufficient to generate an adequate electrospray. Contrary, the flow rates in CE are considerably lower (<200 nL/min). In order to close the contact of the CE circuit and electrospray while increasing the flow rate, an additional make-up liquid is usually implemented for CE-MS coupling referred to as sheath liquid (SL) [56]. The CE capillary is positioned in the needle tip of a coaxial sheath liquid sprayer surrounded by SL (a). In addition, through an outer tube a hot nitrogen stream is applied, supporting the nebulization process. The electric field extracts electrons from the liquid, continuously generating additional cations. Due to the excess of cations and the electric field force a so called “Taylor cone” (b) is formed at the tip of the needle. The edge of the Taylor cone gets nebulized and multiple

charged droplets are produced (c). The charges are mainly located at the surface of the droplets. Because of the high temperature of the source the droplets shrink until they reach a point where the repulsion of the charges is exceeding the surface tension of the droplets, referred to as "Rayleigh limit" (d). At this moment, a coulomb explosion takes place generating smaller multiple charged droplets. This process is repeated a few times depending on the initial droplet size (typically around 1.5 μm), until very small charged droplets are produced (e). The final step of the ESI process (f) is still critically discussed. Nevertheless three different models are acknowledged depending on the type of analyte ion: (i) ion evaporation model (IEM), (ii) charge residue model (CRM), and (iii) charge ejection model (CEM) illustrated in Figure 9.

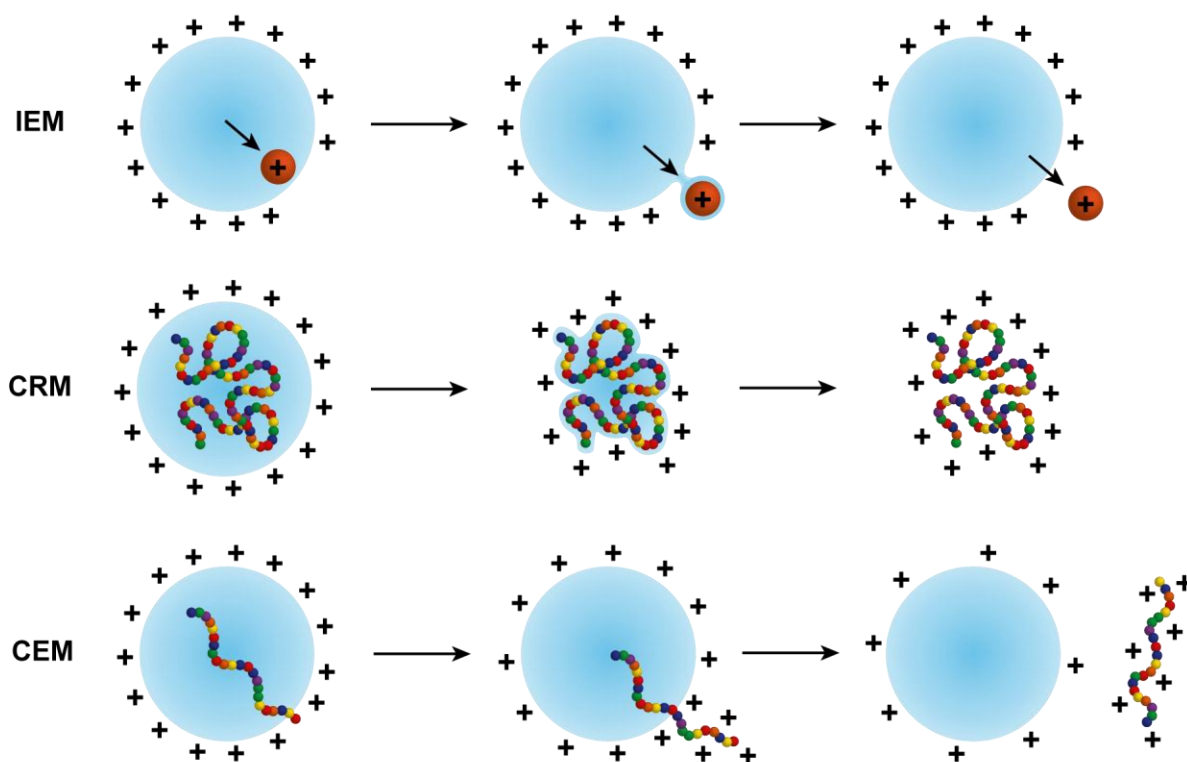


Figure 9: Three major models describing the final step of the ESI process: ion evaporation model (IEM), charge residue model (CRM) and charge ejection model (CEM). IEM involves direct evaporation of small ions from charged droplets. In CRM, the solvent evaporates completely and the charge remains on the molecule, considered the major mechanism for (native) proteins. In CEM, rather non-polar polymer chains (e.g. unfolded proteins) are ejected from the droplet over time entraining charge.

Small analyte ions usually behave according to the IEM. Hence, the ion migrates towards the droplet surface and is directly ejected/evaporated leaving the remaining solvent droplet behind. In the case of native proteins (compact, hydrophilic) the CRM

is regarded appropriate. Here, a single protein resides in the droplet while the remaining solvent evaporates until dryness leaving the charges on the protein as it is transferred to the gas-phase. However, if a protein is denatured, non-polar residues are exposed and accessible to the solvent. For unfolded proteins (extended, hydrophobic) the CEM is considered a fitting mechanism. In this case, the unfolded protein moves to the droplet surface followed by sequential ejection. It is apparent that the CEM shares similarities to the IEM but is clearly distinct from the CRM.

For large molecules, such as proteins, multiple charged ions are commonly produced by ESI. This is highly beneficial as it does not only improve sensitivity at the detector, but also makes protein analysis accessible to mass analyzers with an m/z cut-off. For this reason, ESI represents a highly suitable ionization technique for proteins that were previously separated by liquid separation techniques such as CE or LC.

4.2 ESI-interfering CE electrolytes

Efficient ESI premises the absence of non-volatile constituents, in order to avoid ion suppression and contamination of the MS instrument [57]. However, in CE certain non-volatile electrolyte compounds are often required to achieve sufficient selectivity and separation efficiency. These compounds include, among others, the electrolyte itself, ampholytes, polymeric compounds for sieving, complexing agents and surfactants. As a consequence, interference with the electrospray ionization process represents a common issue, impeding direct coupling of such systems to MS. In certain CE modes, including capillary gel electrophoresis (CGE) or capillary isoelectric focusing (CIEF), ESI-interfering compounds are even essential components of the general separation mechanism. Though CZE is the separation mode that often allows the application of volatile electrolytes, such as acetic acid (HAc) or formic acid (FAc) based BGEs, there is a variety of efficient and routinely applied CZE methods based on ESI-interfering constituents. The application of ESI-interfering electrolytes in CZE is not limited to a particular class of compounds but ranging from small (**manuscript I**) to large molecules, such as mAbs (**manuscript II**). Still, several options exist to obtain adequate mass spectra after separation, including off-line fractionation, alternative ionization, dilution of ESI-interfering compounds, or the change to volatile constituents, which are discussed critically in more detail in **manuscript III**.

However, all these options are a compromise between separation performance and sensitivity of mass spectrometric detection. Contrary, CE-CE-MS systems represent a promising alternative to overcome the aforementioned challenges, as they allow the use of existing methods with optimized separation performance in combination with sensitive mass characterization. In this regard, the development and application of such CE-CE-MS methods represents one of the core objectives of this work.

4.3 Time-of-flight mass analyzer

Time-of-flight (TOF) is considered the most straightforward concept of mass analyzers. Designs of first instruments have already been introduced in 1955 [58]. Still, due to the challenges regarding electronics and handling of large amounts of generated data TOF-MS instruments started to play a major role in the late 1980s [59] (pp. 126-142). In the TOF mass analyzer ions are accelerated into a field-free flight path and separated based on their different velocities. Hence, the electric potential energy (E_{el}) gained from the acceleration unit is converted to kinetic energy (E_{kin}) leading to equation 4.1:

$$e \cdot z \cdot U = E_{el} = E_{kin} = \frac{1}{2} \cdot m \cdot v^2 \quad (4.1)$$

E_{el}	:	electric potential energy
e	:	elementary charge
z	:	charge number
U	:	acceleration potential
E_{kin}	:	kinetic energy
m	:	mass of ion
v	:	velocity of ion

Since the velocity (v) is the quotient between the separation length (L) and time (t), it can be substituted accordingly and equation 4.1 can be solved for mathematical term of time resulting in the following connectedness:

$$t^2 = \frac{m}{z} \cdot \left(\frac{L^2}{2 \cdot e \cdot U} \right) \quad (4.2)$$

t : time to traverse the flight path

L : length of separation section

The time it takes for an ion to traverse the flight path is proportional to the square root of its mass-to-charge ratio (m/z). Consequently, the flight time is measured and converted to the respective m/z of the detected ion species. All other factors are either a natural constant (e) or kept constant as instrument parameters (L, U). Advantages of TOF-MS instruments include the following: (i) generation of mass spectra in micro-seconds, resulting in comparable high sensitivity; (ii) high mass accuracy (error < 5 ppm) and resolution ($R > 10000 m/\Delta m$); and (iii) a theoretical infinite mass range [60]. Therefore, TOF-MS instruments are well-suited for protein analysis.

4.4 Quadrupole mass analyzer

A quadrupole (Q) mass analyzer consists of four parallel aligned metal rods acting as electrodes. Alternating current (AC) and direct current (DC) voltages are applied between these rods in order to affect the trajectory of ions passing through [61]. For specific AC/DC settings only ions with a certain m/z ratio (mass window of ~ 1 Da) are able to pass the mass analyzer. By scanning the AC/DC settings for stable trajectories from low to high m/z ratios a mass spectrum of the desired m/z range is obtained. However, the scan rate and thus the generation of a full mass spectrum is rather slow compared to above-mentioned TOF-MS instruments. Nevertheless, the opportunity to select ions with a specific m/z ratio, referred to as selected ion monitoring, represents a big advantage of this type of mass analyzer. In addition, if only AC voltages are applied, which is called "radio frequency (RF) only" mode, the quadrupole acts as an ion guide enabling a broad m/z range to pass. For this reason, multipoles are oftentimes applied as mass filter, ion guides, or collision cells in other types of MS instruments [62].

4.5 Quadrupole time-of-flight mass spectrometer

The combination of Q- and TOF-MS technology represents one of the most successful types of MS instrumentation, especially for the analysis of protein samples. A scheme of the general setup of an electrospray ionization (ESI)-QTOF-MS instrument as applied in this thesis is depicted in Figure 10. First and foremost, through the entire ion path region (a-e) prior to the TOF section a DC potential cascade is applied guiding the desired type of ions (anions or cations) towards the orthogonal acceleration unit of the flight tube (f). The instrument is equipped with an ESI source (a), where the effluent of a hyphenated separation technique or the sample itself is nebulized and ionized. The generated ions enter the transfer capillary (b) through a narrow orifice. Remaining solvent is dried while traversing through the transfer capillary. In modern ESI-QTOF-MS instruments, ion funnels are applied directly after the transfer capillary section as part of the ion guides (c). Ion funnels are stacked ring electrodes with decreasing diameter in direction of the ion path [63]. Repulsive RF potentials are applied to adjacent electrodes, focusing the ions radially to the center of this ion guide. An additional DC gradient is used to route the ions through the funnel. Ion funnels exhibit higher transfer efficiencies compared to the previously applied ion skimmer technology. In addition, they enable the implementation of a vertical offset of the ion path, which is especially beneficial to remove remaining neutral molecules. Following the ion funnels is a multipole (hexa- or octupole) in RF only mode before entering the next section. The subsequent isolation Q (d) is either operated in RF only mode to function as a simple ion guide or used to isolate certain m/z species prior to the collision cell (e). The collision cell is typically another Q that is operated at higher pressures ($\sim 10^{-3}$ mbar) to fragment incoming ions by collision induced dissociation if desired.

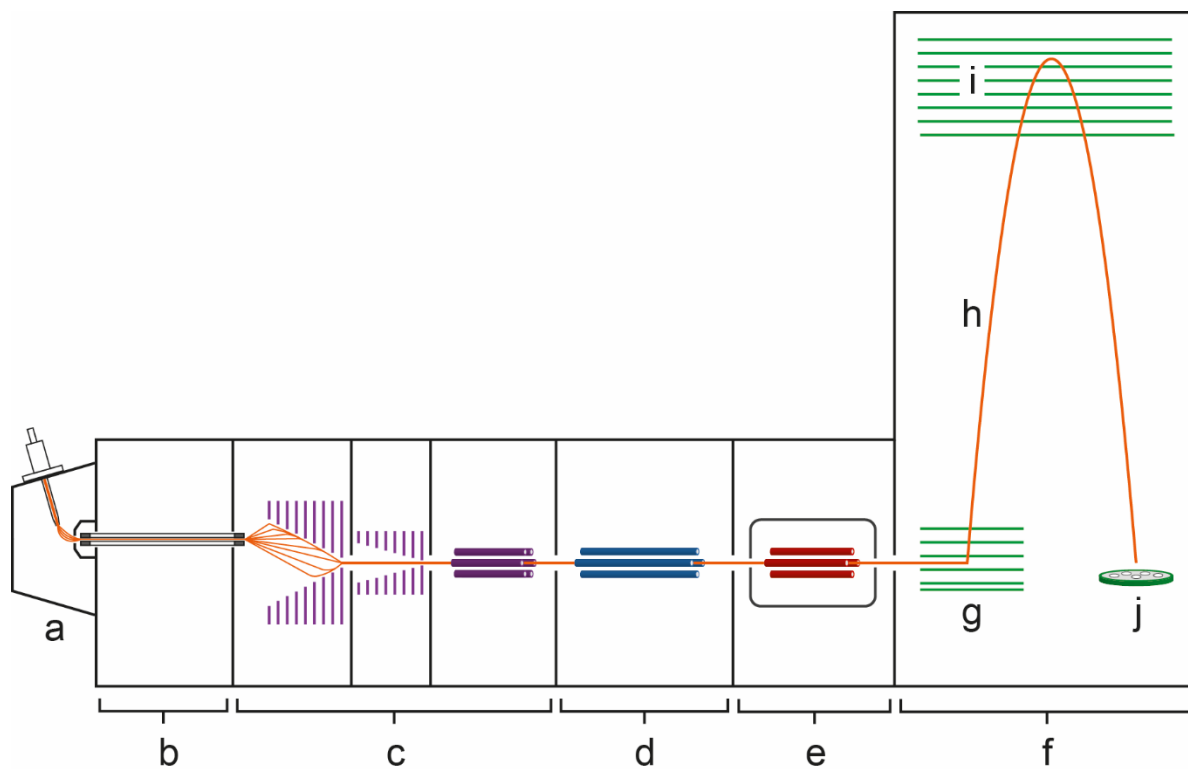


Figure 10: Scheme of ESI-QTOF-MS setup: Ions are generated by ESI (a), enter the instrument through the transfer capillary (b), and traverse the ion guides (c) towards the isolation Q (d) where a certain m/z species can be isolated if desired. The following quadrupole is operated at higher pressure and acts as collision cell (e) for potential fragmentation experiments before entering the orthogonal acceleration (g) into the field-free flight path (h). Ions are deflected vertically by the reflectron (i) and detected by a microchannel plate (j).

Afterwards, intact and/or fragment ions enter the flight tube (f) where they are accelerated orthogonally (g) into a field-free region (h) in a pulsed manner. Separation of ions in dependence of their m/z value takes place as described above. One issue of the pulsed orthogonal acceleration is that the kinetic energy is not absolutely the same for each ion, due to various factors such as the exact spatial position when the electric pulse is initiated. This results in a distribution of the flight time of ions having the same m/z , negatively affecting the obtainable resolution. Therefore, most modern QTOF-MS instruments possess a reflectron unit (i) on the opposite site to the orthogonal acceleration electrodes [64]. Reflectrons are comprised of stacked ring electrodes where increasing repulsing potentials are applied. Incoming ions penetrate the reflectron until their kinetic energy is nullified and get accelerated to the opposite direction towards the microchannel plate detector (j).

Conclusively, the reflectron setup provides two major advantages: (i) the separation path length is increased considerably and (ii) a correction of the flight time narrowing the kinetic distribution for each m/z species. Both of these characteristics result in improved resolution and mass accuracy. Nevertheless, ESI-QTOF-MS instruments need to be mass calibrated frequently (daily or weekly basis) to correct e.g. minor temperature fluctuations.

Due to their high mass accuracy and resolution, ESI-QTOF-MS systems are well-suited for the characterization of high-molecular weight species such as glycoproteins. In this context, the obtainable mass accuracy for mAbs (~ 150 kDa) was critically evaluated in **manuscript II**. In this work, an additional mass calibration of the developed CZE-CZE-MS method for mAb charge variant characterization was performed for each analysis by infusing via SL. In this way, the achievable mass accuracy and precision was even increased resulting in mass errors in the lower ppm range. A more detailed description can be found in the discussion section.

5 Ion mobility spectrometry based separation

A recent trend in the field of separation science represents the hyphenation of MS detection with preceding separation by ion mobility spectrometry (IMS) technology. IMS is an analytical technique that separates ions in the gas-phase based on their size-to-charge ratios as well as their interactions with buffer gas in an applied electric field [65]. Briefly, compact, highly charged molecules travel faster through an IMS cell than more extended, less charged ones. IMS can be considered the gas-phase equivalent of CE, where ions are separated in a similar way but in condensed phase. IMS bares the potential to separate structural isomers, conformers and even chiral components with high duty cycles. Since both IMS and MS require gas-phase ions and their duty cycles complement each other (IMS: ms; TOF-MS: μ s) they can be coupled successively in one instrument. These instruments are referred to as ion mobility mass spectrometers (IM-MS).

Although IMS is a relatively old analytical technique, first coupled to MS already in 1962 [66], it has become significantly more important in the last few years. This conclusion can be derived from the number of yearly publications related to IMS as illustrated in Figure 11 [67]. Among others, this development can be attributed to the

pioneering work of protein conformer separation demonstrated by Clemmer *et al.* [68]. Development and commercialization of novel instrumentation utilizing different IMS techniques coupled to MS has generated recent interest in the scientific community. Four general types of commercial IM-MS devices are distinguished: field-asymmetric ion mobility spectrometry mass spectrometry (FAIMS-MS), travelling wave ion mobility mass spectrometry (TWIM-MS), drift time ion mobility mass spectrometry (DTIM-MS), and the most recently introduced trapped ion mobility spectrometry mass spectrometry (TIMS-MS) [65, 69].

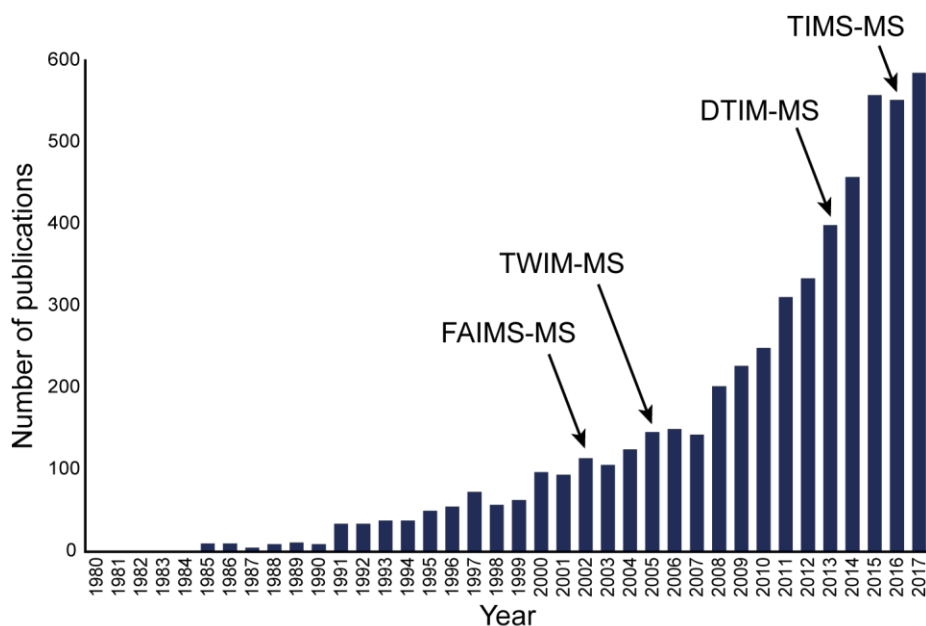


Figure 11: Number of peer-reviewed papers published annually. Data was generated using Web of Science with the search term "ion mobility spectrometry" [67]. The arrows mark the year the different IMS technologies were made commercially available.

5.1 Drift-tube ion mobility mass spectrometry

DTIM-MS instruments are the most straightforward concept of IMS technology. Ions are introduced into a drift tube, filled with a drift gas such as nitrogen. The drift tube consists of stacked ring electrodes, where a static uniform electric field is applied along the drift tube and guiding ions axially towards the MS detector [70].

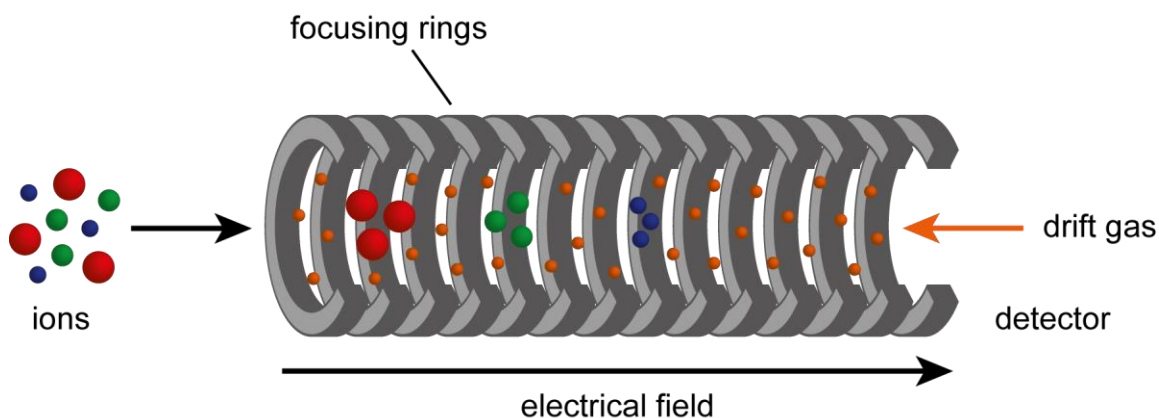


Figure 12: General principle of DTIMS. The DTIMS cell consists of stacked ring electrodes where a homogenous electric field is applied. It is filled with drift gas (e.g. N_2) streaming against the ion movement.

The drift velocity (v_d) of an ion traversing through the drift tube is directly related to its mobility (K) and the resulting electrical field (E) as expressed in the following equation:

$$v_d = K \cdot E \quad (5.1)$$

v_d : drift velocity
 K : mobility of ion

An important parameter of IMS in general is the so called “collisional cross section” (CCS). The CCS describes the averaged rotational area covered by a molecule depending on its size, charge and shape [70]. Ions with an elongated structure interact with drift gas molecules more frequently than ions with more compact structures, consequently leading to longer drift times. CCS (Ω) values are calculated based on the work of Mason and Schamp in 1958 [71] as illustrated in equation 5.2. However, there are certain limitations to this mathematical approach, since it can only be applied for lower electric fields typically between 5-100 V. This threshold is referred to as the “low field limit”. Nevertheless, DTIM-MS is the only ion mobility technique that allows the direct determination of CCS values.

$$\Omega = \frac{3ze}{16N} \left(\frac{2\pi}{\mu k_B T} \right)^{1/2} \frac{1}{K_0} \quad (5.2)$$

- Ω : collisional cross section
 N : number density of drift gas
 μ : reduced mass of ion-neutral drift gas pair
 k_b : Boltzmann constant
 T : drift gas temperature
 K_0 : reduced mobility (standard conditions)

In combination with its comparable high resolving power ($R > 100 \Omega/\Delta\Omega$), DTIM-MS is well-suited to obtain structural information about ions, e.g. folding conformations of proteins or isomer characterization of small molecules. In the past, DTIM-MS suffered from poor duty cycles, due to the dispersion of the ions during the transfer. In this particular case, duty cycles describe the percentage of ions that could be detected compared to those generated by the ionization source. Nevertheless, sensitivity has been considerably improved by the application of ion trapping funnels in front of the drift cell, which can accumulate ions prior to the injection into the drift cell [72].

6 Two-dimensional separation systems

Two-dimensional (2D) separations represent a powerful and common strategy for the analysis of complex samples by improving peak capacity, resolving power and separation efficiency compared to their one-dimensional (1D) counterparts [73]. In this context, two hyphenated analytical techniques should ideally possess orthogonal separation mechanisms in order to obtain maximum peak capacity [74]. A general aspect of 2D separation is that the solvent of fractions that are transferred from a 1st dimension needs to be compatible with the 2nd separation dimension. In the case of off-line 2D systems, fractions from a 1st separation dimension are collected and later injected individually to a 2nd dimension for further analysis [75]. Though these systems enable additional sample treatment in-between, e.g. buffer exchange, they are very time-consuming and labor-intensive. Furthermore, CE peak volumes are

typically in the low nL range but have to be collected at least in a few μL of solvent. Consequently, if CE effluent is collected off-line, high dilution factors need to be accepted.

A more elegant but at the same time more challenging approach is to hyphenate two analytical separation techniques directly, referred to as on-line coupling. First, pure chromatographic based separation techniques were on-line hyphenated, e.g. 2D gas chromatography or 2D LC and there exists a wide range of methods and applications [76, 77]. It is evident that the hyphenation of electrophoretic separation techniques is more complex due to their smaller dimensions and the application of electrical fields [73]. The most crucial step of an on-line 2D system represents the sample transfer from the 1st to the 2nd dimension. Three general strategies are distinguished as illustrated in Figure 13: (i) single heart-cut: “-” symbol, (ii) multiple heart-cut: “+” symbol, and (iii) comprehensive: “x” symbol [75].

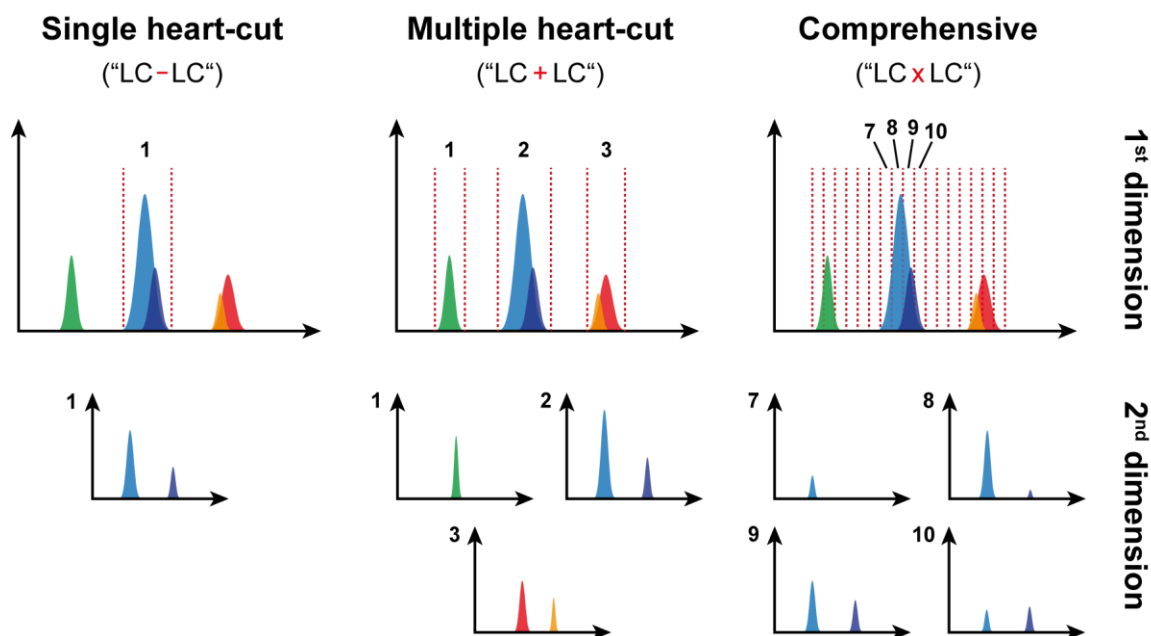


Figure 13: Overview of 2D transfer strategies: (i) single heart-cut, where only one fraction is transferred to the 2nd dimension; (ii) multiple heart-cut, where few fractions are forwarded; and (iii) comprehensive, where the entire first dimension is transferred fraction-wise.

Applying single heart-cut strategies, only one peak or fraction of the sample is transferred from the 1st to the 2nd separation dimension. Consequently, the separation time of the 2nd dimension is not limited, which allows to optimize the method for the

analyte of interest without run time restrictions in order to achieve best separation performance. Still, only a small fraction of sample can be analyzed per run. These methods are of particular interest if only few but difficult to separate analytes are characterized. In comprehensive 2D approaches, the entire 1st dimension is forwarded to the 2nd dimension at high sampling frequencies. As a result, the 2nd dimension needs to be considerably faster than the 1st dimension, oftentimes exhibiting method run times of less than a minute. This demand strongly restricts the options concerning combinations of separation techniques coupled in this way. Nevertheless, the entire sample is analyzed per run, e.g. applied for non-target analysis of complex samples. A compromise between these two strategies represents multiple heart-cutting by transferring few peaks or fractions of interest per 2D run.

6.1 CE-CE-MS

Besides the traditional idea behind 2D separation to improve resolution and separation efficiency, CE-CE-MS can be used to enable MS detection of samples previously separated in an ESI-interfering BGE as 1st dimension (see chapter 4.2). In general, it is possible to perform 2D CE in a single capillary without the need of an additional coupling device [78]. Hence, a first CE separation takes place until a majority of matrix left the capillary and the analyte of interest is located near the capillary outlet. Subsequently, the analyte is transported backwards and positioned again at the capillary inlet either by reversing the polarity or applying a hydrodynamic flow. The electrolyte is exchanged and the second CE separation is performed. Though this concept is technically straightforward, the coupling with MS is not possible due to the need of a (pressurized) outlet vial [75].

In the last years, various types of CE-CE interfaces were developed including, among others, dialysis membranes, porous junctions, tee-unions, flow gating, nicked-sleeve, hanging droplet interfaces, and mechanical valves described in more detail elsewhere [73, 75]. Thus far, only few CE-CE interfaces were applied in combination with MS detection, due to additional challenges such as (i) the lack of a (pressurized) outlet electrolyte reservoir. Flow gating types are not only the most frequently applied CE-CE interfaces in general, but were also implemented in CE-CE-MS setups by the Dovichi group [79, 80]. The general concept and principle of transverse flow gating interfaces is illustrated in Figure 14 A1. Two capillaries are positioned in a connector

device with a small gap in-between. A transverse liquid flow can be applied at the cross section. Heart-cut sample transfer takes place as shown in Figure 14 A2: Initially, the 1st dimension separation is performed while the transverse flow is switched on directing the effluent to waste (step 1). When an analyte of interest reaches the gap the transverse flow is switched off for injection (step 2).

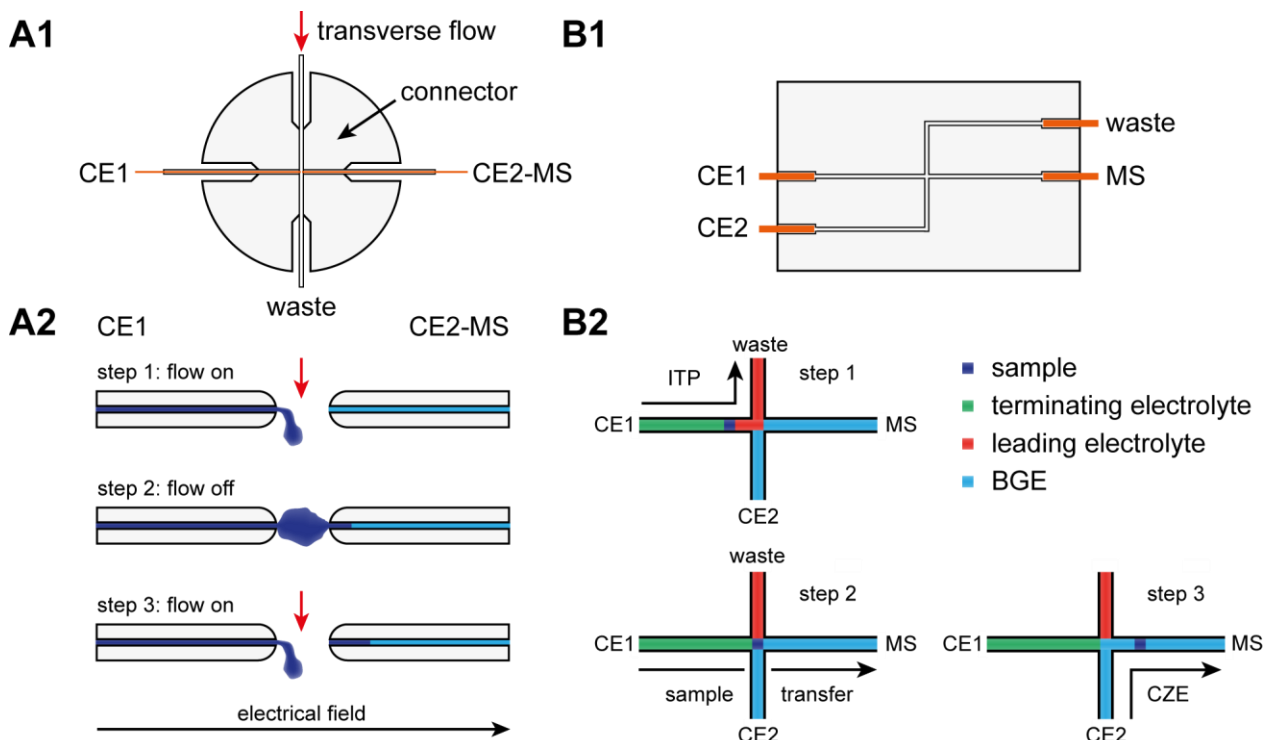


Figure 14: Generic designs and sample transfer process of transverse flow gating (A1, A2) and hybrid capillary microchip interface (B1, B2). A more detailed description can be found in the main text.

Due to the applied electrical field the analyte ions migrate towards the entrance of the 2nd dimension capillary. The transverse flow is switched on again after the injection is finished (step 3). Despite flow gating interfaces possess an elegant design and low dead volumes, the accurate amount of sample which is injected into the 2nd dimension usually cannot be determined and low transfer efficiencies are critical parameters. If the 2nd dimension is coupled to an MS instrument, coating procedures are often challenging to perform due to the missing (pressurized) outlet vial.

An alternative type of interface that was applied for CE-CE-MS represent hybrid capillary-microchip devices. A generic 2D setup including a typical cross-channel section is illustrated in Figure 14 B1. The microfluidic chip comprises 4 channels

converging at the cross-section. Capillaries are connected to the respective ports of the channels (e.g. by adherence) including the inlet of the 1st dimension (CE1), the inlet of the 2nd dimension (CE2), an outlet waste vial, and the capillary hyphenated to the MS instrument. In Figure 14 B2, sample transfer is exemplarily shown for isotachopheresis (ITP)-CZE-MS: An electrical field is applied between the CE1 inlet and the waste vial for ITP separation (step 1). When an analyte of interest reaches the cross-channel section the direction of the electrical field is changed (CE1 to MS) for injection to the CZE dimension (step 2). Subsequently, HV is applied between the CE2 inlet and the MS instrument to perform separation in the 2nd dimension towards the MS (step 3). Such a design was developed and applied for ITP-CZE-MS by the Huhn group [81, 82]. A critical part of this hybrid setup was the connection between the CE capillaries and the microfluidic chip, resulting in additional dead volumes and consequently peak broadening. In a consecutive study an advanced design was introduced using selective laser induced etching processes during manufacturing of the glass chips to create circular channels [83]. In addition, dead volumes of capillary connections could be reduced significantly. In this way, peak tailing/broadening was improved and demonstrated for the separation of L-arginine and L-lysine. Still, only ITP was performed as 1st dimension and thus other CE modes should be evaluated in further studies. Moreover, similar to flow gating interfaces, the 1st and 2nd dimension are not physical separated and transfer volumes cannot be determined accurately. Contrary, defined sample volumes can be transferred applying a mechanical valve as CE-CE interface. Furthermore, both dimensions are physically separated enabling independent operation e.g. rinsing or coating steps, which represents a great benefit especially if the 2nd dimension is coupled to MS detection (open system without an outlet vial). Mechanical 6-port-valves, traditionally utilized in LC, were applied to couple CIEF and capillary electrochromatography for the analysis of proteins and peptides [84, 85]. However, no MS detection was performed and rather large sample volumes (130 and 500 nL) were transferred from 1st to 2nd dimension, well-suited for CEC but too large for typical CZE.

In our working group, a mechanical 4-port-valve (VICI AG International: Schenkon, Switzerland) was tested as CE-CE interface for CE-CE-MS as illustrated in Figure 15 A [86]. This 4-port-valve consists of three major parts: (1) motor, (2) rotor comprising a 20 nL sample loop, and (3) stator including four capillary connections. Rotor and

stator are manufactured from polymer material (Valcon E®, PEEK/PTFE composition). The general concept of heart-cut sample transfer is illustrated in Figure 15 B. During separation in the 1st dimension the valve is kept in loading position, where the sample loop is connected to the inlet of a CE instrument (CE1) and the outlet is placed in a grounded external vial (EV) filled with BGE. An external UV detector is positioned a few cm in front of the valve in order to determine the correct time when an analyte of interest is located in the center of the sample loop. A more detailed description of this procedure can be found in the discussion section. Subsequently, the voltage in the 1st dimension is turned off and the valve is switched to inject position. Consequently, the sample loop is connected to the inlet of the second CE instrument (CE2) and the MS instrument. HV is applied in the 2nd dimension and separation takes place. Preliminary results were achieved indicating the promising perspective of this approach [86]. Hence, a simple phosphate based BGE was utilized as 1st CZE dimension for the separation of peptides to demonstrate the general functionality of the 4-port valve as CE-CE interface. In this case, a similar separation could be achieved using a volatile BGE system. Consequently, real applications still have to be developed, especially using more challenging BGEs as 1st separation dimension.

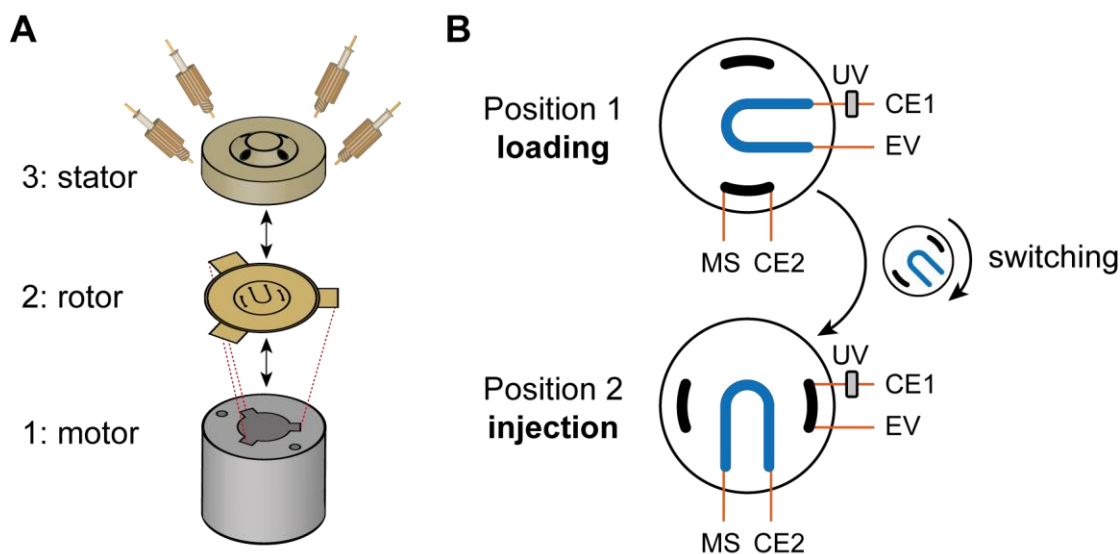


Figure 15: (A) Scheme of mechanical 4-port valve consisting of three major part: (1) motor, (2) rotor incorporating a sample loop, and (3) stator including capillary connections. (B) General principle of heart-cut sample transfer including loading and injection positions. A more detailed description can be found in the main text.

Moreover, the 2D setup needs to be improved further, including e.g. implementation of precise heart-cutting procedures. These two aspects were the first core objective of the presented thesis. Applications developed during this project include the characterization of degradation products of small pharmaceuticals (**manuscript I**), as well as the in-depth MS characterization of mAb charge variants (**manuscript II**). In addition, all CE-CE-MS setups and applications developed in our working group related to the aforementioned 4-port valve were summarized and critically discussed in a trend article (**manuscript III**).

6.2 LC-CE-MS

LC-CE-MS systems are expected to possess high separation efficiency for a wide range of molecules, including the analysis of intact glycoproteins in complex biological samples [87]. In this context, the hyphenation of RPLC (hydrophobic interaction) and CZE (electrophoretic mobility) is of particular interest, since these two techniques possess nearly orthogonal separation mechanisms. In addition, LC-CE-MS benefits from the larger injection volumes of LC systems compared to traditional CE-MS, potentially resulting in improved sensitivity. For an adequate hyphenation of LC and CE technology certain demands need to be fulfilled: (i) compatibility of LC and CE conditions including flow rates, geometries and eluent constitution (ii) transfer of LC peaks in the low to mid-nL range, and (iii) electrical insulation required in CE.

Online coupling of chromatographic and electrophoretic separation with optical detection was pioneered by the Jorgenson group using a grounded 6-port valve in the early 90's [88, 89]. Nonetheless, a majority of the sample of the LC dimension was lost due to the large transfer volumes (sample loop: 10 μ L), whereby only a minor fraction could be injected into the CZE dimension. Yet, in a majority of works flow gating types of LC-CE interfaces have been applied in a similar fashion to CE-CE coupling described in the previous chapter [87]. However, as stated before, these interfaces are often difficult to combine with MS e.g. considering coating procedures of the CE dimension or the desire to have complete independent operation of both separation dimensions. Due to the aforementioned challenges, only a couple of studies have been published performing LC-CE-ESI-MS [90–94]. In 1997, Jorgenson *et al.* demonstrated the application of a classical transverse flow gating interface for the analysis of tryptic peptides [90]. Based on the application of capillary RPLC (flow

rate: 15 $\mu\text{L}/\text{min}$) as 1st dimension in combination with the flow gating interface, only a minor fraction of sample could be transferred to the 2nd dimension. Bergström *et al.* developed a modified version of a flow gating interface which exhibited reduced dead volumes and a simplified fabrication process [91, 92]. Still, the general characteristics remained the same and no follow-up work has been published since 2006. The Ramsey group demonstrated LC-CE-MS using microfluidic devices. [93, 94]. Microfluidic chips provide unique characteristics, such as near-zero dead volume connections and potentially exceptional fast CE separations. Nevertheless, these systems are less flexible and individual separation dimensions are not physically separated as addressed in chapter 6.1.

The aforementioned mechanical 4-port valve represents an interesting alternative as LC-CE interface coupled to subsequent MS detection, allowing the application of nanoRPLC as 1st dimension, perfectly matching the geometries of subsequent CZE-MS analysis. Furthermore, the auspicious analysis of intact proteins by LC-CE-MS has not been described in the literature up to date. Therefore, the development and application of a nanoRPLC-CZE-MS system for intact glycoprotein analysis was the second core objective of the presented thesis. Results of a proof-of-concept study can be found in **manuscript IV**.

6.3 CE-IM-MS

As addressed in chapter 5.1, the combination of separation based on electrophoretic mobility in the liquid (CE) and gas phase (IM-MS) highlighted in a recent trend article is highly auspicious [95]. Yet, this interesting topic was covered in only few studies [96]. CE was hyphenated with FAIMS-MS [97] and TWIM-MS [98, 99]. However, in these works IMS was not particularly applied as additional separation dimension but more to reduce spectral noise (FAIMS) or to gain information about enzyme kinetics (TWIM-MS). Preliminary attempts to perform CE-DTIM-MS were carried out in the late 80's by the Hill group analyzing model substances such as caffeine [100]. However, spray instability was a common issue and hindered its further application at that time. Thus far, the orthogonality of CE and IM-MS has not been evaluated carefully.

In the last decade, IM-MS based approaches such as DTIM-MS have been particularly useful for the analysis of released glycans, including isomer characterization [101].

Nonetheless, there is still room for improvement regarding peak capacity and separation efficiency especially considering larger glycan structures. In some cases, the combination of LC and IM-MS technology was applied to gain an additional separation dimension [96, 102]. However, considering the high polarity of glycans, RPLC is not well-suited for their separation and more adequate LC modes such as ion exchange chromatography still need to be examined in detail considering the hyphenation to IM-MS. In this context, CE-IM-MS represents an interesting and auspicious alternative to improve separation capabilities which has not been investigated for glycan analysis thus far [95]. A CZE-DTIM-MS method was developed for the characterization of released native and derivatized *N*-glycans as described in detail in **manuscript V**.

Objectives

Demands imposed on analytical techniques are constantly increasing. In this regard, CE hyphenated to MS technology is becoming more and more important, especially for the analysis of proteins in a biological and/or pharmaceutical context. This is mainly due to the separation mechanism of CE based on the electrophoretic mobility of ions in liquid phase, which is ideal e.g. for separating proteins with minor structural differences. However, certain limitations are associated with CE-MS analysis including the following: (i) many CE methods are highly ESI-interfering and thus usually restricted to optical detection. Nevertheless, these electrolyte systems are essential to achieve the required selectivity leading to sufficient separation performance. (ii) Sensitivity in CE-MS is often limited, attributed to a major extend to the minor injection volumes (few nL) in standard CE analysis. (iii) Though often exhibiting high separation efficiency, the selectivity and peak capacity of CE-MS is not sufficient in particular cases, e.g. considering complex protein samples. In this regard, multidimensional separation techniques coupled to MS represent an auspicious approach to overcome these challenges. The thesis can be divided into three major parts:

1) The first and main part of this thesis is dedicated to development and application of a fully functional CZE-CZE-MS system utilizing a mechanical 4-port valve as CE-CE interface based on previous works in our group [86]. Hence, the focus is set to enable MS characterization of analytes priorly separated in validated and routinely applied ESI-interfering electrolyte systems (1st dimension) ranging from small molecules to intact proteins such as mAbs (**manuscript I to III**).

2) The application of the aforementioned 4-port valve interface for the hyphenation nanoLC and CZE-MS technology should be investigated for two main reasons: (i) utilizing the increased injection volumes of the nanoLC system (up to few μL) to increase sensitivity compared to traditional CE-MS, and (ii) improvement of separation performance for protein analysis by benefiting from the combination of both, selectivity of chromatography and electrophoresis (**manuscript IV**).

3) The detailed evaluation of the combination of CZE and DTIMS-MS as an alternative multidimensional approach to take advantage of electrophoretic mobilities in the liquid and gas-phase. This method is of particular interest for the characterization of protein (e.g. mAb) glycosylation (**manuscript V**).

List of manuscripts

Manuscript I

S. Neuberger, K. Jooß, C. Ressel, C. Neusüß (shared first author)

Quantification of ascorbic acid and acetylsalicylic acid in effervescent tablets by CZE-UV and identification of related degradation products by heart-cut CZE-CZE-MS

Analytical and Bioanalytical Chemistry (2016) 408(30):8701-8712

Manuscript II

K. Jooß, J. Hühner, S. Kiessig, B. Moritz, C. Neusüß (paper in forefront)

Two dimensional capillary zone electrophoresis-mass spectrometry for the detailed characterization of intact monoclonal antibody charge variants, including deamidation products

Analytical and Bioanalytical Chemistry (2017) 409(26):6057-6067

Manuscript III

J. Schlecht, K. Jooß, C. Neusüß

Two-dimensional capillary electrophoresis-mass spectrometry (CE-CE-MS): coupling MS-interfering capillary electromigration methods with mass spectrometry

Analytical and Bioanalytical Chemistry (2018) 410(25):6353-6359

Manuscript IV

K. Jooß, N. Scholz, J. Meixner, C. Neusüß

Heart-cut nanoLC-CZE-MS for the characterization of proteins on the intact level

Electrophoresis (2018) DOI: 10.1002/elps.201800411

Manuscript V

K. Jooß, S. W. Meckelmann, J. Klein, O. J. Schmitz, C. Neusüß (paper in forefront)

Capillary zone electrophoresis coupled to drift tube ion mobility-mass spectrometry for the analysis of native and APTS-labeled N-glycans

Analytical and Bioanalytical Chemistry (2018) DOI: 10.1007/s00216-018-1515-7

I. Setup of CZE-CZE-MS system and first application to small pharmaceuticals

Quantification of ascorbic acid and acetylsalicylic acid in effervescent tablets by CZE-UV and identification of related degradation products by heart-cut CZE-CZE-MS

S. Neuberger, K. Jooß, C. Ressel, C. Neusüß (shared first author)

Analytical and Bioanalytical Chemistry (2016) 408(30):8701-8712

A CZE-UV method was developed and validated for the simultaneous quantification of acetylsalicylic acid (ASA), ascorbic acid (ASC) and related degradation products in effervescent tablets. Due to the highly ESI-interfering BGE (100 mM tricine, pH = 8.8) a direct coupling to MS was not possible. Therefore, the first fully functional CZE-CZE-MS system, utilizing a mechanical 4-port valve as CZE-CZE interface, was developed to enable mass spectrometric characterization of the observed degradation products. In this context, a generally applicable hydrodynamic heart-cut strategy was implemented for sample transfer from the 1st to the 2nd CZE dimension. Besides the initial real application of CZE-CZE-MS utilizing the 4-port valve interface, relevant degradation products originating from the combination of ASA and ASC (one- and twofold acetylation of ASC by ASA) could be identified. These degradation products have not been described in the literature up to this point.

Candidate's contribution:

Planning of validation and degradation study experiments and (statistical) data evaluation considering the CZE-UV method. Development of the CZE-CZE-MS setup, especially the hydrodynamic heart-cut sample transfer strategy, which consequently lead to a functional 2D system. Performance of CZE-CZE-MS experiments, data evaluation, literature search and preparation of manuscript was divided equally between S. Neuberger and myself.

RESEARCH PAPER

Quantification of ascorbic acid and acetylsalicylic acid in effervescent tablets by CZE-UV and identification of related degradation products by heart-cut CZE-CZE-MS

Sabine Neuberger¹ · Kevin Jooß¹ · Christian Ressel¹ · Christian Neusüß¹Received: 12 April 2016 / Revised: 16 June 2016 / Accepted: 21 June 2016 / Published online: 12 July 2016
© Springer-Verlag Berlin Heidelberg 2016

Abstract Capillary electrophoresis is commonly applied for the analysis of pharmaceutical products due to its high separation efficiency and selectivity. For this purpose, electrospray-ionization-(ESI)-interfering additives or electrolytes are often required, which complicates the identification of impurities and degradation products by mass spectrometry (MS). Here, a capillary zone electrophoresis (CZE) method with ultraviolet (UV) absorption detection for the simultaneous determination and quantification of ascorbic acid and acetylsalicylic acid in effervescent tablets was developed. Related degradation products were identified via CZE-CZE-MS. Systematic optimization yielded 100 mM tricine (pH = 8.8) as appropriate background electrolyte, resulting in baseline separation of ascorbic acid, acetylsalicylic acid, and related anionic UV-active degradation products. The CZE-UV method was successfully validated regarding the guidelines of the Food and Drug Administration. The validated method was applied to trace the degradation rate of the active pharmaceutical ingredients at defined ambient conditions. A heart-cut CZE-CZE-MS approach, including a 4-port-nL-valve, was performed for the identification of the observed degradation products. This 2D setup enables a precise cutting of accurate sample volumes (20 nL) and the independent operation of two physically separated CZE dimensions, which is especially

beneficial regarding MS detection. Hence, the ESI-interfering tricine electrolyte components were separated from the analytes in a second electrophoretic dimension prior to ESI-MS detection. The degradation products were identified as salicylic acid and mono- and diacetylated ascorbic acid. This setup is expected to be generally applicable for the mass spectrometric characterization of CZE separated analytes in highly ESI-interfering electrolyte systems.

Keywords Two-dimensional separation · Mechanical valve · Capillary zone electrophoresis-mass spectrometry · Interference-free electrospray-ionization · Interface

Abbreviations

AA	Ascorbic acid
APIs	Active pharmaceutical ingredients
ASA	Acetylsalicylic acid
BGE	Background electrolyte
CE	Capillary electrophoresis
CEC	Capillary electrochromatography
CIEF	Capillary isoelectric focusing
CZE	Capillary zone electrophoresis
DHAA	Dehydroascorbic acid
DKG	2,3-Diketogulonic acid
EOF	Electroosmotic flow
ESI	Electrospray-ionization
HPLC	High-performance liquid chromatography
IS	Internal standard
LOD	Limit of detection
MS	Mass spectrometry
NSA	2-Naphthalenesulfonic acid
PVA	Poly(vinyl alcohol)
RSD	Relative standard deviation
S/N	Signal-to-noise

Published in the topical collection *Fundamental Aspects of Electromigrative Separation Techniques* with guest editors Carolin Huhn and Pablo A. Kler.

Sabine Neuberger and Kevin Jooß contributed equally to this work.

✉ Christian Neusüß
Christian.Neusuess@hs-aalen.de

¹ Faculty of Chemistry, Aalen University, Beethovenstraße 1,
73430 Aalen, Germany

SA	Salicylic acid
SL	Sheath liquid

Introduction

Acetylsalicylic acid (ASA), also referred as aspirin, represents one of the most commonly applied substances in pharmaceutical formulations. ASA shows analgesic and antipyretic properties and can be utilized as an anti-inflammatory agent. In addition, it is prescribed as painkiller for moderate types of pain. However, there are known adverse reactions associated with ASA intake, including gastric bleeding or the formation of gastrointestinal ulcers [1]. Since these serious consequences are caused by the release of oxygen radicals during the ASA metabolism, ascorbic acid (AA), known as vitamin C, is added to ASA in many formulations. In this way, the analgesic and antipyretic effect of ASA is combined with the antioxidant property of AA. Appropriate storage conditions are of great importance, in order to fulfill the quality requirements of pharmaceutical products. The active pharmaceutical ingredients (APIs) of ASA effervescent tablets, including AA, degrade relatively fast, if the samples are exposed to oxygen and/or humidity. This could be caused by, e.g., inappropriate storage or manufacturing conditions [2, 3].

In order to ensure the high quality of commercial medicines, it is necessary to analyze these pharmaceutical products, including the identification and quantification of the APIs and related degradation products. Spectroscopic techniques, such as UV/VIS [4–6] and Raman Spectroscopy [7], are often applied for the determination of AA and/or ASA in pharmaceuticals. However, the data interpretation requires elaborate statistical data evaluation and a clear identification of degradation products is difficult. During the last years, several methods based on high-performance liquid chromatography (HPLC) have been developed for the simultaneous determination of ASA and AA in pharmaceutical products [8–14]. Thomis et al. [12] demonstrated the first HPLC-UV approach, which enables the concurrent quantification of ASA, AA and their main degradation products in tablets within 35 min. However, two of the observed degradation products were not baseline separated and could not be clearly identified by HPLC-UV. Up to this point, only Wabaidur et al. [13] performed HPLC-mass spectrometry (MS) for the simultaneous quantification of AA and ASA in effervescent tablets, achieving a remarkable fast separation within 2 min. Nevertheless, no degradation products were analyzed in this approach. AA and ASA are small polar organic molecules, which are dissociated to a large extent in solution at neutral or basic pH. Thus, capillary zone electrophoresis (CZE) provides a promising approach as separation technique for these kinds of analytes. CZE represents a rather simple system setup with low reagent and sample consumption, often combined with a minimum of

sample pretreatment. Koh et al. [15] developed a CZE-UV method for the quantitative analysis of AA in fruit beverages and biological fluids with minor sample preparation, utilizing a tricine-based background electrolyte (BGE) system. Later on, AA was determined by CZE [16, 17] or micellar electrokinetic chromatography [17]. Wei et al. [18] demonstrated a CZE-UV method for the determination of ASA by using β -cyclodextrine as additive in a phosphate based BGE. Marra et al. [19] separated ASA and salicylic acid (SA) with a 20 mM tris(hydroxymethyl)aminomethane buffer at pH 8.4 by adding 10 mM 3,4-dimethoxycinnamate. In conclusion, a variety of complex BGE systems have been applied for the determination of ASA or AA. To the best of our knowledge, there is no work published applying an electromigrative separation technique for the simultaneous determination of ASA and AA, neither by UV nor MS detection. Moreover, no identification via MS of related degradation products separated by electromigrative techniques was reported up to date.

In order to ensure a stable ionization, prevent ion suppression of the electrospray-ionization (ESI) process and contamination of the MS, nonvolatile electrolytes and additives should be avoided applying capillary electrophoresis-mass spectrometry (CE-MS) [20]. However, these ESI-interfering substances are often required to achieve sufficient selectivity. Therefore, different concepts for the hyphenation of nonvolatile CE methods with MS detection by multidimensional electrophoretic separation techniques have been tested and evaluated in recent years [21–23]. One possible approach represents the offline hyphenation of two CE systems by fraction collection between the separation dimensions. Nevertheless, the collection of the low CE effluent is associated with high dilution of the desired analytes [22, 24]. In order to realize an online hyphenation of two electromigrative separation techniques special coupling techniques are required, due to the small volumes and strong electrical fields in CE. In general, the online hyphenation of two CE systems can be carried out by utilizing different types of interfaces [21–23]: The Cottet group introduced a heart-cut 2D-CE in a single capillary approach [25, 26], which later on was pursued by the Quirino group [27, 28]. Several sophisticated flow gating interfaces based on the original work from Jorgenson et al. [29] have been developed in recent years [30–32], which are in general compatible with MS detection. However, compared to flow gating interfaces, accurate sample volumes can be transferred to the 2nd dimension applying a mechanical valve. Moreover, both dimensions are physically separated allowing individual operation, e.g. rinsing or coating, which represents a great benefit especially if the 2nd dimension is coupled to MS detection (open system without an outlet vial). Zhang et al. [33] and Wei et al. [34] demonstrated the online coupling of capillary isoelectric focusing (CIEF) with capillary electrochromatography (CEC) for the analysis of proteins

and peptides applying a mechanical 6-port-valve. Hence, rather large sample volumes (>100 nL) were transferred from the 1st to the 2nd dimension, which is well-suited for chromatographic-based 2nd dimensions. Recently, we introduced a proof of concept using a mechanical valve with a sufficiently small volume for CZE-CZE-MS [35]. Hence, a cationic model system (protein digest) was separated in a phosphate-based electrolyte system in the 1st dimension and transferred to a volatile 2nd separation dimension coupled to MS.

In this work, a CZE-UV method was developed and validated for the simultaneous quantification of ASA and AA and related degradation products. The CZE-UV method was applied for a degradation study of ASA + AA effervescent tablets to demonstrate the capability to trace changes of the APIs. In order to identify the observed degradation products, the ESI-interfering tricine-based CZE-UV system was online hyphenated to CZE-ESI-MS using a mechanical 4-port-valve. With this heart-cut 2D setup it was possible to identify all anionic components separated and observed in the CZE-UV approach. The applicability of this CZE-CZE-MS system to separate ESI-interfering substances prior to MS detection is discussed.

Materials and methods

Materials

Methanol, 2-propanol (all ROTISOLV® ≥99.95 %, LC-MS grade), ammonia (ROTIPURAN® 30 %, p.a., ACS), ammonium acetate (≥97 %, p.a.), ammonium hydrogen carbonate (≥99 %, p.a.), formic acid (ROTIPURAN® ≥98 %, p.a., ACS), and acetic acid (ROTIPURAN® 100 %, p.a.) were purchased from Carl Roth (Karlsruhe, Germany) and used without further purification. Acetylsalicylic acid (≥99 %, p.a.), L-ascorbic acid (reagent grade), salicylic acid (≥99 %, p.a.), glutaraldehyde solution (50 % in H₂O, suitable for photographic applications), 2-naphthalenesulfonic acid (technical grade, 70 %), and poly(vinyl alcohol) (≥99 %, average MW 89,000 – 98,000) were received from Sigma-Aldrich (Steinheim, Germany). Tricine was purchased from Alfa Aesar (Karlsruhe, Germany). Sodium hydroxide (p.a.), hydrochloric acid (37 %, p.a.), boric acid (p.a.), and sodium dihydrogen phosphate (pure) were purchased from Merck (Darmstadt, Germany). Ultrapure H₂O of an electrical resistivity >18 MΩcm was supplied by an UltraClear UV system (Siemens water technologies, Günzburg, Germany) and was used for the preparation of all samples, rinsing solutions and background electrolytes (BGEs). Fused silica capillaries (50 μm inner diameter, 363 μm outer diameter) were obtained from Polymicro Technologies (Phoenix, AZ, USA).

Different BGE solutions were prepared: 25 mM boric acid (pH 6 and 9) and 25 mM sodium dihydrogen phosphate (pH 6 and 9), pH values were adjusted with 4 M NaOH; 25 mM ammonium acetate (pH 6, 7, 7.5 and 9) and 25 mM ammonium hydrogen carbonate (pH 9), pH values were adjusted with 30 % ammonia; 25 mM ammonium formate (pH 6 and 9) was prepared by mixing formic acid and 30 % ammonia, pH values were adjusted with 30 % ammonia; and 25, 50, 100, and 200 mM tricine, pH 8.8 was adjusted with 4 M NaOH.

Effervescent tablets (ASS + C - ratiopharm®) with an amount of 600 mg ASA and 200 mg AA (vitamin C) were obtained from ratiopharm (Ulm, Germany). The tablets contained adipic acid, sodium bicarbonate, citric acid, sodium dihydrogen citrate, povidon (K25), lemon flavor, and sodium saccharin as excipients. Prior to the CZE-UV measurements, the effervescent tablets were dissolved in 80 mL internal standard (IS) solution (2-naphthalenesulfonic acid (NSA) with a concentration of 70 mg/L) and further diluted to desired concentrations. For the CZE-CZE-MS measurements, the effervescent tablets were dissolved in 80 mL ultrapure H₂O (initial concentration: 7500 mg/L ASA and 2500 mg/L AA). Afterwards, the solutions were sonicated for 10 min to degas the samples. All samples and standards were measured directly after preparation or stored at -20 °C.

For the degradation study, 18 effervescent tablets (ASS + C - ratiopharm®) were stored in a desiccator placed in an incubator (30 °C) for 72 h. In this way, the tablets were shielded from the laboratory atmosphere. In order to simulate a realistic degradation occurring during storage at inappropriate conditions, e.g. outside of the original packaging, the tablets were stored intact and not grinded for the degradation study. The relative humidity (RH) was adjusted to 75 % by using a supersaturated solution of sodium chloride filled in the desiccator. The RH was monitored via a thermo-hygrometer (Albert Mebus GmbH & Co. KG, Haan, Germany) during the whole storage period. Two tablets were taken out after 1, 3, 6, 9, 12, 24, 36, 48, and 72 h, respectively; each was solved in 250 mL NSA (70 mg/L) and subsequently measured via CZE-UV. Two freshly unpacked effervescent tablets were analyzed directly to obtain data of a 0 h storage period.

CZE-UV

CZE-UV measurements were performed on an HP ^{3D}CE electrophoresis instrument from Agilent (Agilent Technologies, Waldbronn, Germany) using capillaries with an inner diameter of 50 μm and a total length of 50 cm. New bare fused silica capillaries were preconditioned by flushing (approximately 1 bar) with methanol (5 min), H₂O (5 min), 1 M NaOH (20 min), H₂O (5 min), and BGE (10 min). In addition, in order to ensure a constant electroosmotic flow (EOF) the capillary was reconditioned every 10–15 runs by flushing with H₂O

(3 min), 1 M NaOH (10 min), H₂O (3 min), and BGE (5 min). In the final CZE-UV method, the BGE was composed of 100 mM tricine at pH 8.8. The pH of the BGE was adjusted with 4 M NaOH. Prior each sample injection, the capillary was flushed with BGE for 4 min. Samples were injected hydrodynamically (50 mbar, 12 s), followed by dipping the capillary into a H₂O vial in order to prevent contamination of the BGE. A constant voltage of +20 kV was applied during separation, resulting in a typical current of 42–44 μ A. The sample tray was cooled down to 10 °C, in order to prevent degradation of the sample during storage in the equipment. Due to the short analysis time, an additional cooling of the capillary was abstained and it was kept at 25 °C. Analytes were detected using a diode array detector at a wavelength of 220 nm for ASA and 270 nm for AA.

CZE-CZE-MS

An online hyphenation of an ESI-interfering CZE-UV system with a CZE-MS approach was realized by implementing a mechanical 4-port-valve as interface in between the separation dimensions. Both electrophoretic dimensions and the 4-port-valve interface are described individually in the following sections:

First dimension - CZE-UV

The CZE measurements applying UV detection in the 1st dimension was performed using a Beckman Coulter PA 800 plus CE system (Beckman Coulter, Krefeld, Germany). The same electrolyte system (100 mM tricine, pH 8.8) as for the 1D CZE-UV experiments was utilized. A 55 cm long bare-fused silica capillary was preconditioned as described above for the 1D approach. Afterwards, the capillary was cut into two parts and connected via a 4-port-valve. The first part between the CE inlet and the valve was 35 cm long, possessing a window at a distance of 4.5 cm in front of the valve. An external UV detector from J&M Analytik AG (Essingen, Germany), which enables the detection of the different analytes at 220 and 270 nm, was positioned at the capillary window. This results in a total distance of 5.0 cm from the detection window to the center of the valve. The second part of the capillary located between the valve and the external outlet vial was 20 cm long. In contrast to our proof of concept study [35] the implemented external outlet vial resulted in a shorter total capillary length of 55 cm for the 1st dimension, which is in the typical range for standard CE applications. Prior to each run, the capillary was rinsed with BGE for 10 min. Samples were injected hydrodynamically (50 mbar, 12 s). The injection was followed by a H₂O dipping step. A high voltage of +7.5 kV was applied for separation. A grounded ampere meter was placed inside the external outlet vial of the 1st dimension, acting as counter electrode. By

comparison of the currents measured at each electrode, it was possible to monitor the stability of the current through the system.

Mechanical 4-port-valve

A microinjector 4-port-valve with an internal 20 nL sample loop, including the rotor and stator made out of polymer material (Valcon E®, PTFE/PEAK composition), was purchased from VICI AG International (Schenkon, Swiss). The 4-port-valve consists of 3 parts: the stator, the rotor comprising the 20 nL loop, and the motor. A detailed description of the general valve design can be found elsewhere [35]. Briefly, the capillaries of the 1st and 2nd dimension were connected with 4 junctions to the stator via finger tight screws. The inlet and outlet capillary of the 1st dimension were connected to the valve at position S and W, respectively (see Fig. 1a). The inlet and outlet capillary of the 2nd dimension were connected to the valve at position P and C, respectively. The stator, rotor, and motor were pushed tight together via two screws, in order to avoid leakages during the measurements. During the 1st dimension, the mechanical valve was kept in Position 1 (Loading), connecting the sample loop (20 nL) to channel S and W (see Fig. 1b). The separation was stopped when the analyte reached its peak in the UV detector. Subsequently, low pressure (50 mbar) was applied to transport the analyte into the sample loop followed by switching the valve to Position 2 (Injection). In this way, the sample loop was connected to channel P and C. The analyte was pushed (50 mbar, 30 s) into the 2nd dimension towards the MS detector. Prior to the separation in the 2nd dimension, the valve was switched back to Position 1.

Second dimension - CZE-MS

The CZE-MS analysis was performed with an HP ^{3D}CE electrophoresis instrument from Agilent (Agilent Technologies, Waldbronn, Germany) using poly(vinyl alcohol) (PVA)-coated capillaries with an inner diameter of 50 μ m and a total length of 121 cm. The capillary was cut into two parts: The inlet part, between CE instrument and valve, was 52 cm and the second part, between valve and ESI interface, was 69 cm long, respectively. The PVA coating was performed in-house as follows, based on a method from Xu et al. [36]. The capillary was flushed with MeOH for 20 min, H₂O for 20 min, 1 M NaOH for 120 min, and H₂O for 20 min and dried with air (approximately 5 bar) for 20 min. Afterwards, the capillary was rinsed (approximately 5 bar), first with glutaraldehyde solution (3.25 pM in 1.21 M HCl) followed by PVA solution (45 mg/mL in 0.6 M HCl) for 5 min. Finally, the capillary was dried (approximately 5 bar) with air at 100 °C for 130 min in an LC oven. The BGE consisted of 25 mM ammonium acetate at pH 6. The capillaries were flushed prior to each measurement for

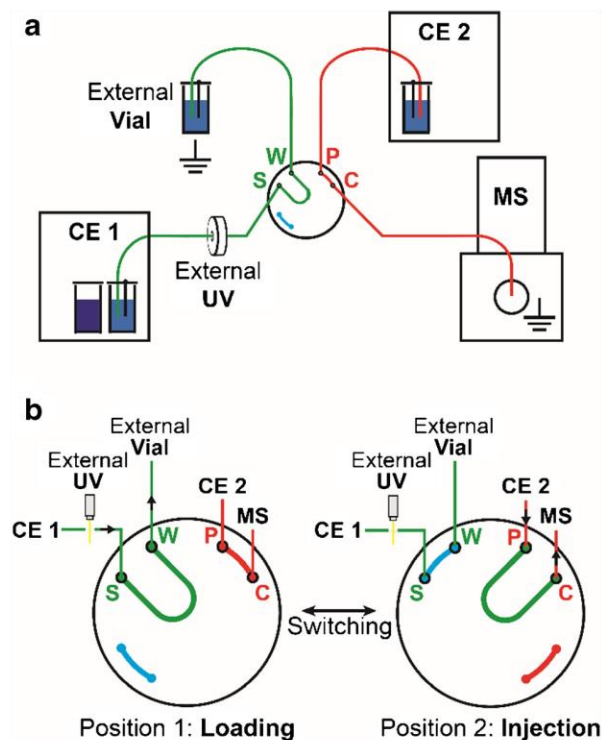


Fig. 1 Scheme of the complete 2D setup (a): The inlet (CE 1) and outlet capillary (external vial) of the 1st dimension are connected to channel S and W of the 4-port-valve, respectively. An electrode is placed in the external vial for grounding. An external UV detector cell is positioned 4.5 cm in front of the valve through the inlet of the 1st dimension. In the 2nd dimension the inlet (CE 2) and outlet capillary (MS) are connected to channel P and C of the 4-port-valve, respectively. Scheme of the switching of the rotor located in the applied 4-port-valve (b): During the 1st dimension the mechanical valve is kept in Position 1 (Loading), where the sample loop (20 nL) is connected to channel S and W. When the desired analyte is located in the sample loop, the valve is switched to Position 2 (Injection) in order to transfer the sample from the 1st in the 2nd dimension. In this way, the sample loop is connected to channel P and C. Subsequently, the analytes are flushed (50 mbar, 30 s) into the 2nd dimension towards the MS detector. Prior to the separation in the 2nd dimension, the valve is switched back to Position 1

10 min with BGE. The CZE analyses were performed applying a constant separation voltage of -10 kV resulting in currents of $7-8$ μ A.

The CZE-ESI-MS coupling was carried out using a commercial triple-tube sheath liquid (SL) interface (Agilent Technologies). A mixture of 2-propanol, H_2O and 25 mM aqueous ammonium acetate with adjusted pH = 6 (5:4:1, v/v) was used as SL, delivered at a flow rate of 3 μ L/min by a syringe pump (Cole-Parmer®, IL, USA) equipped with a 5-mL syringe (5MDF-LL-GT, SGE Analytical Science, Melbourne, Australia).

A microOTOF-Q II quadrupole time-of-flight MS controlled by microOTOF control software (Bruker Daltonik, Bremen, Germany) was used. While the transfer capillary was kept at a constant voltage of +4500 V (negative ion

polarity mode), the ESI sprayer was grounded. The dry gas (nitrogen) flow rate was set to 4 L/min and the dry gas temperature to 170 °C. The nebulizer gas (nitrogen) pressure was adjusted to 1.0 bar. The measurements were divided into two segments. During the first 12 min of an acquisition, all source voltages and the nebulizer gas were switched off. Afterwards, all voltages were altered to the abovementioned values. The ion optics were optimized to the highest possible intensity in the mass range of 30 to 400 m/z by direct infusion using a sodium formate cluster solution (5 mL 2-propanol mixed with 4.9 mL ultrapure H_2O , 50 μ L formic acid, and 50 μ L 1 M NaOH). The same solution was used for the mass calibration of the QTOF-MS, which was performed at least once a day. In addition, a one point mass correction using the tricine peak was performed for each measurement. Data processing was carried out using the Bruker Compass Data Analysis software (Version 4.1, Bruker Daltonik).

Results and discussion

Method development and validation of the CZE-UV method

The first objective of this work was the development of a CZE-UV method which enables the simultaneous quantification of AA and ASA, including the determination of related degradation products. Therefore, standard mixtures and ASA + AA effervescent tablet solutions (API amount: 200 mg AA and 600 mg ASA, solved in 250 mL NSA solution (70 mg/L), containing 800 mg/L of AA and 2400 mg/L ASA each, were measured to evaluate the performance of several BGE systems (detailed preparations described in the “Materials and methods” section): 25 mM boric acid pH 6 and 9, 25 mM ammonium hydrogen carbonate buffer pH 9, 25 mM sodium dihydrogen phosphate pH 6 and 9, 25 mM ammonium formate pH 6 and 9, and 25 mM ammonium acetate pH 6 and 9. However, none of the tested BGEs resulted in sufficient separation of AA, ASA, and related degradation products (data not shown). In order to quantify AA in fruit beverages and biological fluids, Koh et al. [15] developed an EOF driven system based on a BGE of 100 mM tricine at pH 8.8. Here, this method was adapted by altering capillary dimensions, separation voltage, injection volumes, and detection wavelengths. In addition, different concentrations of tricine (25, 50, 100, and 200 mM) were tested. 25 and 50 mM lead to insufficient separation of the analyte peaks. Using a 100 mM tricine BGE analyzing a standard mixture containing 800 mg/L AA and 2400 mg/L ASA, a successful separation within less than 10 min was achieved (data not shown). 200 mM tricine did only showed minor improvement regarding resolution and separation efficiency and resulted in considerable longer analysis time compared to 100 mM tricine. Thus, 100 mM tricine (pH = 8.8) was

chosen as BGE. Besides the two main peaks of AA and ASA, an additional small, rather broad asymmetric peak was observed in the standard mixture. This peak shape likely originates from electrodispersion effects of slow migrating anions. By spiking experiments and taking the UV spectra in consideration this peak was identified as SA, which is well-known as the main degradation product of ASA [37, 38]. NSA was applied as IS noticeably improving precision of the peak areas, leading to a sharp signal between the AA and SA peak as displayed in Fig. 2a. IS correction was performed for all following experiments dividing the peak area of the analyte by the peak area of NSA and multiplying by the respective analyte response factor and concentration of NSA. The analyte response factors were determined in a previous experiment with 5 measurements of AA, ASA, and NSA standards. Migration times were not IS corrected.

Subsequently, the CZE-UV method was applied to effervescent tablet solutions (tablets solved in 250 mL NSA solution (70 mg/L) resulting in 800 mg/L AA and 2400 mg/L ASA). Two clearly separated main peaks and two additional smaller peaks could be observed, as displayed in Fig. 2b. Spiking experiments were performed and the first, second and fourth peak were successfully assigned to AA, ASA and SA, respectively. Compared with the results received for the standard mixture, an additional peak was present in the electropherogram. Consequently, the tablet sample was spiked with different quantities of sodium saccharin (1000 mg/L). An increase in peak area was observed combined with no noticeable alteration of the UV profile and thus, the third peak was assigned to the matrix component saccharin.

The optimized CZE-UV method was validated regarding the quantification of AA and ASA in effervescent tablets. As a first approach, the matrix effect of the tablets was evaluated in order to ensure the applicability of an external calibration. Therefore, ten replicates of an ASA + AA effervescent tablet solution and a standard mixture containing equal amounts of AA (2500 mg/L) and ASA (7500 mg/L) solved in NSA (70 mg/L) solution were measured and compared. Slightly higher peak areas were observed for the effervescent tablet samples referred to the values of the standard mixture (AA $109.43 \pm 1.19\%$ and ASA $113.64 \pm 2.53\%$). However, applying NSA for IS correction the matrix effect could be greatly reduced (AA $98.29 \pm 1.64\%$ and ASA $101.98 \pm 1.28\%$). A further migration time correction of the peak area values was considered and evaluated, but did not show any additional improvement regarding matrix effect and/or precision (data not shown). Thereupon, the method was validated for AA and ASA with respect to precision, accuracy, linear dynamic range as well as limit of detection (LOD) according to the Food and Drug Administration (FDA) guidelines [39] (see Table 1). Hence, intra-/interday precision and accuracy were determined at three different concentration levels ($n = 5$). For AA the intra- and interday precision of peak areas were

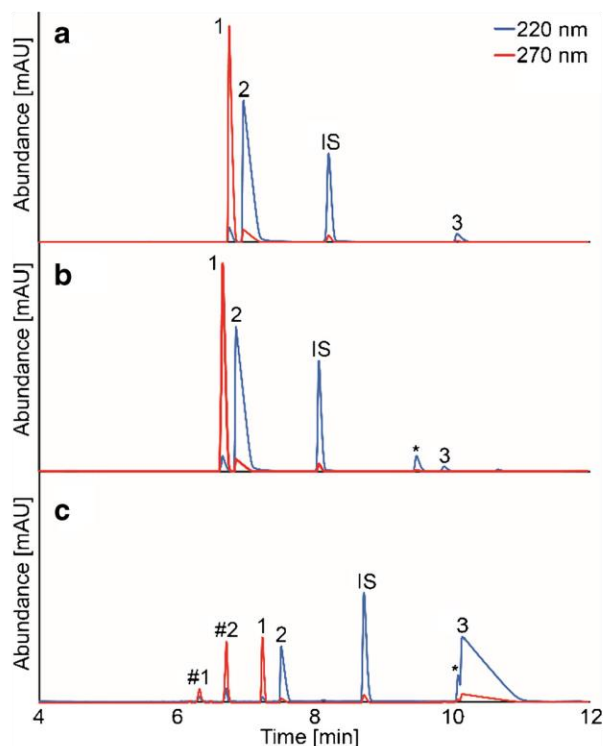


Fig. 2 Electropherograms of AA/ASA standard mixture (a), a freshly unpacked (b), and a degraded (c) ASA + AA effervescent tablet dissolved in 250 mL NSA (70 mg/L) solution (final concentration: 800 mg/L AA and 2400 mg/L ASA). The measurements were applied at two different wavelengths: 220 nm (blue line) and 270 nm (red line). The degraded effervescent tablet was exposed to an environment of defined humidity (75 %) and temperature (30 °C) for 72 h. The CZE-UV separation was performed using a 50 cm fused silica capillary, 100 mM tricine (pH 8.8) as BGE and a separation voltage of +20 kV. The peaks were assigned to AA (1), ASA (2), SA (3), NSA (IS) as internal standard, saccharin (asterisk), degradation product 1 (#1) and 2 (#2). Later, #1 and #2 were identified as di- and monoacetylated AA via heart-cut CZE-CZE-MS

between 0.75–1.12 % and 0.95–1.15 %. In terms of ASA the intra- and interday precision of peak areas were determined to be 0.47–1.03 % and 0.35–0.87 %. The accuracy for AA and ASA was between 101.14 ± 1.02 – $103.46 \pm 0.24\%$ and 97.26 ± 0.45 – $103.42 \pm 0.69\%$, respectively. Furthermore, carry over experiments were performed by analyzing a high concentrated tablet solution (2500 mg/L AA and 7500 mg/L ASA, solved in 80 mL NSA (70 mg/L) solution) and a blank sample alternating five consecutive times. No significant signal for AA or ASA and thus, no carry over was observed in all five blank measurements (data not shown). A linear regression was performed using six concentration levels, a zero sample (blank + IS), and a blank sample with five repetitions each. The linearity for AA was determined to be in the range of 25–2500 mg/L ($R^2 = 0.999$) and for ASA between 30 and 7500 mg/L ($R^2 = 1$). These concentration ranges are sufficient to quantify all amounts of AA and

Table 1 Results of the validation experiments for the CZE-UV method for the determination of ascorbic acid and acetylsalicylic acid

Analyte	Conc. [mg/L]	RSD area intraday [%] (n = 5)	RSD area interday [%] (n = 10)	RSD MT intraday [%] (n = 5)	RSD MT interday [%] (n = 10)	Linear range [mg/L]	R ²	LOD [mg/L]	Conc. [mg/L]	Accuracy [%] (n = 5)
Ascorbic acid	2500	1.12	0.95	0.16	1.45	25-2500	0.999	0.8	2500	101.63 ± 0.67
	250	0.75	1.15	0.44	1.43				800	103.46 ± 0.24
	25	1.01	1.14	0.16	3.32				40	101.14 ± 1.02
Acetylsalicylic acid	7500	1.03	0.87	0.13	1.41	30-7500	1	0.7	7500	103.42 ± 0.69
	750	0.67	0.53	0.18	0.99				2400	102.23 ± 0.04
	75	0.47	0.35	0.17	3.30				120	97.26 ± 0.45

ASA to be expected in fresh and degraded effervescent tablet solutions. By using the signal-to-noise (S/N) ratio of the lowest analyzed concentration the LOD (S/N = 3) was determined. The LOD was estimated to be around 0.8 mg/L for AA and 0.7 mg/L for ASA. These results demonstrate the applicability of the presented CZE-UV method for the quantification of AA and ASA in effervescent tablets. In conclusion, all investigated parameters were successfully validated reaching the demands of the FDA [39].

Application of the developed CZE-UV method for a degradation study

A degradation study of ASA + AA effervescent tablets was performed in order to quantitatively trace the degradation of the APIs. In order to simulate a realistic degradation, such as occurring during inappropriate storage conditions, the tablets were stored and degraded intact. Furthermore, the capability of the CZE-UV method for the early detection of chemical changes should be demonstrated. Therefore, 18 effervescent tablets were exposed to an environment of defined humidity (75 %) and temperature (30 °C) for 72 h, in order to facilitate the degradation of the tablet samples. Three replicates of two tablet samples (n = 6) were measured after 0, 1, 3, 6, 9, 12, 24, 36, 48, and 72 h, respectively. The tablet samples were dissolved in 250 mL NSA solution (70 mg/L) resulting in an initial concentration of 800 mg/L of AA and 2400 mg/L ASA. An example electropherogram of a tablet stored at these conditions for 72 h is displayed in Fig. 2c. Compared with the results obtained for a freshly unpacked effervescent tablet (Fig. 2b), clear differences between both electropherograms could be observed: On the one hand, the peak area of AA and ASA decreased as expected. On the other hand, the peak area of SA increased and moreover, two unknown peaks appeared in front of the AA peak. Both AA and ASA degrade fast under the aforementioned conditions as displayed in Fig. 3. During the first 12 h the curve progression of AA and ASA is almost parallel, implying that both degradation processes could be

directly related during this stage of the storage period. However, an accurate interpretation of the kinetics is challenging due to the intentional inhomogeneous degradation of the tablet samples and thus, was not further investigated in this study. Moreover, reactions in solution were not particularly evaluated and even tried to be avoided during the degradation study by cooling the sample tray to 10 °C and measurements directly after sample preparation. A significant decrease of AA (t-test: $\alpha = 0.05$, $p = 1.6 \cdot 10^{-5}$) and ASA (t-test: $\alpha = 0.05$, $p = 0.028$) could already be detected after 1 h. In contrast, minor visual changes of the tablet color (from white to yellowish) occurred after at least 12 h. Beyond 12 h storage time,

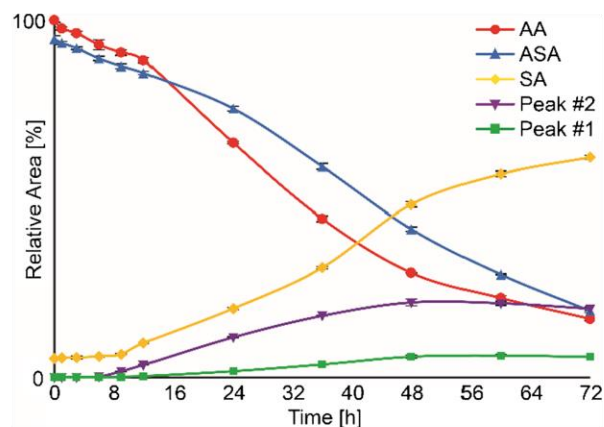


Fig. 3 ASA + AA effervescent tablets were exposed to an environment of defined humidity (75 %) and temperature (30 °C) for 72 h. Detailed description of the degradation conditions can be found in the “Materials and methods” section. The lines indicate the percentage degradation of AA (red, circle), ASA (blue, triangle) and the formation of three degradation products 1# (green, square), 2# (purple, triangle) and SA (yellow, rhombus). The concentration of SA was determined using an external calibration and was set in ratio to the concentration of ASA. The initial concentration of SA (t_0) was subtracted from the concentration of ASA. The formation of the degradation products 1# and 2# was set in ratio to the initial concentration of AA. The same absorption coefficient for AA and the two degradation products was assumed. Later, #1 and #2 were identified as di- and monoacetylated AA via heart-cut CZE-CZE-MS

the AA concentration decreased faster than ASA, which could be explained by time-delayed additional degradation processes of AA. After 72 h, more than 80 % of both APIs were already degraded. As mentioned above, associated with the degradation of the APIs an increase of the SA concentration was observed (see Figs. 2c and 3), which is in agreement with the known degradation pathways [11, 12, 14]. In addition, two unknown peaks appeared over time. DHAA and 2,3-diketogulonic acid (DKG) which are described in the literature [10, 11, 40, 41] as main degradation products for AA are not likely due to their low UV activity at the detected wavelengths (220 and 270 nm). Since there was no prior knowledge about these peaks, an unequivocal identification by CZE-UV only was not possible. In general, the formation of the peaks could result either from the degradation of the APIs or matrix compounds, such as tablet excipients. Thus, in order to clearly identify the degradation products MS detection was aspired. As previously described, the application of a volatile BGE did not result in separation of AA and ASA and the observed degradation products and thus, no direct CE-ESI-MS could be performed. Because of the high concentrated ESI-interfering tricine a direct coupling of the CZE-UV method to an ESI-MS instrument was abstained, due to expected signal suppression and contamination of the instrument. Therefore, a two-dimensional (2D) heart-cut CZE-CZE-MS was performed in order to characterize the degradation products.

CZE-CZE-MS measurements

The online hyphenation of the tricine-based CZE-UV system and CZE-MS was realized by implementing a mechanical 4-port-valve as interface in between the separation dimensions [35]. Regarding such a valve certain requirements must be fulfilled. In order to be able to apply high voltages, a fully isolated valve is required and thus, metal components in direct contact or near proximity of the electrolyte solutions must be avoided. Therefore, a mixture of polyether ether ketone and polytetrafluoroethylene was chosen as rotor and stator material, possessing a dielectric strength of ~20 kV/mm. Prior to assembling the valve, all channels and surfaces were carefully cleaned to avoid contamination. Due to the short distances between the individual channels (<1 mm) of the 4-port-valve +7.5 kV (1st dimension) and -10 kV (2nd dimension) were applied to prevent current leakages and ensure a stable system setup. Current leakage was not observed during all measurements ($\pm 0.2 \mu\text{A}$).

In the 2nd dimension a separation of the remaining ESI-interfering tricine from the analytes must be achieved prior to MS detection. Thus, various BGE systems were tested in a 1D CZE-MS approach, such as 25 mM ammonium hydrogen carbonate (pH = 6), 25 mM ammonium formate (pH = 6 and 9), and ammonium acetate at different pH values (pH = 6, 7, 7.5 and 9) using an AA sample solved in tricine BGE (1000 mg/L in

100 mM tricine). No full separation of analytes and tricine could be achieved applying an EOF driven system in normal polarity mode (data not shown). Using 25 mM ammonium acetate at pH 6 as BGE in an EOF suppressed system (PVA-coated capillaries) in reversed polarity mode, a separation between AA/ASA and tricine was achieved with the analyte being detected first. In order to balance the small remaining EOF, the nebulizer pressure was adapted (see “Materials and methods”). On the one hand, lower pH values lead to neutral forms of AA/ASA which hinders their migration towards the MS. On the other hand, higher pH values resulted in a loss of separation efficiency and an increasing risk of remaining reversed EOF causing issues regarding current stability.

As a first test of the complete 2D system a standard solution (AA, 6000 mg/L) was injected and separated in the 1st dimension, applying +7.5 kV. Hence, the electrophoretic velocity of ions in the 1st dimension is not constant through the whole analysis, i.e. due to field inhomogeneities directly after injection. Furthermore, possible dead volumes caused by the capillary junctions of the valve might influence the electric field and the migration time of the analytes. Thus, an accurate heart-cut by only applying high voltage and one detector is challenging. Therefore, the separation was stopped when the analyte reached the UV detector (4.5 cm in front of the valve) and the analyte was transported into the loop of the valve applying low pressure (50 mbar). The required flushing time was calculated using the distance from the detector to the center of the loop and the flow rates at 50 mbar pressure. The flow rates were determined prior to the analysis by injecting a standard solution (AA, 6000 mg/L) and flushing with 50 mbar till the AA plug passed the external UV detector. The required time was used for the calculation of the flow rate. When the desired analyte was positioned in the center of the loop, the valve was switched to inject position (see Fig. 1), and 50 mbar pressure was applied for 30 s to forward the analyte out of the loop into the separation capillary of the 2nd dimension. Afterwards, the valve was switched back and -10 kV were applied to the 2nd dimension, resulting in typical currents of 4.0–4.4 μA . This procedure improved the overall system stability of the 2nd dimension. An electropherogram of the baseline separated AA and tricine in the 2nd dimension is displayed in Fig. 4. A high concentrated sample is shown to demonstrate that even under overloading conditions a baseline separation between tricine and analyte is ensured. The baseline separation between the ESI-interfering tricine and the analyte signal was achieved for all analytes. Due to the high tricine concentration and a potential associated destacking effect (BGE 25 mM ammonium acetate; 100 mM tricine) the ESI-interfering tricine shows a very broad migration window. The general shape of the detected tricine peak was consistent for all measurements. There exists a large variety of CZE methods for the separation of organic and inorganic ions including the most commonly applied BGE

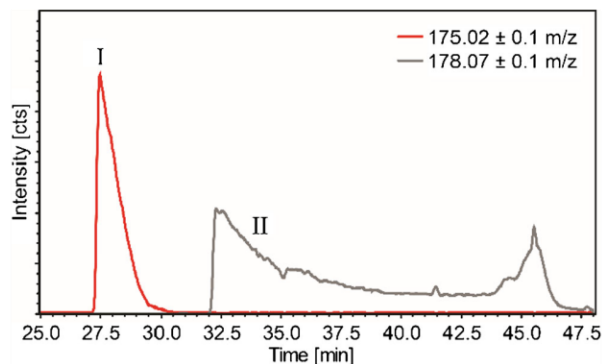


Fig. 4 Extracted ion electropherograms of AA (I; $m/z = 175.02 \pm 0.1$) and tricine (II; $m/z = 178.07 \pm 0.1$) in the 2nd dimension of the heart-cut CZE-CZE-MS approach. 1st dimension: a separation voltage of +7.5 kV, 100 mM tricine at pH 8.8 as BGE and bare fused silica capillaries (total length 55 cm) were applied. 2nd dimension: a separation voltage of -10 kV, 25 mM ammonium acetate at pH 6 as BGE and PVA-coated capillaries (total length 121 cm) were used

systems for CZE-UV. The selectivity of the 2nd dimension can be adjusted and even the migration order can be reversed varying the pH of the BGE system or applying capillary coatings. Thus, we expect it is possible to find appropriate conditions for the separation of a variety of different analytes from ESI-interfering BGE components in the 2nd dimension.

Subsequently, degraded ASA + AA effervescent tablets (48 h @ 75 % humidity and 30 °C) were analyzed in the CZE-CZE-MS system. Therefore, the tablets were dissolved in 80 mL ultrapure H₂O resulting in a concentration of 2500 mg/L AA and 7500 mg/L ASA. As displayed in Fig. 5 all peaks observed in the electropherogram of the external UV detector were cut in a heart-cut approach (at least 3 repetitions for each signal) following the procedure described above. For any individual cut the sample was injected anew and separated in the 1st dimension. The obtained relative standard deviation (RSD) values ($n = 3$) for the migration time of all analytes in the 2nd dimension were between 0.74 and 4.75 %. Based on a 1D experiment, the LOD of the 2nd dimension was estimated to be in the lower ppm range. In agreement with the previous CZE-UV measurements, the peaks 1, 2 and 3 could successfully be assigned to AA, ASA and SA with a mass deviation <5 ppm compared with the calculated accurate masses (see Fig. 5b, c, and f). In order to identify the unknown peaks #1 and #2, the respective m/z values (#1 = 217.0358 and #2 = 259.0455) were compared to the accurate masses of known degradation products described in the literature [10–12, 14, 40]. However, none of the previously described degradation products were in accordance with the observed m/z values (see Fig. 5d, e). The mass difference between peak #2 and AA was determined to be +42.0106 Da, which corresponds to an acetylation (exact

mass: 42.0100 Da). The determined mass difference (+42.0105 Da) between peak #2 and #1 is in accordance with the presence of an additional, second, acetylation (see Fig. 5d, e). Furthermore, the elemental composition of the observed m/z values was calculated. Peak #2 ($m/z = 217.0358$) and Peak #1 ($m/z = 259.0455$) were determined to be C₈H₁₀O₇ (mass deviation: 1.8 ppm) and C₁₀H₁₂O₈ (mass deviation: 2.1 ppm) with score values of 100 %. All other suggested elemental compositions were implausible. Thus, the degradation products were identified as di- and monoacetylated AA, which is additionally substantiated by the migration time shift to shorter values compared to AA.

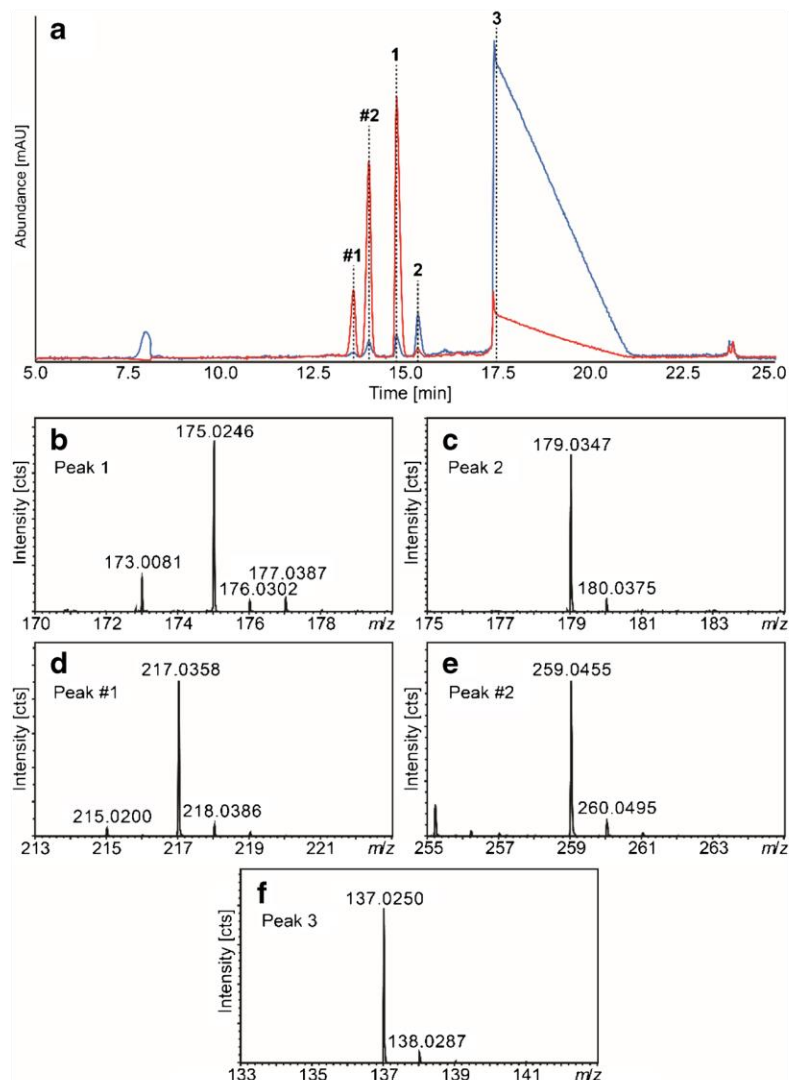
Thomis et al. [12] hypothesized the formation of monoacetylated AA; however, they could not confirm its presence by HPLC-UV applying an ESI-interfering phosphate buffer. Taking the molecular structure of AA in consideration, the 3-hydroxy group can be acetylated relatively easily due to its vinylogous structure, e.g. by using acetic anhydride in aqueous solution [42]. Furthermore, it has been demonstrated that ASA acetylates reactive hydroxyl-groups of different pharmaceuticals, e.g. phenylephrine hydrochloride [43]. Here, a similar mechanism is proposed involving AA and ASA. A direct acetylation of the 2-hydroxy group by ASA is unlikely, due to its considerable high p_{ka} of 11.5. However, the p_{ka} of the 2-hydroxy group is significantly lowered in 3-*O*-acetylated AA and expected to be around 5.5 [42] and thus, a second acetylation is possible.

The only published works utilizing a mechanical (6-port)-valve for 2D electrophoretic separation from Zhang et al. [33] and Wei et al. [34] were applied to CIEF-CEC-UV with the objective to achieve high separation efficiency by the combination of CIEF and CEC and not to enable MS detection of an ESI-interfering electrolyte system. In addition, rather large sample volumes (130 nL [33] and 500 nL [34]) were transferred to the 2nd dimension well-suited for CEC, but not for CZE applications. On the one hand, a classical 6-port-valve enables the injection of flexible sample volumes. On the other hand, it is not possible to transfer precise volumes in the lower nL range. In contrast, applying the presented 4-port-valve this limitation is overcome (precise transfer volume: 20 nL) and thus, this valve is in general more applicable for CZE-CZE-MS.

Conclusion

The developed and validated CZE-UV method enables the simultaneous quantification of AA and ASA in ASA + AA effervescent tablets including the determination of

Fig. 5 Electropherogram of a degraded ASA + AA effervescent tablet at two different wavelengths: 220 nm (blue line) and 270 nm (red line) (a). The effervescent tablets were exposed to an environment of defined humidity (75 %) and temperature (30 °C) for 72 h. The separation was performed using the heart-cut CZE-CZE-MS approach. 1st dimension: a separation voltage of +7.5 kV, 100 mM tricine at pH 8.8 as BGE and bare fused silica capillaries (total length 55 cm) were used. 2nd dimension: a separation voltage of -10 kV, 25 mM ammonium acetate at pH 6 as BGE and PVA-coated capillaries (total length 121 cm) were applied. Mass spectra of peak 1 (b), peak 2 (c), peak 3 (f), degradation product #1 (d) and #2 (e). Due to the determination of accurate masses the peaks were assigned to AA (peak 1), ASA (peak 2), SA (peak 3), diacetylated AA (#1) and monoacetylated AA (#2)



related degradation products. A degradation study of ASA + AA effervescent tablets demonstrates the capability of the CZE-UV method for the detection of significant chemical changes, already after short storage periods (1 h @ 75 % humidity and 30 °C) prior to visual changes of the tablets. Due to the ESI-interfering tricine electrolyte system, a direct coupling of the CZE-UV method to an MS instrument for peak characterization is not possible. Our previous proof of concept study has demonstrated the applicability of a mechanical valve for 2D CE coupled to MS detection using a model phosphate-based electrolyte system in the 1st dimension. Here, the application of the mechanical 4-port-valve has been expanded to a first real case study of an MS-incompatible CZE electrolyte system. Hence, this heart-cut CZE-CZE-MS approach enables the online

MS characterization of anionic degradation products from a tricine-based CZE-UV separation. In this way, the unknown degradation products have been successfully identified as mono- and diacetylated AA. Thus, the CZE-CZE-MS setup represents a straightforward approach for the detailed characterization of CZE-separated analytes in non-MS-compatible electrolyte systems. Moreover, the online hyphenation of two physically separated CZE systems provides certain benefits, such as individual and simultaneous conditioning of both dimensions. We expect that the general 2D setup can be transferred to other electrolyte systems, providing a wide range of possible applications for the MS identification of CZE separated analytes in BGEs containing ESI-interfering constituents. Nevertheless, this still has to be shown in future work.

Acknowledgments The authors acknowledge the partners within the MIME project: J&M Analytic AG, LabCognition Analytical Software GmbH & Co. KG, Glatt GmbH Systemtechnik, Pharma Test AG, Bundeskriminalamt Wiesbaden (BKA) and University of Münster and the Federal Ministry of Education and Research (BMBF) for financial support in the course of the announcement “Sicherung der Warenketten” within the scope of the program “Forschung für die zivile Sicherheit” of the Federal Government (FKZ 13 N12009). We thank Norbert Schaschke and Jens Hühner from the University of Aalen for helpful suggestions.

Compliance with ethical standards

Conflict of interest The authors declare that they have no conflict of interest.

References

- Pohle T, Brzozowski T, Becker JC, van Dervoort IR, Markmann A, Konturek SJ, et al. Role of reactive oxygen metabolites in aspirin-induced gastric damage in humans: gastroprotection by vitamin C. *Aliment Pharmacol Ther.* 2001;15:677–87.
- Mylrea M, Robertson S, Haywood A, Glass B. Stability of dispersible aspirin tablets repacked into dosette boxes. *J Pharm Pract Res.* 2012;42(3):204–7.
- Pavlovská G, Tanevská S. Influence of temperature and humidity on the degradation process of ascorbic acid in vitamin C chewable tablets. *J Therm Anal Calorim.* 2013;111(3):1971–7.
- Dinç E, Baleanu D. Ratio spectra-continuous wavelet transform and ratio spectra-derivative spectrophotometry for the quantitative analysis of effervescent tablets of vitamin C and aspirin. *Rev Chim (Bucharest, Rom).* 2008;59(5):499–504.
- Dinç E, Ozdemir A, Baleanu D. Comparative study of the continuous wavelet transform, derivative and partial least squares methods applied to the overlapping spectra for the simultaneous quantitative resolution of ascorbic acid and acetylsalicylic acid in effervescent tablets. *J Pharm Biomed Anal.* 2005;37(3):569–75.
- Toral MI, Lara N, Richter P, Tassara A, Tapia AE, Rodríguez C. Simultaneous determination of ascorbic acid and acetylsalicylic acid in pharmaceutical formulations. *J AOAC Int.* 2001;84(1):37–42.
- Neuberger S, Neusüß C. Determination of counterfeit medicines by Raman spectroscopy: systematic study based on a large set of model tablets. *J Pharm Biomed Anal.* 2015;112:70–8.
- Di Pietra AM, Gatti R, Andrisano V, Cavrini V. Application of high-performance liquid chromatography with diode-array detection and on-line post-column photochemical derivatization to the determination of analgesics. *J Chromatogr A.* 1996;729(1-2):355–61.
- Khan MR, Allothman ZA, Naushada M, Ghfar AA, Wabaidur SM. Simultaneous analysis of Vitamin C and aspirin in aspirin C effervescent tablets by high performance liquid chromatography-photodiode array detector. *J Liq Chromatogr Relat Technol.* 2012;35(17):2454–61.
- Klimczak I, Gliszczynska-Świągło A. Comparison of UPLC and HPLC methods for determination of vitamin C. *Food Chem.* 2015;175:100–5.
- Kmetec V. Simultaneous determination of acetylsalicylic, salicylic, ascorbic and dehydroascorbic acid by HPLC. *J Pharm Biomed Anal.* 1992;10:1073–6.
- Thomis R, Roets E, Hoogmartens J. Analysis of tablets containing aspirin, acetaminophen, and ascorbic acid by high-performance liquid chromatography. *J Pharm Sci.* 1984;73(12):1830–3.
- Wabaidur SM, Allothman ZA, Khan MR. A rapid method for the simultaneous determination of L-ascorbic acid and acetylsalicylic acid in aspirin C effervescent tablet by ultra performance liquid chromatography-tandem mass spectrometry. *Spectrochim Acta Part A.* 2013;108:20–5.
- Akay C, Ismail Tuncer D, Ahmet S, Aydin A, Özkan Y, Gül H. Rapid and simultaneous determination of acetylsalicylic acid, paracetamol, and their degradation and toxic impurity products by HPLC in pharmaceutical dosage forms. *Turk J Med Sci.* 2008;38:167–73.
- Koh EV, Bissell MG, Ito RK. Measurement of vitamin C by capillary electrophoresis in biological fluids and fruit beverages using a stereoisomer as an internal standard. *J Chromatogr A.* 1993;633(1-2):245–50.
- Dong S, Zhang S, Cheng X, He P, Wang Q, Fang Y. Simultaneous determination of sugars and ascorbic acid by capillary zone electrophoresis with amperometric detection at a carbon paste electrode modified with polyethylene glycol and Cu(2)O. *J Chromatogr A.* 2007;1161(1-2):327–33.
- Zykova EV, Sandetskaya NG, Ostrovskii OV, Verovskii VE. Determining ascorbic acid in medicinal preparations by capillary zone electrophoresis and micellar electrokinetic chromatography. *Pharm Chem J.* 2010;44(8):463–5.
- Wei W, Yu X, Ju H. Simultaneous determination of several antalgic drugs based on their interactions with -cyclodextrin by capillary zone electrophoresis. *J Chromatogr Sci.* 2004;42(3):155–60.
- Marra MC, Cunha RR, Vidal DTR, Munoz RAA, do Lago CL, Richter EM. Ultra-fast determination of caffeine, dipyrone, and acetylsalicylic acid by capillary electrophoresis with capacitively coupled contactless conductivity detection and identification of degradation products. *J Chromatogr A.* 2014;1327:149–54.
- Whitehouse CM, Dreyer RN, Yamashita M, Fenn JB. Electrospray interface for liquid chromatographs and mass spectrometers. *Anal Chem.* 1985;57(3):675–9.
- Kler PA, Sydes D, Huhn C. Column-coupling strategies for multidimensional electrophoretic separation techniques. *Anal Bioanal Chem.* 2015;407(1):119–38.
- Kohl FJ, Sánchez-Hernández L, Neusüß C. Capillary electrophoresis in two-dimensional separation systems: techniques and applications. *Electrophoresis.* 2015;36(1):144–58.
- Grochocki W, Markuszewski MJ, Quirino JP. Multidimensional capillary electrophoresis. *Electrophoresis.* 2015;36(1):135–43.
- Santos B, Simonet BM, Ríos A, Valcárcel M. Integrated 2-D CE. *Electrophoresis.* 2007;28(9):1345–51.
- Cottet H, Biron J, Taillades J. Heart-cutting two-dimensional electrophoresis in a single capillary. *J Chromatogr A.* 2004;1051(1-2):25–32.
- Anouti S, Vandenabeele-Trambouze O, Cottet H. Heart-cutting 2D-CE with on-line preconcentration for the chiral analysis of native amino acids. *Electrophoresis.* 2010;31(6):1029–35.
- Kukusamude C, Srijaranai S, Quirino JP. Stacking and separation of neutral and cationic analytes in interface-free two-dimensional heart-cutting capillary electrophoresis. *Anal Chem.* 2014;86(6):3159–66.
- Kukusamude C, Srijaranai S, Quirino JP. Interface-free two-dimensional heart-cutting capillary electrophoresis for the separation and stacking of anionic and neutral analytes. *J Sep Sci.* 2015;38(14):2532–7.
- Lemmo AV, Jorgenson JW. Transverse flow gating interface for the coupling of microcolumn LC with CZE in a comprehensive two-dimensional system. *Anal Chem.* 1993;65(11):1576–81.
- Michels DA, Hu S, Schoenherr RM, Eggertson MJ, Dovichi NJ. Fully automated two-dimensional capillary electrophoresis for high sensitivity protein analysis. *Mol Cell Proteomics.* 2001;1(1):69–74.
- Michels DA, Hu S, Dambrowitz KA, Eggertson MJ, Lauterbach K, Dovichi NJ. Capillary sieving electrophoresis-micellar

- electrokinetic chromatography fully automated two-dimensional capillary electrophoresis analysis of *Deinococcus radiodurans* protein homogenate. *Electrophoresis*. 2004;25(18-19):3098–105.
32. Flaherty RJ, Huge BJ, Bruce SM, Dada OO, Dovichi NJ. Nicked-sleeve interface for two-dimensional capillary electrophoresis. *Analyst*. 2013;138(13):3621–5.
 33. Zhang M, El Rassi Z. Two-dimensional microcolumn separation platform for proteomics consisting of on-line coupled capillary isoelectric focusing and capillary electrochromatography. 1. Evaluation of the capillary-based two-dimensional platform with proteins, peptides, and human serum. *J Proteome Res*. 2006;5(8):2001–8.
 34. Wei J, Gu X, Wang Y, Wu Y, Yan C. Two-dimensional separation system by on-line hyphenation of capillary isoelectric focusing with pressurized capillary electrochromatography for peptide and protein mapping. *Electrophoresis*. 2011;32(2):230–7.
 35. Kohl FJ, Montealegre C, Neusiß C. On-line two-dimensional capillary electrophoresis with mass spectrometric detection using a fully electric isolated mechanical valve. *Electrophoresis*. 2016;37(7):954–8.
 36. Xu L, Dong X, Sun Y. Electroosmotic pump-assisted capillary electrophoresis of proteins. *J Chromatogr A*. 2009;1216(32):6071–6.
 37. Edwards LJ. The hydrolysis of aspirin. A determination of the thermodynamic dissociation constant and a study of the reaction kinetics by ultra-violet spectrophotometry. *Trans Faraday Soc*. 1950;46:723.
 38. Leeson LJ, Mattocks AM. Decomposition of aspirin in the solid state. *J Pharm Sci*. 1958;47(5):329–33.
 39. Food and Drug Administration. Guidance for Industry - Bioanalytical Method Validation; 2001 [cited 2015 Nov 10]. Available from: URL:<http://www.fda.gov/ucm/groups/fdagov-public/@fdagov-drugs-gen/documents/document/ucm070107.pdf>.
 40. Kimoto E, Tanaka H, Ohmoto T, Choami M. Analysis of the transformation products of dehydro-L-ascorbic acid by ion-pairing high-performance liquid chromatography. *Anal Biochem*. 1993;214(1):38–44.
 41. Rubin SH, DeRitter E, Johnson JB. Stability of vitamin C (ascorbic acid) in tablets. *J Pharm Sci*. 1976;65(7):963–8.
 42. Paulssen RB, Chatterji D, Higuchi T, Pitman IH. Acylation of ascorbic acid in water. *J. Pharm. Sci*. 1975; 64(8).
 43. Troup AE, Mitchner H. Degradation of phenylephrine hydrochloride in tablet formulations containing aspirin. *J Pharm Sci*. 1964;53(4):375–9.

II: Extension of CZE-CZE-MS applications towards intact protein analysis

Two dimensional capillary zone electrophoresis-mass spectrometry for the detailed characterization of intact monoclonal antibody charge variants, including deamidation products

K. Jooß, J. Hühner, S. Kiessig, B. Moritz, C. Neusüß (paper in forefront)

Analytical and Bioanalytical Chemistry (2017) 409(26):6057-6067

CZE-UV methods utilizing ϵ -aminocaproic acid (EACA) based electrolytes are routinely applied as biopharmaceutical applications for the separation of monoclonal antibody (mAb) charge variants. Though being highly ESI-interfering, these electrolytes are necessary to achieve sufficient separation efficiency of the various potential mAb charge variants. Thus, these CZE methods represent an ideal challenge to expand the application field of the CZE-CZE-MS setup towards intact protein analysis. In this regard, a generic EACA based CZE-UV method was applied as first dimension. It was possible to generate interference-free, highly precise mass data of Trastuzumab charge variants. In this way, the first on-line generated MS data of mAb variants was generated applying an EACA-based electrolyte system. Furthermore, it was possible to differentiate between main and deamidated forms of mAbs ($\Delta m = 1$ Da) on the intact level for the first time. This approach has the potential to become a compelling analytical tool for MS characterization of mAb charge variants.

Candidate's contribution:

Planning of experiments and development of CZE-CZE-MS method. Performance of majority of experiments. Entire interpretation and evaluation of data. Literature search and preparation of major parts of the manuscript including creation of figures.

Two-dimensional capillary zone electrophoresis–mass spectrometry for the characterization of intact monoclonal antibody charge variants, including deamidation products

Kevin Jooß^{1,2} · Jens Hühner^{1,3} · Steffen Kiessig⁴ · Bernd Moritz⁴ · Christian Neusüß¹

Received: 1 June 2017 / Revised: 14 July 2017 / Accepted: 20 July 2017 / Published online: 12 August 2017
© Springer-Verlag GmbH Germany 2017

Abstract Capillary zone electrophoresis (CZE) is a powerful tool that is progressively being applied for the separation of monoclonal antibody (mAb) charge variants. Mass spectrometry (MS) is the desired detection method concerning identification of mAb variants. In biopharmaceutical applications, there exist optimized and validated electrolyte systems for mAb variant quantification. However, these electrolytes interfere greatly with the electrospray ionization (ESI) process. Here, a heart-cut CZE–CZE–MS setup with an implemented mechanical four-port valve interface was developed that used a generic ϵ -aminocaproic acid based background electrolyte in the first dimension and acetic acid in the second dimension. Interference-free, highly precise mass data (deviation less than 1 Da) of charge variants of trastuzumab, acting as model mAb system, were achieved. The mass accuracy obtained (low parts per million range) is discussed regarding both measured and calculated masses. Deamidation was detected for the intact model antibody, and related mass differences were significantly confirmed on the deglycosylated

level. The CZE–CZE–MS setup is expected to be applicable to a variety of antibodies and electrolyte systems. Thus, it has the potential to become a compelling tool for MS characterization of antibody variants separated in ESI-interfering electrolytes.

Keywords Antibody analysis · ϵ -Aminocaproic acid · Electrospray ionization · Capillary zone electrophoresis–mass spectrometry · Two-dimensional interface · Mechanical valve · Pharmaceutical application

Abbreviations

BGE	Background electrolyte
CE	Capillary electrophoresis
CZE	Capillary zone electrophoresis
EACA	ϵ -Aminocaproic acid
ESI	Electrospray ionization
FAc	Formic acid
HAc	Acetic acid
IEC	Ion-exchange chromatography
IPA	Isopropyl alcohol
mAb	Monoclonal antibody
MS	Mass spectrometry
PTM	Posttranslational modification
PVA	Poly(vinyl alcohol)
QqTOF	Quadrupole–quadrupole time of flight
RSD	Relative standard deviation
SL	Sheath liquid
TM	Tuning mix

Parts of this work were presented at ANAKON 2017 Tübingen, Germany.

Electronic supplementary material The online version of this article (doi:10.1007/s00216-017-0542-0) contains supplementary material, which is available to authorized users.

✉ Christian Neusüß
christian.neuss@hs-aalen.de

¹ Faculty of Chemistry, Aalen University, Beethovenstr. 1, 73430 Aalen, Germany

² Research Unit Analytical BioGeoChemistry, Helmholtz Zentrum München, Ingolstädter Landstr. 1, 85764 Neuherberg, Germany

³ Institute of Pharmaceutical Sciences, University of Tübingen, Auf der Morgenstelle 8 (Haus B), 72076 Tübingen, Germany

⁴ F. Hoffmann-La Roche AG Ltd, Grenzacherstrasse 124, 4070 Basel, Switzerland

Introduction

Monoclonal antibodies (mAbs) are considered to be the fastest growing group of pharmaceuticals, achieving sales of almost

\$75 billion in 2013 [1]. Starting with the first therapeutic mAb in 1986, more than 30 mAbs are now available and currently approved by the US Food and Drug Administration [2]. The fields of application of mAbs include, among others, the treatment of cancer, transplants, and cardiovascular, infectious, or chronic inflammatory diseases [3]. During manufacture, purification, and storage of these complex proteins, different variants besides the main form can occur [4]. Changes in microheterogeneity may lead to attenuated therapeutic efficacy [5]. Modifications encompass, for example, disulfide bond scrambling, change in glycosylation pattern, deamidation, pyroglutamate formation, loss of C-terminal lysine, oxidation (e.g. methionine), and amino acid substitution [6]. The characterization of such variants plays an important role regarding product quality, including technical development, release testing, and control of manufacturing processes.

Important techniques for the characterization of mAbs include chromatographic approaches such as reversed-phase liquid chromatography [7, 8], ion-exchange chromatography (IEC) [9], size-exclusion chromatography [10], hydrophobic interaction chromatography [11], and hydrophilic interaction liquid chromatography [12]. In addition, electrophoresis-based separation techniques are commonly applied for the analysis of biopharmaceutical proteins, including capillary isoelectric focusing [13], capillary gel electrophoresis [14], and capillary zone electrophoresis (CZE) [5, 15–18]. A detailed comparison discussing the benefits and limitations of these techniques can be found in recent reviews [1, 2, 19]. Use of chromatography in IEC mode, especially cation-exchange chromatography, is considered the benchmark for the determination of charge variants of therapeutic antibodies [9].

Because of their high selectivity, high resolving power, and low solvent and sample consumption, electrophoresis-driven separation approaches have been commonly applied for the analysis of biopharmaceuticals, especially on the protein level [1]. Capillary isoelectric focusing [13] and capillary gel electrophoresis [14] are more quantitative and less time-consuming alternatives to classic slab gel analysis. CZE is the most straightforward electrophoretic separation technique, where ionic analyte species are separated on the basis of their charge-to-size ratio. Thus, this technique is well suited for the separation of charge variants of intact antibodies [20]. Because of the small difference in molecular mass between mAb charge variants (e.g., deamidation $\Delta m \approx 1$ Da), the difference in charge and not in hydrodynamic radius is often the important factor regarding separation efficiency. To increase resolution and avoid protein adsorption on the capillary wall, sophisticated electrolyte systems and capillary coatings have been developed [4, 15, 16, 18, 21]. In the last few years, several CZE methods based on ϵ -aminocaproic acid (EACA) as the background electrolyte (BGE) have been introduced [5, 15, 22–24]. Moreover, a generic EACA system, which was successfully applied for the charge heterogeneity

profiling of 23 mAbs (pI 7.4–9.2), has been tested in an extensive interlaboratory study for the analysis of a monoclonal IgG1, showing impressive precision (standard deviations of approximately 1% for the main peak) [5]. These EACA-based electrolyte systems are already an integrated part of the pharmaceutical industry as a tool additional to classic IEC with UV detection for the characterization of mAb charge variants [5, 15, 22].

Mass spectrometry (MS) has been demonstrated to be a powerful tool for the characterization of mAb variants [25]. Thus, MS is well established in the field of mAb analysis, providing information on the primary sequence, posttranslational modifications (PTMs), and higher-order structures [26]. In general, high resolution MS allows the discrimination of analyte species even with minor mass differences. Nevertheless, the isotopic envelope of high-mass molecules such as mAbs is broad (approximately 25 Da at full width at half maximum), limiting the information provided [2]. Because of overlapping small mass shifts caused by deamidation (+1 Da) or even larger shifts, for example, oxidation (+16 Da) or N-terminal pyroglutamate formation (–18 Da), mAb variants are difficult to resolve by MS alone. Therefore, electrophoretic or chromatographic separation is often performed before MS detection. However, the separation buffers or electrolytes that are required for chromatographic and electrophoretic separations often interfere with the electrospray ionization (ESI) process. The aforementioned EACA-based CZE systems represent a good example for considerable ESI interference. Different approaches have been pursued to enable online capillary electrophoresis (CE)–MS detection [27]. One way is to alter the electrolyte conditions (e.g., lower concentrations) and capillary coatings or to replace the nonvolatile components by MS-compatible electrolytes. In this way, mAb charge variants were separated and characterized by MS by application of an acetic acid based BGE in a microfluidic device by Redman et al. [4, 21]. On the other hand, EACA-based CZE–UV methods are very robust, precise, and quantitative, and are thus routinely used in biopharmaceutical applications [5, 22]. In this regard, another promising attempt involves the removal of the ESI-interfering components of such electrolyte systems before MS detection. One straightforward concept is the collection of previously separated fractions of mAb variants and either reinjection of the fractions in a second MS-compatible separation dimension or pretreatment of the sample in between to remove interfering components before MS detection. Nevertheless, the collection of low amounts of effluent in CE is associated with high dilution of the desired analytes [28]. A more elegant approach is to hyphenate the ESI-interfering buffer system online with a second separation dimension coupled to an MS system. Because of the low flow rates and dimensions of CE in general, the application of another electrophoresis-based separation technique as the second dimension is beneficial, especially CZE because of available volatile BGE systems.

To realize the online hyphenation of two electromigrative separation techniques, special coupling techniques are required because of the small volumes and strong electrical fields in CE. In the last few years, different types of sophisticated interfaces have been developed [28, 29]. Recently, we introduced a mechanical four-port valve with sufficiently small volume (low nanoliter range) for CE–CE–MS [30]. Different applications have been reported, demonstrating the potential of this cutting-edge two-dimensional setup [30–33].

Here, a heart-cut CZE–CZE–MS method was developed that uses the aforementioned mechanical four-port valve for the MS characterization of mAb charge variants previously separated in a highly ESI-interfering generic EACA-based electrolyte system. In this way, assignment of MS data to the respective peaks in the UV separation should be achieved. The characterization of deamidation products is one of the biggest and latest challenges regarding intact mAb charge variant analysis, because of their minor differences compared with the main form. Trastuzumab is well characterized and known for possessing several potential deamidation sites [34, 35]. Thus, it was selected as a model system to demonstrate the capability of the CZE–CZE–MS setup. On the basis of the low mass differences expected from deamidation products, another objective of this work was to critically elucidate the obtainable mass accuracy and related theoretical calculations.

Materials and methods

Materials

Ultrapure water (electrical resistivity greater than 18 M Ω cm) from an UltraClear UV system (Siemens Water Technologies, Günzburg, Germany) was used to prepare all BGEs, samples, and rinsing solutions. Methanol (MS grade), isopropyl alcohol (IPA; MS grade), sodium hydroxide (98% or greater), ammonia solution (ROTIPURAN®, 30%, p.a.), ammonium hydrogen carbonate (99% or greater, p.a.), formic acid (FAc; ROTIPURAN®, 98% or greater, p.a., ACS), and acetic acid (HAc; ROTIPURAN®, 100%, p.a.) were obtained from Carl Roth (Karlsruhe, Germany). (Hydroxypropyl)methyl cellulose (molecular mass approximately 26 kDa), triethylenetetramine (97.0% or greater), glutaraldehyde solution (50% in H₂O, suitable for photographic applications), poly(vinyl alcohol) (PVA; (molecular mass 89–98 kDa, 99+% hydrolyzed), *N*-glycosidase F (recombinant from *Escherichia coli*), and caffeine (99%) were purchased from Sigma-Aldrich (Steinheim, Germany). Hydrochloric acid (37%, p.a.) and phosphoric acid (85%, p.a.) were obtained from Häffner (Asberg, Germany). EACA (pure) was obtained from Merck (Darmstadt, Germany). Trastuzumab (Herceptin® from F. Hoffmann-La Roche) was used. ESI-L low-concentration tuning mix (TM)

was obtained from Agilent Technologies (Santa Clara, CA, USA). Bare fused-silica capillaries (50- μ m inner diameter, 363- μ m outer diameter) were purchased from Polymicro Technologies (Phoenix, AZ, USA). Nanosep 10K omega centrifugal devices were obtained from Pall Life Sciences (Ann Arbor, MI, USA). The C4N-4354-.02D microinjector four-port valve, including rotors (internal sample loops 20 and 10 nL) and stators out of plastic material (Valcon E®, polytetrafluorethylene/polyether ether ketone composition), was obtained from VICI AG International (Schenkon, Switzerland). The external UV detector applied in the first dimension of the CZE–CZE–MS setup was purchased from J+M Analytik (Essingen, Germany).

Neutral coating of capillaries with PVA, to prevent protein adsorption at the capillary wall and eliminating the electroosmotic flow, was performed in-house. A detailed description of the coating procedure applied can be found elsewhere [32]. Deglycosylation of trastuzumab samples was performed with *N*-glycosidase F as described in the electronic supplementary material

CZE–UV detection

CZE–UV measurements were performed with an HP ^{3D}CE electrophoresis instrument from Agilent Technologies (Waldbronn, Germany) using capillaries with an inner diameter of 50 μ m and a length of 60.0 cm. Bare fused-silica capillaries were preconditioned every morning by rinsing (approximately 1 bar) with 0.1 M hydrochloric acid (10 min) and EACA-based BGE (10 min), followed by the application of +10 kV for 10 min. The BGE consisted of 380 mM EACA, 1.9 mM triethylenetetramine, and 0.05% w/w (hydroxypropyl)methyl cellulose (pH 5.7, adjusted with HAc), adapted from He et al. [22] Before each run, the capillary was rinsed (approximately 1 bar) consecutively with 0.1 M hydrochloric acid (5 min), H₂O (2 min), and BGE (4 min). For long-term or overnight storage, the capillary was rinsed (approximately 1 bar) with 0.1 M phosphoric acid for 5 min and placed in vials filled with H₂O. Samples were injected hydrodynamically (50 mbar, 24 s). Constant voltages of +10 kV were applied during separations, and UV detection was performed at a wavelength of 214 nm.

CZE–ESI-MS

CZE–ESI-MS was performed with an HP ^{3D}CE electrophoresis instrument from Agilent Technologies coupled to a compact™ quadrupole–quadrupole time-of-flight (QqTOF) mass spectrometer from Bruker Daltonik (Bremen, Germany). PVA-coated capillaries (60.0 cm) were used. The CZE–ESI-MS coupling was performed with a commercial triple-tube sheath liquid (SL) interface (Agilent Technologies, Waldbronn, Germany). Different BGE solutions were applied: 0.2 and 1 M FAc; 0.5, 1, 2, 3, and 5 M HAc. The SL was based

on IPA–H₂O (1:1), and different amounts (0.2 and 1.0% v/v) of FAc and HAC were tested as additives. The SL was delivered at a flow rate of 4 μ L/min by a syringe pump (Cole-Parmer, Vernon Hills, IL, USA) equipped with a 5-mL syringe (5MDF-LL-GT, SGE Analytical Science, Melbourne, Australia). For separation, +10 kV was applied. Samples were injected hydrodynamically (50 mbar, 24 s). Two different MS methods were applied: a wide-range method for the simultaneous detection of EACA and antibodies and a high-mass method optimized for sensitive mAb detection. The most important parameters are summarized in the Table S1. Data processing was performed by Bruker Compass Data Analysis (version 4.2, Bruker Daltonik, Bremen, Germany). For overnight or long-term storage, the PVA-coated capillaries were flushed (approximately 1 bar) with H₂O and dried with air for 10 min.

Heart-cut CZE–CZE–MS

The EACA-based CZE–UV system was coupled online to the CZE–MS system by implementation of a mechanical four-port valve as the interface. Both electrophoretic dimensions and the four-port valve interface are described individually in the following sections:

First dimension: CZE–UV detection

Fused-silica capillaries were connected to the four-port valve as described in detail in Fig. 1. The same procedures (+10 kV for preconditioning and separation) were used as applied in the one-dimensional approach described earlier. Separation was performed until the desired analytes reached the UV detector. At this point, the separation was stopped, and the analytes were transferred into the loop of the valve by application of 50 mbar. Flow rates were determined before each analysis by injection of a small caffeine plug (1 mg/mL, 50 mbar, 12 s) and flushing with 50 mbar until it passed the external UV detector. Flow rates were calculated as described in our previous work [32].

Four-port valve

A mechanical four-port valve was applied as the interface between the first dimension and the second dimension, and consisted of three major parts (see Fig. 1a): the stator, the rotor with the sample loop, and the motor. A more detailed description of the valve and its characteristics can be found elsewhere [30, 31]. Two different sample loop sizes (20 and 10 nL) were applied during the experiments (see Fig. 1c). The rotor with the 10-nL sample loop was used in most of the experiments. The application of the 20-nL loop is mentioned in the text accordingly. The capillaries in the first and second dimensions were connected to the stator with four junctions (S, W, P, and

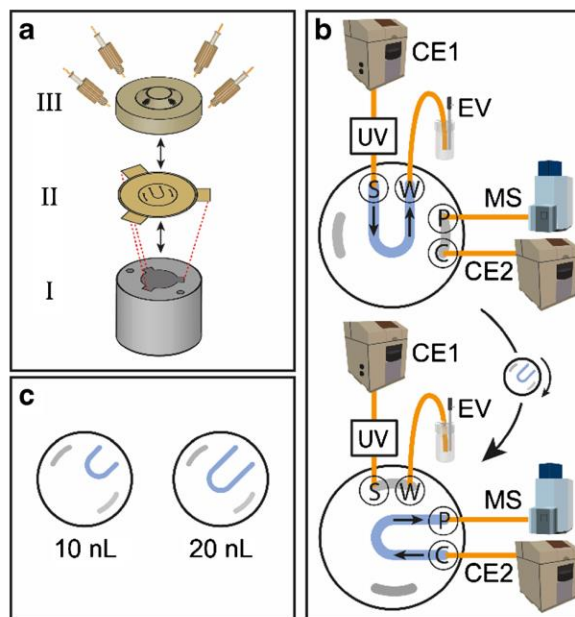


Fig. 1 General setup of the capillary zone electrophoresis (CZE)–CZE–mass spectrometry system applied. **a** The three major parts of the mechanical four-port valve: motor (*I*), rotor including the sample loop (*II*), and the stator with associated capillary connections (*III*). **b** The complete two-dimensional setup. The inlet capillary (fused silica, 40 cm) and outlet capillary (fused silica, 20 cm), which is placed in a grounded external vial (*EV*) of the first dimension [capillary electrophoresis system 1 (*CE1*) to *EV*] are connected to channels *S* and *W* of the four-port valve respectively. An external UV detector cell is positioned 4.5 cm in front of the valve through the inlet of the first dimension. The inlet capillary [poly(vinyl alcohol) (PVA) coated, 40 cm] and outlet capillary (PVA coated, 40 cm) of the second dimension (capillary electrophoresis system 2 (*CE2*) to mass spectrometer (*MS*)] are connected to channels *P* and *C* of the four-port valve respectively. During the separation in the first dimension, the mechanical valve is kept in the loading position (*top*), where the sample loop is connected to channels *S* and *W*. When the desired analyte is located in the sample loop, the valve is switched to the inject position (*bottom*), transferring the analyte from the first dimension to the second dimension. Subsequently, +10 kV is applied for separation. **c** The rotors: 10- and 20-nL sample loop volumes

C). During the first-dimension separation, the mechanical valve was kept in the “loading position” (see Fig. 1b, top). When the desired analytes were located in the sample loop, the valve was switched to the “inject position” (see Fig. 1b, bottom).

Second dimension: CZE–ESI–MS

PVA-coated capillaries (total length 80.0 cm) were cut into two parts (each 40.0 cm) and connected to the valve at junctions *C* and *P* (see Fig. 1). The BGE was composed of 2 M HAC. During the separation in the first dimension, the PVA-coated capillaries were conditioned (approximately 3 bar, 10 min) with BGE. After the analytes had been transferred to the second dimension, +10 kV was applied for separation.

Directly after the analyte reached the mass spectrometer, a 20- μ L plug of calibrant (TM solution) was injected via the SL connection with use of the integrated six-port valve of the mass spectrometer. The TM signals were used for external calibration of each individual data file. A maximum entropy deconvolution was performed with the 12 most abundant charge states (2680–3400 m/z) in the raw mass spectrum.

Results and discussion

Method development

Before application of the complete CZE–CZE–MS setup, the separation dimensions were developed individually in a one-dimensional approach. For the first dimension, a generic CZE–UV method for mAb charge variant separation was selected with typical values for an EACA-based BGE system [5]. A one-dimensional separation of trastuzumab (12.5 mg/mL) through the four-port valve using the complete two-dimensional setup was performed, as depicted in Fig. 2. The separation pattern of trastuzumab obtained is in good agreement with the observations described in the literature [23], showing a small basic peak in the front of the peak corresponding to main variant and some acidic forms migrating subsequently. The resolution of the first CZE–UV dimension could likely be enhanced further by optimization of the electrolyte conditions. However, this was not the objective of this work, which was rather to use a more universal BGE system that had already been applied for a variety of different mAbs [5].

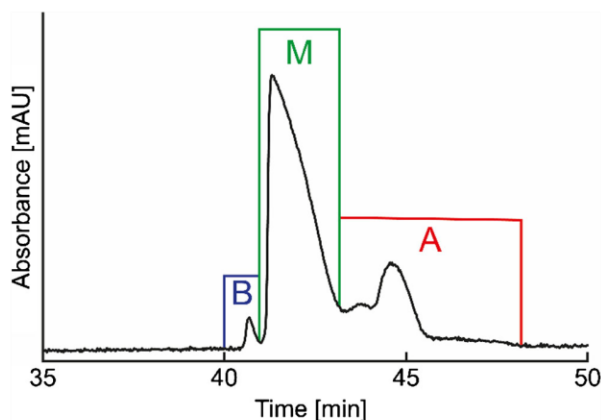


Fig. 2 Electropherogram of trastuzumab (12.5 mg/mL) in the first dimension: capillary zone electrophoresis–UV detection separation was performed through the four-port valve with the complete two-dimensional setup and a total capillary length of 60 cm (the UV detector was located 35.5 cm from the injection end). The background electrolyte consisted of 380 mM ϵ -aminocaproic acid, 1.9 mM triethylenetetramine, and 0.05% (hydroxypropyl)methyl cellulose. UV detection was performed at 214 nm, and +10 kV was applied for separation. The monoclonal antibody profile is divided into three regions: basic (B), main (M), and acidic (A) variants

The main purpose of the second CZE dimension is to separate the remaining ESI-interfering molecules, including the highly concentrated EACA (380 mM) originating from the BGE of the first dimension from the desired mAb variant. Thus, the second-dimension separation is not performed to achieve higher peak capacities or resolution like in a classic two-dimensional approach, but can be seen more as an online electrophoretic cleanup step before MS detection. To test the capability of EACA and mAb separation, trastuzumab (12.5 mg/mL) was dissolved in the BGE of the first dimension and analyzed via one-dimensional CZE–MS. For this experiment the settings of the QqTOF mass spectrometer were adapted in a way that both EACA and the intact mAb molecules could be detected, which is also referred as a “wide-range” MS method (see Table S1). A variety of different volatile BGE compositions were tested: 0.5 and 1 M FAc; 0.5, 1, 2, 3, and 5 M HAc (data not shown). No separation of mAb and EACA could be achieved with FAc-based electrolytes. With 1 M HAc as the BGE, the mAb ions begin to separate from the EACA ions (dimer to heptamer observed in the MS due to high concentration), which migrate in front of the mAb. When the BGE concentration was increased to 2 M HAc, the separation was improved, and an example electropherogram is displayed in Fig. 3. Higher concentrations of HAc did not result in any additional improvement regarding separation efficiency. Thus, 2 M HAc was selected as the BGE for all further experiments. The very broad steplike signal of the EACA ions migrating directly in front of the mAb suggests the presence of (transient) isotachopheresis, due to large a difference of conductivity in the EACA (cut of 380 mM) zone. This results

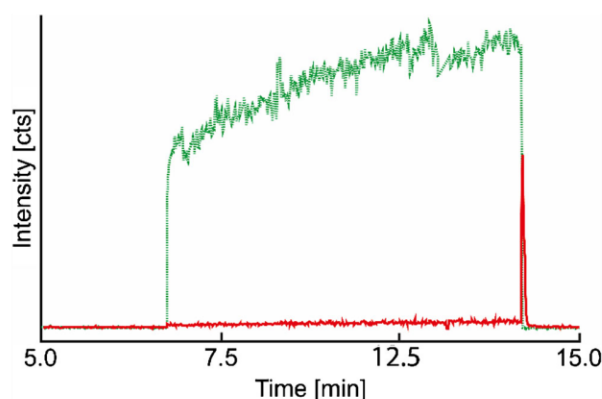


Fig. 3 Electropherogram of trastuzumab (12.5 mg/mL) in the second dimension: capillary zone electrophoresis–mass spectrometry separation was performed in poly(vinyl alcohol)-coated capillaries (total length 60 cm) and 2 M acetic acid as the background electrolyte. The mass spectrometry settings were adjusted to the “wide-range” method parameters (see Table S1), and +10 kV was applied for separation. Extracted ion electropherograms of the ϵ -aminocaproic acid (EACA) dimer (green line) and the sum of the 15 highest-abundance monoclonal antibody (mAb) charge states (red line) are displayed. Separation of EACA and mAb was achieved

in a sharp and concentrated signal for the mAb molecules. A similar effect was observed in our previous work cutting peaks from a 100 mM tricine BGE [32]. Subsequently, the same sample was analyzed with injection via the four-port valve using the complete two-dimensional setup to ensure that the separation efficiency of the one-dimensional CZE–ESI–MS is preserved. Therefore, the capillary of the first dimension was filled with sample before the valve was switched for injection in the second dimension. In this way, analogous results were achieved. To improve the sensitivity of the MS measurement, the influence of the SL composition on the intensity of the mAb signal was evaluated. First, the MS settings were adapted to achieve the highest possible intensity for high-mass molecules with use of TM infusion (see Table S1). Subsequently, the influence of acidic additives in the SL was tested via one-dimensional CZE–ESI–MS analyzing the sample dissolved in the BGE. The SL was composed of 1:1 IPA–H₂O, and different amounts of FAc and HAc were added: 0.2 and 0.5% FAc; 0.2, 0.5, and 1% HAc (data not shown). In general, in comparison with FAc, HAc resulted in higher mAb signals. The highest sensitivity was achieved with 1% HAc, and consequently this SL composition was selected for all further experiments.

One crucial part of the two-dimensional setup is the transfer of analytes from the first dimension to the second dimension. Therefore, precise positioning of the desired analyte in the sample loop is mandatory. An obvious and simple approach is to calculate the time required for the analyte to migrate from the external UV detector to the center of the sample loop during the separation in the first dimension. In principle, only the time for the analyte to reach the external UV detector and the respective distances (capillary inlet to external UV detector, and external UV detector to center of loop) are required. Still, this method premises a constant migration velocity throughout the whole separation in the first dimension. However, because of field inhomogeneities directly after injection and possible dead volumes caused by the capillary junctions of the valve, the migration velocity of the analytes appears to be not perfectly consistent throughout the separation. In this way, precise cutting with this method is challenging. A second, more promising, method is to stop the analysis when the desired analyte reaches the external UV detector and push the analyte into the sample loop by application of a defined low pressure (50 mbar). The time required was calculated with the flow rate at 50 mbar, which was determined before the analysis. To compensate for even minor variations in the flow profile, potentially resulting from switching of the valve, and to achieve a very precise cutting, the flow rate determination was performed before each individual analysis.

The obtainable mass accuracy and precision of the QqTOF mass spectrometer play an essential role for the characterization of mAb variants, especially because of their high molecular mass and structural similarities. To achieve highly accurate results, external calibration of the MS data in a time frame

close to the analyte signal was implemented in the second dimension, which is exemplarily displayed for a cut of the main variant of trastuzumab (18 mg/mL) in Fig. 4a. Thereby, a TM solution (20 µL) is infused via the SL tubing

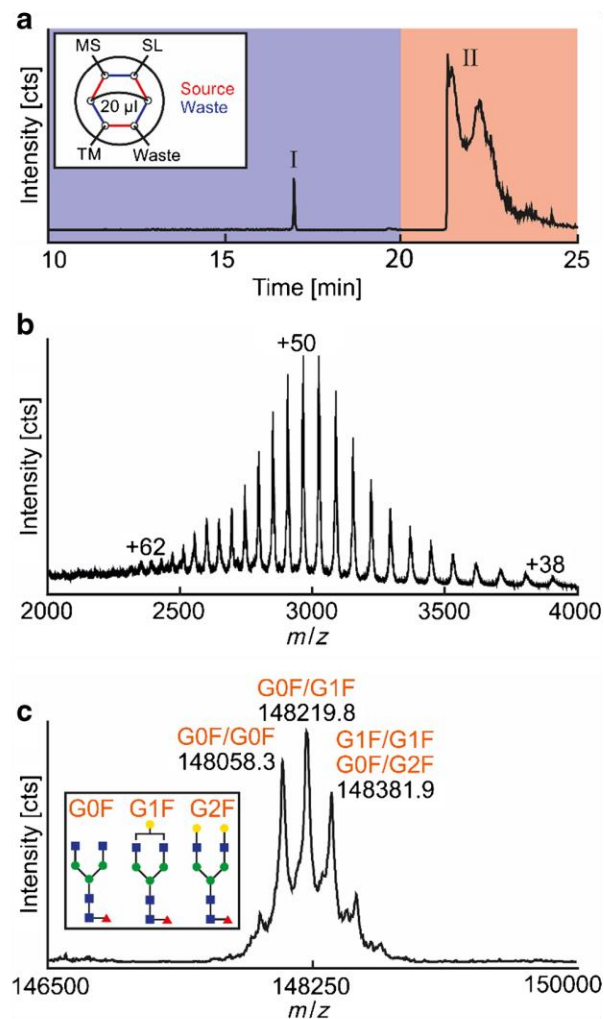


Fig. 4 **a** Base peak electropherogram (2500–5000 m/z) in the second dimension cutting the main variant of trastuzumab (18 mg/mL) via capillary zone electrophoresis (CZE)–CZE–mass spectrometry. The electropherogram was divided into two sections: migration of monoclonal antibody toward the mass spectrometer (MS; I) and infusion of tuning mix (TM) via sheath liquid (SL) tubing for postanalysis mass calibration (II). The inset contains a scheme of the six-port valve integrated in the quadrupole–quadrupole time-of-flight mass spectrometer. During section I the sample loop (20 µL) of the six-port valve was filled with TM (position waste) and infused to the mass spectrometer via the SL tubing during section II (position source). The TM signals were used to recalibrate the mass spectrometry data. **b** Mass spectrum of the main variant of trastuzumab. Charge states ranging from +38 to +62 were observed. **c** Deconvoluted mass spectrum of trastuzumab main variant. The three highest peaks of the spectrum were assigned to the corresponding glycoform. The inset contains the structure of the three common glycans (G0F, G1F, and G2F) present in trastuzumab: red triangle fucose, blue square *N*-acetylglucosamine, green circle mannose, yellow circle galactose

directly after the mAb is detected in the mass spectrometer with use of the integrated six-port valve of the QqTOF mass spectrometer. The resulting TM signals were used to recalibrate the mass spectra during data evaluation (quadratic regression model). In this way, variations in the instrument performance could be corrected subsequently.

Glycosylated mAb samples

The mass spectrum of the cut main variant of glycosylated trastuzumab (18 mg/mL), demonstrating the general applicability of the two-dimensional setup, is displayed in Fig. 4b. Charge states ranging from +38 to +62 were observed in the raw mass spectrum. The CZE–CZE–MS setup was validated regarding migration time, single intensity, current, and flow rate stability by cutting the main variant of trastuzumab several times (12.5 mg/mL). The results of the validation are summarized in Table 1. The current in both dimensions was stable [intraday relative standard deviation (RSD) 1.2–1.8%, interday RSD 1.5–2.9%], and no current leakage was observed throughout all measurements. As stated before, the flow rate in the first dimension was determined before each run to ensure the highest possible precision of the cutting procedure. Nevertheless, RSDs of 0.9% (intraday) and 4.4% (interday) were achieved for the flow rate. The intraday precision of the migration time in the first and second dimensions was 0.8% and 1.7% respectively. The interday precision of the migration time in the first and second dimensions was 3.1% and 6.2% respectively. The external UV signal showed only minor variation in intensity (intraday RSD 1.1%, interday RSD 2.1%). The intraday and interday RSDs of the mass spectrum signal intensity in the second dimension were 12.1% and 16.9% respectively. These values are in the expected range for ESI-MS measurements without the application of specific internal standards. Since the main purpose of the CZE–CZE–MS setup was the characterization and not the quantification of mAb variants, these RSDs were considered acceptable for this kind of application.

The raw mass spectra as well as the deconvoluted mass spectra showed the typical glycoform pattern of trastuzumab, as illustrated in Fig. 4b and c. The mass differences (161.5–162.1 Da) between the three main glycoforms match well with the expected difference of one hexose molecule (162.1 Da). For the three highest-abundance glycoforms, G0F/G0F, G0F/

G1F, and G1F/G1F (G0F/G2F), average masses of $148,059.1 \pm 0.8$ Da, $148,220.1 \pm 0.5$ Da, and $148,381.6 \pm 0.6$ Da ($n = 5$) respectively were determined. This corresponds to a deviation of +20.2, +13.0, and +8.4 ppm compared with the theoretically calculated average masses (148,056.1, 148,218.2, and 148380.4 Da) obtained with the “representative isotopic distributions” of IUPAC [36]. The masses obtained are well within the expected accuracy, taking the MS data of other published work for trastuzumab into consideration (approximately +22 to +38 ppm, calculated on the basis of illustrated mass spectra and data) [2, 25]. The data presented as well as the literature data show a general tendency to slightly higher masses compared with the calculated values. There are several possible explanations for this observation, including a not considered PTM, a shift caused by the mass calibration procedure, the formation of adducts affecting the average mass, or a divergent isotopic distribution of elements. Trastuzumab has been studied thoroughly over the years on all types of analytical levels. Thus, the presence of an unknown, not considered, PTM causing a minor positive shift in mass can be excluded. In addition, different calibration models (quadratic and linear) were tested. The calibration model applied caused only a minor, nonsystematic difference in the resulting mass (e.g., G0F/G1F, quadratic $148,220.1 \pm 0.5$ Da, linear $148,220.2 \pm 0.5$ Da). Therefore, the calibration model applied can be excluded as a source of the observed slightly higher masses. Furthermore, the influence of adduct formation on the determined mass was investigated. Adducts, including ammonium or sodium adducts, are not fully resolved from the protonated species because of the broad isotopic pattern of the intact antibody (approximately 25 Da at full width at half maximum). It does not appear unlikely for one or a few of the protons (38–62) to be exchanged for another cation. For this purpose, a simple simulation was performed, taking the mass distribution of the protonated form, the sodium adduct, and the ammonium adduct of the mAb into consideration. If in 20% of cases one proton is exchanged by one ammonium (or in 41% of cases by one sodium), a shift of +1 Da is observed for the mAb signal. This corresponds to a proton exchange of 0.3–0.5% by ammonium (or 0.7–1.1% by sodium) considering all available protons. On the other hand, the relative amount of ^{13}C in the “representative isotopic distributions” of IUPAC ($\delta^{13}\text{C} = -37$) [36] is already out of range regarding the natural isotopic distribution of carbon in

Table 1 Results of the validation of the Capillary zone electrophoresis (CZE)–CZE–mass spectrometry system

Dimension	Intraday RSD (%), $n = 5$				Interday RSD (%), $n = 10$			
	Current	Flow rate	Migration time	Peak intensity	Current	Flow rate	Migration time	Peak intensity
1st	1.8	0.9	0.8	1.1	2.9	4.4	3.1	2.1
2nd	1.2	-	1.7	12.1	1.5	-	6.2	16.9

RSD relative standard deviation

organic material (C_3 , C_4 , and crassulacean acid metabolism plants, $\delta^{13}C = -10$ to -33) [37]. Thus, a deviation in the isotopic distribution of carbon could be a plausible explanation for the observed masses. Taking the entire width of the natural organic carbon distribution into account, the theoretically calculated values for the three main glycoforms are 148,057.2 Da (G0F/G0F), 148,219.4 Da (G0F/G1F), and 148,381.5 Da (G1F/G1F and G0F/G2F), with a range of ± 0.8 Da. With these ranges, a mass deviation between -5.1 and $+17.9$ ppm was determined for the measured masses. If the measurement uncertainty (2σ) is taken into consideration, the observed masses are in agreement with these calculated masses. In conclusion, an accurate assessment of the mass accuracy was not possible because of missing information regarding the exact isotopic distribution of elements, especially carbon, in trastuzumab. Additional information (e.g., the origin of the amino acids applied in the manufacturing of trastuzumab) could result in a more precise value for the theoretically calculated masses, highlighting the challenge of accurate mass calculation for high-mass molecular species.

In general, basic and acidic variants of mAbs are considerably less concentrated compared with the main form. Thus, it is important to verify that the resulting measured mass is not significantly influenced by the concentration. In this regard, the main variant was cut five times on the different concentrations: 30, 18, and 9 mg/mL. No significant difference was

observed between all three concentrations (G0F/G1F $148,220.0 \pm 0.4$ Da, $148,220.1 \pm 0.5$ Da, and $148,220.4 \pm 0.5$ Da respectively).

Subsequently, the most intensive acidic variant of trastuzumab (30 mg/mL) was cut. A slightly higher mass (approximately 1–3 Da) was observed compared with the main variant (data not shown). The signal was very noisy, and thus not sufficient for a repeatable accurate mass determination (standard deviation 1.8 Da; $n = 5$). Therefore, a detailed interpretation of the data was not possible. Furthermore, the analysis of higher concentrations did not result in better data quality, because of loss of resolution and peak broadening in the first dimension. Nevertheless, a slightly higher mass of the intact mAb in combination with a noticeable shift to higher migration times implies the presence of potential deamidation processes.

Deglycosylated mAb samples

To increase the sensitivity and simultaneously simplify the spectrum, a deglycosylation of trastuzumab samples was performed with *N*-glycosidase F. An electropherogram from the first dimension analyzing deglycosylated trastuzumab (6 mg/mL) is shown in Fig. 5a. It is apparent that the mAb profile changed compared with that for the glycosylated sample (see Fig. 2), resulting in distinct higher intensities for the acidic

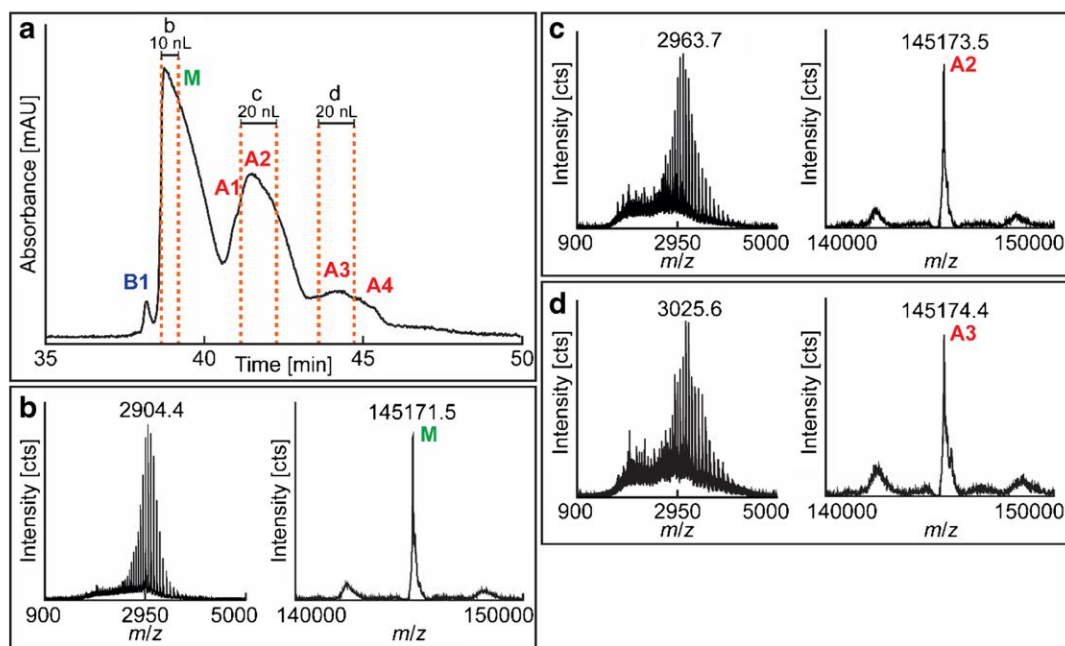


Fig. 5 a Capillary zone electrophoresis (CZE)–UV electropherogram of deglycosylated trastuzumab (6 mg/mL). Separation was performed with the CZE–CZE–mass spectrometry setup. In the first dimension, a separation voltage of +10 kV, 380 mM ϵ -aminocaproic acid, 1.9 mM triethylenetetramine, and 0.05% (hydroxypropyl)methyl cellulose (pH 5.7) as the background electrolyte, and bare fused-silica capillaries

(total length 60 cm) were used. In the second dimension, a separation voltage of +10 kV, 2 M acetic acid as the background electrolyte, and poly(vinyl alcohol)-coated capillaries (total length 80 cm) were used. Raw and deconvoluted mass spectra of the main variant (10-nL cut) (b), acidic variant A2 (20-nL cut) (c), and acidic variant A3 (20-nL cut) (d). For the cut of A3, a more concentrated sample was used (30 mg/mL)

variants. This implies a chemical alteration of the sample induced by the *N*-glycosidase F treatment. First, the main variant was cut five consecutive times. An example deconvoluted mass spectrum of the main variant is displayed in Fig. 5b. A mass of $145,171.5 \pm 0.4$ Da was observed, showing no distinct signals of remaining glycosylated variants. Similar results were obtained by analysis of a less concentrated trastuzumab sample (4 mg/mL), giving a mass of $145,171.5 \pm 0.5$ Da ($n = 4$) for the main mAb variant. Thus, for both glycosylated and deglycosylated samples, mass spectra with high reproducibility (standard deviation less than 1 Da) at different concentrations have been obtained.

Subsequently, the highest-abundance acidic variant A2 was cut multiple times ($n = 5$). An example of a deconvoluted mass spectrum is shown in Fig. 5c. As already indicated by the analysis of the glycosylated sample, a slightly higher mass compared with the main variant was observed ($145,173.5 \pm 0.6$ Da), which corresponds to a shift of +2.0 Da. The mass difference from the main variant was confirmed to be statistically significant (t test $\alpha = 0.05$; $p < 10^{-5}$). To achieve sufficient signal intensity, a more concentrated deglycosylated sample (30 mg/mL) was analyzed. A mass of $145,174.6 \pm 0.8$ Da was detected, which corresponds to a mass difference of +3.1 Da compared with the main variant. The mass difference ($\Delta m = 1.1$ Da) between A2 and A3 was confirmed to be statistically significant (t test $\alpha = 0.05$; $p = 0.018$).

As stated before, the acidic variants can most likely be attributed to deamidation products, because of the slightly higher masses combined with a considerable shift to longer migration times. Thus, the acidic variants A2 and A3 could correspond to a double and a triple deamidation respectively. In principle, trastuzumab possesses several positions in the peptide chain that can be potentially deamidated [34]. Most studies are focused on Asn30 in the light chain. However, Asn55 located in complementarity-determining region 2 of the heavy chain is also known to be susceptible to deamidation at elevated pH values (greater than 7.5). This hypothesis is additionally substantiated by the elevated intensity of the acidic variants after deglycosylation at pH 8 (see Figs. 2 and 5a). Furthermore, *N*-glycosidase F treatment is known to cause significant amounts of additional chemical deamidation [38]. In summary, the occurrence of deamidation products is a plausible and compelling explanation for the identity of the acidic variants A2 and A3.

Conclusion

Besides IEC, mAb charge variants are routinely quantified in biopharmaceutical applications by EACA-based CZE–UV methods [5]. We have developed and validated a heart-cut CZE–CZE–MS method for the detailed MS characterization of mAb charge variants using a generic EACA-based

electrolyte. A clear online assignment of MS data to the peaks in this ESI-interfering CZE–UV system is possible. Highly precise mass data (standard deviation 0.4–0.8 Da) of glycosylated and deglycosylated variants of trastuzumab as a model mAb system were obtained. The measured and calculated masses were in good agreement (low parts per million range). Remaining uncertainty likely originates, for example, from potential adduct formation during the measurement and the relative isotopic abundances used for the calculation, highlighting the challenge of accurate mass determination for high-mass molecular species. Combining the electrophoretic separation and the highly precise masses, we identified potential deamidation products for an intact antibody. The entire system is expected to be applicable to a variety of different BGEs. Thus, extensively optimized electrolyte conditions for specific mAbs can be coupled with MS in the CZE–CZE–MS setup presented. Still, there is room for improvement regarding sensitivity and sample pretreatment (generation of additional deamidation caused by deglycosylation procedure) to characterize even very low abundance charge variants. The overall analysis time is rather long; however, the actual CZE–CZE–MS method is needed only for characterization purposes, whereas the underlying first-dimension separation (CZE–UV detection) is applied routinely for reliable quantitation. The CZE–CZE–MS system presented has the potential to become a compelling tool for the characterization of mAb charge variants separated in MS-incompatible BGE systems.

Compliance with ethical standards

Conflict of interest The authors declare that they have no conflict of interest.

References

1. Fekete S, Guillarme D, Sandra P, Sandra K. Chromatographic, electrophoretic, and mass spectrometric methods for the analytical characterization of protein biopharmaceuticals. *Anal Chem.* 2016;88(1):480–507.
2. Sandra K, Vandenheede I, Sandra P. Modern chromatographic and mass spectrometric techniques for protein biopharmaceutical characterization. *J Chromatogr A.* 2014;1335:81–103.
3. Li J, Zhu Z. Research and development of next generation of antibody-based therapeutics. *Acta Pharmacol Sin.* 2010;31(9):1198–207.
4. Redman EA, Batz NG, Mellors JS, Ramsey JM. Integrated microfluidic capillary electrophoresis-electrospray ionization devices with online MS detection for the separation and characterization of intact monoclonal antibody variants. *Anal Chem.* 2015;87(4):2264–72.
5. Moritz B, Schnaible V, Kiessig S, Heyne A, Wild M, Finkler C, et al. Evaluation of capillary zone electrophoresis for charge heterogeneity testing of monoclonal antibodies. *J Chromatogr B.* 2015;983–984:101–10.

6. Liu H, Ponniah G, Zhang H-M, Nowak C, Neill A, Gonzalez-Lopez N, et al. In vitro and in vivo modifications of recombinant and human IgG antibodies. *mAbs*. 2014;6(5):1145–54.
7. Visser J, Feuerstein I, Stangler T, Schmiederer T, Fritsch C, Schiestl M. Physicochemical and functional comparability between the proposed biosimilar rituximab GP2013 and originator rituximab. *BioDrugs*. 2013;27(5):495–507.
8. Liu H, Jeong J, Kao Y-H, Zhang YT. Characterization of free thiol variants of an IgG1 by reversed phase ultra high pressure liquid chromatography coupled with mass spectrometry. *J Pharm Biomed*. 2015;109:142–9.
9. Stoll DR, Harnes DC, Danforth J, Wagner E, Guillaume D, Fekete S, et al. Direct identification of rituximab main isoforms and subunit analysis by online selective comprehensive two-dimensional liquid chromatography-mass spectrometry. *Anal Chem*. 2015;87(16):8307–15.
10. Woodard J, Lau H, Latypov RF. Nondenaturing size-exclusion chromatography-mass spectrometry to measure stress-induced aggregation in a complex mixture of monoclonal antibodies. *Anal Chem*. 2013;85(13):6429–36.
11. Birdsall RE, Shion H, Kotch FW, Xu A, Porter TJ, Chen W. A rapid on-line method for mass spectrometric confirmation of a cysteine-conjugated antibody-drug-conjugate structure using multidimensional chromatography. *mAbs*. 2015;7(6):1036–44.
12. Reusch D, Habegger M, Maier B, Maier M, Kloseck R, Zimmermann B, et al. Comparison of methods for the analysis of therapeutic immunoglobulin G Fc-glycosylation profiles—part I: separation-based methods. *mAbs*. 2015;7(1):167–79.
13. Zhang Z, Perrault R, Zhao Y, Ding J. SpeB proteolysis with imaged capillary isoelectric focusing for the characterization of domain-specific charge heterogeneities of reference and biosimilar rituximab. *J Chromatogr B*. 2016;1020:148–57.
14. Szekrényes A, Roth U, Kerékgyártó M, Székely A, Kurucz I, Kowalewski K, et al. High-throughput analysis of therapeutic and diagnostic monoclonal antibodies by multicapillary SDS gel electrophoresis in conjunction with covalent fluorescent labeling. *Anal Bioanal Chem*. 2012;404(5):1485–94.
15. He Y, Lacher NA, Hou W, Wang Q, Isele C, Starkey J, et al. Analysis of identity, charge variants, and disulfide isomers of monoclonal antibodies with capillary zone electrophoresis in an uncoated capillary column. *Anal Chem*. 2010;82(8):3222–30.
16. Gassner A-L, Rudaz S, Schappler J. Static coatings for the analysis of intact monoclonal antibody drugs by capillary zone electrophoresis. *Electrophoresis*. 2013;34(18):2718–24.
17. Jaccoulet E, Smadja C, Prognon P, Taverna M. Capillary electrophoresis for rapid identification of monoclonal antibodies for routine application in hospital. *Electrophoresis*. 2015;36(17):2050–6.
18. Shi Y, Li Z, Qiao Y, Lin J. Development and validation of a rapid capillary zone electrophoresis method for determining charge variants of mAb. *J Chromatogr B*. 2012;906:63–8.
19. Fekete S, Gassner A-L, Rudaz S, Schappler J, Guillaume D. Analytical strategies for the characterization of therapeutic monoclonal antibodies. *Trends Anal Chem*. 2013;42:74–83.
20. Dai H, Li G, Krull I. Separation and quantitation of monoclonal antibodies in cell growth medium using capillary zone electrophoresis. *J Pharm Biomed*. 1998;17(6–7):1143–53.
21. Redman EA, Mellors JS, Starkey JA, Ramsey JM. Characterization of intact antibody drug conjugate variants using microfluidic capillary electrophoresis-mass spectrometry. *Anal Chem*. 2016;88(4):2220–6.
22. He Y, Isele C, Hou W, Ruesch M. Rapid analysis of charge variants of monoclonal antibodies with capillary zone electrophoresis in dynamically coated fused-silica capillary. *J Sep Sci*. 2011;34(5):548–55.
23. la Garza E-de, Carlos E, Perdomo-Abúndez FC, Padilla-Calderón J, Uribe-Wiechers JM, Pérez NO, et al. Analysis of recombinant monoclonal antibodies by capillary zone electrophoresis. *Electrophoresis*. 2013;34(8):1133–40.
24. Glover ZWK, Gennaro L, Yadav S, Demeule B, Wong PY, Sreedhara A. Compatibility and stability of pertuzumab and trastuzumab admixtures in i.v. infusion bags for coadministration. *J Pharm Sci*. 2013;102(3):794–812.
25. Beck A, Wagner-Roussel E, Ayoub D, van Dorsselaer A, Sanglier-Cianfèrani S. Characterization of therapeutic antibodies and related products. *Anal Chem*. 2013;85(2):715–36.
26. Habegger M, Leiss M, Heidenreich A-K, Pester O, Hafenmair G, Hook M, et al. Rapid characterization of biotherapeutic proteins by size-exclusion chromatography coupled to native mass spectrometry. *mAbs*. 2016;8(2):331–9.
27. Gahoual R, Beck A, Leize-Wagner E, François Y-N. Cutting-edge capillary electrophoresis characterization of monoclonal antibodies and related products. *J Chromatogr B*. 2016;1032:61–78.
28. Kohl FJ, Sánchez-Hernández L, Neusüß C. Capillary electrophoresis in two-dimensional separation systems: techniques and applications. *Electrophoresis*. 2015;36(1):144–58.
29. Kler PA, Sydes D, Huhn C. Column-coupling strategies for multi-dimensional electrophoretic separation techniques. *Anal Bioanal Chem*. 2015;407(1):119–38.
30. Kohl FJ, Montealegre C, Neusüß C. On-line two-dimensional capillary electrophoresis with mass spectrometric detection using a fully electric isolated mechanical valve. *Electrophoresis*. 2016;37(7–8):954–8.
31. Hühner J, Neusüß C. CIEF-CZE-MS applying a mechanical valve. *Anal Bioanal Chem*. 2016;408(15):4055–61.
32. Neuberger S, Jooß K, Ressel C, Neusüß C. Quantification of ascorbic acid and acetylsalicylic acid in effervescent tablets by CZE-UV and identification of related degradation products by heart-cut CZE-CZE-MS. *Anal Bioanal Chem*. 2016;408(30):8701–12.
33. Hühner J, Jooß K, Neusüß C. Interference-free mass spectrometric detection of capillary isoelectric focused proteins, including charge variants of a model monoclonal antibody. *Electrophoresis*. 2017;38(6):914–21.
34. Bults P, Bischoff R, Bakker H, Gietema JA, van de Merbel, Nico C. LC-MS/MS-based monitoring of in vivo protein biotransformation: quantitative determination of trastuzumab and its deamidation products in human plasma. *Anal Chem*. 2016;88(3):1871–7.
35. Harris RJ, Kabakoff B, Macchi FD, Shen FJ, Kwong M, Andya JD, et al. Identification of multiple sources of charge heterogeneity in a recombinant antibody. *J Chromatogr B*. 2001;752(2):233–45.
36. Berglund M, Wieser ME. Isotopic compositions of the elements 2009 (IUPAC technical report). *Pure Appl Chem*. 2011;83(2):397–410.
37. O'Leary MH. Carbon isotopes in photosynthesis. *Bioscience*. 1988;38(5):328–36.
38. Palmisano G, Melo-Braga MN, Engholm-Keller K, Parker BL, Larsen MR. Chemical deamidation: a common pitfall in large-scale N-linked glycoproteomic mass spectrometry-based analyses. *J Proteome Res*. 2012;11(3):1949–57.



Kevin Jooß is a PhD student at Aalen University and Helmholtz Zentrum München. He has been working on the analysis of small-molecule drugs, complex proteins, and *N*-glycans by applying capillary zone electrophoresis–mass spectrometry. His PhD project is related to the development and application of two-dimensional electromigrative separation techniques coupled with mass spectrometry. His latest interest is focused on the characterization of monoclonal

antibody charge variants, including detailed interpretation of mass-spectrometric information.



Bernd Moritz is a group head in the Analytical Development and Quality Control Department of Pharma Technical Development Europe (Biologics) Analytics at F. Hoffmann-La Roche Ltd, Basel, Switzerland. He works in the field of developing, validating, and characterizing methods for the physicochemical analysis of proteins, mainly antibodies, for release and stability testing with focus on separation techniques such as capillary electrophoresis.



Jens Hühner is a former PhD student at Aalen University and the University of Tübingen. During his PhD studies he worked on the development and application of two-dimensional electromigrative separation techniques coupled with mass spectrometry, especially for the characterization of capillary isoelectric focused proteins. Since February 2017, he has been a product manager and support engineer for workflow and instrument diagnostic software at Agilent Technologies. In this role, he focuses on new and intuitive workflows for method scouting and development.

ware at Agilent Technologies. In this role, he focuses on new and intuitive workflows for method scouting and development.



Christian Neusüß is Full Professor in the Faculty of Chemistry at Aalen University. His research interests include sophisticated separation techniques coupled with (high-resolution) mass spectrometry. He is an expert in capillary electrophoresis–mass spectrometry with various applications, especially in the biopharmaceutical field. His latest research focus is on the development of two-dimensional electromigrative separation techniques coupled with mass spectrometry.



Steffen Kiessig is a group head in the Analytical Development and Quality Control Department of Pharma Technical Development Europe (Biologics) Analytics at F. Hoffmann-La Roche Ltd, Basel, Switzerland. He works in the field of developing and validating methods for the physicochemical analysis of proteins, mainly antibodies, for release and stability testing with focus on separation techniques such as chromatography and capillary electrophoresis.

III: Overview of CE-CE-MS applications developed for ESI-interfering electrolytes

Two-dimensional capillary electrophoresis-mass spectrometry (CE-CE-MS): coupling MS-interfering capillary electromigration methods with mass spectrometry

J. Schlecht, K. Jooß, C. Neusüß

Analytical and Bioanalytical Chemistry (2018) 410(25):6353-6359

Based on the success of the CE-CE-MS system utilizing the mechanical 4-port valve interface, we were invited to submit a trend article involving the coupling of MS-interfering CE methods with mass spectrometry. In the first section, alternative approaches to CE-CE-MS are critically discussed including off-line fraction collection, alternative ionization, dilution, or the change to volatile electrolyte constituents. Nevertheless, all of these options represent a compromise between separation efficiency and sensitivity of MS detection. The second part of the article revolves around the advantages, limitations and applications of the CE-CE-MS system including future perspectives.

Candidate's contribution:

Preparation of second part of the manuscript (CE-CE-MS section) including literature search. Creation of all presented figures in the manuscript.



Two-dimensional capillary electrophoresis-mass spectrometry (CE-CE-MS): coupling MS-interfering capillary electromigration methods with mass spectrometry

Johannes Schlecht^{1,2} · Kevin Jooß^{1,3} · Christian Neusüß¹Received: 16 April 2018 / Revised: 17 May 2018 / Accepted: 23 May 2018 / Published online: 4 June 2018
© Springer-Verlag GmbH Germany, part of Springer Nature 2018

Abstract

Electromigration separation techniques often demand certain compounds in the electrolyte to achieve the required selectivity and efficiency. These compounds, including the electrolyte itself, ampholytes, polymeric compounds for sieving, complexing agents, tensides, etc. are often non-volatile. Thus, interference with the electrospray ionization process is a common issue, impeding direct coupling of such electrolyte systems to mass spectrometry. Still, several options exist to obtain mass spectra after separation, including offline fractionation, alternative ionization, dilution, or the change to volatile constituents. In the first part of this article, these methods are discussed. However, all of these options are a compromise of separation performance and sensitivity of mass spectrometric detection. Two-dimensional capillary electrophoresis-mass spectrometry (CE-CE-MS) systems represent a promising alternative to the aforementioned challenges, as they allow the use of existing methods with best separation performance in combination with sensitive mass characterization. In this context, the second part of this article is dedicated to the advantages, limitations, and applications of this approach. Finally, an outlook towards future developments is given.

Keywords Capillary electrophoresis · Electrospray ionization · Two-dimensional separation · Interference-free mass spectrometry · Pharmaceutical analysis · 2D interface

Abbreviations

2D	Two dimensional	CIEF	Capillary isoelectric focusing
AA	Ascorbic acid	CZE	Capillary zone electrophoresis
ACE	Affinity capillary electrophoresis	ESI	Electrospray ionization
APCI	Atmospheric pressure chemical ionization	ICP	Inductive-coupled plasma
APPI	Atmospheric pressure photo ionization	mAb	Monoclonal antibody
ASA	Acetylsalicylic acid	MALDI	Matrix-assisted-laser desorption/ionization
BGE	Background electrolyte	MEKC	Micellar electrokinetic chromatography
CD	Cyclodextrin	MS	Mass spectrometry
CE	Capillary electrophoresis	SDS	Sodium dodecyl sulfate
CSE	Capillary sieving electrophoresis		

✉ Christian Neusüß
Christian.Neusuess@hs-aalen.de

¹ Faculty of Chemistry, Aalen University, Beethovenstrasse 1, 73430 Aalen, Germany

² Pharmaceutical/Medicinal Chemistry, Institute of Pharmacy, Friedrich-Schiller-University Jena, Philosophenweg 14, 07743 Jena, Germany

³ Research Unit Analytical BioGeoChemistry, Helmholtz Zentrum München, Ingolstädter Landstr. 1, 85764 Neuherberg, Germany

Introduction

Electromigration techniques such as capillary electrophoresis (CE) enable highly selective and efficient separation for a variety of ionic compounds. Since its introduction in the early 1980s, CE has emerged as a powerful analytical routine tool in the fields of environmental analysis [1, 2], forensic analysis [3], food analysis [4], and bioanalytical analysis [5]. Electromigration includes several techniques such as capillary zone electrophoresis (CZE), capillary isoelectric focusing (CIEF), capillary sieving electrophoresis (CSE), micellar

electrokinetic chromatography (MEKC), and affinity capillary electrophoresis (ACE).

The most common mode of operation is CZE. Separation in CZE occurs according to different electrophoretic mobilities of ions based on their charge-to-size ratio in an electric field. Typical analytes span from small to large molecules, such as proteins including monoclonal antibodies (mAbs) [6]. The selectivity is mainly given by pH (charge of the analyte) and the background electrolyte (BGE). It can be altered by the type of solvent (non-aqueous capillary electrophoresis). Furthermore, additives are often used to modify the mobility, e.g., cyclodextrins can be applied for enantiomeric separation (chiral CZE) or affinity interaction can be studied by adding, e.g., antigens.

By adding a (pseudo)gel, molecules with similar charge-to-size ratio but different size can be separated referred as capillary sieving electrophoresis (CSE). This principle is widely applied for DNA sequencing [7] and protein separation [8] (after complexing with sodium dodecyl sulfate (SDS)). In CIEF, proteins and peptides are separated in a pH gradient formed in a capillary after applying an electric field. The pH gradient is formed utilizing an acidic anolyte, a basic catholyte, and ampholytes in the BGE. In MEKC, analytes are separated by the use of a pseudostationary phase consisting of micelles.

Mass spectrometry is a major technique for the characterization and identification of analytes separated in gas or liquid phase. Electrospray ionization (ESI) is an efficient way to transfer analytes separated in liquid phase into the mass analyzer, especially ionic species as separated in CE. Efficient ESI premises the absence of non-volatile constituents, which often can be achieved in liquid chromatography (LC) without compromising separation. However, most capillary electromigration techniques (as discussed above) require dedicated compounds in the electrolyte for selective separation, compatible with optical detection (UV-Vis absorption, fluorescence) but not with ESI-MS. Nevertheless, possible solutions to obtain online mass spectra from such electromigration techniques exist and are discussed in this paper.

Strategies for direct coupling of MS-interfering capillary electromigration methods to mass spectrometry

Capillary electrophoresis coupled with mass spectrometry (CE-MS) has become a powerful routine tool for analysis of a broad range of analytes. In recent years, several applications about CE-MS have been published highlighting its diversity and importance, including metabolite and intact protein analysis [9–12]. In these applications, almost entirely volatile BGEs have been used.

The pH is the most important parameter for selectivity in CZE. The availability of volatile BGE systems in CZE, covering almost the entire pH range, enables the direct coupling of these methods to ESI-MS. Most common BGEs for CZE-MS applications are formic acid (HFA) and acetic acid (HAc) for low pH values and their respective ammonium salts for acidic to neutral pH values. Other volatile buffers for higher pH ranges include ammonium carbonate ((NH₄)₂CO₃) as well as ammonium hydroxide (NH₄OH). The mentioned volatile buffer electrolytes cover the total pH range. However, the type of BGE and possible additives can also influence the selectivity in CE separations, which can limit their applicability to CZE-MS. The separation of anionic active ingredients and their degradation products in effervescent tablets using different BGEs is shown in Fig. 1. In this case, only the highly ESI-interfering 100 mM tricine electrolyte enables the complete separation of all analytes. Both, the use of a lower concentrated tricine and the use of volatile acetate- or formate-based BGE are insufficient in this regard. The low number of different electrolytes suitable for CZE-MS does not only restrict the versatility of the separation itself, but also the possible use of preconcentration techniques such as transient-isotachopheresis.

CE modes such as CIEF (ampholytes, anolyte, catholyte), chiral CZE (cyclodextrins), and MEKC (surfactants) often rely on ESI-interfering electrolyte compounds. For these techniques, the complete exchange of the BGE system, avoiding non-volatile or ESI-interfering compounds is often very difficult preserving the original separation efficiency and selectivity. Nevertheless, e.g., for MEKC, volatile [13, 14] or at least semi-volatile [15] surfactants can be used in certain applications. If this most straightforward approach using volatile electrolytes is not accessible, other options need to be considered.

Another approach is the use of BGEs with low concentrated interfering compounds. Still, a compromise between MS compatible conditions and separation performance of the CE method has to be made as shown for tricine-based separation of anions in Fig. 1. In addition, low electrolyte concentration limits the possible injection volume. The most common strategy for coupling CIEF with ESI-MS is the direct hyphenation using low ampholyte concentrations. Tang et al. [16] described the first direct hyphenation of CIEF with MS using an ampholyte concentration of 0.5% for a compromise between CIEF resolution and ESI-MS detection. Further approaches of direct CIEF-MS are described in detail in a recent review [17]. Another alternative is the use of partial filling techniques, which have been applied especially for the coupling of chiral CZE and MEKC to ESI-MS [18, 19]. In these cases, the EOF and the migration direction/order play a crucial role and need to be optimized during method development.

Most CE-MS applications have been performed using a sheath liquid interface, where a sheath liquid at a flow rate in the low microliter-per-minute range provides the contact

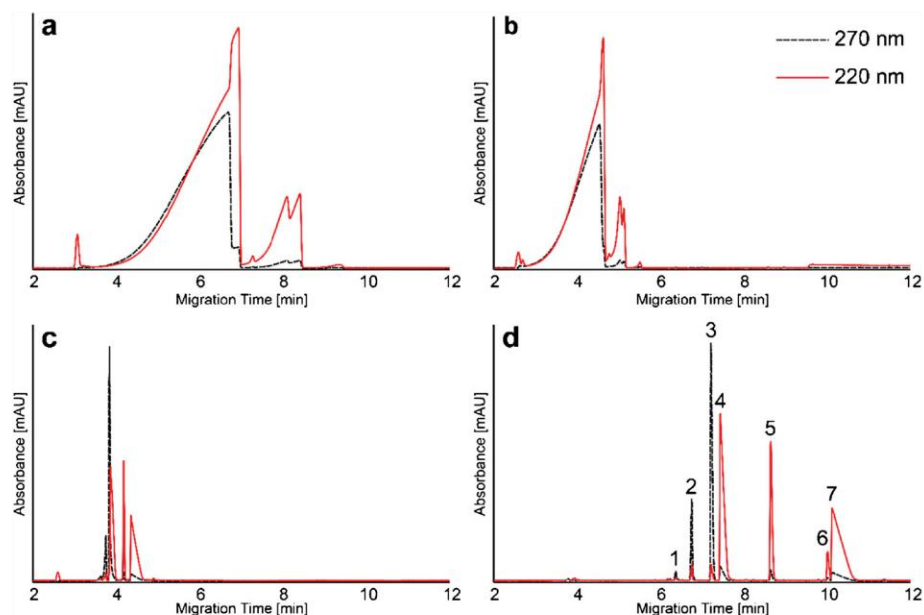


Fig. 1 Comparison of different BGEs for the separation of ascorbic acid (AA), acetylsalicylic acid (ASA), and related degradation products in degraded effervescent tablets (RH 75%, $T = 30\text{ }^{\circ}\text{C}$, $t = 72\text{ h}$). The CZE-UV separation was performed applying +20 kV in a 50-cm fused silica capillary. Two different wavelengths were used: 220 nm (red, solid) and 270 nm (black, dashed). Four different BGEs are compared: 25 mM

ammonium formate, pH = 6 (a); 25 mM ammonium acetate, pH = 9 (b); 25 mM tricine, pH = 8.8 (c); 100 mM tricine, pH = 8.8 (d). The peaks in the 100 mM tricine BGE were assigned to diacetylated AA (1), monoacetylated AA (2), AA (3), ASA (4), naphthalenesulfonic acid as internal standard (5), saccharin (6), and salicylic acid (7)

between the capillary outlet and a surrounding metal needle. In the last years, nanospray interfaces have become more popular, especially since the commercialization of the porous tip and a nanosheath liquid interface. For details of coupling, we refer to recent reviews [20, 21]. NanoESI processes (flow rates < 1000 nL/min) are generally more tolerant to ESI-interfering compounds and offer higher sensitivity. Thus, these interfaces are expected to be more useful for coupling ESI-interfering CE methods with MS. The field of application regarding nanoESI in combination with non-volatile BGEs is relatively new. Nevertheless, the direct hyphenation of CIEF with MS was recently introduced by Dai et al. utilizing a nanosheath liquid interface [22]. Still, there is need for further systematic investigations regarding the degree of compromise considering the concentration of interfering substances, if nanoESI interfaces are used.

A different approach for coupling CE to MS and reduce BGE-related MS interference is the use of alternative ion sources to ESI. Examples are matrix-assisted laser desorption/ionization (MALDI) [23], atmospheric pressure chemical ionization (APCI) [24], atmospheric pressure photo ionization (APPI) [25], and inductive-coupled plasma (ICP) [26]. However, ICP is limited to elemental analysis, especially metals, whereas APCI and APPI are more suited for small, less polar analytes, which are typically not accessible by electromigration separation techniques. The use of MALDI for CE separations is limited to spotted fractions.

Still, in order to maintain the original separation performance in combination with a sensitive mass spectrometric detection, further approaches such as multidimensional separation methods need to be considered.

CE-CE-MS for coupling MS-interfering capillary electromigration methods to mass spectrometry

Two-dimensional (2D) separation techniques are commonly used to increase peak capacity by combining two separation techniques/modes with different selectivities (e.g., combination of LC and CE methods). Hence, superior separation performance can be achieved compared with the respective individual separation dimensions [27]. Here, we discuss an alternative purpose to allow interference-free mass spectrometric detection of analytes separated in highly ESI-interfering electrolyte systems applied as the 1st dimension [28]. Remaining interfering electrolyte compounds of the 1st dimension are either completely removed from the sample or separated from the analytes of interest in the 2nd dimension prior to MS detection. Considering any CE mode as 1st dimension, there are generally two different approaches classified as offline and online.

Applying offline 2D coupling methods, fractions of a 1st separation dimension are collected and subsequently

transferred to a 2nd separation dimension. This approach is rather simple and often preferred, especially if additional sample preparation steps in between the two separation methods are required (e.g., solvent exchange, derivatization, or digestion). Nevertheless, fraction collection in CE is associated with high dilution of the sample, as typical fractions in CE are in the lower nanoliter range which have to be collected in at least a few microliters of solvent [29]. This challenge can be tackled by performing an additional concentration step prior to injection in the 2nd dimension; however, this makes the entire 2D system more complex and sensitive against disturbances. In general, offline methods are time consuming, labor intensive, and also automation is limited. Thus, in contrast with LC, fraction collection is rarely applied in CE.

In contrast, online coupling of two CE dimensions potentially enables a direct sample transfer with minor dilution. For online coupling a dedicated sample transfer in the nanoliter range from the 1st to a 2nd dimension is required. A variety of 2D concepts have been developed, including dialysis, flow gating interfaces, and microfluidic chips [30, 31]. Still, most of this work has been performed with optical detection and ESI-interfering electrolyte systems in the 2nd dimension. Especially, flow-gating interfaces and interface-free microfluidic chips are challenging to couple to MS, due to the open nature of the system (absence of outlet vial).

Mechanical-valve-based interfaces are frequently used in LC-LC coupling. Regarding the use of such a valve for CE-CE, certain other requirements need to be fulfilled. Due to the high voltages applied in CE, a fully isolated valve is required and thus, metal components in direct contact or near proximity of the electrolyte solutions must be avoided. Furthermore, based on the miniature nature of CE, the transfer of very small volumes (low nanoliter range) from the 1st to the 2nd separation dimension needs to be achieved. In recent years, our group has developed a CE-CE-MS system using a four-port mechanical valve as interface. A scheme of the general CE-CE-MS setup is depicted in Fig. 2. The valve consists of three major parts: the stator, the rotor comprising the sample loop (4–20 nL), and the motor. A mixture of polyether ether ketone and polytetrafluoroethylene was chosen as rotor and stator material to provide sufficient resistivity and tightness of the valve. Due to the material properties and the close distance of the rotor channels, up to ± 15 kV can be applied in both dimensions in order to avoid potential current breakthroughs [28]. The inlet and outlet capillaries of the 1st and 2nd separation dimension are connected to the four-port valve, respectively. In general, the 1st dimension can be operated in any CE mode (CZE, CIEF, CE(SDS), etc.) and usually UV detection is applied provided by an external detector placed right in front of the valve through the inlet. During the CE separation of the 1st dimension, the mechanical valve is kept in loading position, where the sample loop is connected to the 1st dimension, until the analyte of interest is positioned in the sample

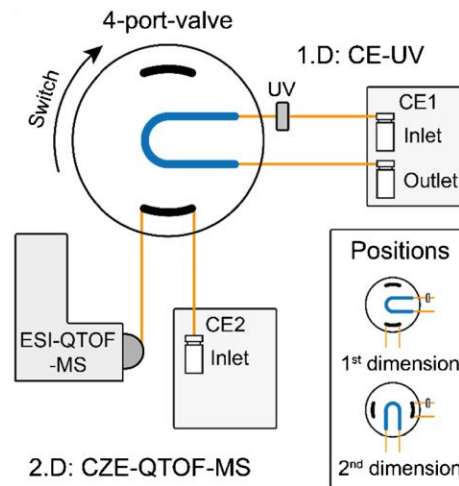


Fig. 2 General setup of the CE-CE-MS system developed in our group. The inlet and outlet capillary of the 1st dimension CE-UV method (CE1 instrument) are connected to the four-port valve (upper, right side). An external UV detector cell is positioned in front of the valve through the inlet of the 1st dimension. Various CE separation modes can be applied as 1st dimension including CZE, CIEF, and CE(SDS). The inlet and outlet capillaries of the 2nd-dimension CZE-QTOF-MS (CE2 and MS instrument) are connected to the remaining channels of the four-port valve (lower part). During the CE(UV) separation, the mechanical valve is kept in loading position where the sample loop is connected to the 1st dimension. When the desired analyte is located in the sample loop, the valve is switched to inject position transferring the analyte from the 1st to the 2nd dimension. Subsequently, high voltage (10 to 15 kV) is applied for separation. The insert contains the position of the valve for the separation in the 1st dimension and the position of the valve for the separation in the 2nd dimension

loop. The external UV detector and the known distance between detector cell and center of the sample loop is used to determine the correct time to cut desired peaks. Subsequently, the valve is switched to inject position transferring the analyte from the 1st to the 2nd dimension and high voltage (± 10 to 15 kV) is applied for separation. Typically, CZE is performed in the 2nd dimension due to the availability of volatile BGEs (e.g., formate or acetate). A major characteristic of this 2D setup is, that both dimension are operated completely independent (e.g., coating and equilibration procedures).

Several applications have been developed utilizing the above-mentioned CE-CE-MS system. In our group, a CZE-UV for the simultaneous determination of ascorbic acid (AA), acetylsalicylic acid (ASA), and their related degradation products in effervescent tablets has been developed. Since the BGE contains 100 mM tricine, direct coupling of this method to ESI-MS was not possible. Thus, this method was the first showcase for a highly ESI-interfering CZE method applied as 1st dimension in the CE-CE-MS setup. In this way, it was possible, for the first time, to identify mono- and diacetylated AA as major degradation products of AA in the presence of ASA [32]. Another example of an MS-incompatible CZE method as 1st dimension was the

characterization of intact monoclonal antibody (mAb) charge variants using a generic ϵ -aminocaproic acid (EACA)-based BGE [33]. These electrolyte systems are routinely applied as pharmaceutical application and cannot be coupled directly to MS [6]. The CZE-UV electropherogram of the deglycosylated model mAb Trastuzumab is shown in Fig. 3a. Three peaks, including the main form (1) and two acidic variants (2 + 3), were cut in a heart-cut approach, transferred, and analyzed via CZE-MS in the 2nd dimension. It was possible to separate the co-transferred ESI-interfering EACA in the 2nd separation dimension prior to MS detection, as indicated in Fig. 3b. In this way, interference-free, highly precise mass data (deviation 0.4–0.8 Da) of intact charge variants of Trastuzumab were achieved (Fig. 3c–e). In combination with the electrophoretic separation, the acidic variant peaks 2 and 3 were identified as deamidation products. Another application was the separation and characterization of hemoglobin and its glycosylated form ($\Delta pI = 0.036$) by CIEF-CZE-MS setup [34]. In addition, Trastuzumab was analyzed with the same CIEF-CZE-MS setup, and the results were in accordance with the findings of the CZE-CZE-MS measurements [35]. In this work, the possibility to perform multiple heart-cuts in

the same CIEF analysis was evaluated and confirmed. In addition, the 2D system was extended to imaging (i)CIEF as 1st dimension, which is a powerful technique commonly applied for the analysis of biopharmaceuticals [36]. In this work, the larger injection volume enabled the characterization of a basic variant of Trastuzumab. The observed mass shift could be explained by either succinimide formation (–17 Da) or partial cyclisation of N-terminal glutamic acid (–18 Da). Another interesting field of high ESI interference are CE methods utilizing SDS for mAb impurity analysis. We have developed a CZE method for the characterization of SDS-complexed samples based on the co-injection of positively charged surfactants and methanol as organic solvent to remove SDS from proteins. This method can be applied as 2nd dimension enabling the mass spectrometric characterization of mAb fragments and impurities (manuscript in preparation).

All these examples demonstrate the versatility of this CE-CE-MS approach using a mechanical valve. This is of special interest for the MS coupling of generic and validated methods, utilizing ESI-interfering electrolytes as frequently applied in the pharmaceutical context.

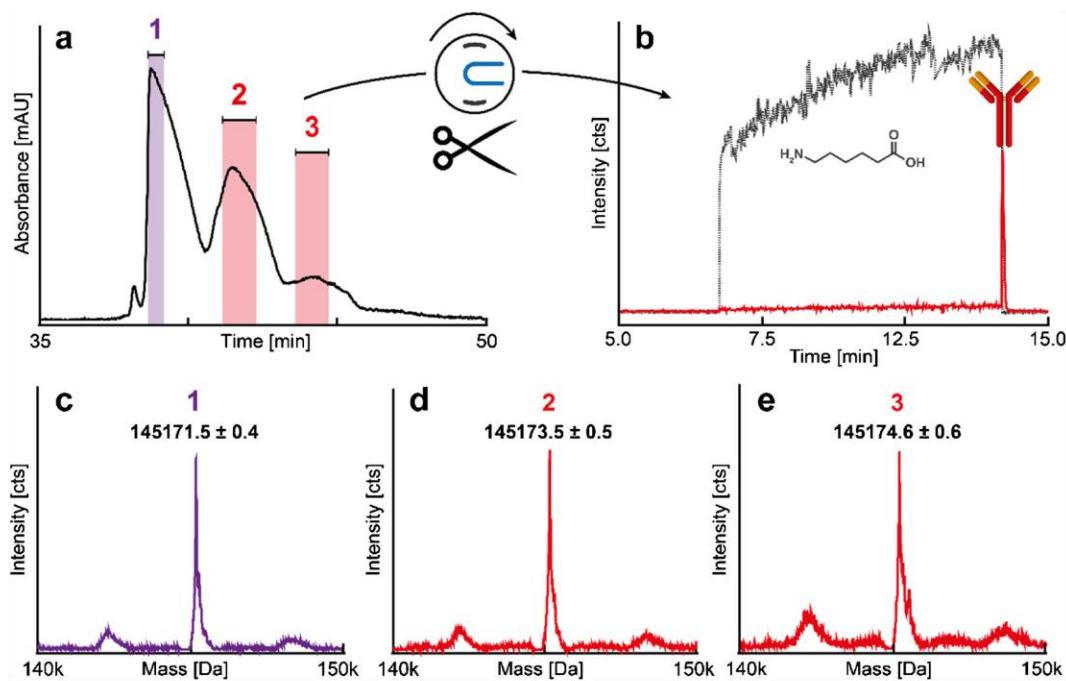


Fig. 3 CZE-CZE-MS for the characterization of intact monoclonal antibody (mAb) charge variants. 1st-dimension CZE-UV electropherogram of deglycosylated model mAb Trastuzumab (6 mg/mL) (a) at 380 mM EACA, 1.9 mM TETA, and 0.05% HPMC (pH = 5.7) was used as BGE, commonly used as pharmaceutical application [6]. A separation voltage of +10 kV was applied. Analyte peaks (10–20 nL) were transferred in a heart-cut approach from the CZE-UV to the CZE-MS 2nd dimension. CZE-MS (2nd dimension) electropherogram of highly ESI-interfering EACA (gray, dashed) and mAb variant (red, solid) (b):

2 M HAc was used as BGE and in-house PVA-coated capillaries were applied. A separation voltage of +10 kV was applied. The co-transferred ESI-interfering EACA was successfully separated from the mAb signal in the 2nd CZE dimension prior to MS detection. Deconvoluted mass spectra of the main form M (peak 1, 10 nL cut) (c) and acidic variant A1 (peak 2, 20 nL cut) (d) and A2 (peak 3, 20 nL cut) (e). The minor mass difference of +2.0 and +3.1 Da is an indication for the presence of deamidation products. For the cut of acidic variant 3, a higher concentrated sample was applied (30 mg/mL). Modified from ref. [33]

Outlook

Despite the ongoing development of new CE methods, many applications are still not compatible with MS detection due to the nature of the electrolytes used. Thus, there is a need for techniques to enable MS detection of analytes separated in such ESI-interfering BGEs. Nanospray interfacing will certainly make CE-MS more powerful in both, existing and new fields of application. Still, to what extent this will also enable direct coupling of ESI-interfering CE methods with MS remains open.

The introduced CE-CE-MS setup based on a mechanical valve interface is a promising approach to face the above-mentioned challenges, which is substantiated by the presented applications. Despite the already achieved results, there is still room for improvement of this design. So far, the maximum applicable voltage is limited (± 15 kV) which influences the total method run time. A complete automation of the mechanical valve-based CE-CE-MS setup is aspired, being supported also by a detection closer to or even in the loop. In addition, interfacing for 2D coupling can be improved potentially by the use of different materials and larger distances of the channels. These characteristics will be tackled in future studies. Such improvements will contribute to expand the application of CE-MS toward classical 2D approaches for the analysis of complex samples. In this context, the combination of chromatographic and electromigration techniques is of major interest. Furthermore, the role of microfluidic chips in one and two-dimensional electromigration techniques will certainly grow in the future.

Funding information The authors thank Hoffman-La Roche Ltd. (Basel, Switzerland) for financial support.

Compliance with ethical standards

Conflict of interest The authors declare that they have no conflict of interest.

References

- Menzinger F, Schmitt-Kopplin P, Freitag D, Kettrup A. Analysis of agrochemicals by capillary electrophoresis. *J Chromatogr A*. 2000;891(1):45–67.
- Fukushi K, Takeda S, Chayama K, Wakida S-I. Application of capillary electrophoresis to the analysis of inorganic ions in environmental samples. *J Chromatogr A*. 1999;834(1–2):349–62.
- Anastos N, Barnett NW, Lewis SW. Capillary electrophoresis for forensic drug analysis: a review. *Talanta*. 2005;67(2):269–79.
- Frazier RA, Papadopoulou A. Recent advances in the application of capillary electrophoresis for food analysis. *Electrophoresis*. 2003;24(22–23):4095–105.
- Kraly J, Fazal MA, Schoenherr RM, Bonn R, Harwood MM, Turner E, et al. Bioanalytical applications of capillary electrophoresis. *Anal Chem*. 2006;78(12):4097–110.
- Moritz B, Schnaible V, Kiessig S, Heyne A, Wild M, Finkler C, et al. Evaluation of capillary zone electrophoresis for charge heterogeneity testing of monoclonal antibodies. *J Chromatogr B Analyt Technol Biomed Life Sci*. 2015;983-984:101–10.
- Mitnik L, Novotny M, Felten C, Buonocore S, Koutny L, Schmalzing D. Recent advances in DNA sequencing by capillary and microdevice electrophoresis. *Electrophoresis*. 2001;22(19):4104–17.
- Zhu Z, Lu JJ, Liu S. Protein separation by capillary gel electrophoresis: a review. *Anal Chim Acta*. 2012;709:21–31.
- Schmitt-Kopplin P, Frommberger M. Capillary electrophoresis-mass spectrometry: 15 years of developments and applications. *Electrophoresis*. 2003;24(22–23):3837–67.
- Desiderio C, Rossetti DV, Iavarone F, Messana I, Castagnola M. Capillary electrophoresis-mass spectrometry: recent trends in clinical proteomics. *J Pharm Biomed Anal*. 2010;53(5):1161–9.
- Klepárník K. Recent advances in combination of capillary electrophoresis with mass spectrometry: methodology and theory. *Electrophoresis*. 2015;36(1):159–78.
- Monton MRN, Terabe S. Recent developments in capillary electrophoresis-mass spectrometry of proteins and peptides. *Anal Sci*. 2005;21(1):5–13.
- Petersson P, Jörintén-Karlsson M, Stålebro M. Direct coupling of micellar electrokinetic chromatography to mass spectrometry using a volatile buffer system based on perfluorooctanoic acid and ammonia. *Electrophoresis*. 2003;24(6):999–1007.
- van Biesen G, Bottaro CS. Ammonium perfluorooctanoate as a volatile surfactant for the analysis of N-methylcarbamates by MEKC-ESI-MS. *Electrophoresis*. 2006;27(22):4456–68.
- Moreno-González D, Haselberg R, Gámiz-Gracia L, García-Campaña AM, de JGJ, Somsen GW. Fully compatible and ultra-sensitive micellar electrokinetic chromatography-tandem mass spectrometry using sheathless porous-tip interfacing. *J Chromatogr A*. 2017;1524:283–9.
- Tang Q, Harrata AK, Lee CS. Capillary isoelectric focusing-electrospray mass spectrometry for protein analysis. *Anal Chem*. 1995;67:3515–9.
- Hühner J, Lämmerhofer M, Neusüß C. Capillary isoelectric focusing-mass spectrometry: coupling strategies and applications. *Electrophoresis*. 2015;36(21–22):2670–86.
- Silva M. MEKC: an update focusing on practical aspects. *Electrophoresis*. 2007;28(1–2):174–92.
- Simó C, García-Cañas V, Cifuentes A. CE-MS C. *Electrophoresis*. 2010;31(9):1442–56.
- Týčová A, Ledvína V, Klepárník K. Recent advances in CE-MS coupling: instrumentation, methodology, and applications. *Electrophoresis*. 2017;38(1):115–34.
- Lindenburger PW, Haselberg R, Rozing G, Ramautar R. Developments in interfacing designs for CE-MS: towards enabling tools for proteomics and metabolomics. *Chroma*. 2015;78(5–6):367–77.
- Dai J, Lamp J, Xia Q, Zhang Y. Capillary isoelectric focusing-mass spectrometry method for the separation and online characterization of intact monoclonal antibody charge variants. *Anal Chem*. 2018;90(3):2246–54.
- Stutz H. Advances in the analysis of proteins and peptides by capillary electrophoresis with matrix-assisted laser desorption/ionization and electrospray-mass spectrometry detection. *Electrophoresis*. 2005;26(7–8):1254–90.
- Isoo K, Otsuka K, Terabe S. Application of sweeping to micellar electrokinetic chromatography-atmospheric pressure chemical ionization-mass spectrometric analysis of environmental pollutants. *Electrophoresis*. 2001;22(16):3426–32.
- Mol R, de JGJ, Somsen GW. Atmospheric pressure photoionization for enhanced compatibility in on-line micellar electrokinetic

- chromatography-mass spectrometry. *Anal Chem.* 2005;77(16):5277–82.
26. Chen J, Fu F, Wu S, Wang J, Wang Z. Simultaneous detection of zinc dimethyldithiocarbamate and zinc ethylenebisdithiocarbamate in cabbage leaves by capillary electrophoresis with inductively coupled plasma mass spectrometry. *J Sep Sci.* 2017;40(19):3898–904.
 27. Malerod H, Lundanes E, Greibrokk T. Recent advances in on-line multidimensional liquid chromatography. *Anal Methods.* 2010;2(2):110–22.
 28. Kohl FJ, Montealegre C, Neusüß C. On-line two-dimensional capillary electrophoresis with mass spectrometric detection using a fully electric isolated mechanical valve. *Electrophoresis.* 2016;37(7–8):954–8.
 29. Helmja K, Borissova M, Knjazeva T, Jaanus M, Muinasmaa U, Kaljurand M, et al. Fraction collection in capillary electrophoresis for various stand-alone mass spectrometers. *J Chromatogr A.* 2009;1216(17):3666–73.
 30. Kohl FJ, Sánchez-Hernández L, Neusüß C. Capillary electrophoresis in two-dimensional separation systems: techniques and applications. *Electrophoresis.* 2015;36(1):144–58.
 31. Kler PA, Sydes D, Huhn C. Column-coupling strategies for multi-dimensional electrophoretic separation techniques. *Anal Bioanal Chem.* 2015;407(1):119–38.
 32. Neuberger S, Jooß K, Ressel C, Neusüß C. Quantification of ascorbic acid and acetylsalicylic acid in effervescent tablets by CZE-UV and identification of related degradation products by heart-cut CZE-CZE-MS. *Anal Bioanal Chem.* 2016;408(30):8701–12.
 33. Jooß K, Hühner J, Kiessig S, Moritz B, Neusüß C. Two-dimensional capillary zone electrophoresis-mass spectrometry for the characterization of intact monoclonal antibody charge variants, including deamidation products. *Anal Bioanal Chem.* 2017;409(26):6057–67.
 34. Hühner J, Neusüß C. CIEF-CZE-MS applying a mechanical valve. *Anal Bioanal Chem.* 2016;408(15):4055–61.
 35. Hühner J, Jooß K, Neusüß C. Interference-free mass spectrometric detection of capillary isoelectric focused proteins, including charge variants of a model monoclonal antibody. *Electrophoresis.* 2017;38(6):914–21.
 36. Montealegre C, Neusüß C. Coupling imaged capillary isoelectric focusing with mass spectrometry using a nanoliter valve. *Electrophoresis.* 2018; <https://doi.org/10.1002/elps.201800013>

IV: Setup of LC-CE-MS system and first application to intact glycoprotein analysis

Heart-cut nanoLC-CZE-MS for the characterization of proteins on the intact level

K. Jooß, N. Scholz, J. Meixner, C. Neusüß

Electrophoresis (2018) DOI: 10.1002/elps.201800411

The demands for the analysis of complex samples, especially in proteomics, are constantly increasing. In this context, the combination of RPLC in the nanoscale and CZE is of highest interest due to their nearly orthogonal separation mechanism and well-suited geometries/dimensions. Here, a heart-cut nanoLC-CZE-MS setup was developed utilizing a mechanical 4-port valve as LC-CE interface to increase separation performance for glycoprotein analysis. As desired, this 2D setup exhibits higher separation efficiency compared to the 1D methods. A model protein mix was first separated by nanoLC followed by heart-cut transfer of individual LC peaks and subsequent characterization of their glycoforms by CZE-MS. Additionally, higher sensitivity was achieved due to the exploitation of the injection volumes (200 nL) of the nanoLC system compared to traditional CZE (few nL), which resulted in estimated LODs in the low $\mu\text{g/mL}$ range. Furthermore, this proof-of-concept study represents the first application of an LC-CE-MS system for intact protein analysis.

Candidate's contribution:

Development of nanoLC-CZE-MS setup based on preliminary results. Planning of experiments. Partial performance of experiments. Data evaluation including validation. Preparation of manuscript including creation of figures.

1
2
3
4
5
6
7
8
9
10
11
12
13
14
15
16
17
18
19
20
21
22
23
24
25
26
27
28
29
30
31
32
33
34
35
36
37
38
39
40
41
42
43
44
45
46
47
48
49
50
51
52
53
54
55
56
57
58
59
60

Short Communication

Heart-cut nanoLC-CZE-MS for the characterization of proteins on the intact level

Kevin Jooß^{1,2}, Nico Scholz¹, Jens Meixner^{1,#}, Christian Neusüß^{1,*}

¹Faculty of Chemistry, Aalen University, Aalen, Germany

²Research Unit Analytical BioGeoChemistry, Helmholtz Zentrum München, Neuherberg, Germany

[#]now at Agilent Technologies R&D and Marketing GmbH & Co. KG, Waldbronn, Germany

***Correspondence:** Prof. Dr. Christian Neusüß, Beethovenstr. 1, 73430 Aalen, Germany, Christian.Neusuess@hs-aalen.de

To be submitted to Electrophoresis

Abbreviations: ribonuclease B (RNase B), reversed phase liquid chromatography (RPLC)

Keywords: glycoproteins, LC-CE interfacing, mechanical valve, two-dimensional separation

Total number of words including Figure and Table legends: 2300

ELECTROPHORESIS

Abstract

Multidimensional separation techniques play an increasingly important role in separation science, especially for the analysis of complex samples such as proteins. The combination of reversed phase liquid chromatography in the nanoscale and CZE is especially beneficial due to their nearly orthogonal separation mechanism and well-suited geometries/dimensions. Here, a heart-cut nanoLC-CZE-MS setup was developed utilizing for the first time a mechanical 4-port valve as LC-CE interface. A model protein mixture containing four different protein species was first separated by nanoLC followed by heart-cut transfer of individual LC peaks and subsequent CZE-MS analysis. In the CZE dimension, various glycoforms of one protein species were separated. Improved separation capabilities were achieved compared to the 1D methods which was exemplarily shown for ribonuclease B and its different glycosylated forms. LODs in the lower $\mu\text{g/mL}$ range were determined, which is considerably lower compared to traditional CZE-MS. In addition, this study represents the first application of an LC-CE-MS system for intact protein analysis. The nanoLC-CZE-MS system is expected to be applicable to various other analytical challenges.

Color online: See article online to view Figs. 1 and 2 in color.

Additional supporting information may be found in the online version of this article at the publisher's web-site.

1
2
3 LC and CZE are both powerful separation techniques that can adequately resolve components
4
5 in various samples. Still, the demands for sensitive analysis and high separation power are
6
7 constantly increasing. One way to improve separation capabilities is to perform
8
9 multidimensional analysis [1]. In this regard, LC-CE combinations are of great interest:
10
11 reversed phase liquid chromatography (RPLC) involving hydrophobic interactions and CZE
12
13 utilizing differences in the electrophoretic mobilities of ionic substances possess nearly
14
15 orthogonal separation mechanisms. Certain challenges need to be faced considering the
16
17 hyphenation of LC and CE technology: (i) compatibility of LC and CE conditions including
18
19 flow rates, geometries and eluent constitution (ii) transfer of LC peaks in the low to mid-nL
20
21 range and (iii) electrical insulation required in CE. Nevertheless, first online couplings of
22
23 chromatographic and electrophoretic separation were already performed in the early 90's [2, 3].
24
25 Up to date, in a majority of works flow gating types of LC-CE interfaces have been applied [4].
26
27 However, these interfaces are often difficult to combine with MS, e.g. considering coating
28
29 procedures of the CE dimension or the desire to have complete independent operation of both
30
31 separation dimensions. Nevertheless, MS represents the detection technology of choice
32
33 especially for the analysis of complex samples including intact proteins. Due to the
34
35 aforementioned challenges, only few studies have been published performing LC-CE-ESI-MS
36
37 [5–10]. In this context, a mechanical valve based interface represents an interesting alternative
38
39 and has not been evaluated for LC-CE-MS so far. Hence, both dimensions are physically
40
41 separated which is beneficial for e.g. rinsing or coating procedures. Coated capillaries are
42
43 essential in CE especially for protein analysis in order to prevent protein adsorption on the
44
45 capillary wall. Nevertheless, the sample transfer volumes of mechanical valves, usually in the
46
47 range of at least a few hundred nanoliter, and the requirement for the application of electric
48
49 fields limited their implementation for LC-CE coupling. In recent years, our group has
50
51 developed a general CE-CE-MS setup based on a 4-port valve interface capable of transferring
52
53 minor volumes (4 – 20 nL) from a first to a second separation dimension in a reproducible
54
55
56
57
58
59
60

ELECTROPHORESIS

1
2
3 manner [11, 12]. The focus of our previous studies was set on enabling MS detection despite
4 using highly ESI-interfering BGEs as first dimension. This setup was utilized for the
5 characterization of various proteins, including monoclonal antibodies [13–15]. Taking flow
6 rates and geometry in consideration, nanoLC represents the ideal choice for the hyphenation
7 with CZE. Here, a heart-cut nanoLC-CZE-MS setup was developed utilizing the
8 aforementioned 4-port valve as its core to enhance separation performance for intact protein
9 analysis. A protein mixture was first separated by nanoLC followed by heart-cut transfer of
10 certain protein species and subsequent CZE-MS analysis.
11
12
13
14
15
16
17
18
19
20
21

22 A scheme of the complete nanoLC-(UV)-CZE-MS setup and its mode of operation is illustrated
23 in Figure 1. The first dimension (nanoLC-UV) consisted of the following parts: an Agilent
24 G2226A nano pump (1200 series), the 6-port valve of a *compact* QTOF-MS instrument from
25 Bruker Daltonik (Bremen, Germany), a ZORBAX 300SB C8 nanoLC column (50×0.075 mm;
26 $3.5 \mu\text{m}$) from Agilent Technologies (Waldbronn, Germany), a home-built LC oven set, and an
27 external UV detector from ECOM UV-VIS (Prague, Czech Republic). The outlet flow of the
28 nanoLC column was connected to a mechanical 4-port-valve (20 nL sample loop) applied as
29 interface between the nanoLC and CZE dimension which is described in detail elsewhere [11].
30
31
32
33
34
35
36
37
38
39
40
41
42
43
44
45
46
47
48
49
50
51
52
53
54
55
56
57
58
59
60

51 As an initial step, a nanoLC-UV method for protein separation was developed. The 6-port valve
52 of the QTOF-MS instrument was used for injection. For this purpose, a 10 cm PVA coated
53 capillary with an inner diameter of $50 \mu\text{m}$ was applied as sample loop, resulting in a total
54 injection volume of 200 nL. The PVA coating procedure is described in our previous work [13].
55
56
57
58
59
60 A model protein mix containing ribonuclease (RNase) B, cytochrome c, lysozyme c and

1
2
3 myoglobin was analyzed. Different gradients and eluent compositions including types of
4
5 organic solvents and additives were evaluated. The final nanoLC method was as follows:
6
7 mobile phase A was 10% ACN with 0.05% TFA, while mobile phase B was 100% ACN with
8
9 0.05% TFA. A 44 min gradient was applied as follows: 0 – 2 min: 0% B, 2 – 30 min: 0 – 100%
10
11 B, 30 – 34 min: 100% B, 34 – 36 min: 100 – 0% B, 36 – 44 min: 0% B. In addition, a home-
12
13 built LC oven was constructed and different temperatures were tested during method
14
15 development including 40, 50, 55 and 60°C. Hence, resolution between peaks was considered
16
17 the most important parameter. As a result, a temperature of 50°C was selected for the final
18
19 method since it exhibited the highest resolution (improvement factors: 1.17 – 1.25) compared
20
21 to room temperature (data not shown).
22
23
24

25
26
27 Another general aspect which needs to be attributed is that a majority of proteins elute at
28
29 considerable organic content. Thus, it is important to examine the influence of organic solvents
30
31 on CZE-MS methods, especially the current stability. For this reason, a standard of RNase B
32
33 (1000 µg/mL) was solved in different amounts of ACN or methanol (10 – 70% (v/v)) and
34
35 subsequently analyzed by CZE-MS using 1 M acetic acid as generic BGE. The obtained current
36
37 profiles are illustrated in Figure S1. No current breakdown could be observed only a slight
38
39 decrease in the overall current at higher methanol content. Moreover, the separation
40
41 performance was not affected noticeably. Thus, it can be concluded that typical elution
42
43 conditions for LC can be applied in the nanoLC-CZE setup without a major influence on the
44
45 CZE-MS dimension.
46
47
48

49
50
51 Different electrolyte systems were tested as BGE for the CZE dimension including 1, 2, 3, 5, 7
52
53 M acetic acid and 0.2, 0.5 M formic acid in a CZE-UV approach. Based on its high variability
54
55 in glycoforms, RNase B was selected as model protein to evaluate the separation performance.
56
57 0.2 M formic acid showed the highest resolution (see Figure S2) and thus, was selected as BGE
58
59 for all further experiments. In a subsequent analysis, the protein mix was injected and analyzed.
60

ELECTROPHORESIS

1
2
3 It turned out that the different proteins overlap in the electropherogram and could not be
4 resolved adequately, which substantiates the need for higher separation performance.
5
6

7
8
9 As a first test for the complete nanoLC-CZE-MS, a standard of myoglobin (250 $\mu\text{g/mL}$) was
10 analyzed (see Figure S3). In the CZE dimension, RSD values ($n = 3$) of 0.21% for the migration
11 time and 18.2% for peak intensity (based on extracted ion electropherograms of the 11 major
12 charge states of the respective glycoform) were determined. In this way, the general
13 functionality of the 2D setup including a precise cutting procedure was demonstrated.
14
15 Subsequently, the protein mix was analyzed and RNase B was cut out from the nanoLC run
16 and transferred to CZE-MS. In the CZE dimension the different glycoforms of RNase B were
17 segregated. Both, the nanoLC chromatogram and the CZE electropherogram are illustrated in
18 Figure 2A and B. As expected, the non-glycosylated form of RNase B migrates first and the
19 respective raw and deconvoluted mass spectrum is shown in Figure 2C and D. In general,
20 RNase B exhibits high-mannose *N*-glycans ranging from five to nine mannose units, which
21 migrate later and are partly resolved. The migration time increased with the size of the attached
22 glycan. An average mass spectrum covering the whole range of glycosylated RNase B is
23 illustrated in Figure 2E. The respective deconvoluted mass spectrum is depicted in Figure 2F.
24
25 About 14% of the nanoLC peak was transferred to the CZE-MS dimension taking peak
26 width/shape, nanoLC flow rate and sample loop volume (20 nL) in consideration. This value is
27 expected to be better than in most flow-gating approaches. For example, Lemmo and Jorgenson
28 calculated a transfer efficiency of roughly 1% [16]. Still, the transfer efficiency can be further
29 improved, e.g. by reducing the flow rate in nanoLC and/or by increasing the transfer volume of
30 the valve. This would not only increase the sensitivity but also reduce the risk of errors in
31 relative quantitation by potential pre-separation of glycoforms within the nanoLC peak. In the
32 case of RNase B, the latter could be excluded here by direct nanoLC-MS showing no pre-
33 separation of glycoforms.
34
35
36
37
38
39
40
41
42
43
44
45
46
47
48
49
50
51
52
53
54
55
56
57
58
59
60

1
2
3 IEC-RPLC-MS is a common tool to separate complex (peptide) mixtures based on different
4 ionic interaction in the first dimension and hydrophobic interaction in the second dimension.
5
6
7
8 Contrary, in the here presented LC-CE-MS concept, intact proteins are initially segregated
9
10 according to their hydrophobicity (type of protein) and subsequently based on differences in
11
12 charge-to-size ratio (glycoforms). For intact protein analysis, our approach is certainly more
13
14 appropriate, since all glycoforms of one protein are expected to be detected in one single run of
15
16 the second dimension.
17

18
19
20 In a subsequent experiment different concentrations of RNase B in the protein mix were
21
22 characterized including 10, 50 and 500 $\mu\text{g}/\text{mL}$ with 3 repetitions per concentration level (data
23
24 not shown). Exemplarily, linearity was confirmed ($R^2 = 0.9998$) for the most abundant RNase
25
26 B variant ($\text{Man}_5\text{GlcNAc}_2$) in the examined concentration range and an LOD of 3 $\mu\text{g}/\text{mL}$
27
28 ($S/N = 3$) was determined.
29

30
31
32 In conclusion, a mechanical valve was utilized for the first time to hyphenate LC with CE
33
34 technology in the context of MS characterization. The performance of the nanoLC-CZE-MS
35
36 setup was tested in a proof-of-concept study. Improved separation capabilities compared to the
37
38 1D methods were achieved which was shown for the analysis of RNase B variants. It should
39
40 be mentioned that intact proteins have not been analyzed by LC-CE-MS up to date. The 2D
41
42 system benefits from the greater injection volumes of nanoLC compared to standard CZE
43
44 injections leading to estimated LOD values in the lower $\mu\text{g}/\text{mL}$ range. Larger injection volumes,
45
46 including the applications of trap columns for sample enrichment, will be covered in future
47
48 studies in addition to the analysis of relevant biological samples.
49
50
51

52 53 **Conflict of interest**

54
55
56 *The authors have declared no conflict of interest.*
57
58
59
60

ELECTROPHORESIS

References

1. Giddings, J. C., *J. High Resol. Chromatogr.* 1987, 10 (5), 319–323.
2. Yamamoto, H., Manabe, T., Okuyama, T., *J. Chromatogr.* 1989, 480, 277–283.
3. Bushey, M. M., Jorgenson, J. W., *Anal. Chem.* 1990, 62 (10), 978–984.
4. Ranjbar, L., Foley, J. P., Breadmore, M. C., *Anal. Chim. Acta* 2017, 950, 7–31.
5. Lewis, K. C., Opiteck Gregory J., Jorgenson, J. W., Sheely, D. M., *J. Am. Soc. Mass Spectrom.* 1997 (8), 495–500.
6. Bergström, S. K., Samskog, J., Markides, K. E., *Anal. Chem.* 2003, 75 (20), 5461–5467.
7. Bergström, S. K., Dahlin, A. P., Ramström, M., Andersson, M., Markides, K. E., Bergquist, J., *Analyst* 2006, 131 (7), 791–798.
8. Zhang, J., Hu, H., Gao, M., Yang, P., Zhang, X., *Electrophoresis* 2004, 25 (14), 2374–2383.
9. Chambers, A. G., Mellors, J. S., Henley, W. H., Ramsey, J. M., *Anal. Chem.* 2011, 83 (3), 842–849.
10. Mellors, J. S., Black, W. A., Chambers, A. G., Starkey, J. A., Lacher, N. A., Ramsey, J. M., *Anal. Chem.* 2013, 85 (8), 4100–4106.
11. Kohl, F. J., Montealegre, C., Neusüß, C., *Electrophoresis* 2016, 37 (7-8), 954–958.
12. Schlecht, J., Jooß, K., Neusüß, C., *Anal. Bioanal. Chem.* 2018, 410 (25), 6353–6359.
13. Hühner, J., Jooß, K., Neusüß, C., *Electrophoresis* 2017, 38 (6), 914–921.
14. Jooß, K., Hühner, J., Kiessig, S., Moritz, B., Neusüß, C., *Anal. Bioanal. Chem.* 2017, 409 (26), 6057–6067.
15. Montealegre, C., Neusüß, C., *Electrophoresis* 2018, 39 (9-10), 1151–1154.
16. Lemmo, A. V., Jorgenson, J. W., *Anal. Chem.* 1993, 65 (11), 1576–1581.

Figure Captions

Figure 1. Scheme of the nanoLC-CZE-MS setup: The first dimension consists of a nanoLC pump (flow rate = 500 nL/min) connected to the 6-port-valve of a QTOF-MS instrument, which is used for sample injection. Prior to the run the 6-port-valve is kept in position **A** and the sample is loaded ($V_{\text{loop}} = 200$ nL) using a syringe. For injection, the 6-port-valve is switched to position **B** and the sample is transferred to the nanoLC column, which is placed in a home-built LC oven ($T = 50^{\circ}\text{C}$). The outlet of the column is connected to the 4-port-valve through an external UV detector placed 8.6 cm in front of the valve. The sample loop is directly incorporated on the rotor of the 4-port-valve ($V_{\text{loop}} = 20$ nL). The inlet capillary of the second dimension (CZE) is connected to one of the remaining two connections of the 4-port-valve. A second capillary is connected to the remaining port and the ESI-QTOF-MS instrument to complete the CZE-MS dimension. During separation in the first dimension, the 4-port-valve is kept in position **C**. The external UV detector (214 nm detection wavelength) is used to determine the correct time when the analyte of interest is positioned in the sample loop and the 4-port-valve can be switched to position **D**. Subsequently, +15 kV is applied in the second dimension and separation towards the MS takes place.

Figure 2. Analysis of protein mix by nanoLC-CZE-MS. The mix contained RNase B (100 $\mu\text{g}/\text{mL}$), cytochrome c (80 $\mu\text{g}/\text{mL}$), lysozyme c (80 $\mu\text{g}/\text{mL}$) and myoglobin (50 $\mu\text{g}/\text{mL}$). First dimension: **(A)** nanoLC chromatogram (214 nm detection wavelength) of the separation of different proteins. Second dimension: **(B)** CZE-MS electropherogram obtained after heart-cut of RNase B peak (transfer volume: 20 nL). Separation of various RNase B glycoforms observed. The 11 most abundant charge states of the individual glycoforms were used to create the ion traces, respectively. Raw **(C)** and deconvoluted **(D)** mass spectrum of non-glycosylated RNase B (range: 26.1 – 26.3 min). Raw **(E)** and deconvoluted **(F)** mass spectrum including all glycosylated forms of RNase B (range: 27.9 – 29.5 min).

ELECTROPHORESIS

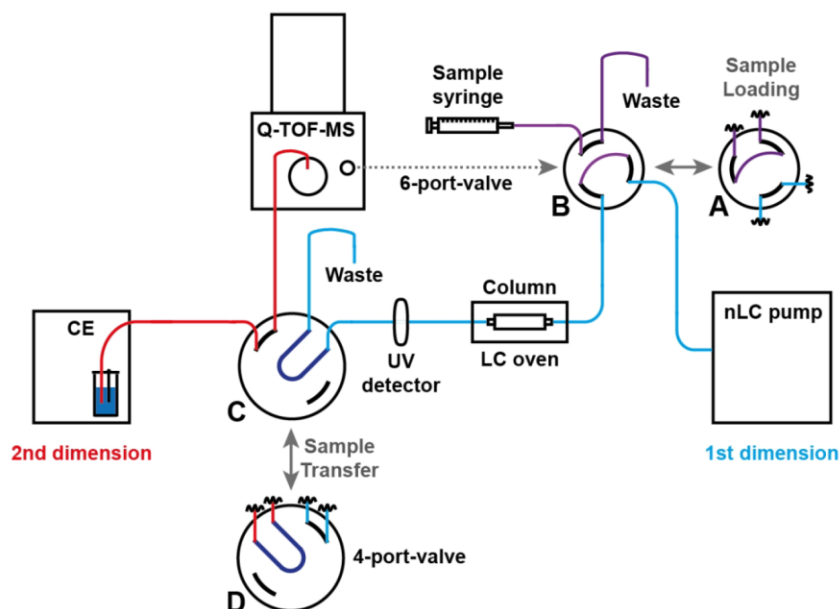


Figure 1. Scheme of the nanoLC-CZE-MS setup: The first dimension consists of a nanoLC pump (flow rate = 500 nL/min) connected to the 6-port-valve of a QTOF-MS instrument, which is used for sample injection. Prior to the run the 6-port-valve is kept in position A and the sample is loaded ($V_{loop} = 200$ nL) using a syringe. For injection, the 6-port-valve is switched to position B and the sample is transferred to the nanoLC column, which is placed in a home-built LC oven ($T = 50$ °C). The outlet of the column is connected to the 4-port-valve through an external UV detector placed 8.6 cm in front of the valve. The sample loop is directly incorporated on the rotor of the 4-port-valve ($V_{loop} = 20$ nL). The inlet capillary of the second dimension (CZE) is connected to one of the remaining two connections of the 4-port-valve. A second capillary is connected to the remaining port and the ESI-QTOF-MS instrument to complete the CZE-MS dimension. During separation in the first dimension, the 4-port-valve is kept in position C. The external UV detector (214 nm detection wavelength) is used to determine the correct time when the analyte of interest is positioned in the sample loop and the 4-port-valve can be switched to position D. Subsequently, +15 kV is applied in the second dimension and separation towards the MS takes place.

105x78mm (300 x 300 DPI)

1
2
3
4
5
6
7
8
9
10
11
12
13
14
15
16
17
18
19
20
21
22
23
24
25
26
27
28
29
30
31
32
33
34
35
36
37
38
39
40
41
42
43
44
45
46
47
48
49
50

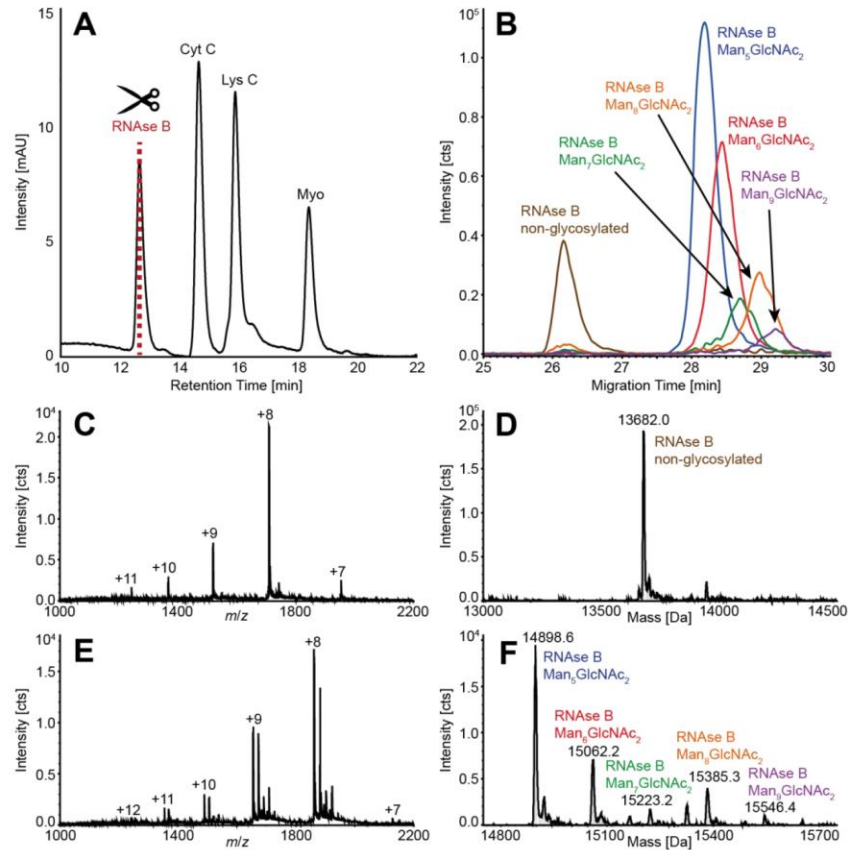


Figure 2. Analysis of protein mix by nanoLC-CZE-MS. The mix contained RNase B (100 $\mu\text{g}/\text{mL}$), cytochrome c (80 $\mu\text{g}/\text{mL}$), lysozyme c (80 $\mu\text{g}/\text{mL}$) and myoglobin (50 $\mu\text{g}/\text{mL}$). First dimension: (A) nanoLC chromatogram (214 nm detection wavelength) of the separation of different proteins. Second dimension: (B) CZE-MS electropherogram obtained after heart-cut of RNase B peak (transfer volume: 20 nL). Separation of various RNase B glycoforms observed. The 11 most abundant charge states of the individual glycoforms were used to create the ion traces, respectively. Raw (C) and deconvoluted (D) mass spectrum of non-glycosylated RNase B (range: 26.1 – 26.3 min). Raw (E) and deconvoluted (F) mass spectrum including all glycosylated forms of RNase B (range: 27.9 – 29.5 min).

125x128mm (300 x 300 DPI)

V: Development of a CZE-DTIM-MS method for the analysis of protein glycosylation

Capillary zone electrophoresis coupled to drift tube ion mobility-mass spectrometry for the analysis of native and APTS-labeled *N*-glycans

K. Jooß, S. W. Meckelmann, J. Klein, O. J. Schmitz, C. Neusüß (paper in forefront)

Analytical and Bioanalytical Chemistry (2018) DOI: 10.1007/s00216-018-1515-7

In recent years, drift tube ion mobility mass spectrometry (DTIM-MS) has emerged as a fast alternative to traditional separation techniques. The combination of CZE based on electrophoretic mobility in the liquid phase and DTIM-MS based on mobilities in the gas-phase represents an interesting approach for a two-dimensional separation concept. Here, the first on-line coupling of CZE and DTIM-MS was performed as an alternative to traditional two-dimensional liquid phase separation. The aim was to further improve separation capabilities for the analysis of native and APTS-labeled *N*-glycans released from different protein sources including monoclonal antibodies. Each individual glycan signal separated in CZE exhibited an unexpectedly high number of peaks observed in the IMS dimension. Their origin could be explained by the presence of isomeric forms, including different linkages, and/or gas-phase conformers which do not interconvert on the time-scale of the ion mobility separation. Without prior separation in the CZE dimension, the complexity of some *N*-glycans could not be resolved by DTIM-MS alone. This highlights the benefits obtained by the combination of these powerful analytical techniques. Summarized, the combination of CZE and DTIM-MS technology displays a high potential and is expected to find various applications in the future.

Candidate's contribution:

Planning and performance of experiments, data evaluation, literature search, preparation of manuscript including creation of figures.



Capillary zone electrophoresis coupled to drift tube ion mobility-mass spectrometry for the analysis of native and APTS-labeled *N*-glycans

Kevin Jooß^{1,2} · Sven W. Meckelmann^{3,4} · Julia Klein^{3,4} · Oliver J. Schmitz^{3,4} · Christian Neusüß¹Received: 24 August 2018 / Revised: 16 October 2018 / Accepted: 23 November 2018
© Springer-Verlag GmbH Germany, part of Springer Nature 2018

Abstract

Capillary zone electrophoresis (CZE) based on electrophoretic mobility in the liquid phase and ion mobility spectrometry (IMS) based on mobilities in the gas phase are both powerful techniques for the separation of complex samples. Protein glycosylation is one of the most common post-translational modifications associated with a wide range of biological functions and human diseases. Due to their high structural variability, the analysis of glycans still represents a challenging task. In this work, the first on-line coupling of CZE with drift tube ion mobility-mass spectrometry (DTIM-MS) has been performed to further improve separation capabilities for the analysis of native and 8-aminopyrene-1,3,6-trisulfonic acid (APTS)-labeled *N*-glycans. In this way, a complexity of glycan signals was revealed which could not be resolved by these techniques individually, shown for both native and APTS-labeled glycans. Each individual glycan signal separated in CZE exhibited an unexpectedly high number of peaks observed in the IMS dimension. This observation could potentially be explained by the presence of isomeric forms, including different linkages, and/or gas-phase conformers. In addition, the type of sialic acid attached to glycans has a significant impact on the obtained drift time profile. Furthermore, the application of α 2-3 neuraminidase enabled the partial assignment of peaks in the arrival time distribution considering their sialic acid linkages (α 2-3/ α 2-6). This work is a showcase for the high potential of CZE-DTIM-MS, which is expected to find various applications in the future.

Keywords Glycan analysis · CE-IM-MS · Isomer separation · Liquid- and gas-phase separation

Abbreviations

AGP	α -1-Acid glycoprotein	ESI	Electrospray ionization
APTS	8-Aminopyrene-1,3,6-trisulfonic acid	FAIMS-MS	High-field asymmetric waveform ion mobility spectrometry mass spectrometry
ATD	Arrival time distribution	HILIC	Hydrophilic interaction chromatography
BGE	Background electrolyte	IMS	Ion mobility spectrometry
CE	Capillary electrophoresis	mAb	Monoclonal antibody
CZE	Capillary zone electrophoresis	MS	Mass spectrometry
DT	Drift time	NeuNAc	<i>N</i> -Acetylneuraminic acid
DTIM-MS	Drift tube ion mobility-mass spectrometry	NeuNGc	<i>N</i> -Glycolylneuraminic acid

Published in the topical collection *Close-Up of Current Developments in Ion Mobility Spectrometry* with guest editor Gérard Hopfgartner.

Electronic supplementary material The online version of this article (<https://doi.org/10.1007/s00216-018-1515-7>) contains supplementary material, which is available to authorized users.

✉ Christian Neusüß
Christian.Neusuess@hs-aalen.de

¹ Faculty of Chemistry, Aalen University, 73430 Aalen, Germany

² Research Unit Analytical BioGeoChemistry, Helmholtz Zentrum München, Ingolstädter Landstr. 1, 85764 Neuherberg, Germany

³ Applied Analytical Chemistry, University of Duisburg-Essen, Universitätsstr. 5, 45141 Essen, Germany

⁴ Teaching and Research Center for Separation, University of Duisburg-Essen, Universitätsstr. 5, 45141 Essen, Germany

SA	Sialic acid
SL	Sheath liquid
TOF-MS	Time-of-flight mass spectrometry
TWIM-MS	Traveling wave ion mobility-mass spectrometry

Introduction

Glycosylation represents the most common post translational modification of proteins with an estimation that approximately 50% of all proteins are glycosylated in eukariotic systems [1]. A variety of biological functions have been associated with protein glycosylation including immune response, protein regulation/interactions, apoptosis, and recognition of signals on the cell surface [2]. Furthermore, glycans are known to be involved in the development and progression of human diseases, especially cancer, inflammantoy diseases, rheumatoid arthritis, and Alzheimers disease [3]. Increased insight in the molecular and structural characteristics of glycans in biological processess led to the development of biotherapeutics, e.g., monoclonal antibodies (mAbs), with specific glycoforms [4].

Glycoproteins synthesized in living cell systems usually comprise macro- and micro-heterogeneity based on the complexity of the involved glycosylation processes [5]. On the one hand, macro-heterogeneity is described by the variability of glycosylation sites and number of attached glycans. In general, glycosylation can occur on asparagine (*N*-glycans) or on serine/threonine (*O*-glycans) residues. On the other hand, micro-heterogeneity is related to the variety of different glycan structures that can occur. Furthermore, even for glycans with the same elemental composition, the micro-heterogeneity can be extensively complex due to stereoisomers of monomer units, several potential linkage sites, anomeric configurations of glycosidic bonds, and the occurrence of multiple branching patterns [6].

Thus, the characterization of glycosylation remains challenging usually requiring several orthogonal methods. Besides analyses on the intact glycoprotein and glycopeptide level, the detailed characterization of glycosylation based on released glycans represents an important analytical task. In order to determine three-dimensional structures of glycans, nuclear magnetic resonance spectroscopy and X-ray crystallography can be applied [7]. Still, these techniques require pure and highly concentrated samples.

Matrix-assisted laser desorption/ionization time-of-flight mass spectrometry (TOF-MS) can be applied for rapid profiling of released glycans. Thereby, glycans are usually permethylated to improve ionization efficiency and stabilize sialylated glycans in positive ionization mode [8]. For liquid chromatography-based and mass spectrometry (MS)-based characterization, released glycans are often labeled with a fluorescence tag, such as 2-aminobenzamide, using reductive

amination [9]. Common chromatographic techniques for released glycan analysis include hydrophilic interaction chromatography (HILIC), reversed-phase liquid chromatography, anion exchange chromatography, and porous graphitized carbon chromatography [10].

Besides chromatographic approaches, electromigrative separation techniques represent efficient tools to separate glycan isomers in complex samples. In this regard, capillary sieving electrophoresis coupled to laser-induced fluorescence detection using 8-aminopyrene-1,3,6-trisulfonic acid (APTS) as fluorescence tag exhibits high selectivity/sensitivity and is commonly applied in pharmaceutical analysis [9]. However, due to the lack of available glycan standards and the incompatibility of the electrolyte system with electrospray ionization (ESI), the assignment of peaks, especially for new glycan structures, is difficult or even not possible. Thus, in recent years, we have introduced a capillary zone electrophoresis (CZE)-MS method based on an ϵ -aminocaproic acid background electrolyte (BGE) showing similar separation performance [11]. In addition, this method can be applied for native and APTS-labeled *N*-glycan analysis. Still, the glycan structure characterization remains challenging due to the isomeric and branched nature of glycans.

In recent years, ion mobility spectrometry (IMS) in combination with MS has gained importance. TOF-MS is usually selected as mass analyzer due to the well-fitting duty cycles (IMS: ms range; TOF-MS: μ s range). Several different IMS technologies have been developed, which are discussed in detail elsewhere [12]. In general, ions are separated according to their charge, size, and shape while traversing through a cell, filled with neutral inert gas, and guided by an electric field. In this way, isomers can potentially be separated. IMS technology has been frequently applied for the analysis of glycans [13]. Despite the already promising results achieved, the separation efficiency of IMS needs to be improved, especially for larger complex type *N*-glycans.

On the one hand, the separation mechanism in CZE is based on the electrophoretic mobility in the liquid phase, which can be manipulated depending on the choice of BGE, additives, and coatings. On the other hand, IMS is associated with gas-phase mobilities and thus, different selectivities can be expected. Therefore, the combination of these two powerful techniques represents a promising approach to gain further separation performance, which was highlighted in a recent trend article [14]. Still, their orthogonality has not been carefully evaluated so far [15]. Capillary electrophoresis (CE) has been hyphenated with high-field asymmetric waveform ion mobility spectrometry mass spectrometry (FAIMS-MS) [16] and traveling wave ion mobility-mass spectrometry (TWIM-MS) [17, 18]. Yet, the focus of these works was to reduce the mass spectral noise (FAIMS-MS) or to obtain simultaneous information on the conformational distribution and activity of enzymes (TWIM-MS), and not to gain additional separation

performance. Preliminary attempts to perform CE-DTIM-MS have been carried out in the late 1980s by the Hill group [19]. However, spray instability was an issue and hindered its application at that time.

Here, the aforementioned CZE-MS method for glycan analysis was coupled to drift tube ion mobility-mass spectrometry (DTIM-MS). To the best of our knowledge, this is the first successful hyphenation of CZE to DTIM-MS technology to improve the performance of the separation. APTS-labeled *N*-glycans released from a model mAb were characterized. In addition, native complex type *N*-glycans released from fetuin and α -1-acid glycoprotein (AGP) were analyzed. Furthermore, native glycan samples were treated with α 2-3 neuraminidase and reanalyzed and changes in the glycan profile were investigated.

Materials and methods

Materials

Ultrapure water (electrical resistivity > 18 M Ω cm) from an UltraClear UV system (Siemens water technologies, Günzburg, Germany) was used to prepare all BGEs, samples, and rinsing solutions. Methanol (MS-grade), isopropyl alcohol (MS-grade), acetonitrile (MS-grade), sodium hydroxide ($\geq 98\%$), ammonia solution (ROTIPURAN® 30% p.a.), ammonium hydrogen carbonate ($\geq 99\%$, p.a.), and acetic acid (ROTIPURAN® 100%, p.a.) were obtained from Carl Roth (Karlsruhe, Germany). *N*-Glycosidase F (rec. *E. coli*), AGP (bovine serum 99%), and fetuin (fetal calf serum) were purchased from Sigma Aldrich (Steinheim, Germany). ϵ -Aminocaproic acid (pure) was obtained from Merck (Darmstadt, Germany). *N*-Glycans released from a monoclonal antibody were labeled with APTS based on the procedure in our previous work [11]. α 2-3 Neuraminidase S from New England Biolabs (Frankfurt, Germany) was applied. Bare fused-silica capillaries (50 μ m inner diameter, 363 μ m outer diameter) were purchased from Polymicro Technologies (Phoenix, AZ, USA).

Deglycosylation of AGP and fetuin samples was performed with *N*-glycosidase F. Accordingly, 200 μ g of protein was solved in 20 μ L digestion buffer (25 mM ammonium hydrogen carbonate, pH = 8.2 adjusted with 30% ammonia). Subsequently, samples were transferred to safe-lock tubes containing 15 units of *N*-glycosidase F and incubated for 24 h at 37 °C. The reaction was stopped by heating the samples to 100 °C for 5 min. For the cleavage of α 2-3-linked sialic acids (SA), 4 μ L of α 2-3 neuraminidase (1 mg/mL) was added and the samples were incubated for 3 h at 37 °C (pH 6 adjusted with acetic acid).

CZE-IM-MS

CZE

An Agilent 7100 CE System (Agilent Technologies, Waldbronn, Germany) was applied for CZE separation using bare fused-silica capillaries with an inner diameter of 50 μ m and a length of 80.0 cm. The BGE consisted of 0.1 M ϵ -aminocaproic acid and 0.5 M ammonia solved in methanol/water 1:1 [11]. The capillaries were preconditioned once by rinsing (using approximately 1 bar) with methanol (5 min), water (5 min), 1.2 M hydrochloric acid (5 min), water (5 min), 1 M sodium hydroxide (20 min), water (5 min), and BGE (10 min). For long-term or overnight storage, the capillary was rinsed (using approximately 1 bar) with water and air for 5 min, respectively. Every morning, the capillary was preconditioned briefly (using approximately 1 bar) with 1.2 M hydrochloric acid (1.5 min), water (5 min), 0.1 M sodium hydroxide (10 min), water (5 min), and BGE (10 min). Samples were injected hydrodynamically (50 mbar, 18 s). A constant voltage of +30 kV was applied during separation. Electropherograms were slightly smoothed using a Quartic/Quintic Savitsky-Golay algorithm.

ESI-DTIM-MS

An Agilent 6560 Ion Mobility Quadrupole Time-of-Flight Mass Spectrometer (Agilent Technologies, Waldbronn, Germany) was used. The CZE-ESI-IM-MS coupling was performed with a commercial triple-tube sheath liquid interface (Agilent Technologies, Waldbronn, Germany). Bare fused-silica capillaries were positioned in such a way that they stuck visibly outside of the sheath liquid sprayer needle (approximately 1/5 of the capillary diameter). Different sheath liquid (SL) compositions were tested: isopropyl alcohol/water 1:1, 3:7, 7:3; methanol/water 1:1; and acetonitrile/water 1:1. The SL was delivered at a flow rate of 4 μ L/min by a syringe pump (Cole-Parmer®, IL, USA) equipped with a 5-mL syringe (5MDF-LL-GT, SGE Analytical Science, Melbourne, Australia). The Agilent Jetstream Source was operated in the negative mode under the following conditions: gas temperature 220 °C, drying gas 2 L/min N₂, sheath gas temperature 200 °C, sheath gas flow 5 L/min N₂, VCap 3500 V, nozzle voltage 2000 V, and fragmentor 400 V. DTIM-MS parameters were as follows: nitrogen (3.95 Torr) applied as drift gas, trap fill time 30 ms, trap release time 150 μ s, and maximum drift time was 60 ms. The drift voltage was 18.5 V/cm (drift tube entrance 1700 V, drift tube exit 250 V, drift tube length 78.236 cm). Data processing was carried out by using Agilent MassHunter Qualitative Analysis Navigator (B.08.00) and IM-MS Browser (B.08.00). Identification of glycan species was based on their *m/z* value in combination

with the known literature [20]. All extracted ion electropherograms (EIEs) were extracted with $\Delta m = \pm 0.1$ Da.

Results and discussion

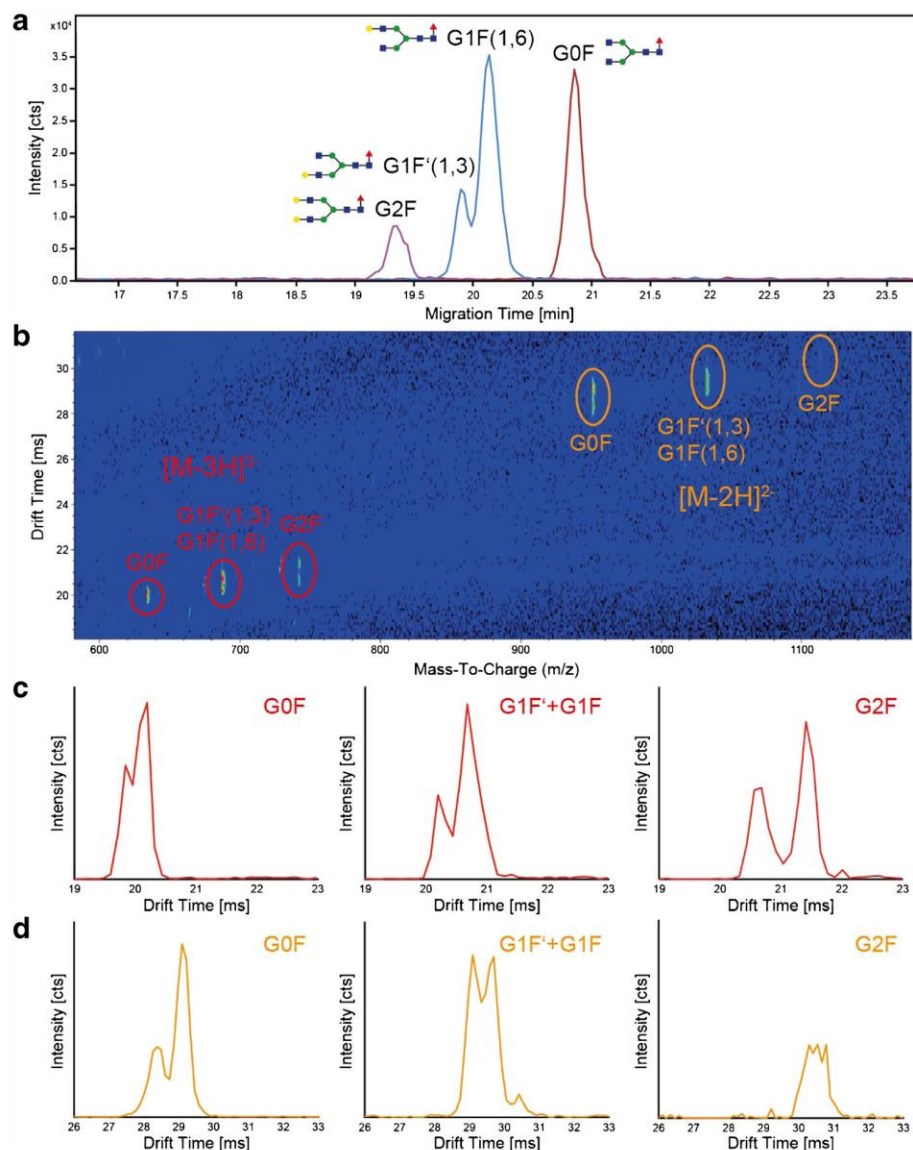
APTS-labeled glycans: mAb

Derivatization with APTS is a common labeling procedure for CZE characterization of *N*-glycans. Thus, as an initial test for the CZE-IM-MS setup, APTS-labeled *N*-glycans released from a model mAb were analyzed. To the best of our knowledge, the obtained results represent the first IMS data of *N*-glycans with this type of labeling. As expected, a typical CZE

separation profile was obtained including the mAb-based glycans G0F, the isomers G1F'(1,3) and G1F(1,6), and G2F as shown in Fig. 1a [11]. Multiple deprotonated ionic species ($[M-2H]^{2-}$ and $[M-3H]^{3-}$) were detected with the negative charges located at the highly acidic APTS label (Fig. 1b).

Interestingly, each individual arrival time distribution (ATD) of the glycan signals resolved in the CZE exhibits multiple peaks. Two prominent peaks were observed for the $[M-3H]^{3-}$ species as displayed in Fig. 1c. The $[M-3H]^{3-}$ profiles of G0F, G1F'(1,3)/G1F(1,6), and G2F are quite similar. Still, with increasing molecular mass, the DT peaks are not only shifted to higher drift times, as expected, but also better resolved. In addition, a third, small signal is appearing at higher drift times in the G2F spectra, indicating the presence

Fig. 1 CZE electropherogram of APTS-labeled *N*-glycans released from mAb1 including G0F (950.75, 633.50 *m/z*), G1F'(1,3) and G1F(1,6) (1031.77, 687.51 *m/z*), and G2F (1112.80, 741.53 *m/z*) (a). 2D IM-MS plot (19–21.2 min) (b): Heat map (*m/z* vs. DT) of triple- and double-charged ionic species highlighted in red and orange, respectively. ATDs of the glycans G0F (20.6–21.1 min), G1F'(1,3) + G1F(1,6) (19.7–20.5 min), and G2F (19.1–19.6 min) of the triply (c) and doubly (d) charged ions. Multiple peaks were observed in each ATD



of an ionic species with different mobility. Considering the ATD profiles of the $[M-2H]^{2-}$ signals, a change in the relative intensities in the pattern is more apparent than in the $[M-3H]^{3-}$ profiles (Fig. 1d). Still, the rather low signal intensity of G2F was not sufficient to allow an adequate comparison with the ATDs obtained from G0F and G1F'(1,3)/G1F(1,6).

The origin of the multiple peaks observed in the ATD space could not be unambiguously assigned, but could be explained by the presence of isomeric forms and/or conformers that do not interconvert on the time scale of the ion mobility separation. Though structural isomers of G0F and G2F are not described in the literature, an analogous ATD (double peak) was shown for G0F (pyridylamino labeled, $[M+2H]^{2+}$) analyzed by HILIC-IM-MS [21]. However, the authors did not elaborate on this observation. Nevertheless, we observed multiple signals in the ATD of all detected glycans. In recent years, there has been increased evidence that improved separation can be obtained in the IMS for certain isomeric glycans if deprotonated ionic species are analyzed, compared to other ionic species [22]. Still, gas-phase separation of glycan ions in IMS has been mainly focused on sodiated or other metal adducts. In addition, APTS-labeled glycans have not been analyzed by IMS so far. These circumstances complicate the comparison to other IMS related works.

Due to the preceding CZE separation, the isomers G1F'(1,3) and G1F(1,6) can be detected independently in the IMS. The distinct ATDs of the $[M-2H]^{2-}$ and $[M-3H]^{3-}$ ionic species of both G1F'(1,3) and G1F(1,6) are depicted in Fig. 2. It is apparent that the ATDs exhibit significant differences between G1F'(1,3) and G1F(1,6) for both charge states. For the triply charged species, G1F'(1,3) delivers one large peak with a slight shoulder on the lower side of the ATD. On the other hand, the ATD of G1F(1,6) indicates the presence of three different species. Considering the doubly charged ions, G1F'(1,3) exhibits the more complex profile with three prominent species, whereas G1F(1,6) shows only the two main ATD peaks. Summarized, without prior separation in the CZE dimension, the complexity of G1F'(1,3) and G1F(1,6) could not be resolved in the DTIM-MS and would result in overlaid ATDs. This observation highlights the important benefit of the hyphenation of CZE to DTIM-MS, since neither of these techniques would be able to resolve all the detected species individually.

Native glycans: AGP and fetuin

Besides APTS-labeled glycans, the CZE system can also be applied to native sialylated glycans. Therefore, native glycans released from fetuin and AGP were analyzed using the CZE-IM-MS setup. Example electropherograms of glycans released from AGP and fetuin are displayed in Fig. 3a, b. The major glycoforms detected for fetuin were di- and triantennary glycans with at least the same amount of *N*-acetylneuraminic

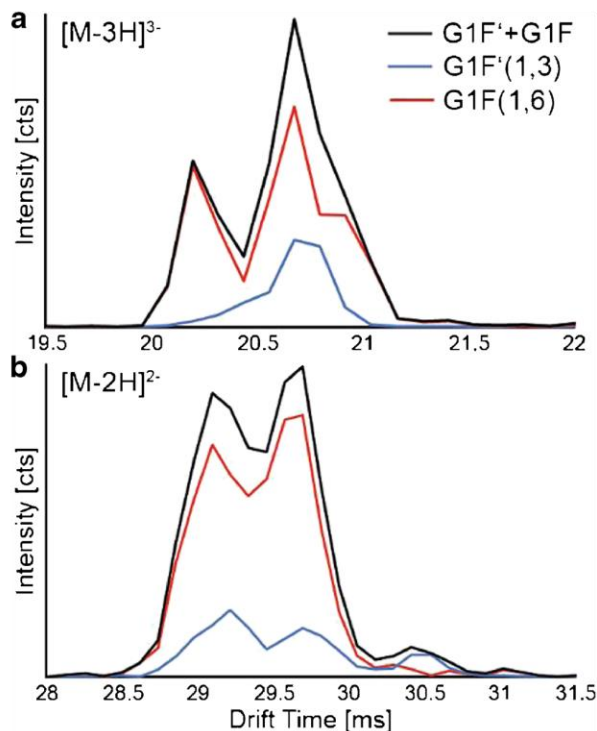
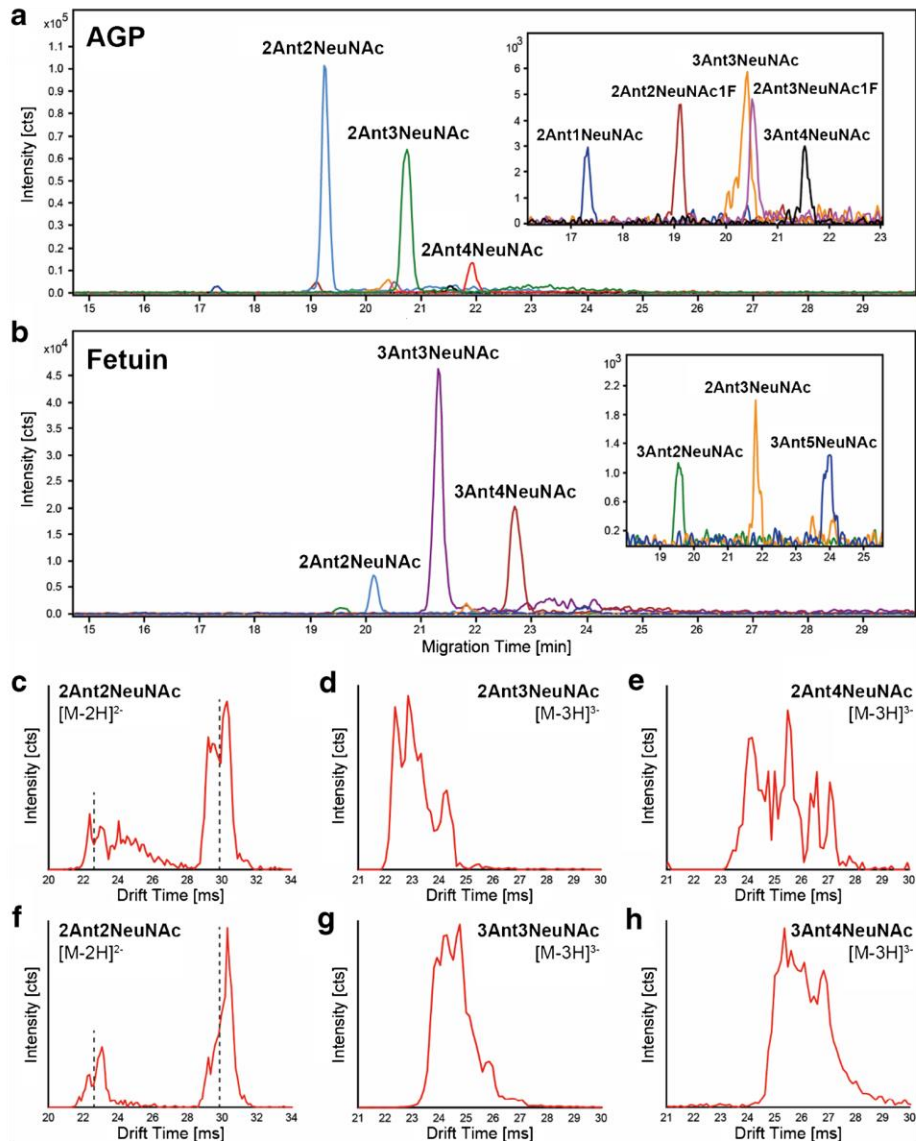


Fig. 2 ATDs of the triple-charged (a) and double-charged (b) ions originating from the mAb glycans G1F'(1,3) (blue, solid line) and G1F(1,6) (red, solid line) priorly separated by CZE. The MT region to extract the ATDs for G1F'(1,3) (19.74–19.89 ms) and G1F(1,6) (20.15–20.25 ms) was selected in certain distance from each other to minimize potential overlap of the ATDs. The combined information of G1F'(1,3) + G1F(1,6) (black, solid line) highlights that the ATDs of G1F'(1,3) and G1F(1,6) would overlap without prior CZE separation which would lead to substantial loss of information

acid (NeuNAc): 2Ant2NeuNAc, 3Ant3NeuNAc, and 3Ant4NeuNAc. On the other hand, AGP exhibits mostly diantennary carbohydrate chains with two to four sialyl residues: 2Ant2NeuNAc, 2Ant3NeuNAc, and 2Ant4NAc. This observation is in accordance with the literature [20]. ATDs of the major glycans for AGP and fetuin are shown in Fig. 3c–e and f–h, respectively. In comparison to the APTS-labeled mAb glycans, a similar or even higher complexity was obtained in the IMS dimension for the individual glycan peaks resolved by CZE. Similarly, Aizpurua-Olaizola et al. have shown more than one signal in the IMS profile of 2Ant1SA priorly separated by HILIC [14].

2Ant2NeuNAc is a major glycan of AGP and fetuin and, thus, allows the direct comparison of a glycan with the same saccharide composition from different protein sources (Fig. 3c, f). First, there are two ATD regions that are present in both proteins, which consist of at least two partly resolved peaks, respectively. However, in both ATD regions, the peaks detected at lower drift times are significantly higher for AGP in comparison to fetuin. Since both proteins were measured under the exact same conditions (instrument setup, BGE, SL composition, etc.), there is

Fig. 3 CZE electropherograms of native sialylated *N*-glycans released from AGP (a) and fetuin (b): Major glycoforms detected include diantennary carbohydrate chains with two to four sialyl residues (AGP) and di- and triantennary glycans with at least the same amount of *N*-acetylneuraminic acid (fetuin). EICs of AGP are generated as a sum of both sialic acid types (NeuNAc and NeuNGc). Inserts show the lower abundant detected glycans, respectively. ATDs of AGP (c–e) and fetuin (f–h) glycans associated with the major peaks separated by CZE



evidence that some features do not correspond to gas-phase conformers, but rather linkage/structural isomers. In addition, AGP exhibits non-resolved signals between these two regions (Fig. 4b), which are barely visible for fetuin.

In contrast to the human form, bovine AGP exhibits glycans containing NeuNAc and/or *N*-glycolylneuraminic acid (NeuNGc) as SA residues increasing the overall complexity. To be more precise, each possible combination (relative amount) of both SA is present as exemplarily shown for the $[M-3H]^{3-}$ species of 2Ant3SA in Fig. 4a. The expected mass shift ($\Delta m/z = 5.33$) related to the exchange of NeuNAc to NeuNGc was observed in the mass spectra. It is also possible to partly separate the different SA types in the CZE dimension, which is exemplarily shown for 2Ant3SA in Fig. S1 (see Electronic Supplementary

Material (ESM)). In the heat map (2D IM-MS plot, Fig. 4b), there appear to be minor differences between the ATDs in dependence of the type of SA residue which gets more evident by taking a closer look at the individual ATDs illustrated in Fig. 4c. The relative intensities of species change systematically with relative amount of NeuNGc. For example, the second observed peak is decreasing (black arrow) and the third one is increasing (blue arrow). An additional example is the ATDs for the $[M-2H]^{2-}$ species of 2Ant2SA (ESM Fig. S2). Similar changes of increasing and decreasing peaks were observed. However, in this regard, a clear statement is not possible due to the limited resolution.

An important parameter for the CZE-DTIM-MS system is the reproducibility of the obtained drift times and ATDs. In general,

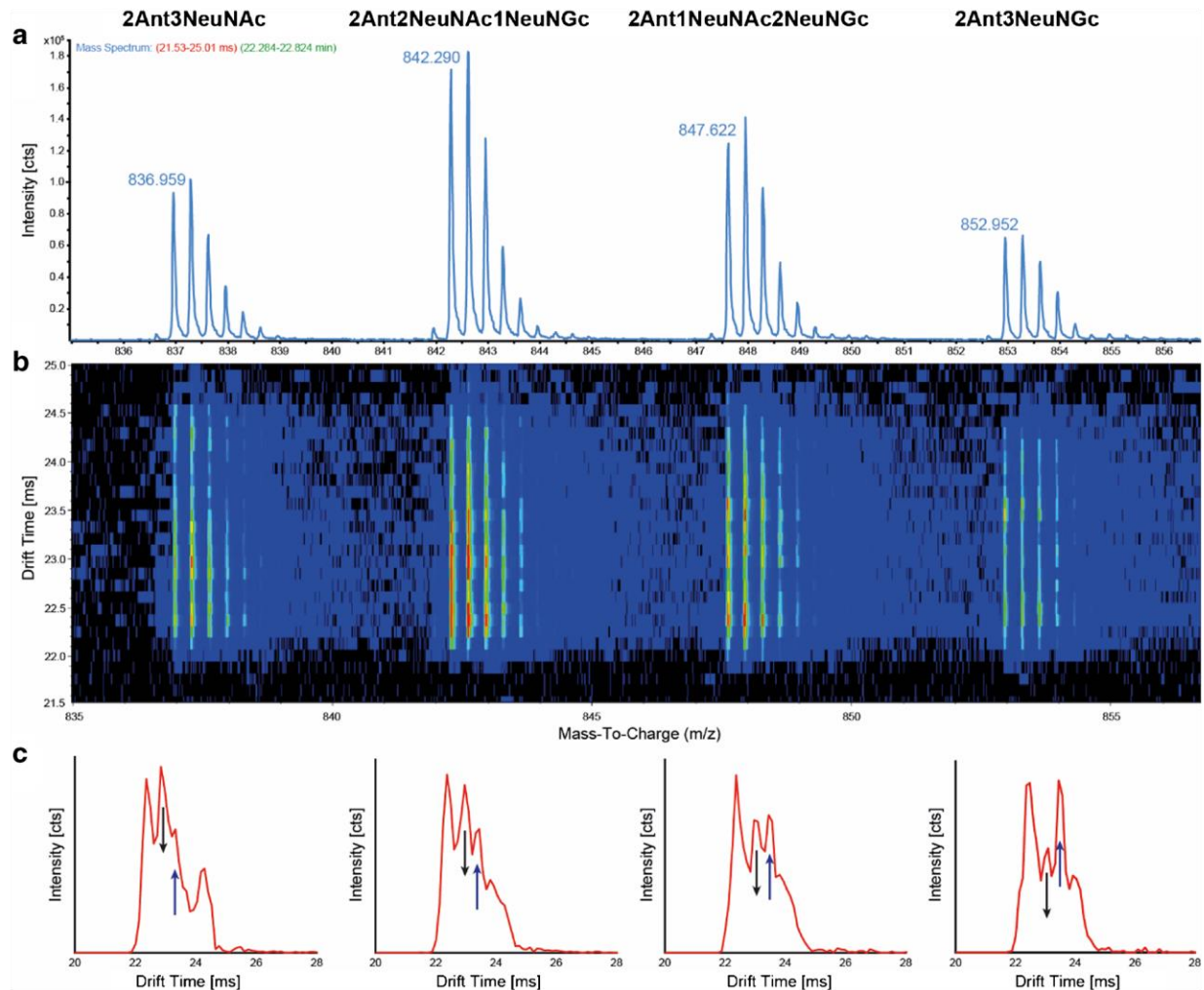


Fig. 4 Separation of 2Ant3SA species (AGP) with different sialic acids containing NeuNAc and/or NeuNGc. Mass spectra of $[M-3H]^{3-}$ ions (**a**) ranging from 2Ant3NeuNAc (836.959 m/z) to 2Ant3NeuNGc (852.952 m/z). Typical distances between sialic acid species were observed ($\Delta m/z = 5.33$). IMS heat map (**b**) associated with the mass spectra.

Slight differences in the ATDs are recognizable. Individual ATDs (**c**) of observed sialic acid species. Changes of relative intensities of signals in the obtained ATD observed in dependence of the type of sialic acid. Most distinct changes are indicated by arrows

the ATDs were reproducible for the entire measurement series. Exemplarily, the ATDs obtained for the glycans 2Ant1NeuNAc1NeuNGc and 2Ant1NeuNAc2NeuNGc of three measurements are shown in ESM Fig. S3. A mean RSD value of 0.20% was calculated for the drift times based on 12 peaks observed in the ATDs of 2Ant2SA (NeuNAc and NeuNGc variants) and 14 peaks observed in the ATDs of 2Ant3SA (NeuNAc and NeuGc variants) with $n_{\text{total}} = 148$. For the lower intense, noisier peaks, the RSD values for the drift times were typically around 0.5%. These values are in the range expected for this type of instrument [23].

In order to evaluate the influence of the sheath liquid on the ATDs, different SL combinations were tested analyzing *N*-glycans released from AGP: isopropyl alcohol/water 1:1, 3:7, 7:3; methanol/water 1:1; and acetonitrile/water 1:1. No

significant changes in the ATDs could be observed (data not shown). In conclusion, the CE-IM-MS system seems to be not depending on the SL applied including the nature and relative amount of organic solvent. Thus, SL compositions can be adapted independently from the IMS dimension, e.g., optimizing ionization efficiency.

To further elucidate the characteristics of the multiple peaks observed in the ATDs, AGP and fetuin samples were treated with α 2-3 neuraminidase. In this way, sialic acids exhibiting a α 2-3 linkage to galactose are specifically cleaved and α 2-6 linkages remain intact. The respective electropherograms of AGP and fetuin can be found in ESM Fig. S4. Interestingly, up to three peaks—corresponding to a single m/z value—are resolved by CZE as exemplarily depicted for 2Ant2SA released from AGP in Fig. 5a. Since liquid-phase conformers are

typically not separated by CZE, it can be assumed that the species resolved are isomers. These glycan structures should only contain α 2-6 linkages after α 2-3 neuraminidase treatment. Thus, the separation in CZE is not related with sialic acid linkages, as commonly observed by porous graphitized carbon chromatography, but can potentially be explained by differences in other linkages such as Gal1-3GlcNAc/Gal1-4GlcNAc in the glycan branches as detected by nuclear magnetic resonance spectroscopy [24]. The individual ATDs of the 2Ant2SA signals resolved in CZE are shown in Fig. 5b. The first and the second CZE peaks showed a similar profile in the ATD. The complexity increased towards the third CZE peak, which exemplarily exhibited a high intense additional feature in the higher ATD region ($t_d = 29.2$ ms). The separation of glycan species in CZE in combination with the further gained resolution in the DTIM-MS indicates again the potential of the hyphenation of these two powerful analytical

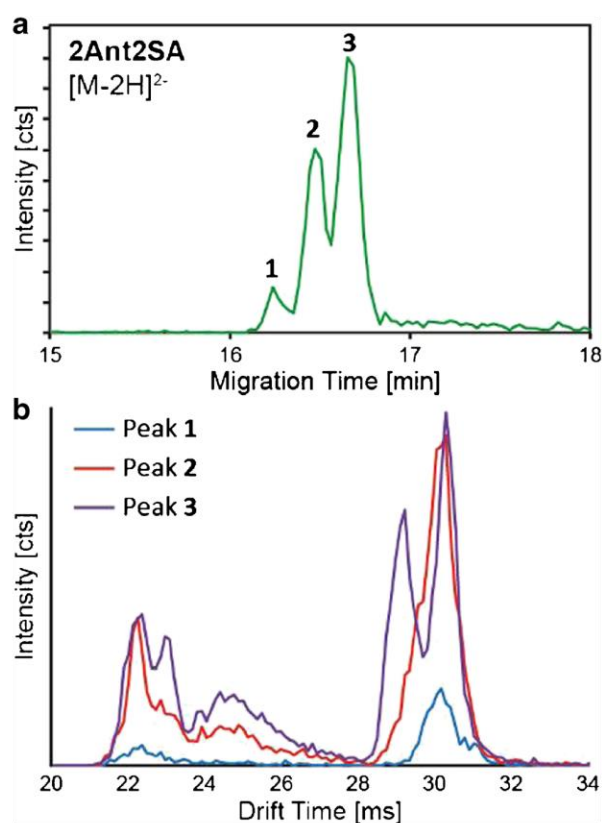


Fig. 5 CZE electropherogram of 2Ant2SA released from AGP and treated with α 2-3 neuraminidase (a). EICs were generated using the combined information of all sialic acid variants related to 2Ant2SA (NeuNAc + NeuNGc). Three distinct peaks could be separated by CZE. Individual ATDs of CZE peaks 1–3 (b). Differences in the ATDs were observed

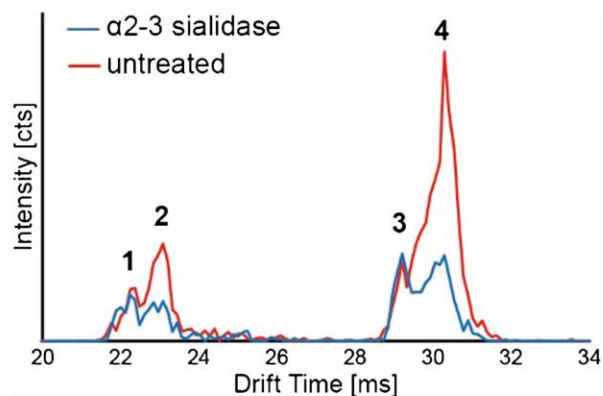


Fig. 6 ATD of 2Ant2NeuNAc ($[M-2H]^{2-}$ species) released from fetuin before (red, solid line) and after (blue, solid line) α 2-3 neuraminidase treatment, divided into four regions (1–4). Decrease of the peaks (2) and (4) observed, whereas (1) and (3) remain similar in intensity

techniques. By comparing the ATDs before and after α 2-3 neuraminidase treatment, it is possible to partly assign signals observed in the ATD. This is especially the case for 2Ant2NeuNAc released from fetuin as illustrated in Fig. 6. In contrast to AGP, fetuin did not exhibit significant amounts of diantennary glycans with more than two sialic acid attached. Thus, only a loss of certain species in the ATD can be expected. The decrease of (2) and (4) is evidence that these regions of the ATD originally contained partly glycans with at least one α 2-3-linked NeuNAc. On the other hand, the signals (1) and (3) in the ATD apparently consist of glycans only containing α 2-6-linked SA. Again, the presence of multiple peaks only constituted of α 2-6-linked SA could potentially be explained by differences in other linkages such as Gal1-3GlcNAc/Gal1-4GlcNAc in the glycan branches.

Conclusion

The combination of CZE and DTIM-MS technology was successfully applied for the separation and characterization of native and APTS-labeled *N*-glycans released from different protein sources. In general, each individual glycan signal resolved in CZE exhibited multiple peaks in the ATD. This observation could be explained by the presence of isomeric forms, including different linkages, and/or gas-phase conformers which do not interconvert on the time scale of the ion mobility separation. Without prior separation in the CZE dimension, the complexity of some *N*-glycans could not be resolved by DTIM-MS alone and would unavoidably lead to overlaid ATDs. This could be shown exemplarily for both APTS-labeled G1F'(1,3)/G1F(1,6) isomers (mAb) and native 2Ant2SA species after α 2-3 neuraminidase treatment (bovine AGP). Since neither CZE nor

DTIM-MS would be able to resolve all the detected species individually, these examples highlight the advantages achieved by the combination of these powerful analytical techniques. For native 2Ant2NeuNAc, differences in the ATD profile were observed depending on the proteins (AGP or fetuin) it originated from, measured under the same conditions. This is evidence that some features do not correspond to gas-phase conformers, but rather to linkage/structural isomers. In addition, it could be shown that the nature and type of SL did not noticeably affect the obtained ATDs. Thus, SL compositions can be optimized regarding ionization efficiency independently from the DTIM-MS dimension. Bovine AGP exhibits a unique feature by possessing two types of SA, NeuNAc and NeuNGc. Besides the partial separation in the CZE dimension, systematic differences in the relative intensities of the ATD were observed in dependence of the type of sialic acid. Furthermore, the use of α -2-3 neuraminidase enables a partial assignment of peaks observed in the DTIM-MS spectra in regard to sialic acid linkages. Summarized, the combination of CZE and DTIM-MS technology displays a high potential and is expected to find various applications in the future.

Compliance with ethical standards

Conflict of interest The authors declare that they have no conflict of interest.

Publisher's Note Springer Nature remains neutral with regard to jurisdictional claims in published maps and institutional affiliations.

References

- Williams JP, Grabenauer M, Holland RJ, Carpenter CJ, Wormald MR, Giles K, et al. Characterization of simple isomeric oligosaccharides and the rapid separation of glycan mixtures by ion mobility mass spectrometry. *Int J Mass Spectrom.* 2010;298(1–3):119–27.
- Rudd PM. Glycosylation and the immune system. *Science.* 2001;291(5512):2370–6.
- Montreuil J, Vliegenthart JFG, Glycoproteins SH. *New comprehensive biochemistry*, vol. 29a. Amsterdam: Elsevier; 1995.
- Dalziel M, Crispin M, Scanlan CN, Zitzmann N, Dwek RA. Emerging principles for the therapeutic exploitation of glycosylation. *Science.* 2014;343(6166):1235681.
- Zhang L, Luo S, Zhang B. Glycan analysis of therapeutic glycoproteins. *MAbs.* 2016;8(2):205–15.
- Dwek RA. Glycobiology: toward understanding the function of sugars. *Chem Rev.* 1996;96(2):683–720.
- Wormald MR, Petrescu AJ, Pao Y-L, Glithero A, Elliott T, Dwek RA. Conformational studies of oligosaccharides and glycopeptides: complementarity of NMR, X-ray crystallography, and molecular modelling. *Chem Rev.* 2002;102(2):371–86.
- Sanchez-De Melo I, Grassi P, Ochoa F, Bolivar J, García-Cózar FJ, Durán-Ruiz MC. N-glycosylation profile analysis of trastuzumab biosimilar candidates by normal phase liquid chromatography and MALDI-TOF MS approaches. *J Proteome.* 2015;127:225–33.
- Ruhaak LR, Zauner G, Huhn C, Bruggink C, Deelder AM, Wuhrer M. Glycan labeling strategies and their use in identification and quantification. *Anal Bioanal Chem.* 2010;397(8):3457–81.
- Melmer M, Stangler T, Premstaller A, Lindner W. Comparison of hydrophilic-interaction, reversed-phase and porous graphitic carbon chromatography for glycan analysis. *J Chromatogr A.* 2011;1218(1):118–23.
- Bunz S-C, Cutillo F, Neusüß C. Analysis of native and APTS-labeled N-glycans by capillary electrophoresis/time-of-flight mass spectrometry. *Anal Bioanal Chem.* 2013;405(25):8277–84.
- Kanu AB, Dwivedi P, Tam M, Matz L, Hill HH. Ion mobility-mass spectrometry. *J Mass Spectrom.* 2008;43(1):1–22.
- Hofmann J, Pagel K. Glycan analysis by ion mobility-mass spectrometry. *Angew Chem Int Ed.* 2017;56(29):8342–9.
- Aizpurua-Olaizola O, Sastre Torano J, Falcon-Perez JM, Williams C, Reichardt N, Boons G-J. Mass spectrometry for glycan biomarker discovery. *TrAC Trends Anal Chem.* 2018;100:7–14.
- Zheng X, Wojcik R, Zhang X, Ibrahim YM, Burnum-Johnson KE, Orton DJ, et al. Coupling front-end separations, ion mobility spectrometry, and mass spectrometry for enhanced multidimensional biological and environmental analyses. *Ann Rev Anal Chem.* 2017;10(1):71–92.
- Li J, Purves RW, Richards JC. Coupling capillary electrophoresis and high-field asymmetric waveform ion mobility spectrometry mass spectrometry for the analysis of complex lipopolysaccharides. *Anal Chem.* 2004;76(16):4676–83.
- Mironov GG, Okhonin V, Khan N, Clouthier CM, Berezovski MV. Conformational dynamics of DNA G-quadruplex in solution studied by kinetic capillary electrophoresis coupled on-line with mass spectrometry. *Chem Open.* 2014;3(2):58–64.
- Mironov GG, Clouthier CM, Akbar A, Keillor JW, Berezovski MV. Simultaneous analysis of enzyme structure and activity by kinetic capillary electrophoresis-MS. *Nat Chem Biol.* 2016;12(11):918–22.
- Hallen RW, Shumate CB, Siems WF, Tsuda T, Hill HH. Preliminary investigation of ion mobility spectrometry after capillary electrophoretic introduction. *J Chromatogr.* 1989;480:233–45.
- Nakano M. Detailed structural features of glycan chains derived from 1-acid glycoproteins of several different animals: the presence of hypersialylated, O-acetylated sialic acids but not disialyl residues. *Glycobiology.* 2004;14(5):431–41.
- Yamaguchi Y, Nishima W, Re S, Sugita Y. Confident identification of isomeric N-glycan structures by combined ion mobility mass spectrometry and hydrophilic interaction liquid chromatography. *Rapid Commun Mass Spectrom.* 2012;26(24):2877–84.
- Struwe WB, Baldauf C, Hofmann J, Rudd PM, Pagel K. Ion mobility separation of deprotonated oligosaccharide isomers – evidence for gas-phase charge migration. *Chem Commun.* 2016;52(83):12353–6.
- Stow SM, Causon TJ, Zheng X, Kurulugama RT, Mairinger T, May JC, et al. An interlaboratory evaluation of drift tube ion mobility-mass spectrometry collision cross section measurements. *Anal Chem.* 2017;89(17):9048–55.
- Cumming DA, Hellerqvist CG, Harris-Brandts M, Michnick SW, Carver JP, Bendiak B. Structures of asparagine-linked oligosaccharides of the glycoprotein fetuin having sialic acid linked to N-acetylglucosamine. *Biochemistry.* 1989;28:6500–12.



Kevin Jooß is currently a Ph.D. student at Aalen University and the Helmholtz Zentrum München. He has been working on the analysis of small molecule drugs, complex proteins, and N-glycans applying capillary zone electrophoresis mass spectrometry. His Ph.D. project is related to the development and application of two-dimensional (electromigrative) separation techniques coupled to mass spectrometry.



Oliver J. Schmitz cofounded the company iGenTraX UG which develops new ion sources and units to couple separation techniques with mass spectrometers. Since 2012, he has been Full Professor at the University of Duisburg-Essen and is Chair of the Institute of Applied Analytical Chemistry. In 2018, he founded the Teaching and Research Center for Separation (TRC) at the University of Duisburg-Essen, which belongs to Agilent's global network of

world-class Centers of Excellence. He is the author/co-author of one textbook and 9 book chapters, 81 papers published in peer-reviewed journals, more than 130 lectures, and 4 patents.



Sven W. Meckelmann is Senior Scientist at the University of Duisburg-Essen in the Department of Applied Analytical Chemistry. His research interests include the development and application of new methods for the identification and quantification of lipids and metabolites in biological samples.



Christian Neusüß is Full Professor at the Faculty of Chemistry at Aalen University. His research interests include sophisticated separation techniques coupled to (high-resolution) mass spectrometry with a focus on CE-MS. His latest research focus is set on the development of two-dimensional electromigrative separation techniques coupled to mass spectrometry. He is the author/co-author of about 100 peer-reviewed publications and several patents and book chapters

as well as numerous lectures at scientific conferences.



Julia Klein is currently a Ph.D. student in the working group of Professor Oliver J. Schmitz for Applied Analytical Chemistry at the University of Duisburg-Essen, Germany. Her research focusses on the analysis of complex samples using liquid chromatography coupled to ion mobility and high-resolution mass spectrometry.

Discussion

The following section contains a discussion about the key findings of the presented work described in the thesis relevant manuscripts, especially in the context of the over-all project.

7. Setup of CZE-CZE-MS system and first application to small pharmaceuticals

7.1 CZE-CZE-MS of small pharmaceuticals

Acetylsalicylic acid (ASA), known as aspirin, is one of the most commonly applied active ingredients in pharmaceuticals due to its analgesic, antipyretic, and anti-inflammatory properties. In order to counteract serious adverse drug effects caused by oxygen radicals formed during the metabolism of ASA, ascorbic acid (ASC, referred to as AA in **manuscript I**) is oftentimes added to the pharmaceutical formulation [103]. Both, ASA and ASC are known to degrade relatively fast if exposed to oxygen and/or humidity [104, 105]. Conclusively, the quantification of ASA, ASC and related degradation products including preceding identification is of utmost importance to ensure the quality of pharmaceutical products. In this context, different HPLC methods have been developed for the quantification of ASA and ASC. However, considering degradation products, either resolution was not sufficient [106], or they have not been detected in general [107]. ASA and ASC are small polar molecules, dissociated at neutral to basic pH. For this reason, CZE appears to be a promising approach for the separation of these analytes. Thus far, no CZE method has been reported for the simultaneous determination of ASA and ASC, let alone related degradation products. Therefore, in the context of another PhD project, the first CZE-UV method was developed for the quantification of ASA, ASC and potential degradation products in effervescent tablets. During method development, several different BGE systems were tested analyzing fresh and degraded effervescent tablet samples including typical volatile BGEs, such as ammonium formate or acetate. In fact, only a BGE containing high amounts of ESI-interfering tricine (100 mM, pH = 8.8) delivered sufficient resolution and separation performance. A more detailed

description of method conditions can be found in **manuscript I**. Concerning degradation products, salicylic acid could be easily identified by spiking experiments. In addition, two other prominent peaks were generated over storage time as illustrated in Figure 16 (peak #1 and #2). These peaks did not match with any known degradation product of ASA or ASC. Therefore, MS characterization was mandatory to identify these unknown substances. The tricine-based CZE-UV method represented the ideal showcase not only to evaluate and improve the CE-CE-MS system further but also to identify important, but previously unknown degradation products of ASA and ASC.

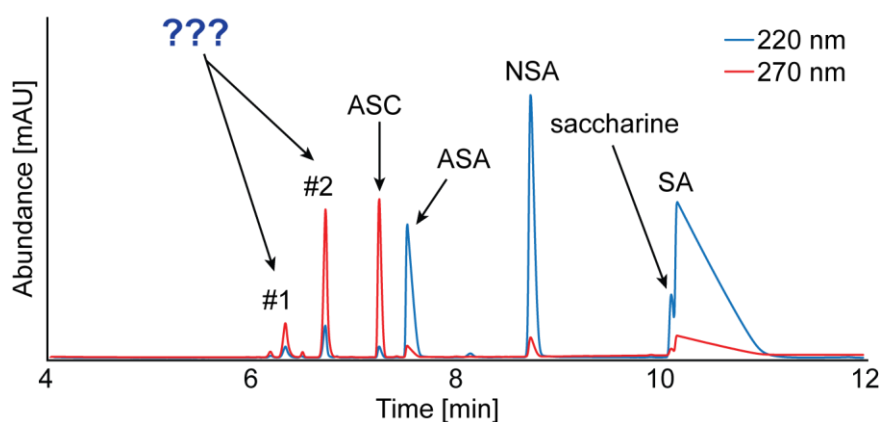


Figure 16: CZE-UV electropherogram of degraded ASA + ASC tablet sample. Original concentrations: 800 mg/mL ASC, 2400 mg/mL ASA and 70 mg/mL 2-naphthalenesulfonic acid (NSA) applied as internal standard. Detection was performed at 220 nm (blue) and 270 nm (red) wavelength. Tablets were exposed to a relative humidity of 52% at 30 °C for 72 h. Separation was performed using FS capillaries (50 cm), 100 mM tricine (pH = 8.8) as BGE, and +20 kV separation voltage. Non-assignable peaks (#1, #2) were observed. More detailed method information can be found in **manuscript I**.

7.2 CE-CE-MS utilizing a 4-port valve interface

The CE-CE-MS setup utilized during this thesis was based on our previous work [86]. A scheme of the general 2D setup can be found in Figure 17 A. The 1st dimension (CE1 instrument) is comprised as follows: An inlet capillary (1.D_{inl}) is connected through the external UV cell to channel S of the mechanical 4-port valve. An outlet capillary (1.D_{out}) is jointed to channel W and placed in a grounded external vial filled with BGE to close the electrical circuit. The inlet (2.D_{inl}) and outlet (2.D_{out}) of the 2nd dimension (CE2 instrument) are connected to channel C and P, respectively. In addition, the outlet is linked to the ESI source of the QTOF-MS instrument. The length

and type of the capillaries (coated, non-coated) vary depending on the application and can be found in the methods & materials section of the respective manuscripts. The motor, rotor and stator were pushed tight together via two screws, in order to avoid leakages during the measurements.

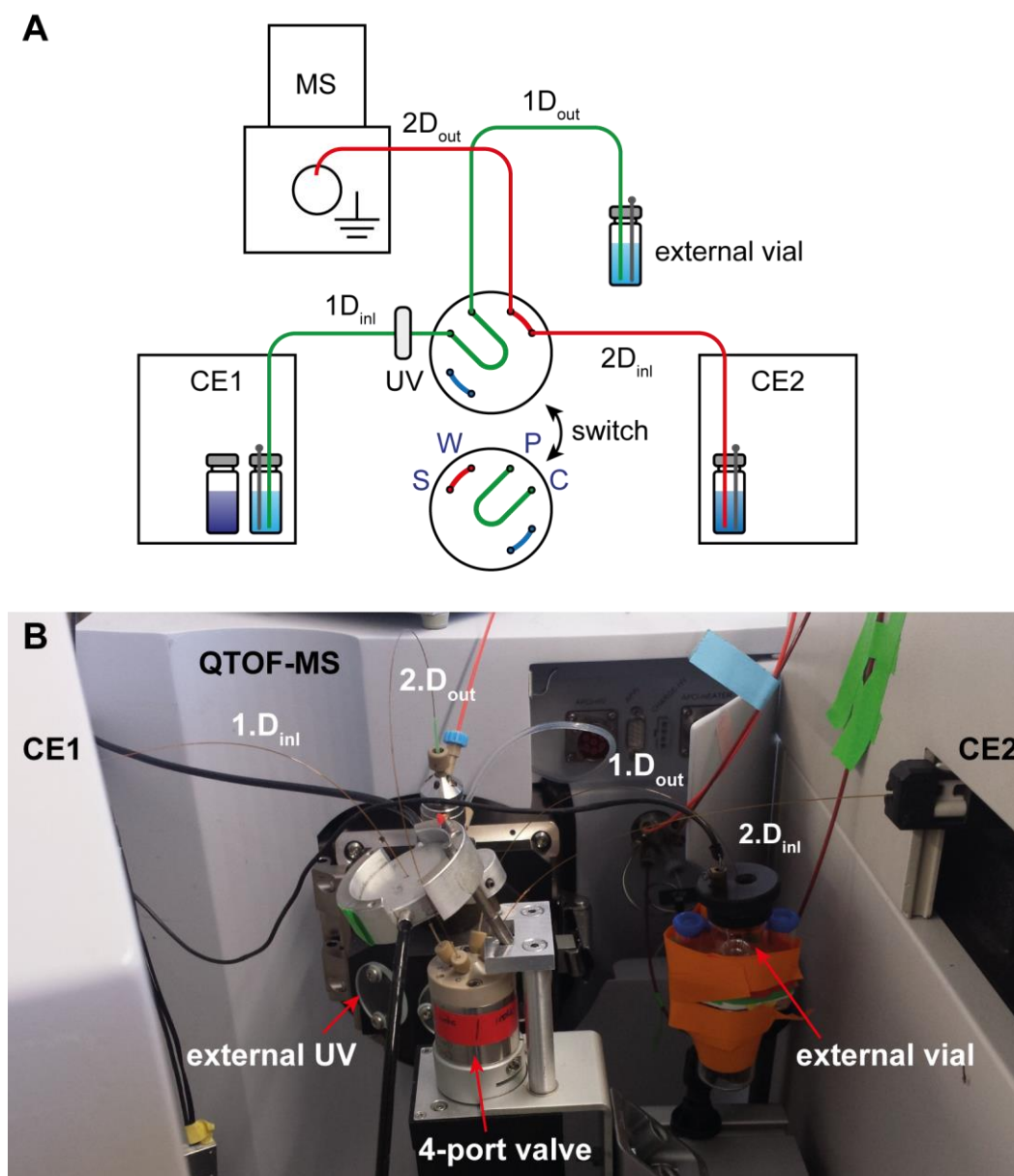


Figure 17: (A) Scheme of general CE-CE-MS setup. The inlet of the 1st dimension (1.D_{inl}) is connected through the external UV cell to channel S of the 4-port valve. The outlet (1.D_{out}) is jointed to channel W and placed in a grounded external vial filled with BGE. The inlet and outlet of the 2nd dimension (2.D_{inl}) are connected to channel C and P, respectively. The outlet (2.D_{out}) is linked to the ESI source of the QTOF-MS instrument. A more detailed description of operation can be found in the main text. (B) Photographic picture of applied CE-CE-MS setup.

The stator and rotor are comprised of a mixture of polyether ether ketone and polytetrafluoroethylene exhibiting a dielectric constant of approximately 22 kV/mm [86]. Thus, considering the rotor geometries and material properties, a voltage between ± 10 to 15 kV is usually applied in order to prevent current breakthroughs and ensure stable operation of the 2D system. A picture of the CE-CE-MS setup is shown in Figure 17 B.

7.3 Development of heart-cut strategy

As stated earlier, the crucial part of the CZE-CZE-MS method represents the sample transfer from the 1st to the 2nd separation dimension. In this context, two different heart-cut sample transfer strategies were evaluated experimentally as depicted in Figure 18. The most straightforward approach to position a desired peak within the sample loop of the 4-port valve is to utilize the electromigration in the 1st dimension (Figure 18 B). Initially, separation is performed in the 1st dimension (step 1). Based on the time it takes for an analyte to migrate towards the external UV detector, its electrophoretic velocity (v_{el}) [cm/min] can be determined as described in equation 7.1 (step 2).

$$v_{el} = \frac{L_{eff}}{t_m} \quad (7.1)$$

- v_{el} : electrophoretic velocity of analyte
 L_{eff} : effective capillary length from CE inlet to UV detector
 t_m : migration time of analyte

Subsequently, the cutting time (t_{cut}) is calculated using the electrophoretic velocity (v_{el}) and the remaining length between the detector and the center of the sample loop of the 4-port valve as shown in equation 7.2. The standard sample loop of the 4-port valve has a volume of 20 nL correlating approximately to a length of 1 cm for a 50 μ m inner diameter capillary. Consequently, the equivalent length to the center of the loop is 0.5 cm which needs to be considered and thus is added to the numerator of the equation.

$$t_{cut} = \frac{L_{tot} - L_{eff} + 0.5}{v_{el}} \quad (7.2)$$

t_{cut} : time to switch 4-port valve

L_{tot} : total capillary length

Separation is prolonged until the cutting time (t_{cut}) is reached and the analyte is located in the sample loop (step 3). Afterwards, the valve is switched and separation in the 2nd dimension is performed (step 4). This strategy was already applied in the previous proof-of-concept study [86]. However, this heart-cut strategy has displayed fundamental drawbacks. It is necessary that the electrophoretic velocity remains constant throughout the whole separation in the 1st dimension. Therefore, the conductivity of the sample and the BGE need to be similar, to avoid field inhomogeneities after injection. In fact, this is not always the case including the tricine-based CZE-UV method.

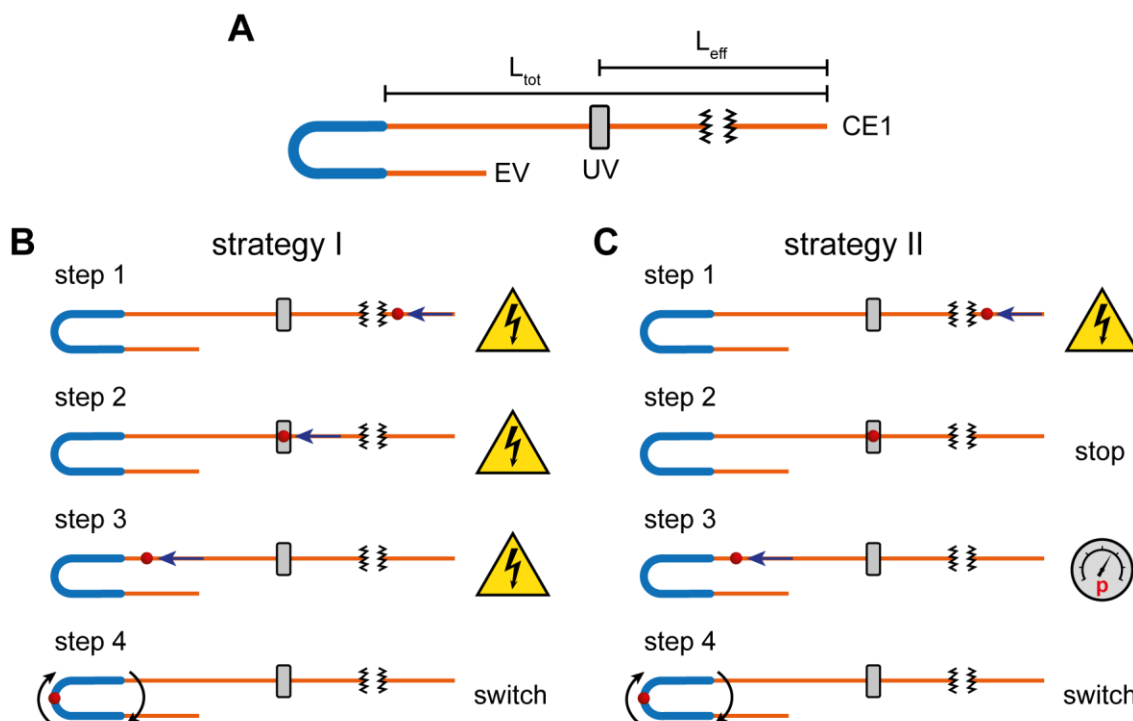


Figure 18: Principle of heart-cut strategies utilizing 4-port valve as CE-CE interface: (A) Definition of different lengths in the 1st dimension. (B) Strategy I, utilizing only electromigration to position analyte in sample loop. (C) Strategy II, including hydrodynamic positioning of analyte from UV detector to sample loop. A more detailed description can be found in the main text.

In addition, potential dead volumes at the capillary junctions and changes in the geometry and surface properties attributed to the 4-port valve might influence the electrophoretic velocity. In fact, the appropriate cutting time can also be determined empirically by stepwise alteration until the highest peak intensity is obtained in the 2nd dimension. Consequently, the calculation can be adapted for a specific type of sample accordingly.

Another way to solve this issue is to use two external detectors in proximity to the 4 port-valve in the 1st dimension. In this way, the electrophoretic velocity can be determined more precisely based on the migration time difference and known distances between the detectors. Such a method was successfully applied for CIEF-CZE-MS utilizing an external UV and conductivity detector [108]. However, it is very elaborate to position two optical detectors directly in front of the 4-port valve, and the setup is fragile due to the need of two capillary windows.

For this reason, an alternative heart-cut strategy was developed as depicted in Figure 18 C. First, separation is performed in the 1st dimension as described for strategy I (step 1). Separation is stopped as soon as the analyte of interest reaches the external UV detector (step 2). Subsequently, low pressure (50 mbar) is applied to position the analyte accurately in the sample loop of the 4-port valve (step 3). The flow rate (\dot{V}_p) is determined prior to the 2D analysis e.g. by injecting a UV active standard and applying low pressure (50 mbar) until it passes the external UV detector. The required time is used to calculate \dot{V}_p as described in equation 7.3.

$$\dot{V}_p = \frac{V_{eff}}{t_{UV}} \quad (7.3)$$

\dot{V}_p : flow rate (50 mbar)

t_{UV} : time for analyte to pass UV detector

The cutting time (t_{cut}) is calculated based on equation 7.4. After positioning of the peak, the valve is switched and separation in the 2nd dimension is performed (step 4). This heart-cut strategy was evaluated empirically and proofed to be more reliable and precise compared to the electromigration based approach.

$$t_{cut} = \frac{V_{tot} - V_{eff} + V_{cl}}{\dot{V}_p} \quad (7.4)$$

- V_{tot} : total volume of capillary
 V_{eff} : effective capillary volume from CE inlet to UV detector
 V_{cl} : volume from capillary connection to center of sample loop

Peak broadening is expected to be low, due to the small applied pressure (50 mbar) and the short distance from the external UV detector to the center of the sample loop (typically 4.5 cm). Differences in the conductivity of the sample and the BGE do not represent a potential issue anymore. Furthermore, this strategy is applicable for any kind of CE method in the 1st dimension as described in **manuscript III**. In case of the tricine-based CZE method the analyte was additionally flushed out of the sample loop into the 2nd dimension (50 mbar for 30 sec) and the valve was switched back to loading position prior to the application of HV in the 2nd dimension (**manuscript I**). Initially, it was believed that this procedure results in a more stable separation. However, follow-up studies revealed that this step is not necessary and HV can be directly applied in the 2nd dimension while the analyte is still located in the sample loop (**manuscript II**).

7.4 Identification of ASA/ASC degradation products

Besides accurate sample transfer, the separation of the co-transferred tricine from the analyte in the 2nd CZE dimension is essential prior to MS detection. In this regard, various BGE systems were tested by 1D CZE-MS analyzing an ASC standard (1000 mg/L) solved in tricine BGE of the 1st dimension. Separation could be achieved using 25 mM ammonium acetate (pH = 6.0) as BGE in reversed polarity mode. The EOF had to be suppressed using poly(vinyl alcohol) (PVA) coating to avoid suction of SL into the separation capillary, creating unstable CE currents. As mentioned before, two distinct peaks were observed in the CZE electropherogram (peak #1 and #2, Figure 16) which could not be attributed to known degradation pathways of neither ASA nor ASC.

Applying CZE-CZE-MS, these peaks could be identified as monoacetylated (#2) and diacetylated (#1) ASC based on their accurate mass and shifts in migration time as illustrated in Figure 19. This conclusion fits well with a proposed reaction mechanism.

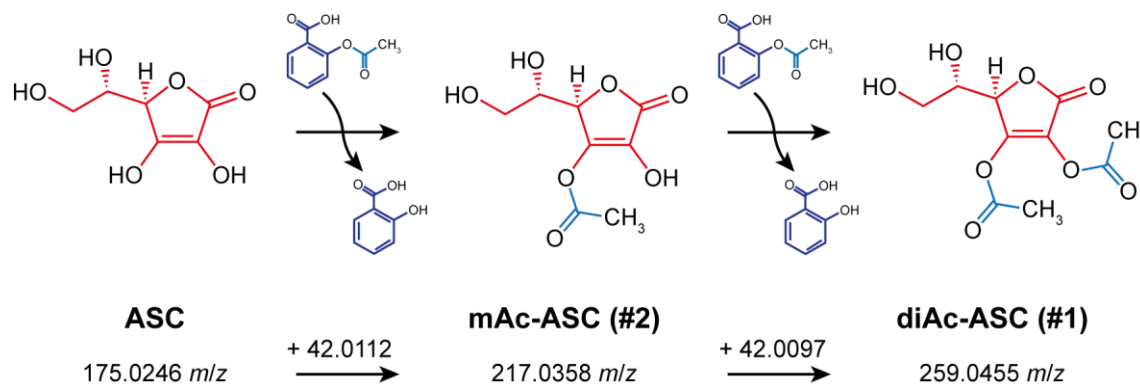


Figure 19: Overview of degradation products originating from ASC in the presence of ASA. ASC is acetylated by ASA forming monoacetylated (mAc)-ASC and diacetylated (diAc)-ASC. Detected m/z values are added below their structure, respectively.

The 3-hydroxy group of ASC is known to be prone to acetylation due to its vinylogous structure [109]. In addition, ASA is capable to acetylate reactive hydroxy groups [110]. Moreover, the pK_A value of the 2-hydroxy group of ASC is lowered from 11.5 to around 5.5 after acetylation of the 3-hydroxy group [109]. Thus, a second acetylation of ASC by ASA is quite plausible.

8. Extension of CZE-CZE-MS applications towards intact protein analysis

8.1 CZE-CZE-MS of mAb charge variants

The characterization of product- and storage-related impurities (e.g. degradation products) of mAbs is an important task of technical development, release testing, control of manufacturing processes, and to ensure the safety of the drug [36]. CZE is well-suited for the analysis of mAb charge variants, due to its high selectivity, resolving power, and low sample consumption. Because of the small deviation in molecular mass between mAb charge variants, the difference in charge and not in hydrodynamic radius is often the important factor regarding separation efficiency. In

recent years, CZE methods were introduced utilizing electrolytes containing, among others, high concentrations of ϵ -aminocaproic acid (EACA) [36, 111, 112]. These EACA-based CZE-UV methods are already an integrated part in the pharmaceutical industry as an additional tool to ion exchange chromatography (IEX)-UV for the characterization of mAb charge variants. In addition, these methods usually exhibit superior separation efficiency and resolution compared to traditional IEX. In order to identify previously separated mAb charge variants, MS characterization has been demonstrated to be a powerful and crucial tool [113]. However, similar to the previously described tricine, EACA is highly ESI-interfering for proteins in positive mode and thus no direct coupling with MS is feasible. Therefore, a heart-cut CZE-CZE-MS method was developed utilizing the aforementioned 4-port-valve. Trastuzumab is well characterized and known to possess several potential deamidation sites [114, 115]. Due to the minor mass difference of deamidated proteoforms ($\Delta m = 1$ Da), a preceding separation is essential prior to MS characterization. For this reason, Trastuzumab was selected as model system to demonstrate the capability of the developed CZE-CZE-MS method.

8.2 CZE-CZE-MS method development

For the 1st dimension, a generic EACA based BGE was selected adapted from Moritz *et al.* [36]. The BGE comprised 380 mM EACA, 1.9 mM triethylentetramine, and 0.05% hydroxypropyl methylcellulose. A more detailed description of 1D and 2D method conditions can be found in **manuscript II**. To reiterate, the 2nd dimension was not performed to achieve higher peak capacities or resolution such as in traditional 2D approaches, but can be seen more as an on-line electrophoretic clean-up step prior to MS detection. Therefore, a variety of different volatile BGE compositions were tested as potential 2nd dimension analyzing Trastuzumab (12.5 mg/mL) dissolved in EACA electrolyte by 1D CZE-MS: 0.5 and 1 M FAc; 0.5, 1, 2, 3 and 5 M HAc. In this context, 2 M HAc was sufficient to separate mAb variants from the EACA electrolyte constituents and thus selected for all further experiments. In subsequent CZE-CZE-MS experiments, single heart-cuts (20 nL) of mAb peaks were performed as described in Figure 18 C. An example cut of the main peak of glycosylated Trastuzumab (12.5 mg/mL) is shown in Figure 20. Interference-free mass spectra could be obtained and typical glycoforms were observed.

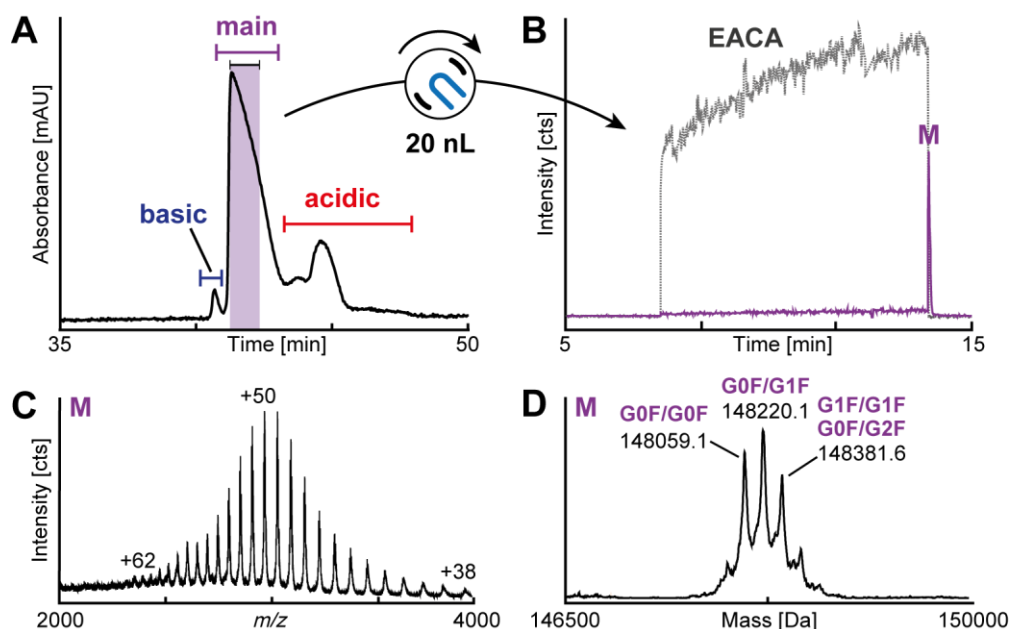


Figure 20: Cut of main peak of glycosylated Trastuzumab (12.5 mg/mL) using CZE-CZE-MS (20 nL transfer volume). (A) CZE-UV electropherogram of 1st dimension including basic, main, and acidic variants. (B) CZE-MS electropherogram of 2nd dimension. (C) Raw and (D) deconvoluted mass spectrum of cut main peak. Typical glycoforms (G0F/G0F to G1F/G1F, G0F/G2F) were observed. Detailed separation conditions can be found in **manuscript I**.

8.3 Mass accuracy of intact mAbs

In general, MS characterization of mAb variants provides information on the primary sequence, PTMs and higher order structures [116]. However, high mass molecules such as intact mAbs (~150 kDa) are usually non-isotopically resolved by most MS instruments, including the applied QTOF-MS instrument. Nonetheless, high resolution MS enables the discrimination of analyte species even with minor differences. Yet, the isotopic envelope of mAbs is rather broad (~25 Da at full width at half maximum) [117]. Small mass shifts caused by deamidation (+1 Da) or even larger shifts, e.g. *N*-terminal pyroglutamate formation (-18 Da) would inevitably overlap in the mass spectrum. Due to the preceding separation of charge variants in the EACA-based BGE the broad isotopic envelope did not represent an issue for the developed CZE-CZE-MS method. Still, a mass precision better than 1 Da is necessary to distinguish deamidated proteoforms. In fact, the obtainable mass accuracy and precision had to be critically evaluated. In order to optimize the achievable mass accuracy and precision an external calibration of the MS data in a close time frame to the analyte signal was implemented in the 2nd dimension. Thereby, tuning mix solution (20 μ L)

was infused via the SL tubing directly after the mAb was detected in the MS using the integrated mechanical 6-port valve of the QTOF-MS instrument depicted in Figure 21.

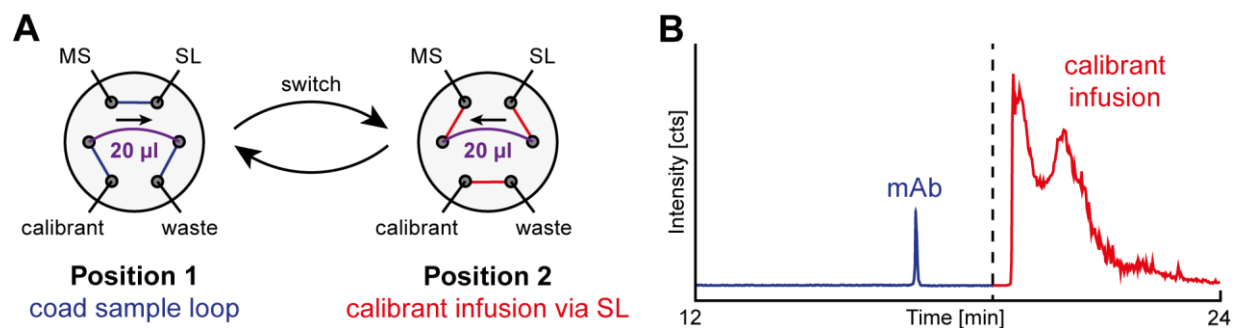


Figure 21: MS calibration procedure based on SL tuning mix infusion. (A) Scheme of 6-port valve of QTOF-MS used for tuning mix infusion (B) CZE-MS electropherogram with implemented tuning mix infusion. A more detailed description can be found in the main text.

During migration of the mAb charge variant, the sample loop (20 µL) of the 6-port valve implemented in the QTOF-MS instrument was filled with tuning mix solution (position 1). After detection of the mAb in the MS the valve is switched and tuning mix is infused via the SL tubing (position 2). The resulting tuning mix signals were used to recalibrate the MS spectra during data evaluation (quadratic regression model). In this way, variations in the instrumental performance could be corrected subsequently improving the overall mass accuracy and precision. In general, the developed calibration procedure can be transferred to any CZE-MS method utilizing a SL based CE-ESI interface and was later applied in our group for CIEF-CZE-MS of intact proteins including mAbs [118]. In this way, highly precise mass data of glycosylated Trastuzumab could be obtained.

For the three highest abundant glycoforms of the main variant G0F/G0F, G0F/G1F and G1F/G1F (G0F/G2F) an average mass of 148059.1 ± 0.8 , 148220.1 ± 0.5 and 148381.6 ± 0.6 ($n = 5$) was determined, respectively. A deviation of +20.2, +13.0 and +8.4 ppm compared to the theoretically calculated average masses (148056.1, 148218.2 and 148380.4 Da) was observed based on the "representative isotopic distributions" of IUPAC [119]. Potential explanations, such as adduct formation, systematic error in deconvolution and mass calibration process were evaluated but conclusively regarded as improbable. However, a general tendency to slightly higher average masses compared to the calculated values could be observed in the literature

as well [113, 117]. The relative amount of ^{13}C in the “representative isotopic distributions” of IUPAC ($\delta^{13}\text{C} = -37$) is based on crude oil, and differs compared to the natural isotopic distribution of carbon in organic material (C3, C4 and CAM plants: $\delta^{13}\text{C} = -10$ to -33) [120]. Thus, a deviation in the isotopic distribution of carbon could be a plausible explanation for the observed mass shift, as exemplarily shown for the glycoform G0F/G1F of the main Trastuzumab peak in Figure 22.

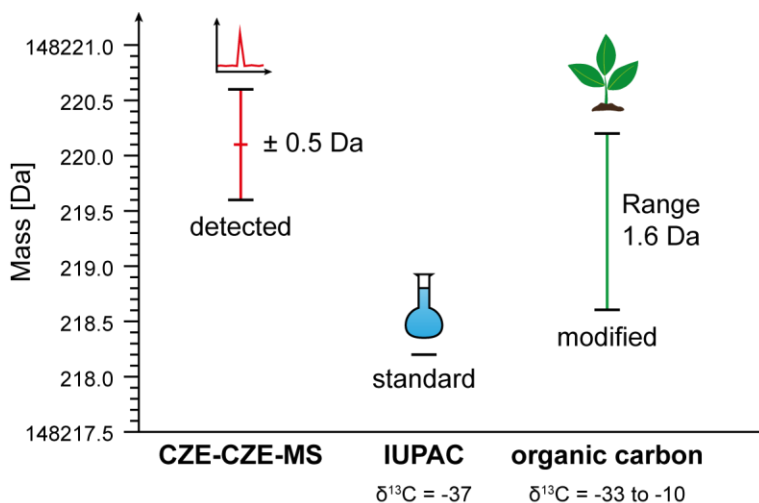


Figure 22: Comparison of detected deconvoluted mass of G0F/G1F glycoform of the main peak of Trastuzumab with calculated masses based on ^{13}C distribution stated by IUPAC [119] and natural organic carbon [120]. A more detailed explanation can be found in the main text.

Taking the entire width of the natural organic carbon distribution into account, the theoretical calculated values for the three main glycoforms are 148057.2 (G0F/G0F), 148219.4 (G0F/G1F) and 148381.5 (G1F/G1F, G0F/G2F) with a range of ± 0.8 , respectively. A corresponding mass deviation between -5.1 to $+17.9$ ppm was determined for the detected masses. By taking the measurement uncertainty in consideration, detected and calculated masses are in agreement. The detailed comparison between detected and theoretical masses of intact proteins could only be performed due to the impressive mass precision (standard deviation = 0.5 – 0.8 Da) achieved by using the developed CZE-CZE-MS method. The attained results highlight the challenge of accurate mass calculation for intact proteins in general. Furthermore, such a detailed evaluation of detected and calculated masses has not been performed for intact mAbs thus far.

8.4 Deamidated charge variants of Trastuzumab

Subsequently, the most intense acidic variant of glycosylated Trastuzumab was cut and analyzed and a slight shift to higher masses ($\sim 1\text{-}3$ Da) was observed compared to its main form, which could be explained by potential deamidation processes. However, the signal quality was not sufficient for accurate mass determination (standard deviation 1.8 Da; $n = 5$). For this reason, deglycosylation of Trastuzumab samples using *N*-glycosidase F was performed, in order to increase sensitivity and simultaneously simplify the obtained mass spectra. Results of the CZE-CZE-MS analysis of the main form and the two most abundant acidic variants are illustrated in Figure 23.

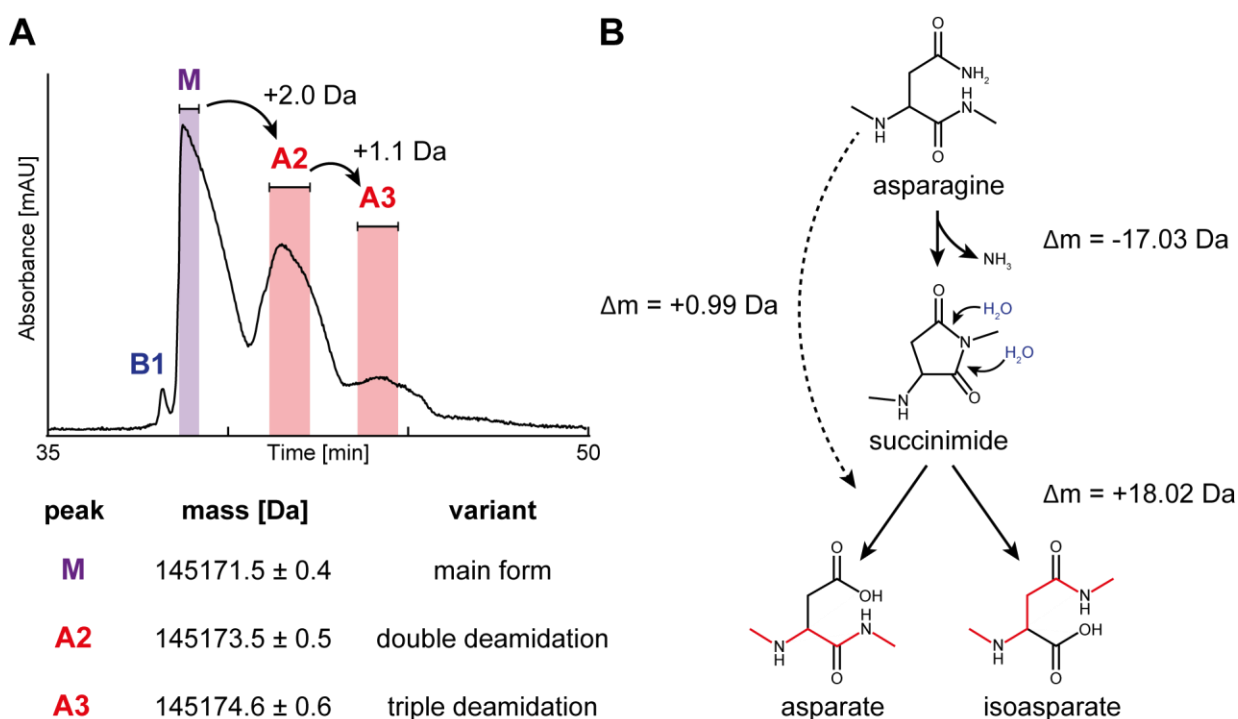


Figure 23: CZE-CZE-MS analysis of deglycosylated Trastuzumab (6 mg/mL). (A) 1st dimension CZE-UV electropherogram. Results of consecutive cuts ($n = 5$) of M, A2, and A3 are summarized below. (B) Reaction pathway of deamidation process. A more detailed description can be found in the main text.

Considerable higher relative intensities for the acidic variants were observed compared to the glycosylated sample, which implies chemical alteration induced by *N*-glycosidase F treatment. The following deconvoluted masses were obtained for 5 consecutive cuts of each peak: M = 145171.5 ± 0.4 Da, A2 = 145173.5 ± 0.5 Da, and A3 = 145174.6 ± 0.6 Da. As already indicated by the analysis of the glycosylated

sample, slightly higher masses compared to the main variant were obtained. Due to the high precision (standard deviation ≤ 0.6 Da), the mass differences were confirmed to be statistically significant (t-test, $\alpha = 0.05$, $p < 0.05$). In addition, deglycosylation by *N*-glycosidase F (pH = 8.0) is known to introduce significant amounts of artificial chemical deamidation [121]. The acidic variants A2 and A3 can most likely be attributed to be deamidation products based on three major criteria: (i) increased migration times, (ii) corresponding mass shift, and (iii) elevated intensity after *N*-glycosidase F treatment.

In conclusion, interference-free mass spectra of mAb charge variants previously separated in highly ESI-interfering BGE were obtained by the application of developed CZE-CZE-MS method. Admittedly, the overall analysis time is rather long, however, the CZE-CZE-MS method is only needed for valuable characterization purposes, whereas the underlying 1st dimension (CZE-UV) can be applied routinely for reliable quantitation. The CZE-CZE-MS method is expected to be applicable to a variety of different BGEs in the 1st dimension. In this way, extensively optimized and validated CZE methods, e.g. targeting a specific type of mAb, can be coupled to MS. Still, there is room for improvement regarding, sensitivity and sample pretreatment (generation of additional deamidation caused by *N*-glycosidase F treatment) to characterize even very low abundant charge variants.

9. Overview of CE-CE-MS applications developed for ESI interfering electrolytes

9.1 Application of different CE modes as 1st dimension

In the context of the CE-CE-MS setup utilizing the 4-port valve interface, the focus of this thesis was to enable mass spectrometric characterization of analytes separated by ESI-interfering CZE methods. Nevertheless, other CE modes causing similar interference with the ionization process can be used as 1st dimension, and respective 2D methods were developed by other members of the working group. All 2D CE-MS applications based on the 4-port valve interface so far were summarized and discussed in **manuscript III**.

In CIEF, ions are separated based on their pI value in a pH gradient applying ampholytes which are typically highly ESI-interfering. For this reason, CIEF-CZE-MS methods were developed in our group for intact protein analysis. Exemplarily, separation and characterization of hemoglobin and its glycosylated form ($\Delta pI = 0.036$) could be achieved [108]. In addition, the results obtained regarding potential deamidation products of Trastuzumab using CZE-CZE-MS could be confirmed by CIEF-CZE-MS, utilizing the hydrodynamic sample transfer strategy developed in this thesis [118]. One feature of CIEF is that the entire capillary can be filled with sample often resulting in higher sensitivity compared to CZE due to the increased injection volume. Another interesting application represent CGE methods utilizing sodium dodecyl sulfate (SDS) for mAb impurity characterization. These methods are routinely applied in the pharmaceutical industry and thus of particular interest. Protein-DS complexes are particularly strong and cannot be disrupted easily. In order to overcome this issue, a sophisticated CZE method was developed based on the co-injection of positively charged surfactants and methanol as organic solvent to break up these complexes [122]. This CZE method could be successfully applied as 2nd dimension in the CE-CE-MS system (manuscript in preparation). All these examples, including the CZE-CZE-MS methods developed during this thesis, emphasize the versatility of the CE-CE-MS system.

10. Setup of LC-CE-MS system and first application to intact glycoprotein analysis

10.1 NanoLC-CZE-MS of glycoproteins

Proteome analysis is considered one of the current biggest challenges in the field of (bio)analytical chemistry [123]. Due to the enormous diversity of protein species and variants, a single analytical method is simply not sufficient to reveal the entire complexity of a cell proteome. In this regard, the hyphenation of nanoscale RPLC and CZE is of particular interest due to their nearly orthogonal separation mechanism and well-suited geometries/dimensions, especially in combination with characterization by MS. Up to this point, the 4-port valve interface has not been applied in the context of “traditional” 2D analysis, in order to increase separation efficiency and resolving power. In addition, no chromatographic based separation technique has been

integrated in our 2D system. Therefore, a heart-cut nanoLC-CZE-MS method was developed for the proof-of-concept analysis of glycoproteins utilizing the 4-port valve as LC-CE interface (see **manuscript IV**).

10.2 Development of nanoLC-CZE-MS method

Based on the recent success of our previous work related to CE-CE-MS, a nanoLC pump was provided by Agilent Technologies (Waldbronn, Germany) to evaluate the potential of the 4-port valve interface for nanoLC-CZE coupling. However, no adequate sample injection system ($V_{inj} < 1 \mu\text{L}$) was available in our lab. Thus, an alternative injection system for nanoLC had to be developed. The integrated mechanical 6-port valve of the ESI-QTOF-MS system was evaluated for sample injection in the nanoLC system as illustrated in Figure 24.

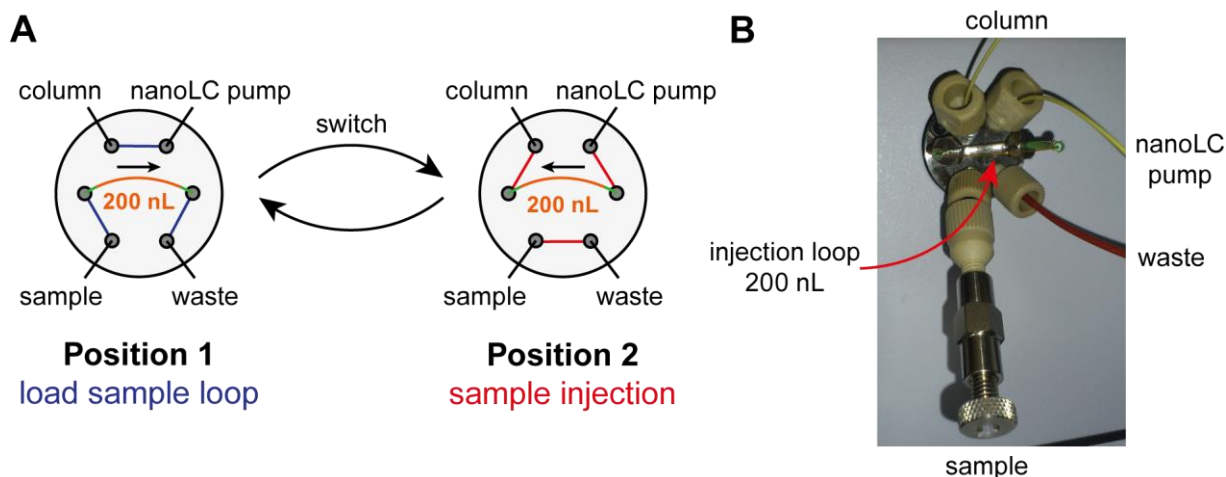


Figure 24: (A) Scheme of 6-port valve used for sample injection for nanoLC system. Sample is loaded via a syringe while the 6-port valve is kept in position 1 (loading volume: 200 nL). Injection was performed by switching to position 2. (B) Picture of 6-port valve. A more detailed description can be found in the main text.

Here, a PVA coated capillary with an inner diameter of 50 μm and a length of 10 cm was applied as sample loop resulting in an injection volume of about 200 nL. PVA-coated capillaries were used to prevent protein adsorption on the capillary wall which would cause incomplete sample injection and potential carry over. Prior to injection, the complete loop was filled with sample solution using a syringe while the valve is kept in position 1. Subsequently, the valve was switched for 60 sec to position B in

order to ensure the injection of the complete sample onto the column, utilizing a nanoLC flow rate of 0.5 $\mu\text{l}/\text{min}$. The injection method was tested and confirmed to be reproducible for nanoLC-UV by analyzing ribonuclease B (RNase B) as model protein ($c = 100 \mu\text{g}/\text{ml}$).

During nanoLC-UV method development several gradients and eluent compositions were evaluated, including different types of organic solvents and additives, analyzing a model protein mix: RNase B (100 $\mu\text{g}/\text{mL}$), cytochrome c (80 $\mu\text{g}/\text{mL}$), lysozyme c (80 $\mu\text{g}/\text{mL}$) and myoglobin (50 $\mu\text{g}/\text{mL}$). The final nanoLC method was as follows: mobile phase A was 10% ACN with 0.05% TFA, while mobile phase B was 100% ACN with 0.05% TFA. A 44 min gradient was applied: 0-2 min: 0% B, 2-30 min: 0-100% B, 30-34 min: 100% B, 34-36 min: 100-0% B, 36-44 min: 0% B. In the context of intact protein analysis, elevated column temperatures have been demonstrated to be beneficial for intact protein separation [124]. For this reason, an LC oven was built and different temperatures were tested during method development including room temperature, 40, 50, 55 and 60 $^{\circ}\text{C}$. A temperature of 50 $^{\circ}\text{C}$ was selected for further experiments exhibiting the highest resolution (improvement factors: 1.17-1.25, compared to room temperature). Since proteins usually elute at high organic content, the influence of organic solvents on CZE-MS had to be evaluated. Therefore, a standard of RNase B (1000 $\mu\text{g}/\text{mL}$) was solved in different amounts of ACN or methanol (10-70% (v/v)) and subsequently analyzed by CZE-MS (BGE 1 M HAc). No major influence on the separation performance and stability was observed. Thus, it can be concluded that typical elution conditions for RPLC can be applied in the 1st dimension of the 2D setup without negative influence on the CZE-MS dimension. Furthermore, different BGE compositions were tested for glycoforms separation analyzing the same RNase B standard resulting in a final BGE of 0.2 M FAc.

10.3 Heart-cut of RNase B from protein mix

Subsequently, the protein mix was analyzed using the complete nanoLC-CZE-MS system. A scheme of the complete 2D setup can be found in **manuscript IV**. First, the different protein species were separated by nanoLC followed by heart-cut transfer of individual LC peaks and subsequent characterization of their glycoforms by CZE-MS. A chromatogram of the 1st dimension separation is illustrated in Figure 25 A. All four protein species were baseline separated. An electropherogram of the 2nd

dimension after heart-cut of the RNase B peak is shown in Figure 25 B. The non-glycosylated form is clearly separated from the partly resolved glycosylated variants (high-mannose *N*-glycans ranging from five to nine Man units). As expected, the migration time increased with the size of the attached glycan.

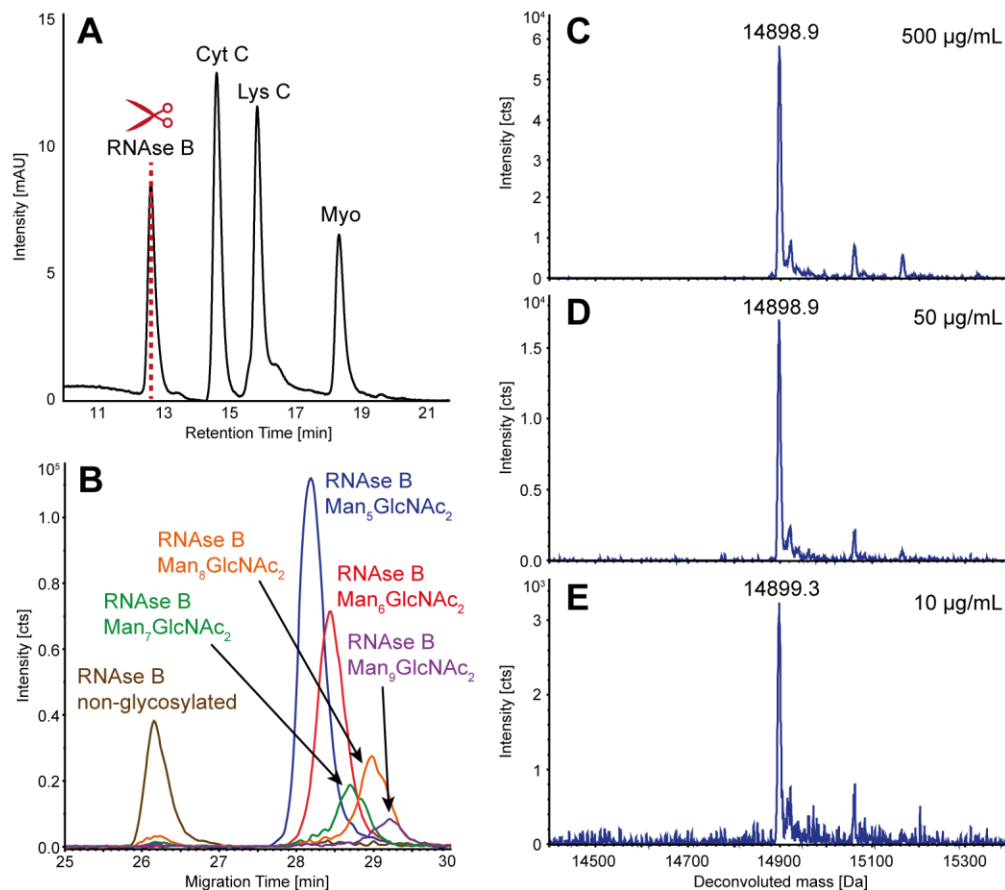


Figure 25: Analysis of protein mix by nanoLC-CZE-MS. 1st dimension: (A) nanoLC chromatogram (214 nm detection wavelength) of the separation of different proteins. 2nd dimension: (B) CZE-MS electropherogram obtained after heart-cut of RNase B peak (transfer volume: 20 nL). Separation of various RNase B glycoforms observed. The 11 most abundant charge states of the individual glycoforms were used to create the ion traces, respectively. (C-E) Deconvoluted mass spectra of main variant of RNase B ($\text{Man}_5\text{GlcNAc}_2$) at three concentration levels: 500, 50, and 10 $\mu\text{g/mL}$.

In addition, the protein mix was analyzed by 1D CZE-MS leading to overlaid electropherograms of the different protein species/variants, substantiating the importance of increased resolution by the nanoLC-CZE-MS method. Linearity was confirmed ($R^2 = 0.9998$) exemplarily for the main glycosylated form of RNase B ($\text{Man}_5\text{GlcNAc}_2$) by cutting three different concentrations ($n = 3$ per level) of RNase B

out of a protein mix: 500, 50, and 10 $\mu\text{g}/\text{mL}$. Deconvoluted mass spectra are illustrated in Figure 25 C-F. High mass accuracy and precision was achieved even at the lowest concentration: detected 14899.24 ± 0.16 Da, calculated 14899.23 Da. The limit of detection of RNase B ($\text{Man}_5\text{GlcNAc}_2$) was estimated to be about 3 $\mu\text{g}/\text{mL}$ ($S/N = 3$). With respect to the obtained peak widths ($\text{FWHM} \sim 0.25$ min) it is apparent that 20 nL is not sufficient to transfer an entire analyte peak from the 1st to the 2nd dimension. Assuming the heart-cut is accurate and taking peak shapes in consideration transfer efficiencies of RNase B was calculated to be around 14%. This value is expected to be better compared to most flow-gating approaches. For instance, Lemmo and Jorgenson calculated transfer efficiencies of about 1% [125]. Nonetheless, there is still room for improvement in regards of sensitivity which will be covered in future studies.

11. Development of a CZE-DTIM-MS method for the analysis of protein glycosylation

11.1 CZE-IM-MS of *N*-glycans

An interesting alternative to couple two liquid based separation techniques is the combination of CZE (liquid phase) and IMS (gas phase) technology [95]. Both, CZE and IMS have been demonstrated to be highly efficient for glycan separation, especially considering isomeric separation [101, 126]. Yet, the characterization of glycans still represents a challenging task due to their high structural variability [16]. 8-aminopyrene-1,3,6-trisulfonic acid (APTS) is a common labeling agent for the separation of *N*-glycans using CZE coupled to laser-induced fluorescence (LIF) detection [127]. However, due to the lack of available glycan standards and the incompatibility of the electrolyte system with ESI, the assignment of peaks especially for new glycan structures is difficult or even not possible. Therefore, our group has introduced a CZE-MS method utilizing an EACA-based BGE showing similar separation performance than the CZE-LIF methods [126]. In contrast to the aforementioned mAb charge variant analysis, EACA does not noticeably interfere with the ionization of *N*-glycans in negative ion mode. During this thesis, the EACA-based CZE method was hyphenated with DTIM-MS to further improve separation capabilities for the analysis of native and APTS-labeled *N*-glycans (**manuscript V**). DTIM-MS instruments are

already commercially available since 2013. Nevertheless, CZE-DTIM-MS has not been investigated in detail to this day [96].

11.2 Analysis of APTS-labeled mAb *N*-glycans

Initially, APTS-labeled *N*-glycans released from a model mAb were analyzed using the developed CZE-DTIM-MS method. An example CZE electropherogram is shown in Figure 26 A. A typical separation profile of *N*-glycans derived from mAbs was obtained including G2F, G1F'(1,3), G1F(1,6) and G0F. Each individual arrival time distribution (ATD) of the glycan signals resolved in the CZE exhibits multiple peaks which is exemplarily shown for the triple- and double-charged ions of the glycan isomers G1F'(1,3) and G1F(1,6) in Figure 26 B/C, respectively. In addition, the corresponding mass spectra can be found in Figure 26 D-G. Significant differences between the ATDs of G1F'(1,3) and G1F(1,6) were observed for both charge states. Only the preceding CZE separation provides independent detection of G1F'(1,3) and G1F(1,6) in the IMS. Otherwise, their ATDs would be heavily overlaid emphasizing the necessity of the combination of CZE and DTIM-MS separation, since neither of these techniques is able to resolve all the detected species individually. An adequate comparison with other IMS related works was not possible, since APTS-labeled glycans have not been analyzed in this way thus far. The origin of the multiple peaks observed in the ATD space could not be unambiguously assigned, but could be explained by the presence of isomeric forms and/or conformers that do not interconvert on the time-scale of the ion mobility separation.

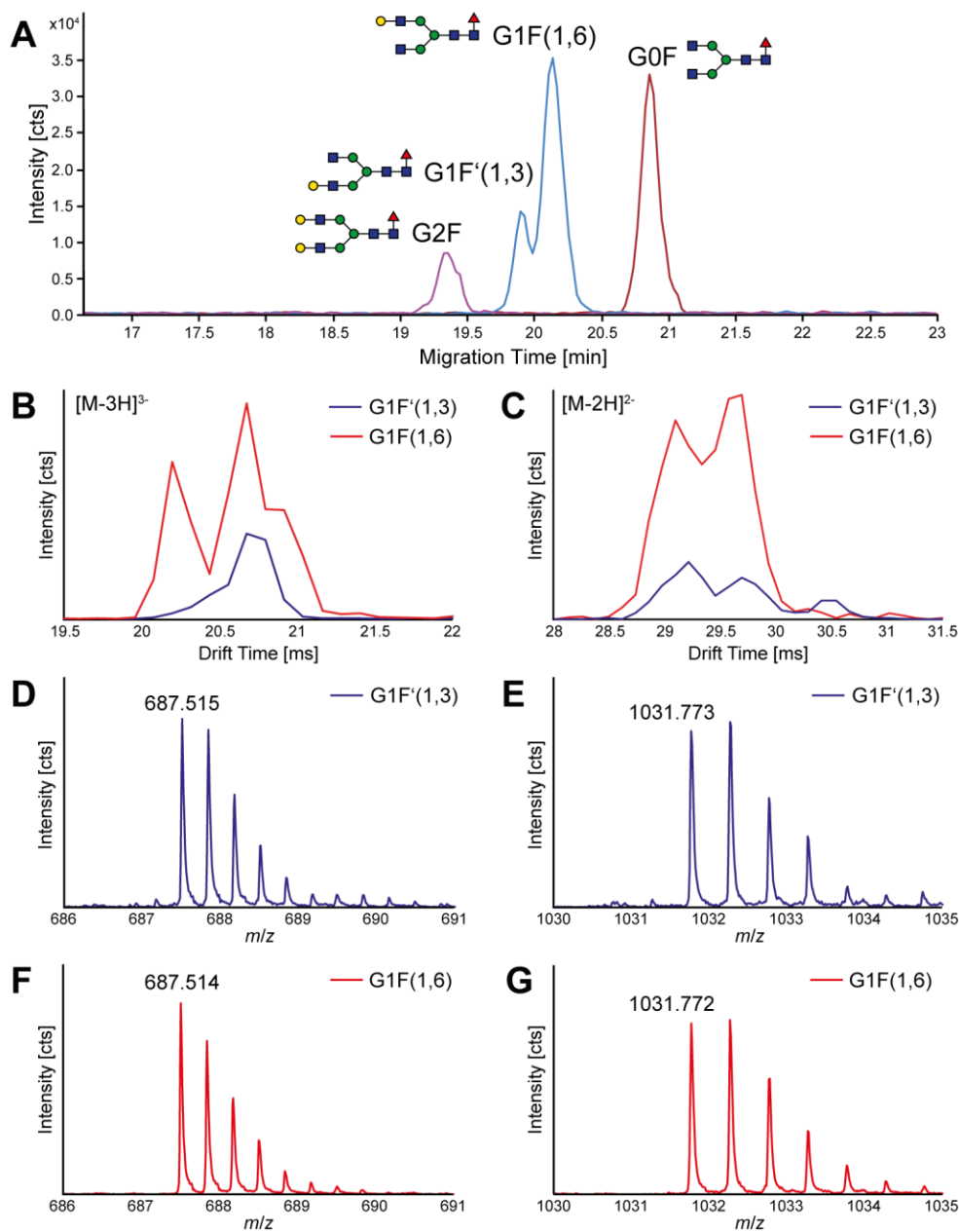


Figure 26: CZE-DTIM-MS of APTS-labeled N-glycans. (A) CZE electropherogram of APTS-labeled N-glycans released from mAb1 including G0F (950.75, 633.50 m/z), G1F'(1,3), G1F(1,6) (1031.77, 687.51 m/z) and G2F (1112.80, 741.53 m/z). ATDs of triple- (B) and double-charged (C) ions originating from the mAb glycans G1F'(1,3) and G1F(1,6) priorly separated by CZE. Corresponding mass spectra of triple- (D, F) and double-charged (E, G) ions. A detailed description of the method conditions can be found in **manuscript V**.

11.3 Analysis of native *N*-glycans

In a subsequent experiment, native *N*-glycans released from fetuin and α -1-acid glycoprotein (AGP) were analyzed using the developed CZE-DTIM-MS method. The major glycoforms detected were in accordance with the known literature [128]: 2Ant2NeuNAc, 2Ant3NeuNAc, 2Ant4NeuNAc originating from AGP, and 2Ant2NeuNAc, 3Ant3NeuNAc, Ant4NeuNAc released from fetuin. Example electropherograms are depicted in Figure 27 A and B. Compared to the APTS-labeled *N*-glycans, a similar or even higher complexity was obtained for ATDs of the individual glycan peaks resolved by CZE, which is exemplarily shown for the *N*-glycan 2Ant2NeuNAc in Figure 27 C/D. Furthermore, there are distinct differences in the ATDs of 2Ant2NeuNAc depending on the protein source. For example, the signal between 29 and 30 ms is significantly lower in the ATD derived from fetuin compared to AGP.

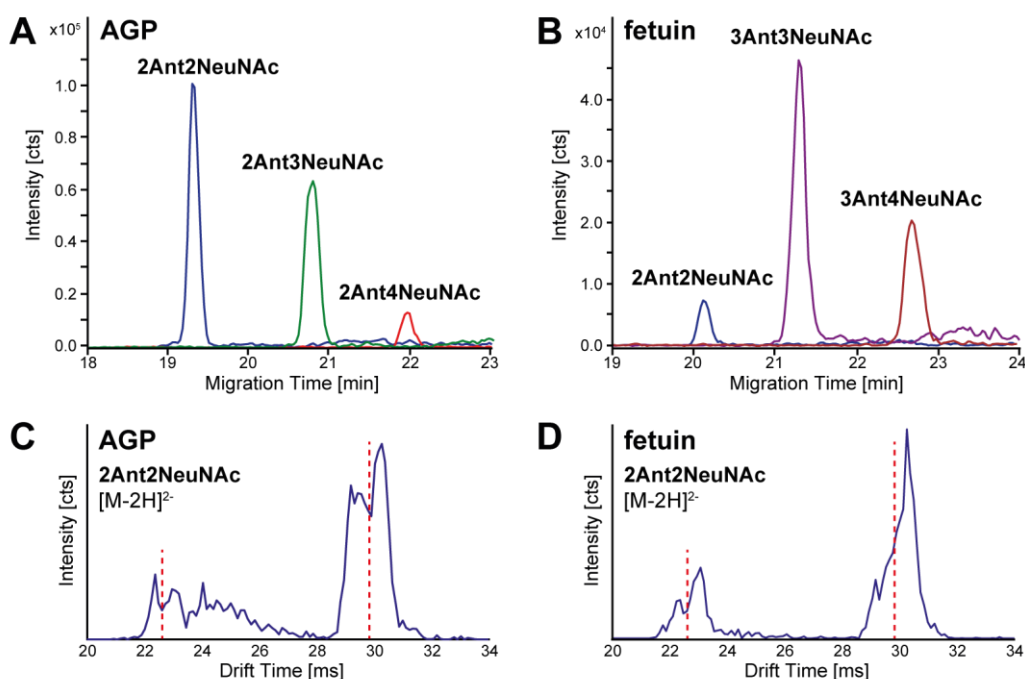


Figure 27: CZE-MS electropherograms of native sialylated *N*-glycans released from AGP (A) and fetuin (B): Major glycoforms detected include diantennary carbohydrate chains with two to four sialyl residues (AGP) and di- and triantennary glycans with at least the same amount of *N*-acetylneuraminic acid (fetuin). ATDs of double-charged ions of 2Ant2NeuNAc released from AGP (C) and fetuin (D). Red dotted lines are added to the ATDs to simplify comparison. A more detailed description about the method conditions can be found in **manuscript V**.

Both samples were analyzed under the same conditions (instrument setup, BGE, SL composition, etc.). This indicates the presence of linkage or structural isomers. To further elucidate the characteristics of the multiple peaks observed in the ATDs, AGP and fetuin derived *N*-glycan samples were treated with α 2-3 neuraminidase. Hence, sialic acids exhibiting an α 2-3 linkage to galactose are specifically cleaved, whereas α 2-6 linkages remain intact. In this way, it was possible to attribute certain peaks in the ATDs of the native *N*-glycans to differences in their sialic acid linkage.

Due to the complex nature of the ATDs the reproducibility of the obtained drift times represents an important parameter of the CZE-DTIM-MS method. Relative standard deviations were calculated between 0.2 and 0.5%. A more detailed description of the applied calculation can be found in **manuscript V**. These values are in the range expected for this type of instrument [129]. Furthermore, different SL combinations were tested analyzing *N*-glycans released from AGP: isopropyl alcohol/water 1:1, 3:7, 7:3, methanol/water 1:1 and acetonitrile/water 1:1. No significant changes in the ATDs could be observed. Consequently, the CZE-IM-MS method seems to be not depending on the applied SL including the nature and relative amount of organic solvent. Thus, it is expected that SL compositions in CZE can be adapted independently from the IMS dimension e.g. to optimize ionization efficiency. Summarized, the high potential of the combination of CZE and DTIM-MS technology could be demonstrated and is expected to find various applications in the future.

Conclusion

CE coupled to MS technology is becoming increasingly important in the academic field as well as in pharmaceutical industry e.g. for the analysis of intact proteins. Nevertheless, certain restrictions still remain impeding the application of CE-MS: (i) ESI-interference of many commonly applied electrolytes, (ii) low concentration sensitivity due to minor injection volumes (typically in the few nL range), and (iii) deficient separation resolution and efficiency in particular cases. Therefore, the main objective of the presented thesis was to develop two dimensional separation systems coupled to MS utilizing a mechanical 4-port valve as CE-CE or LC-CE interface in order to overcome these limitations. A preceding proof-of-concept study in our working group has demonstrated the general applicability of the 4-port valve as CE-CE interface. However, no real application has been developed thus far, and certain issues remained regarding reproducibility and stability of the general CE-CE-MS setup.

For this reason, the first period of this thesis was dedicated to the development and application of a functional CE-CE-MS system, employing highly ESI-interfering CZE methods as 1st separation dimension. Initially, a CZE-CZE-MS method was developed for the identification of previously unknown degradation products of acetylsalicylic acid and ascorbic acid in effervescent tablets. Here, an ESI-interfering tricine-based BGE was applied in the 1st dimension in order to achieve sufficient separation efficiency. The crucial part of the CZE-CZE-MS method is the sample transfer from the 1st to the 2nd separation dimension. In this context, a precise and reliable hydrodynamic heart-cut sample transfer was implemented greatly improving the overall reproducibility of the 2D system. Furthermore, this approach is expected to be applicable for any kind of CE method as 1st dimension, making on-line MS detection accessible for a wide range of ESI-interfering CE electrolytes. In this way, it was possible to identify mono- and diacetylated ascorbic acid as relevant degradation products derived from the combination of ASA and ASC in pharmaceutical formulations for the first time. Subsequently, the field of application for the CE-CE-MS setup was extended to intact protein analysis. CZE-UV methods utilizing EACA based electrolytes are routinely applied in pharmaceutical applications for the separation of mAb charge variants. Similar to the tricine-based CZE method,

significant ESI-interference occurred due to the applied EACA-based BGE. A sophisticated CZE-CZE-MS method was developed for intact mAb charge variant characterization utilizing the EACA-based BGE as 1st dimension. Interference-free mass spectra of Trastuzumab charge variants, acting as a model mAb system, were obtained. Besides the first on-line generated MS data of mAbs separated in such a BGE, differentiation between main and deamidated forms of mAbs on intact protein level ($\Delta m = 1$ Da) was achieved supported by statistical data. The obtainable mass accuracy was critically evaluated. Since the detailed isotopic elemental composition of mAb molecules is usually unknown, especially considering the $^{13}\text{C}/^{12}\text{C}$ ratio, the calculation of the theoretical intact mass exhibits considerable uncertainties (low Da range). This is not only an issue for the developed CZE-CZE-MS method, but for intact protein analysis by MS in general. Nevertheless, values in the lower ppm range could be achieved. A potential work flow for application in the pharmaceutical industry is proposed as follows: The CZE-UV method is applied for routine quantitation and high throughput analysis, whereas the CZE-CZE-MS method is employed for specific samples, e.g. for identification of uncharacterized peaks.

In addition, other CE modes such as CIEF were successfully applied as 1st dimension by our group, utilizing the developed hydrodynamic heart-cut sample transfer, summarized in a recent trend article. This highlights the flexibility and versatility of the developed CE-CE-MS system. Nevertheless, there is still room for improvement for future projects. One remaining issue is the maximal applicable HV of about ± 15 kV. In addition, the 2D setup is still rather elaborate to rig up, including cleaning of rotor and stator. Potential solutions include the application of an alternative valve material exhibiting a higher dielectric constant or a general redesign increasing the distance between the rotor channels. Thinking ahead, automation of the CE-CE-MS system is also aspired, which involves writing an original source code and program to control all elements of the 2D system. Furthermore, direct optical detection on the sample loop would be ideal to avoid the required calculation of cutting times. However, this would probably require more effort than a rather simple redesign of the existing 4-port valve, but might be accomplished by other types of 2D interfaces, e.g. involving transparent microfluidic chips. Nonetheless, already impressive, efficient and sophisticated CZE-CZE-MS methods were developed during this work.

The second part of the thesis involved the development of a heart-cut nanoLC-CZE-MS method for glycoprotein analysis. The hyphenation of nanoscale RPLC and CZE is of major interest in the scientific community due to their nearly orthogonal separation mechanism and well-suited geometries/dimensions. This proof-of-concept study represented the primary attempt to utilize the 4-port valve as LC-CE interface. Exemplarily, a model protein mix was separated by nanoLC followed by heart-cut transfer of RNase B and subsequent characterization of its glycoforms by CZE-MS. As expected, the developed 2D method exhibited higher separation efficiency compared to the 1D methods. LODs in the lower $\mu\text{g/mL}$ range were determined. Taking the width of analyte peaks (FWHM ~ 0.25 min), flow rate (500 nL/min) and the sample loop (20 nL) of the rotor in consideration, transfer efficiencies of about 14% were determined. This nanoLC-CZE-MS method represents an initial step towards increased sensitivity and improved separation performance in regards to intact (glyco)protein analysis. Conclusively, there is still room for improvement including (i) optimization of the 1st dimension to achieve narrower nanoLC peaks, (ii) implementation of larger sample loops on the rotor of the 4-port valve, (iii) integration of trap columns in the 1st dimension, and (iv) application of different type of CE-MS interface (e.g. nano sheath liquid interface). In this way, it is expected that LODs in the low to mid ng/mL range can be achieved, considerably improving sensitivity compared to traditional (SL based) CZE-MS. Future applications include intact protein analysis of pharmaceutical and biological/clinical relevant samples.

The final part of the thesis was dedicated to the development of a CZE-DTIM-MS method for the characterization of native and APTS-labeled *N*-glycans, which represents an interesting and auspicious alternative to traditional 2D liquid based separation. The combination of CZE and DTIM-MS has not been investigated in detail prior to this work. Each individual glycan signal separated in CZE exhibited an unexpectedly high number of peaks observed in the IMS dimension. Their origin could be explained by the presence of isomeric forms, including different linkages, and/or gas-phase conformers which do not interconvert on the time-scale of the ion mobility separation. Some peaks observed in the ATD could be attributed to different sialic acid linkages by treating samples with $\alpha 2\text{-}3$ neuraminidase. In order to elucidate the structures of the different ATD species in more detail, further experiments are required such as stepwise digestion with various exoglycosinases and/or

fragmentation experiments. Without prior separation in the CZE dimension, the complexity of some *N*-glycans could not be resolved by DTIM-MS alone. This emphasizes the benefits obtained by the combination of these powerful analytical techniques. Furthermore, it could be shown that the obtained ATD profiles are independent of the applied SL, which allows the optimization, e.g. optimizing ionization efficiency. It could be demonstrated that the combination of CZE and DTIM-MS technology displays high potential for *N*-glycan analysis and is expected to find various applications in the future. The presented work represents a cornerstone for future work related to CE-IM-MS, e.g. covering detailed glycosylation profiling of biotherapeutics or the analysis of serum samples in the context of diagnosis.

References

1. Nelson DL, Cox MM. Lehninger Biochemie. Mit 131 Tabellen, 4., vollständig überarbeitete und erweiterte Auflage, Übersetzung der 5. amerikanischen Auflage, korrigierter Nachdruck. Springer-Lehrbuch. Springer, Berlin, Heidelberg. 2011.
2. Ambrogelly A, Palioura S, Söll D. Natural expansion of the genetic code. *Nat. Chem. Biol.* 2007;3(1):29–35.
3. Bürkle A. Posttranslational Modification. In: Brenner S, Miller JH, Broughton WJ (eds) Encyclopedia of genetics. 2002;. Academic Press, San Diego, p. 1533.
4. Lanouette S, Mongeon V, Figeys D, Couture J-F. The functional diversity of protein lysine methylation. *Mol. Syst. Biol.* 2014;10:724.
5. Drazic A, Myklebust LM, Ree R, Arnesen T. The world of protein acetylation. *Biochim. Biophys. Acta.* 2016;1864(10):1372–1401.
6. Ardito F, Giuliani M, Perrone D, Troiano G, Lo Muzio L. The crucial role of protein phosphorylation in cell signaling and its use as targeted therapy (Review). *Int. J. Mol. Med.* 2017;40(2):271–280.
7. Jiang H, Zhang X, Chen X, Aramsangtienchai P, Tong Z, Lin H. Protein Lipidation: Occurrence, Mechanisms, Biological Functions, and Enabling Technologies. *Chem. Rev.* 2018;118(3):919–988.
8. Varki A, Cummings RD, Esko JD, Stanley P, Hart GW, Aebi M, Darvill AG, Kinoshita T, Packer NH, Prestegard JH, Schnaar RL, Seeberger PH (eds). 2017. Essentials of glycobiology, Third edition. Cold Spring Harbor Laboratory Press, Cold Spring Harbor, New York.
9. Kornfeld R, Kornfeld S. Assembly of asparagine-linked oligosaccharides. *Annu. Rev. Biochem.* 1985;54:631–664.

10. Williams JP, Grabenauer M, Holland RJ, Carpenter CJ, Wormald MR, Giles K, Harvey DJ, Bateman RH, Scrivens JH, Bowers MT. Characterization of simple isomeric oligosaccharides and the rapid separation of glycan mixtures by ion mobility mass spectrometry. *Int. J. Mass Spectrom.* 2010;298(1-3):119–127.
11. Stanley P, Taniguchi N, Aebi M. N-Glycans. In: *Essentials of Glycobiology*
12. LIS H, SHARON N. Protein glycosylation. Structural and functional aspects. *Eur. J. Biochem.* 1993;218(1):1–27.
13. Mariño K, Bones J, Kattla JJ, Rudd PM. A systematic approach to protein glycosylation analysis: a path through the maze. *Nat. Chem. Biol.* 2010;6(10):713–723.
14. Schwarz F, Aebi M. Mechanisms and principles of N-linked protein glycosylation. *Curr. Opin. Struct. Biol.* 2011;21(5):576–582.
15. Zhang L, Luo S, Zhang B. Glycan analysis of therapeutic glycoproteins. *mAbs.* 2016;8(2):205–215.
16. Dwek RA. Glycobiology: Toward Understanding the Function of Sugars. *Chem. Rev.* 1996;96(2):683–720.
17. Rudd PM. Glycosylation and the Immune System. *Science.* 2001;291(5512):2370–2376.
18. Montreuil J, Vliegenthart JFG, Schachter H. Glycoproteins. *New comprehensive biochemistry.* v. 29a. Elsevier, Amsterdam, New York. 1995.
19. Dalziel M, Crispin M, Scanlan CN, Zitzmann N, Dwek RA. Emerging principles for the therapeutic exploitation of glycosylation. *Science.* 2014;343(6166):1235681.
20. Buxbaum E. *Fundamentals of Protein Structure and Function*, 2nd ed. Springer International Publishing, Cham, s.l. 2015.

21. Xia Z. Structure, Classification, and Naming of Therapeutic Monoclonal Antibodies. In: Liu C, Morrow J (eds) Biosimilars of monoclonal antibodies. A practical guide to manufacturing, preclinical, and clinical development. 2017. vol. 256. John Wiley & Sons, Inc, Hoboken, New Jersey, pp 63–83.
22. Fekete S, Gassner A-L, Rudaz S, Schappler J, Guillarme D. Analytical strategies for the characterization of therapeutic monoclonal antibodies. *TrAC, Trends Anal. Chem.* 2013;42:74–83.
23. Ecker DM, Jones SD, Levine HL. The therapeutic monoclonal antibody market. *mAbs.* 2015;7(1):9–14.
24. Monoclonal Antibodies Approved by the EMA and FDA for Therapeutic Use – ACTIP. <http://www.actip.org/products/monoclonal-antibodies-approved-by-the-ema-and-fda-for-therapeutic-use/>. Accessed 6 November 2018.
25. Li J, Zhu Z. Research and development of next generation of antibody-based therapeutics. *Acta Pharmacol. Sin.* 2010;31(9):1198–1207.
26. Tomita M, Tsumoto K. Hybridoma technologies for antibody production. *Immunotherapy.* 2011;3(3):371–380.
27. Köhler G, Milstein C. Continuous cultures of fused cells secreting antibody of predefined specificity. *Nature.* 1975;256(5517):495–497.
28. Buss NAPS, Henderson SJ, McFarlane M, Shenton JM, Haan L de. Monoclonal antibody therapeutics: history and future. *Curr. Opin. Pharmacol.* 2012;12(5):615–622.
29. Liu JKH. The history of monoclonal antibody development - Progress, remaining challenges and future innovations. *Ann. Med. Surg. (Lond).* 2014;3(4):113–116.
30. Elgundi Z, Reslan M, Cruz E, Sifniotis V, Kayser V. The state-of-play and future of antibody therapeutics. *Adv. Drug Deliv. Rev.* 2017;122:2–19.

31. Chon JH, Zarbis-Papastoitsis G. Advances in the production and downstream processing of antibodies. *N. Biotechnol.* 2011;28(5):458–463.
32. Gronemeyer P, Ditz R, Strube J. Trends in Upstream and Downstream Process Development for Antibody Manufacturing. *Bioengineering (Basel)*. 2014;1(4):188–212.
33. Fahrner RL, Knudsen HL, Basey CD, Galan W, Feuerhelm D, Vanderlaan M, Blank GS. Industrial Purification of Pharmaceutical Antibodies: Development, Operation, and Validation of Chromatography Processes. *Biotechnol. Genet. Eng. Rev.* 2001;18(1):301–327.
34. Liu HF, Ma J, Winter C, Bayer R. Recovery and purification process development for monoclonal antibody production. *mAbs*. 2010;2(5):480–499.
35. Liu H, Ponniah G, Zhang H-M, Nowak C, Neill A, Gonzalez-Lopez N, Patel R, Cheng G, Kita AZ, Andrien B. In vitro and in vivo modifications of recombinant and human IgG antibodies. *mAbs*. 2014;6(5):1145–1154.
36. Moritz B, Schnaible V, Kiessig S, Heyne A, Wild M, Finkler C, Christians S, Mueller K, Zhang L, Furuya K, Hassel M, Hamm M, Rustandi R, He Y, Solano OS, Whitmore C, Park SA, Hansen D, Santos M, Lies M. Evaluation of capillary zone electrophoresis for charge heterogeneity testing of monoclonal antibodies. *J. Chromatogr. B*. 2015;983-984:101–110.
37. Manning MC, Chou DK, Murphy BM, Payne RW, Katayama DS. Stability of protein pharmaceuticals: an update. *Pharm. Res.* 2010;27(4):544–575.
38. Pace AL, Wong RL, Zhang YT, Kao Y-H, Wang YJ. Asparagine deamidation dependence on buffer type, pH, and temperature. *J. Pharm. Sci.* 2013;102(6):1712–1723.

39. Laurer H, Rozing G (eds). 2015. High performance capillary electrophoresis (2nd edition): A primer. Agilent Technologies.
40. Tiselius A. A new apparatus for electrophoretic analysis of colloidal mixtures. *Trans. Faraday Soc.* 1937;33:524.
41. Xuan X, Li D. Analytical study of Joule heating effects on electrokinetic transportation in capillary electrophoresis. *J. Chromatogr. A.* 2005;1064(2):227-237.
42. Hjertén S. Free zone electrophoresis. *Chromatogr. Rev.* 1967;9(2):122–219.
43. Jorgenson JW, Lukacs KD. Free-zone electrophoresis in glass capillaries. *Clin. Chem. (Washington, DC, U. S.).* 1981;27(9):1551–1553.
44. Breadmore MC. Electrokinetic and hydrodynamic injection: making the right choice for capillary electrophoresis. *Bioanalysis.* 2009;1(5):889–894.
45. Höcker O, Montealegre C, Neusüß C. Characterization of a nanoflow sheath liquid interface and comparison to a sheath liquid and a sheathless porous-tip interface for CE-ESI-MS in positive and negative ionization. *Anal. Bioanal. Chem.* 2018;410(21):5265–5275.
46. Fekete S, Guillarme D, Sandra P, Sandra K. Chromatographic, Electrophoretic, and Mass Spectrometric Methods for the Analytical Characterization of Protein Biopharmaceuticals. *Anal. Chem.* 2016;88(1):480–507.
47. Laroy W, Contreras R, Callewaert N. Glycome mapping on DNA sequencing equipment. *Nat. Protoc.* 2006;1(1):397–405.
48. van Deemter JJ, Zuiderweg FJ, Klinkenberg A. Longitudinal diffusion and resistance to mass transfer as causes of nonideality in chromatography. *Chem. Eng. Sci.* 1956;5(6):271–289.

49. MacNair JE, Lewis KC, Jorgenson JW. Ultrahigh-pressure reversed-phase liquid chromatography in packed capillary columns. *Anal. Chem.* 1997;69(6):983-989.
50. Molnár I, Horváth C. Reverse-phase chromatography of polar biological substances: separation of catechol compounds by high-performance liquid chromatography. *Clin. Chem. (Washington, DC, U. S.)*. 1976;22(9):1497-1502.
51. Rafferty JL, Zhang L, Siepmann JI, Schure MR. Retention mechanism in reversed-phase liquid chromatography: a molecular perspective. *Anal. Chem.* 2007;79(17):6551-6558.
52. Karpievitch YV, Polpitiya AD, Anderson GA, Smith RD, Dabney AR. Liquid Chromatography Mass Spectrometry-Based Proteomics: Biological and Technological Aspects. *Ann. Appl. Stat.* 2010;4(4):1797-1823.
53. Mitulovic G, Mechtler K. HPLC techniques for proteomics analysis—a short overview of latest developments. *Briefings Funct. Genomics Proteomics.* 2006;5(4):249-260.
54. Gross JH. Mass spectrometry. A textbook. Springer, 1. ed, corr. 2. print, Berlin. 2004.
55. Yamashita M, Fenn JB. Electrospray ion source. Another variation on the free-jet theme. *J. Phys. Chem.* 1984;88(20):4451-4459.
56. Olivares JA, Nguyen NT, Yonker CR, Smith RD. On-line mass spectrometric detection for capillary zone electrophoresis. *Anal. Chem.* 1987;59(8):1230-1232.
57. Mallet CR, Lu Z, Mazzeo JR. A study of ion suppression effects in electrospray ionization from mobile phase additives and solid-phase extracts. *Rapid Commun. Mass Spectrom.* 2004;18(1):49-58.

58. Wiley WC, McLaren IH. Time-of-Flight Mass Spectrometer with Improved Resolution. *Rev. Sci. Instrum.* 1955;26(12):1150–1157.
59. Hoffmann Ed, Stroobant V. Mass spectrometry. Principles and applications, 3. ed. Wiley, Chichester, West Sussex, England, Hoboken, N.J. 2007;
60. Boesl U. Time-of-flight mass spectrometry: Introduction to the basics. *Mass Spectrom. Rev.* 2017;36(1):86–109.
61. Leary JJ, Schmidt RL. Quadrupole Mass Spectrometers: An Intuitive Look at the Math. *J. Chem. Educ.* 1996;73(12):1142–1144.
62. Morris M, Thibault P, Boyd RK. Characterization of a high-pressure quadrupole collision cell for low-energy collision-induced dissociation. *J. Am. Soc. Mass Spectrom.* 1994;5(12):1042–1063.
63. Kelly RT, Tolmachev AV, Page JS, Tang K, Smith RD. The ion funnel: theory, implementations, and applications. *Mass Spectrom. Rev.* 2010;29(2):294–312.
64. Mamyrin BA. Laser assisted reflectron time-of-flight mass spectrometry. *Int. J. Mass Spectrom. Ion Processes.* 1994;131:1–19.
65. Lanucara F, Holman SW, Gray CJ, Eyers CE. The power of ion mobility-mass spectrometry for structural characterization and the study of conformational dynamics. *Nat. Chem.* 2014;6(4):281–294.
66. McDaniel EW, Martin DW, Barnes WS. Drift Tube-Mass Spectrometer for Studies of Low-Energy Ion-Molecule Reactions. *Rev. Sci. Instrum.* 1962;33(1):2–7.
67. Web of Science [v.5.30] - Citation Report.
https://apps.webofknowledge.com/CitationReport.do?product=WOS&search_mode=CitationReport&SID=D2gPQCjkAKbQtHnInxM&page=1&cr_pqid=6&viewType=summary&colName=WOS. Accessed 11 November 2018.

68. Clemmer DE, Hudgins RR, Jarrold MF. Naked Protein Conformations: Cytochrome c in the Gas Phase. *J. Am. Chem. Soc.* 1995;117(40):10141–10142.
69. Fernandez-Lima FA, Kaplan DA, Park MA. Note: Integration of trapped ion mobility spectrometry with mass spectrometry. *Rev. Sci. Instrum.* 2011;82(12)
70. Marchand A, Livet S, Rosu F, Gabelica V. Drift Tube Ion Mobility: How to Reconstruct Collision Cross Section Distributions from Arrival Time Distributions? *Anal. Chem.* 2017;89(23):12674–12681.
71. Mason EA, Schamp HW. Mobility of gaseous ions in weak electric fields. *Ann. Phys. (Amsterdam, Neth.)*. 1958;4(3):233–270.
72. Clowers BH, Ibrahim Y, Prior DC, Danielson WF, Belov M, Smith RD. Enhanced Ion Utilization Efficiency Using an Electrodynamic Ion Funnel Trap as an Injection Mechanism for Ion Mobility Spectrometry. *Anal. Chem.* 2008;80(3):612–623.
73. Kler PA, Sydes D, Huhn C. Column-coupling strategies for multidimensional electrophoretic separation techniques. *Anal. Bioanal. Chem.* 2015;407(1):119–138.
74. Giddings JC. Concepts and comparisons in multidimensional separation. *J. High Resol. Chromatogr.* 1987;10(5):319–323.
75. Kohl FJ, Sánchez-Hernández L, Neusüß C. Capillary electrophoresis in two-dimensional separation systems: Techniques and applications. *Electrophoresis.* 2015;36(1):144–158.
76. Cortes HJ, Winniford B, Luong J, Pursch M. Comprehensive two dimensional gas chromatography review. *J. Sep. Sci.* 2009;32(5-6):883–904.

-
77. Stoll DR, Carr PW. Two-Dimensional Liquid Chromatography: A State of the Art Tutorial. *Anal. Chem.* 2017;89(1):519–531.
 78. Cottet H, Biron J-P, Taillades J. Heart-cutting two-dimensional electrophoresis in a single capillary. *J. Chromatogr. A.* 2004;1051(1-2):25–32.
 79. Schoenherr RM, Ye M, Vannatta M, Dovichi NJ. CE-microreactor-CE-MS/MS for protein analysis. *Anal. Chem.* 2007;79(6):2230–2238.
 80. Li Y, Wojcik R, Dovichi NJ. A replaceable microreactor for on-line protein digestion in a two-dimensional capillary electrophoresis system with tandem mass spectrometry detection. *J. Chromatogr. A.* 2011;1218(15):2007–2011.
 81. Kler PA, Posch TN, Pattky M, Tiggelaar RM, Huhn C. Column coupling isotachopheresis-capillary electrophoresis with mass spectrometric detection: characterization and optimization of microfluidic interfaces. *J. Chromatogr. A.* 2013;1297:204–212.
 82. Kler PA, Huhn C. Non-aqueous electrolytes for isotachopheresis of weak bases and its application to the comprehensive preconcentration of the 20 proteinogenic amino acids in column-coupling ITP/CE-MS. *Anal. Bioanal. Chem.* 2014;406(28):7163–7174.
 83. Sydes D, Kler PA, Hermans M, Huhn C. Zero-dead-volume interfaces for two-dimensional electrophoretic separations. *Electrophoresis.* 2016;37(22):3020–3024.
 84. Zhang M, El Rassi Z. Two-dimensional microcolumn separation platform for proteomics consisting of on-line coupled capillary isoelectric focusing and capillary electrochromatography. 1. Evaluation of the capillary-based two-dimensional platform with proteins, peptides, and human serum. *J. Proteome Res.* 2006;5(8):2001–2008.

85. Wei J, Gu X, Wang Y, Wu Y, Yan C. Two-dimensional separation system by on-line hyphenation of capillary isoelectric focusing with pressurized capillary electrochromatography for peptide and protein mapping. *Electrophoresis*. 2011;32(2):230–237.
86. Kohl FJ, Montealegre C, Neusüß C. On-line two-dimensional capillary electrophoresis with mass spectrometric detection using a fully electric isolated mechanical valve. *Electrophoresis*. 2016;37(7-8):954–958.
87. Ranjbar L, Foley JP, Breadmore MC. Multidimensional liquid-phase separations combining both chromatography and electrophoresis - A review. *Anal. Chim. Acta*. 2017;950:7–31.
88. Bushey MM, Jorgenson JW. Automated instrumentation for comprehensive two-dimensional high-performance liquid chromatography of proteins. *Anal. Chem*. 1990;62(2):161–167.
89. Bushey MM, Jorgenson JW. A comparison of tryptic digests of bovine and equine cytochrome C by comprehensive reversed-phase HPLC-CE. *J. Micro. Sep.* 1990;2(6):293–299.
90. Lewis KC, Opiteck G. J., Jorgenson JW, Sheely DM. Comprehensive on-line RPLC-CZE-MS of peptides. *J. Am. Soc. Mass Spectrom.* 1997;8(5):495–500.
91. Bergström SK, Samskog J, Markides KE. Development of a poly(dimethylsiloxane) interface for on-line capillary column liquid chromatography-capillary electrophoresis coupled to sheathless electrospray ionization time-of-flight mass spectrometry. *Anal. Chem*. 2003;75(20):5461–5467.

92. Bergström SK, Dahlin AP, Ramström M, Andersson M, Markides KE, Bergquist J. A simplified multidimensional approach for analysis of complex biological samples: on-line LC-CE-MS. *Analyst*. 2006;131(7):791–798.
93. Chambers AG, Mellors JS, Henley WH, Ramsey JM. Monolithic integration of two-dimensional liquid chromatography-capillary electrophoresis and electrospray ionization on a microfluidic device. *Anal. Chem.* 2011;83(3):842–849.
94. Mellors JS, Black WA, Chambers AG, Starkey JA, Lacher NA, Ramsey JM. Hybrid capillary/microfluidic system for comprehensive online liquid chromatography-capillary electrophoresis-electrospray ionization-mass spectrometry. *Anal. Chem.* 2013;85(8):4100–4106.
95. Aizpurua-Olaizola O, Sastre Toraño J, Falcon-Perez JM, Williams C, Reichardt N, Boons G-J. Mass spectrometry for glycan biomarker discovery. *TrAC, Trends Anal. Chem.* 2018;100:7–14.
96. Zheng X, Wojcik R, Zhang X, Ibrahim YM, Burnum-Johnson KE, Orton DJ, Monroe ME, Moore RJ, Smith RD, Baker ES. Coupling Front-End Separations, Ion Mobility Spectrometry, and Mass Spectrometry For Enhanced Multidimensional Biological and Environmental Analyses. *Annu. Rev. Anal. Chem. (Palo Alto Calif)*. 2017;10(1):71–92.
97. Li J, Purves RW, Richards JC. Coupling capillary electrophoresis and high-field asymmetric waveform ion mobility spectrometry mass spectrometry for the analysis of complex lipopolysaccharides. *Anal. Chem.* 2004;76(16):4676–4683.

98. Mironov GG, Okhonin V, Khan N, Clouthier CM, Berezovski MV. Conformational Dynamics of DNA G-Quadruplex in Solution Studied by Kinetic Capillary Electrophoresis Coupled On-line with Mass Spectrometry**. *ChemistryOpen*. 2014;3(2):58–64.
99. Mironov GG, Clouthier CM, Akbar A, Keillor JW, Berezovski MV. Simultaneous analysis of enzyme structure and activity by kinetic capillary electrophoresis-MS. *Nat. Chem. Biol.* 2016;12(11):918–922.
100. Hallen RW, Shumate CB, Siems WF, Tsuda T, Hill HH. Preliminary investigation of ion mobility spectrometry after capillary electrophoretic introduction. *J. Chromatogr. A*. 1989;480:233–245.
101. Hofmann J, Pagel K. Glycan Analysis by Ion Mobility-Mass Spectrometry. *Angew. Chem. Int. Ed. Engl.* 2017;56(29):8342–8349.
102. Lareau NM, May JC, McLean JA. Non-derivatized glycan analysis by reverse phase liquid chromatography and ion mobility-mass spectrometry. *Analyst*. 2015;140(10):3335–3338.
103. Pohle T, Brzozowski T, Becker JC, van der Voort IR, Markmann A, Konturek SJ, Moniczewski A, Domschke W, Konturek JW. Role of reactive oxygen metabolites in aspirin-induced gastric damage in humans: gastroprotection by vitamin C. *Aliment Pharmacol. Ther.* 2001;15(5):677–687.
104. Mylrea M, Robertson S, Haywood A, Glass B. Stability of Dispersible Aspirin Tablets Repacked into Dosette Boxes. *J. Pharm. Pract. Res.* 2012;42(3):204–207.
105. Pavlovska G, Tanevska S. Influence of temperature and humidity on the degradation process of ascorbic acid in vitamin C chewable tablets. *J. Therm. Anal. Calorim.* 2013;111(3):1971–1977.

106. Thomis R, Roets E, Hoogmartens J. Analysis of Tablets Containing Aspirin, Acetaminophen, and Ascorbic Acid by High-Performance Liquid Chromatography. *J. Pharm. Sci.* 1984;73(12):1830–1833.
107. Wabaidur SM, Alothman ZA, Khan MR. A rapid method for the simultaneous determination of L-ascorbic acid and acetylsalicylic acid in aspirin C effervescent tablet by ultra performance liquid chromatography-tandem mass spectrometry. *Spectrochim. Acta, Part A.* 2013;108:20–25.
108. Hühner J, Neusüß C. CIEF-CZE-MS applying a mechanical valve. *Anal. Bioanal. Chem.* 2016;408(15):4055–4061.
109. Paulssen RB, Chatterji D, Higuchi T, Pitman IH. Acylation of Ascorbic Acid in Water. *J. Pharm. Sci.* 1975;64(8):1300–1305.
110. Troup AE, Mitchner H. Degradation of Phenylephrine Hydrochloride in Tablet Formulations Containing Aspirin. *J. Pharm. Sci.* 1964;53(4):375–379.
111. He Y, Lacher NA, Hou W, Wang Q, Isele C, Starkey J, Ruesch M. Analysis of identity, charge variants, and disulfide isomers of monoclonal antibodies with capillary zone electrophoresis in an uncoated capillary column. *Anal. Chem.* 2010;82(8):3222–3230.
112. La Espinosa-de Garza CE, Perdomo-Abúndez FC, Padilla-Calderón J, Uribe-Wiechers JM, Pérez NO, Flores-Ortiz LF, Medina-Rivero E. Analysis of recombinant monoclonal antibodies by capillary zone electrophoresis. *Electrophoresis.* 2013;34(8):1133–1140.
113. Beck A, Wagner-Rousset E, Ayoub D, van Dorsselaer A, Sanglier-Cianférani S. Characterization of therapeutic antibodies and related products. *Anal. Chem.* 2013;85(2):715–736.

114. Bults P, Bischoff R, Bakker H, Gietema JA, van de Merbel NC. LC-MS/MS-Based Monitoring of In Vivo Protein Biotransformation: Quantitative Determination of Trastuzumab and Its Deamidation Products in Human Plasma. *Anal. Chem.* 2016;88(3):1871–1877.
115. Harris RJ, Kabakoff B, Macchi FD, Shen FJ, Kwong M, Andya JD, Shire SJ, Bjork N, Totpal K, Chen AB. Identification of multiple sources of charge heterogeneity in a recombinant antibody. *J. Chromatogr. B.* 2001;752(2):233–245.
116. Haberger M, Leiss M, Heidenreich A-K, Pester O, Hafenmair G, Hook M, Bonnington L, Wegele H, Haindl M, Reusch D, Bulau P. Rapid characterization of biotherapeutic proteins by size-exclusion chromatography coupled to native mass spectrometry. *mAbs.* 2016;8(2):331–339.
117. Sandra K, Vandenheede I, Sandra P. Modern chromatographic and mass spectrometric techniques for protein biopharmaceutical characterization. *J. Chromatogr. A.* 2014;1335:81–103.
118. Hühner J, Jooß K, Neusüß C. Interference-free mass spectrometric detection of capillary isoelectric focused proteins, including charge variants of a model monoclonal antibody. *Electrophoresis.* 2017;38(6):914–921.
119. Berglund M, Wieser ME. Isotopic compositions of the elements 2009 (IUPAC Technical Report). *Pure Appl. Chem.* 2011;83(2):397–410.
120. O’Leary MH. Carbon Isotopes in Photosynthesis. *BioScience.* 1988;38(5):328–336.
121. Palmisano G, Melo-Braga MN, Engholm-Keller K, Parker BL, Larsen MR. Chemical deamidation: a common pitfall in large-scale N-linked glycoproteomic mass spectrometry-based analyses. *J. Proteome Res.* 2012;11(3):1949–1957.

122. Sánchez-Hernández L, Montealegre C, Kiessig S, Moritz B, Neusüß C. In-capillary approach to eliminate SDS interferences in antibody analysis by capillary electrophoresis coupled to mass spectrometry. *Electrophoresis*. 2017;38(7):1044–1052.
123. Staub A, Guillarme D, Schappler J, Veuthey J-L, Rudaz S. Intact protein analysis in the biopharmaceutical field. *J. Pharm. Biomed. Anal.* 2011;55(4):810–822.
124. Martosella J, Zolotarjova N, Liu H, Nicol G, Boyes BE. Reversed-phase high-performance liquid chromatographic prefractionation of immunodepleted human serum proteins to enhance mass spectrometry identification of lower-abundant proteins. *J. Proteome Res.* 2005;4(5):1522–1537.
125. Lemmo AV, Jorgenson JW. Transverse flow gating interface for the coupling of microcolumn LC with CZE in a comprehensive two-dimensional system. *Anal. Chem.* 1993;65(11):1576–1581.
126. Bunz S-C, Cutillo F, Neusüß C. Analysis of native and APTS-labeled N-glycans by capillary electrophoresis/time-of-flight mass spectrometry. *Anal. Bioanal. Chem.* 2013;405(25):8277–8284.
127. Ruhaak LR, Zauner G, Huhn C, Bruggink C, Deelder AM, Wuhrer M. Glycan labeling strategies and their use in identification and quantification. *Anal. Bioanal. Chem.* 2010;397(8):3457–3481.
128. Nakano M, Kakehi K, Tsai M-H, Lee YC. Detailed structural features of glycan chains derived from alpha1-acid glycoproteins of several different animals: the presence of hypersialylated, O-acetylated sialic acids but not disialyl residues. *Glycobiology*. 2004;14(5):431–441.

129. Stow SM, Causon TJ, Zheng X, Kurulugama RT, Mairinger T, May JC, Rennie EE, Baker ES, Smith RD, McLean JA, Hann S, Fjeldsted JC. An Interlaboratory Evaluation of Drift Tube Ion Mobility-Mass Spectrometry Collision Cross Section Measurements. *Anal. Chem.* 2017;89(17):9048–9055.

Appendix

List of Figures

Figure 1: Basic structural composition of peptides and proteins.....	2
Figure 2: Simplified concept of protein synthesis divided into three major steps.....	3
Figure 3: Three general types of N-glycans.....	4
Figure 4: (A) Three-dimensional depiction of IgG class. (B) Scheme of general structure of IgG.	6
Figure 5: Graphical representation of four general types of biotherapeutic mAbs. ...	8
Figure 6: Scheme of general CZE setup.....	10
Figure 7: Formation of EOF in FS capillaries.....	12
Figure 8: ESI process in positive ion mode applying CE-MS.	16
Figure 9: Three major models describing the final step of the ESI process.....	17
Figure 10: Scheme of ESI-QTOF-MS setup.....	22
Figure 11: Number of peer-reviewed papers published annually. Data was generated using Web of Science with the search term "ion mobility spectrometry".	24
Figure 12: General principle of DTIMS.....	25
Figure 13: Overview of 2D transfer strategies.	27
Figure 14: Generic designs and sample transfer process of transverse flow gating and hybrid capillary microchip interface.....	29
Figure 15: (A) Scheme of mechanical 4-port valve consisting of three major part (B) General principle of heart-cut sample transfer.....	31
Figure 16: CZE-UV electropherogram of degraded ASA + ASC tablet sample.	98
Figure 17: (A) Scheme of general CE-CE-MS setup. (B) Photographic picture of applied CE-CE-MS setup.....	99
Figure 18: Principle of heart-cut strategies utilizing 4-port valve as CE-CE interface	101

Figure 19: Overview of degradation products originating from ASC in the presence of ASA.....104

Figure 20: Cut of main peak of glycosylated Trastuzumab (12.5 mg/mL) using CZE-CZE-MS (20 nL transfer volume).106

Figure 21: MS calibration procedure based on SL tuning mix infusion.....107

Figure 22: Comparison of detected deconvoluted mass of G0F/G1F glycoform of the main peak of Trastuzumab with calculated masses based on ¹³C distribution stated by IUPAC and natural organic carbon.108

Figure 23: CZE-CZE-MS analysis of deglycosylated Trastuzumab.....109

Figure 24: (A) Scheme of 6-port valve used for sample injection for nanoLC system.112

Figure 25: Analysis of protein mix by nanoLC-CZE-MS.114

Figure 26: CZE-DTIM-MS of APTS-labeled N-glycans.....117

Figure 27: CZE-MS electropherograms of native sialylated N-glycans released from AGP and fetuin.....118

Supplementary Information Manuscript II

Deglycosylation of Trastuzumab samples

120 μL H_2O and 30 μL Trastuzumab (25 mg/mL) were added to a nanosep 10K omega centrifuge device. The formulation buffer was exchanged by 20 mM ammonium hydrogen carbonate (pH = 8, adjusted with 30% ammonia) at 6000 rpm, leading to a final volume of 40 μL and a theoretical concentration of 18.75 mg/mL Trastuzumab. Subsequently, samples were transferred to a tube containing 20 units of *N*-glycosidase F followed by incubation (37°C, 24 h) to achieve complete deglycosylation. In order to deglycosylate higher concentrated mAb samples, the amount of *N*-glycosidase F was adapted accordingly. Samples were analyzed directly without further purification.

Table S1: Parameters of the applied Q-TOF MS methods.

Parameter	Wide range	High mass
End plate offset	-500 V	-500 V
Capillary voltage	-5000 V	-5000 V
Nebulizer	0.5 bar	0.5 bar
Dry gas	3.0 L/min	3.0 L/min
Dry temperature	170°C	170°C
Mass range	100 – 5000 <i>m/z</i>	700 – 5000 <i>m/z</i>
Pre pulse storage	32.0 μs	32.0 μs
Collision cell transfer time	50 (50%) – 130 (50%) μs	140 μs
Collision cell RF	500 (50%) – 1900 (50%) Vpp	2100 Vpp
Collision cell energy	15 eV	30 eV
Quadrupole ion energy	7 eV	30 eV

Supplementary Information Manuscript IV

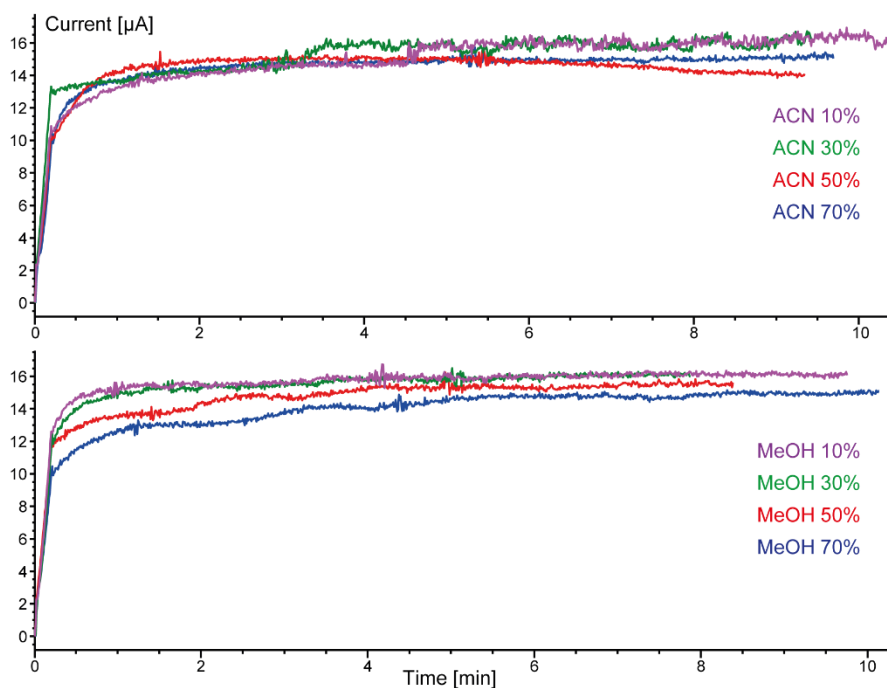


Figure S1: Evaluation of the influence of organic solvent content in the sample on current stability of CZE-MS. RNase B (1000 $\mu\text{g}/\text{mL}$) was solved in different amounts (10-70% (v/v)) of ACN and methanol, respectively. CZE-MS was performed as follows: BGE: 1 M acetic acid, 50 cm PVA coated capillary, injection: 50 mbar for 12 sec, +30 kV separation voltage, sheath liquid: 50% isopropyl alcohol +0.2 M FAC (flow rate = 4 $\mu\text{L}/\text{min}$). No significant influence on the current profile was noticed for acetonitrile (upper part). A slight decrease of the overall current was observed at higher content of methanol (lower part). Still, no current breakdown was observed and the obtained CZE profiles were equivalent with minor differences in the migration time.

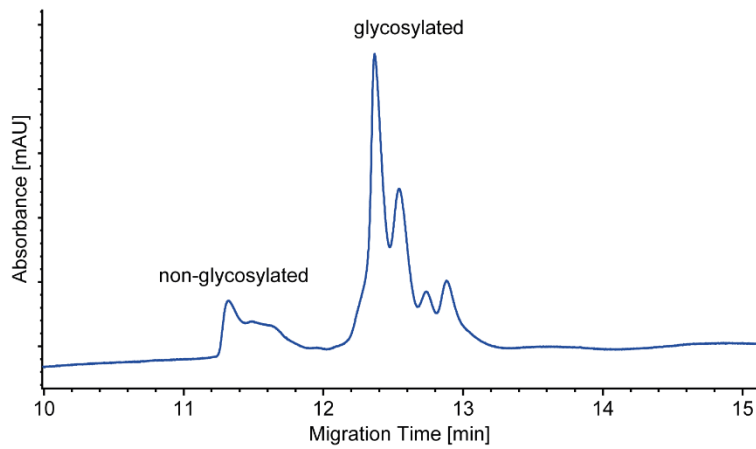


Figure S2: CZE-UV electropherogram of RNase B (1000 $\mu\text{g}/\text{mL}$) using a 90 cm PVA coated capillary and 0.2 M formic as BGE. Hydrodynamic injection was performed for 12 sec at 50 mbar and +30 kV was applied for separation. The detection wavelength was 214 nm. At least 4 different glycosylated forms of RNase B were observed.

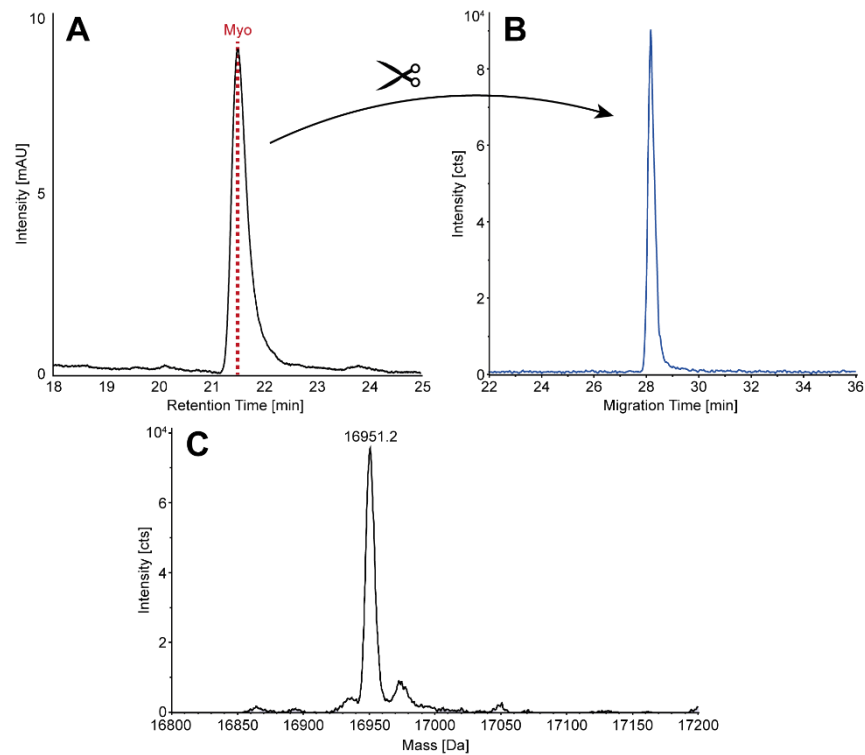


Figure S3: Analysis of myoglobin standard (250 $\mu\text{g}/\text{mL}$) by nanoLC-CZE-MS. First dimension: **(A)** nanoLC chromatogram at 214 nm detection wavelength. Second dimension: **(B)** CZE-MS electropherogram obtained after heart-cut of myoglobin from the nanoLC separation. The 11 most abundant charge states of the individual glycoforms were used to create the ion trace. Deconvoluted mass spectrum of myoglobin **(C)**.

Supplementary Information Manuscript V

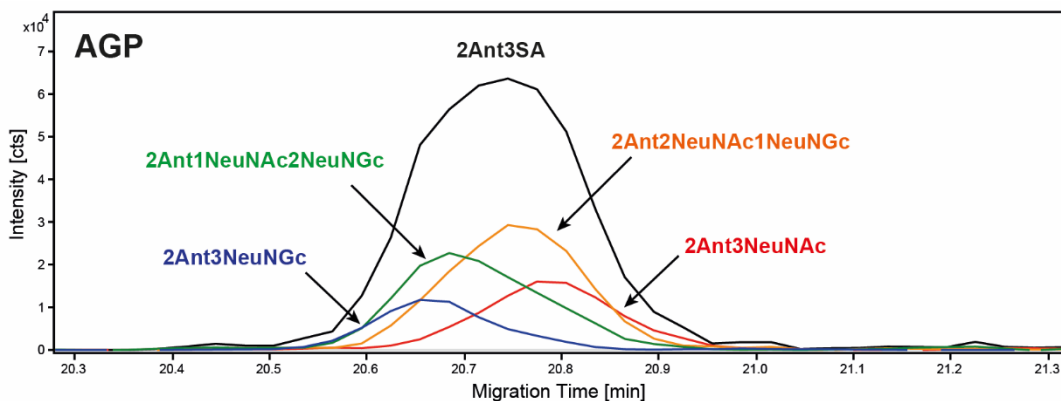


Figure S1: CZE electropherogram of different sialic acid species of 2Ant3SA, released from AGP, containing NeuNAc and/or NeuNGc. EICs of $[M-3H]^{3-}$ ions: 2Ant3NeuNAc (836.952 m/z), 2Ant2NeuNAc1NeuNGc (842.284 m/z), 2Ant1NeuNAc2NeuNGc (847.615 m/z), 2Ant3NeuNGc (852.947 m/z). Combined information of all glycoforms is illustrated by the EIC trace 2Ant3SA. Partial separation of species containing the same core structure but different types of sialic acids.

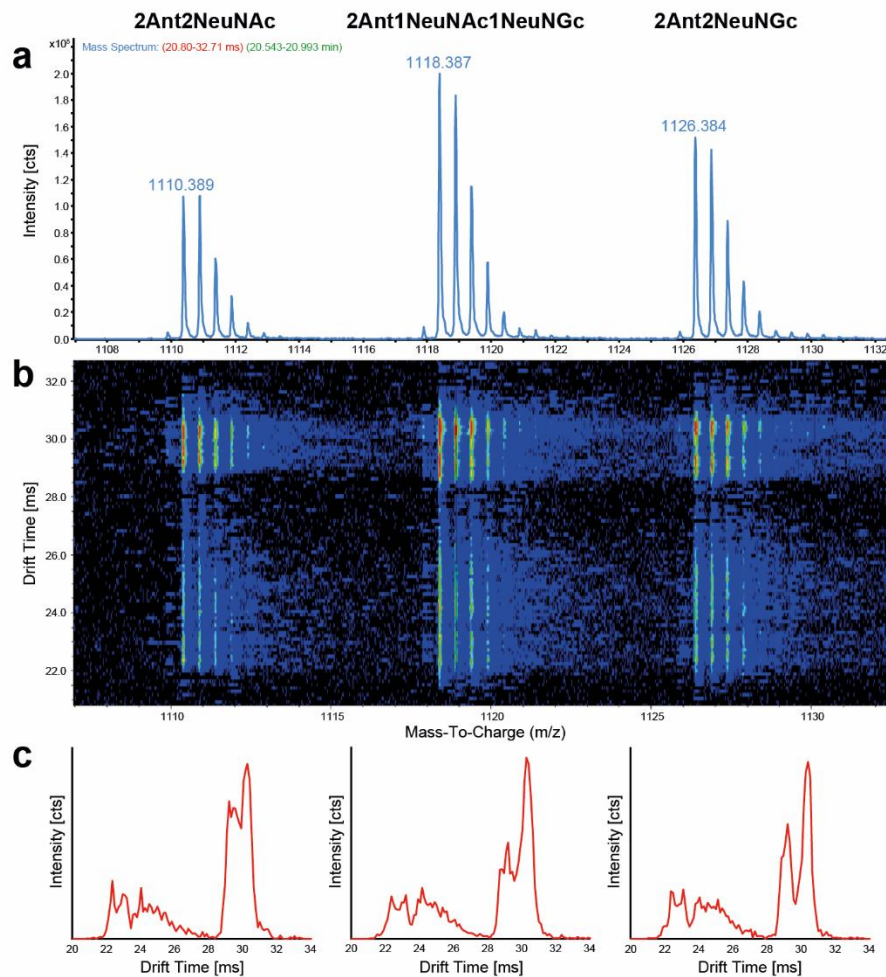


Figure S2: Separation of different sialic acid species of 2Ant2SA, released from AGP, containing NeuNAc and/or NeuNGc. Mass spectra of $[M-2H]^{2-}$ ions (**a**) ranging from 2Ant2NeuNAc (1110.389 m/z) to 2Ant2NeuNGc (1126.384 m/z). Typical distances between sialic acid species was observed ($\Delta m/z = 8.00$ Da). IMS heat map (**b**) associated with the mass spectra. Slight differences in the DT distribution are recognizable. Individual ATDs (**c**) of observed sialic acid species. Changes of relative signal intensities in the ATDs observed in dependence of the type of sialic acid.

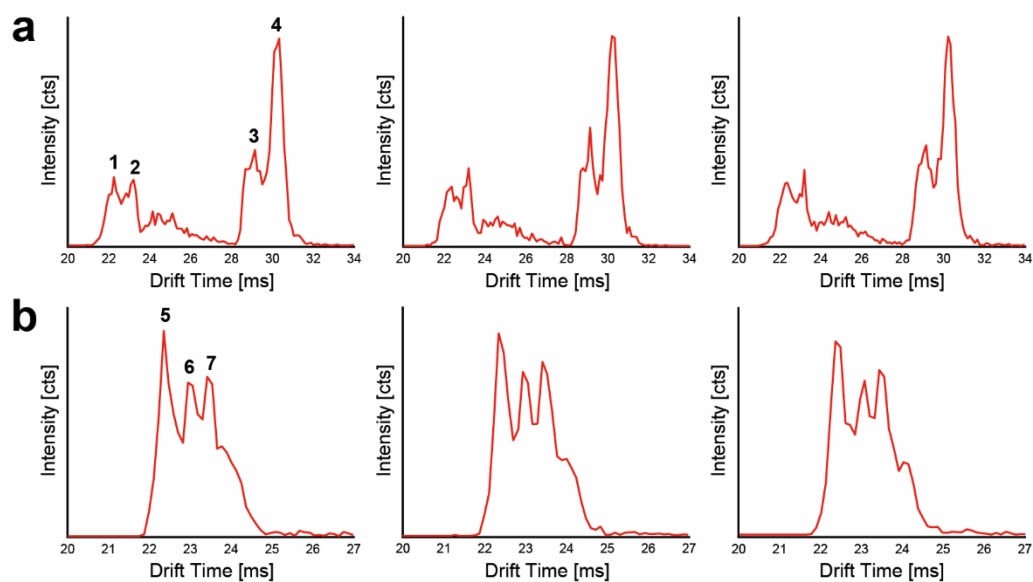


Figure S3: Repeatability experiment: Example ATDs of the glycans (a) 2Ant1NeuNAc1NGc and (b) 2Ant1NeuNAc2NeuNGc obtained for three measurements under the same conditions. The general patterns are reproducible. In addition, for the peaks 1-7 a mean RSD of 0.20% was determined for the drift time ($n = 6$ per peak). These values are in the typical range expected for this type of DTIM-MS instrument.

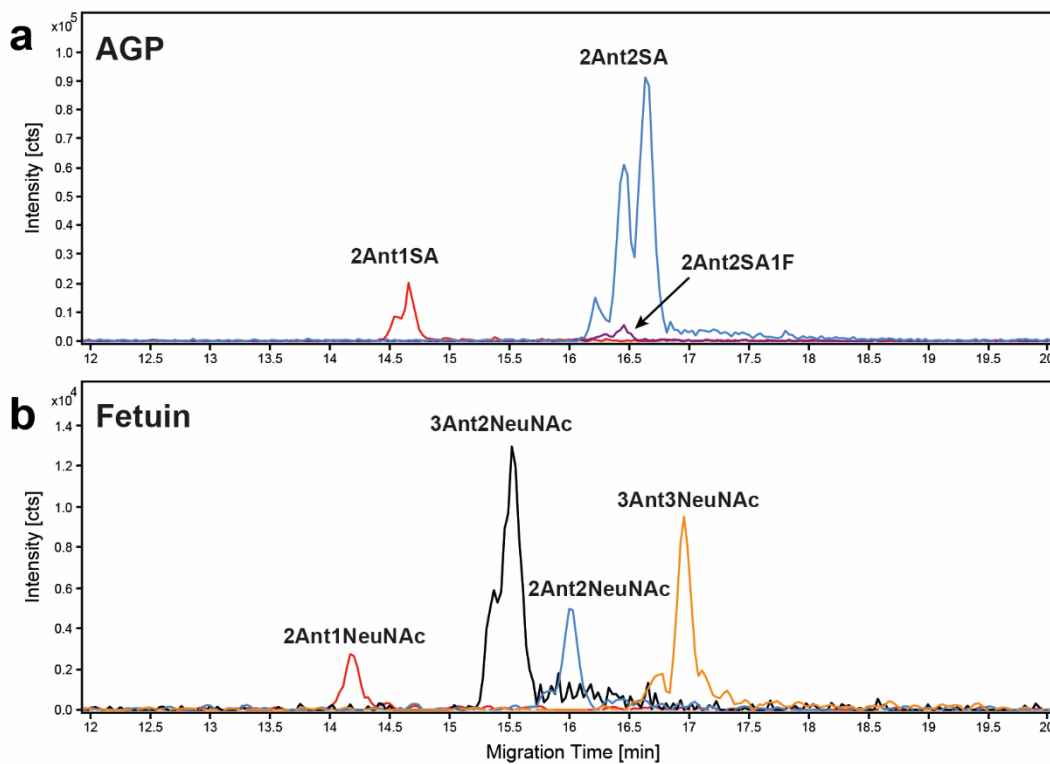


Figure S4: CZE electropherograms of native sialylated *N*-glycans released from AGP **(a)** and fetuin **(b)** after α 2-3 neuramidase treatment. Only glycans containing α 2-6-linked sialic acids should remain. Partly separation of glycan species possessing the same *m/z* value observed.

Scientific contributions

Peer-reviewed publications

K. Jooß, N. Scholz, J. Meixner and C. Neusüß, "Heart-cut nanoLC-CZE-MS for the characterization of proteins on the intact level", *Electrophoresis*, 2018, DOI: 10.1002/elps.201800411

K. Jooß, S. W. Meckelmann, O. J. Schmitz and C. Neusüß, "Capillary zone electrophoresis coupled to drift tube ion mobility spectrometry mass spectrometry for the analysis of native and APTS-labeled *N*-glycans", *Analytical and Bioanalytical Chemistry*, 2018, DOI: 10.1007/s00216-018-1515-7

A. Stolz, K. Jooß, O. Höcker, J. Römer, J. Schlecht and C. Neusüß, "Recent advances in capillary electrophoresis-mass spectrometry: Instrumentation, methodology and applications", *Electrophoresis*, 2018, DOI: 10.1002/elps.201800331

J. Schlecht, K. Jooß, and C. Neusüß, "Two-dimensional capillary zone electrophoresis-mass spectrometry: coupling MS-interfering capillary electromigration methods with mass spectrometry", *Analytical and Bioanalytical Chemistry*, 2018, vol. 410(25), pp. 6353-6359

K. Jooß, J. Hühner, S. Kiessig, B. Moritz and C. Neusüß, "Two-dimensional capillary zone electrophoresis-mass spectrometry for the characterization of intact monoclonal antibody charge variants, including deamidation products", *Analytical and Bioanalytical Chemistry*, 2017, vol. 409(26), pp. 6057-6067

S. Neuberger, K. Jooß, D. Flottmann, G. Scriba and C. Neusüß, "Raman spectroscopy and capillary zone electrophoresis for the analysis of degradation processes in commercial effervescent tablets containing acetylsalicylic acid and ascorbic acid", *Journal of Pharmaceutical and Biomedical Analysis*, 2017, vol. 134, pp. 122-129

J. Hühner, K. Jooß and C. Neusüß, "Interference-free mass spectrometric detection of capillary isoelectric focused proteins, including charge variants of a model monoclonal antibody", *Electrophoresis*, 2017, vol. 38(6), pp. 914-921

S. Neuberger, K. Jooß (shared first author), C. Ressel and C. Neusüß, "Quantification of ascorbic acid and acetylsalicylic acid in effervescent tablets by CZE-UV and identification of related degradation products by heart-cut CZE-CZE-MS", *Analytical and Bioanalytical Chemistry*, 2016, vol. 408(30), pp. 8701-8712

S. Chakrabarty, J. DeLeeuw, D. Woodall, K. Jooss, S. Narayan and S. Trimpin, "Reproducibility and Quantification of Illicit Drugs Using Matrix-Assisted Ionization (MAI) Mass Spectrometry", *Analytical Chemistry*, 2015, vol. 87(16), pp. 8301-8306

K. Jooß, J. Sommer, S. C. Bunz and C. Neusüß, "In-line SPE-CE using a fritless bead string design – Application for the analysis of organic sulfonates including inline SPE-CE-MS of APTS-labeled glycans", *Electrophoresis*, 2014, vol. 35, pp. 1236-1243

Book chapters

Chapter 12: Coupling of Capillary Electromigration Techniques to Mass Spectrometry"
Christian Neusüß, Jennifer Römer, Oliver Höcker and K. Jooß, In: "Capillary Electromigration Separation Methods 1st Edition", Colin F. Poole, Elsevier, 2018, ISBN: 978-0-12-809375-7

Patents

J. Huehner, K. Jooss and C. Neusuess, "Sample transfer device and method for sample transfer", 2017, WO 2017/153451 A1

Contributions to scientific conferences

06/2018

Oral presentation (Invited Lecture) at "Flow Analysis & Capillary Electrophoresis 2018", Hradec Kralove, Czech Republic

Title: 2D-CE to run compounds out of "MS-incompatible" buffers

01/2018

Oral presentation at "Agilent CE-MS User Meeting 2018", Utrecht, Netherlands

Title: 2D-CE to run compounds out of "MS-incompatible" buffers

10/2017

Oral and poster presentation at "1st Joint CE- and FFE Forum 2017", Karlsruhe, Germany

Title: Evaluation of conditions for in-capillary digestion of fractionated mAb variants for the application in a CZE-CZE-MS system

09/2017

Poster presentation at "24th International Symposium on Electro- and Liquid Phase Separation Techniques 2017", Sopot, Poland

Title: Evaluation of conditions for in-capillary digestion of fractionated mAb variants for the application in a CZE-CZE-MS system

06/2017

Oral and poster presentation at "HPLC 2017", Prague, Czech Republic

Title: Two-dimensional capillary zone electrophoresis coupled to mass spectrometry for the characterization of monoclonal antibody variants on the intact level

06/2017

Poster presentation at "65th ASMS Conference on Mass Spectrometry and Allied Topics", Indianapolis, IN, United States

Title: Accurate mass determination of intact monoclonal antibody charge variants including deamidation products using CZE-CZE-QqTOF-MS

10/2016

Oral presentation at "CE Forum 2016", Regensburg, Germany

Title: Two-dimensional capillary zone electrophoresis coupled to mass spectrometry for the characterization of monoclonal antibody variants on the intact level

03/2016

Oral presentation at "Analytical Technologies Europe 2016", Vienna, Austria

Title: Two-dimensional capillary zone electrophoresis coupled to mass spectrometry for the characterization of antibody variants

09/2013

Oral presentation at "7. Conference of Ion Analysis (CIA)", Berlin, Germany

Title: In-line-SPE-CE for the determination of sulfonic acids and APTS-labeled glycans

Eidesstattliche Erklärung

Ich erkläre an Eides statt, dass ich die bei der promotionsführenden Einrichtung
Wissenschaftszentrum Weihenstephan für Ernährung, Landnutzung und Umwelt

der TUM zur Promotionsprüfung vorgelegte Arbeit mit dem Titel:

Development and application of two-dimensional separation techniques coupled to mass spectrometry incorporating capillary electrophoresis

in Chemie am Lehrstuhl für Analytische Lebensmittelchemie

Fakultät, Institut, Lehrstuhl, Klinik, Krankenhaus, Abteilung

unter der Anleitung und Betreuung durch: apl. Prof. Dr. Philippe Schmitt-Kopplin ohne sonstige Hilfe erstellt und bei der Abfassung nur die gemäß § 6 Ab. 6 und 7 Satz 2 angebotenen Hilfsmittel benutzt habe.

Ich habe keine Organisation eingeschaltet, die gegen Entgelt Betreuerinnen und Betreuer für die Anfertigung von Dissertationen sucht, oder die mir obliegenden Pflichten hinsichtlich der Prüfungsleistungen für mich ganz oder teilweise erledigt.

Ich habe die Dissertation in dieser oder ähnlicher Form in keinem anderen Prüfungsverfahren als Prüfungsleistung vorgelegt.

Die vollständige Dissertation wurde in _____ veröffentlicht. Die promotionsführende Einrichtung

_____ hat der Veröffentlichung zugestimmt.

Ich habe den angestrebten Doktorgrad noch nicht erworben und bin nicht in einem früheren Promotionsverfahren für den angestrebten Doktorgrad endgültig gescheitert.

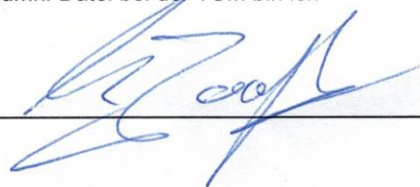
Ich habe bereits am _____ bei der Fakultät für _____
_____ der Hochschule _____
unter Vorlage einer Dissertation mit dem Thema _____
_____ die Zulassung zur Promotion beantragt mit dem Ergebnis: _____

Die öffentlich zugängliche Promotionsordnung der TUM ist mir bekannt, insbesondere habe ich die Bedeutung von § 28 (Nichtigkeit der Promotion) und § 29 (Entzug des Doktorgrades) zur Kenntnis genommen. Ich bin mir der Konsequenzen einer falschen Eidesstattlichen Erklärung bewusst.

Mit der Aufnahme meiner personenbezogenen Daten in die Alumni-Datei bei der TUM bin ich

einverstanden, nicht einverstanden.

Aalen, 17.12.2018, Unterschrift



Short Curriculum Vitae – Kevin Joob

Personal details

Date of birth: 04/29/1989

Place of birth: Heidenheim an der Brenz

Nationality: German

Email: kevin.jooss@gmx.de

Mobile: +49171/8233345

Education

PhD student: Analytical Chemistry

01/2015 – Present

Aalen University | Aalen, Germany

Helmholtz Zentrum München | Munich, Germany

Technical University of Munich | Munich, Germany

Supervisor: Prof. Philippe Schmitt-Kopplin (TUM), Prof. Christian Neusüß (Aalen University)

Thesis title: Development and application of two-dimensional electrophoretic separation techniques coupled to mass spectrometry incorporating capillary electrophoresis

Master of Science (M.Sc.): Analytical and Bioanalytical Chemistry

03/2013 – 12/2014

Aalen University | Aalen, Germany

Thesis title: Development of a Drug Screening Method for Opioids, THC and THC-COOH from Urine Samples Using Matrix-Assisted Ionization Vacuum – Ion Mobility Spectrometry – Mass Spectrometry (Trimpin group, Wayne State University, Detroit, United States)

Bachelor of Science (B.Sc.): Chemistry

09/2008 – 02/2013

Aalen University | Aalen, Germany

Thesis title: In-line-SPE-CE for the determination of sulfonic acids and APTS-labeled glycans (Neusüß group, Aalen University, Aalen, Germany)

Work Experience

03/2011 – 08/2011

Bruker Daltonics | Bremen, Germany

Internship: Contribution to development of novel and commercially available ion source (IonBooster)

Teaching

03/2018 – 08/2018 and 03/2017 – 08/2017

Aalen University | Aalen, Germany

Study program: Analytical and Bioanalytical Chemistry (Master of Science)

Lecture: Chemometrics

03/2015 – 08/2015

Aalen University | Aalen, Germany

Study program: Analytical and Bioanalytical Chemistry (Master of Science)

Lecture: Supplementary Course in Mass Spectrometry

09/2015 – 02/2016, 09/2016 – 02/2017 and 09/2017 – 02/2018

Aalen University | Aalen, Germany

Study program: Chemistry (Bachelor of Science)

Practical Course: Mass Spectrometry

Awards and Grants

10/2017

Best Poster Presentation Award at "1st Joint CE- and FFE Forum 2017", Karlsruhe, Germany

03/2016

Travel Grant Award at "Analytical Technologies Europe 2016", Vienna, Austria

07/2013

Best Thesis Award "Price of Technique and Medicine" of Aalen University, Aalen, Germany

03/2013

Best Graduate of the Year Award (B.Sc. Chemistry), Aalen University, Aalen, Germany

Languages and Technical Competences

German (native speaker), English (fluent, C1 level)

Software: MS Office (Visual Basics), Adobe Illustrator and InDesign

Separation experience: CE, LC, nanoLC

Ion source experience: ESI, HESI, MAI, MALDI

Mass spectrometry experience: QTOF-MS, IT-MS, DTIM-MS, TWIM-MS